Aspects of the life history strategies of the Teredinidae

A thesis submitted in partial fulfilment of its requirements for the award of the degree of Doctor of Philosophy of the University of Portsmouth

By

John Reuben Shipway

Institute of Marine Sciences, School of Biological Sciences

University of Portsmouth

Eastney, Portsmouth

PO49LY

UK

September 2013

‘Thus, from the war of nature, from famine and death, the most exalted object which we are capable of conceiving, namely, the production of the higher animals, directly follows. There is grandeur in this view of life, with its several powers, having been originally breathed into a few forms or into one; and that, whilst this planet has gone cycling on according to the fixed law of gravity, from so simple a beginning endless forms most beautiful and most wonderful have been, and are being, evolved.’

Charles Robert Darwin FRS (1809-1882)

The Origin of Species

Abstract

The Teredinidae are a major economic pest of wooden coastal structures, causing billions of Dollars worth of damage per annum. To fully understand the threat posed by teredinids it is necessary to examine their biology at a number of different levels. These include: the anatomical adaptations which facilitate their wood-boring and wood-feeding life-style; the mechanism of cellulose digestion, which is aided by cellulolytic symbionts retained in bacteriocytes on the teredinid gill; the early life history strategies, particularly larval development; improving the means of teredinid identification for this taxonomically challenging group; and monitoring the spread of teredinids and the impacts global warming may have on their distribution. This thesis set out to address a number of these questions.

The teredinid *Lyrodus pedicellatus* is able to complete a life-cycle feeding exclusively on wood and is one of the most destructive of the marine borers. In this study, X-ray micro-computed tomography (MicroCT) was used to produce a three-dimensional computer-rendered model of *L. pedicellatus*, to examine the anatomical adaptations for wood-digestion. This was complemented by a transcriptomic analysis of the major digestive organs, which set out to determine whether *L. pedicellatus* is capable of independently producing cellulolytic enzymes. Investigation of the early life history strategy aimed to provide new insights into the larval-parent interactions during brooding and development – the most crucial phase in the life-cycle of teredinids. Finally, integrative taxonomy was used to improve the taxonomic resolution of the Teredinidae and these methods helped to confirm the identity of an invasive Caribbean species of teredinid, *Teredothyra dominicensis*, which has recently invaded and established breeding populations in the Mediterranean Sea.

This research provides the first detailed evidence that brooded *L. pedicellatus* larvae derive extra-embryonic nutrition from their parent. This extended parental care allows larvae to settle and metamorphose immediately after release. Development to sexual maturity is then rapid and individuals become gravid with brooded larvae within six weeks.

The examination of the digestive system of *L. pedicellatus* using MicroCT revealed a number of adaptations towards xylotrophy. The elongated stomach, specialised

digestive gland, large caecum with a well developed typhlosole and long intestine are all modifications enabling a more complete utilization of wood for nutrition. These results corresponded with the transcriptomic analysis which suggests the specialised digestive gland produces a range of cellulolytic enzymes.

A phylogenetic survey of the Teredinidae using integrative taxonomy provides a robust model for future identification of species, including cryptic species, within this taxonomically challenging group. This formed the basis for the identification of *T. dominicensis*, a species thought to be confined to the Caribbean and Gulf of Mexico, which has recently invaded the Mediterranean. This species was found to have established a substantial breeding population in the region, which produce large quantities of larvae which could settle and metamorphose. Thus, *T. dominicensis* may be considered an established species in the Mediterranean.

Providing a more accurate means of identification and increasing knowledge on the larval development and early life histories will help efforts to monitor the spread of teredinids and identify areas under threat from the destruction they cause. Furthermore, understanding the anatomical and molecular mechanisms which allow teredinids to deconstruct lignocellulose into monomeric sugars may provide new means of protection for wooden structures and provide novel enzymes for use in the biofuel industry.

Declaration

While registered as a candidate for a doctorate degree, I have not been registered for any other research award. The results and conclusion embodied in this thesis are the work of the named candidate and have not been submitted for any other academic post-graduate degree.

John Reuben Shipway

Acknowledgements

The success of any project departs largely on the assistance, advice and support of many others. First and foremost, I would like to thank my primary supervisor, Dr Simon Cragg, whose council, tutelage and support allowed me to develop as an independent scientist. I would also like to thank my second supervisor, Dr Alex Ford, for his valuable input into this project. I am indebted to Dr Simon Streeter, my unofficial supervisor, whose help and advice greatly enriched this work and Dr Stephen Short, who also provided valuable insights. Dr Johann Müller also deserves a special mention for his continued support. To the borer team, Luisa Borges, Ian Hendy and Sam Stanton, it has been a pleasure working with you. Assistance provided by the technical staff at the Institute of Marine Sciences, namely Lucy Crooks, Adam Bonner, Jenny Mackellar and Marc Martin, was very much appreciated. I am grateful for the funding provided by Mark Jones from the Mary Rose Trust and for the travel grants from both the Malacological Society of London and the Leonardo da Vinci Programme of the European Commission.

I would also like to thank Janet Voight, Andi Wanninger, Dan Distel, Michael Ahrens and Greg Beckham for the interesting discussions. To my colleagues and friends, Chantel, Holly, Laura, Madeline, Mike, Phil, Rob and Scott, thanks for keeping your humour when I lost mine. You made this an unforgettable experience. Finally, this thesis could not have been completed without the love and support of Ann, Angela, Patricia, Sacha and Elina, thank you.

I would like to dedicate this thesis to the late Ruth Turner (1914-2000), curator of Malacology at the Harvard School of Comparative Zoology. Her life-times work on the Teredinidae has provided the foundations for all subsequent research.

Table of Contents

List of Abbreviations

3-D	Three Dimensional
ANOVA	Analysis of Variance
BLAST	Basic local Alignment Search Tool
BP	Base Pair
°C	Degrees Celsius
CAZy	Carbohydrate-Active Enzyme Server
CBM	Carbohydrate Binding Module
CCA	Copper Chromium Arsenic
CD	Catalytic Domain
cDNA	Complementary Deoxyribonucleic Acid
CE	Carbohydrate Esterase
CM	Centimetre
CNAP	Centre for Novel Agricultural Products
COI-5P	Cytochrome c Subunit I Gene
Contig	Contiguous
dH_2O	Distilled Water
DNA	Deoxyribonucleic Acid
dNTP	Deoxyribonucleotide Triphosphate
EC	Enzyme Classification Number
EST	Expressed Sequence Tag
ETS	External Transcribed Spacer
Fig	Figure
FRS	Fellow of the Royal Society
G	Gravity
GH	Glycosyl Hydrolase
GHF	GH Family
HCL	Hydrochloric Acid
HMDS	Hexamethyldisilazane
HRS	Hours
IUBMB	The International Union of Biochemistry and Molecular Biology
IMS	The Institute of Marine Sciences
ISP	Ion Sphere Particle

kV	Kilovolts
K2P	kimura 2-Parameter
L	Litre
M	Molar
MA	Milliampere
MBP	Megabase Pair
MBSL	Meters Below Sea Level
Min	Minute
MicroCT	Micro Computer Tomography
Ml	Millilitres
mm	Millimeters
Mm	Millimolar
mRNA	Messenger Ribonucleic Acid
N/A	Not Applicable
nM	Nano Metres
NJ	Neighbour Joining
P	Probability
PCR	Polymerase Chain Reaction
pH	Percentage Hydrogen
Ph.D	Doctorate of Philosophy
Phyre	Protein Homology analogY Recognition Protein
PL	Polysaccharide Lyase
PolyA	Polyadenylation
PSU	Practical Salinity units
rRNA	Ribosomal Ribonucleic Acid
RNA	Ribonucleic Acid
S	Seconds
S (18S)	Svedberg Unit
SCUBA	Self-Contained Underwater Breathing Apparatus
SE	Standard Error
SEM	Scanning Electron Microscope
Sp	Species
SSU	Small Sub Unit
TBE	TRIS Borate Ethylenediaminetetraacetic Acid
U	Unit

UK	United Kingdom
UV	Ultraviolet
V	Volts
V/V	Volume per Volume
W/V	Weight per Volume

Chapter One: General Introduction

It has been estimated that one-tenth of all forestry products produced per annum are destroyed by wood-degrading organisms, equating to billions of dollars' worth of damage (Goodell *et al.,* 2003). Terrestrial wood degradation is achieved by beetles, termites and basidomycete fungi. Where regular tidal inundation excludes such organisms, wood degradation is continued by the ascomycete fungi, the wood-boring isopods Sphaeromatidae and Limnoriidae, the amphipod Cheluridae and the bivalve families Pholadidae and Teredinidae (Cragg, 2007). Cellulolytic bacteria are capable of degradation in both terrestrial and marine environments, yet at a rate far slower than the aforementioned mentioned organisms (Bjordal & Nilsson, 2008; Singh, 2012). Whilst the degradation of man-made wooden structures represents an enormous waste of resources, these organisms provide an essential nutrient recycling service: without them, our world would be buried under tonnes of cellulose debris (Goodell *et al*., 2003).

This chapter will introduce the marine wood-boring invertebrates before focusing on the ecology, biology and economic impacts of the Teredinidae – the most damaging of the wood degrading consortia and the focus of this thesis.

Wood-boring Crustacea

The majority of wood-boring crustaceans are found in the Isopoda – the same order in which the terrestrial woodlice are found. This group includes the Limnoriidae and Sphaeromatidae, both of which belong to the suborder Flabellifera.

The Limnoriidae

The Limnoriidae, which are commonly referred to as the Gribble (as shown in Fig. 1.1), are considered the most destructive of the crustacean borers (Turner, 1971). Biogeographic distribution is strongly influenced by salinity and temperature and limnoriids are found from sub-polar to tropical seas at depths varying from the inter-tidal zone to over 1000 m below sea level (Turner, 1971; Eaton & Hale, 1993; Cragg, 2007). Figure 1.2 shows the long, narrow tunnels excavated by *Limnoria*. These burrows run along the grain, immediately below the surface of the wood, and are

regularly spaced with perforations which serve as respiratory pits (Turner, 1971; Eaton & Hale, 1993). Adults will pair and mate within the burrow, producing 1-3 egg clutches during the reproductive season. Between 5 -30 eggs are fertilized and are retained in a specialised brood pouch formed by the oostegites, which develop from the peraeopods on the female thorax (Turner, 1971; Cragg, 2007). Development typically lasts between 2 – 4 weeks and juveniles are released into the parental burrow. Eventually the young will begin to excavate their own tunnel, which remains connected to the parental burrow. Migratory behaviour, potentially triggered from competition for food and space, allows dispersal from heavily infested timber (Johnson & Menzies, 1956). Whilst *Limnoria* are capable of swimming using their pleopods, this ability is limited and long-distance dispersal is reliant on transportation via drift wood, wooden sailing vessels or ballast water (Johnson & Menzies, 1956; Oliver, 1962; Quayle, 1992). *Limnoria* have been reported to ingested and digest the particles of wood through which they burrow (Cragg *et al.*, 1999). Whilst *Limnoria* only cause superficial damage, heavily infested timber will rapidly degrade (Fig. 1.3).

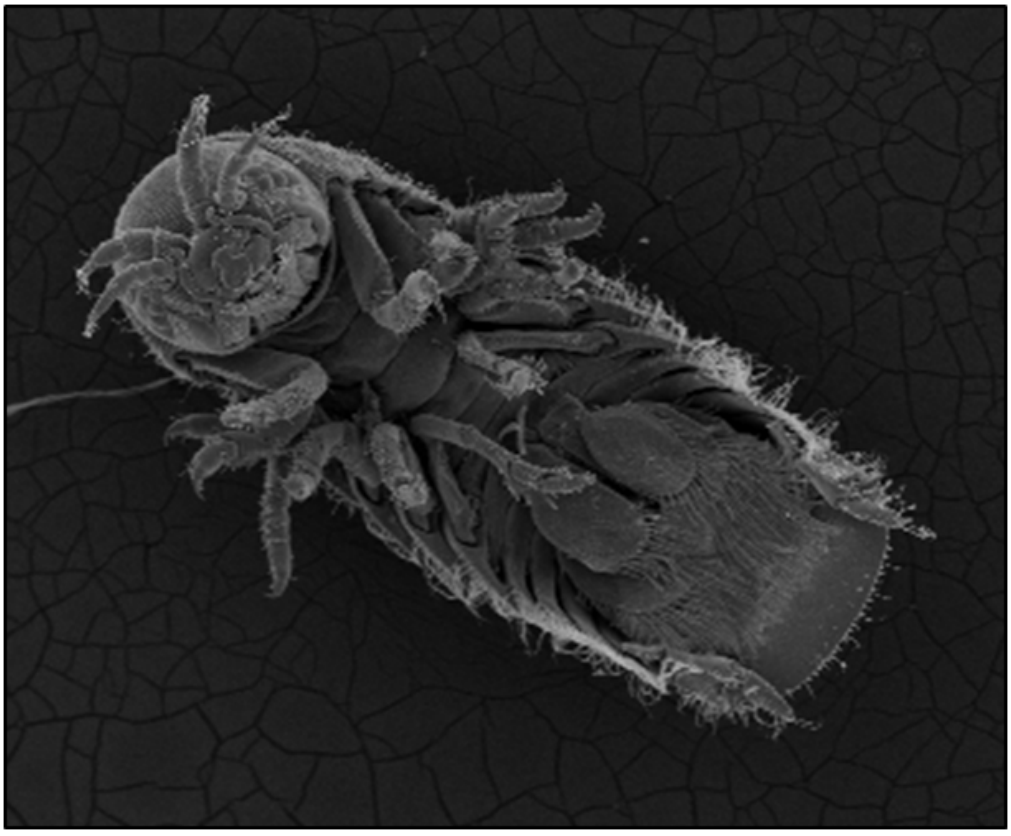

Figure 1.1 a scanning electron microscope image of the wood-boring crustacean *Limnoria tripunctata*. Image by author.

Most organisms capable on wood digestion rely heavily of cellulolytic enzymes provided by symbiotic bacteria, yet the digestive tract of *Limnoria* is effectively sterile with low levels of resident microbes (Boyle & Mitchell, 1978; Daniel *et al*., 1991). This microbial absence suggests limnoriids are capable of wood digestion without symbionts. Indeed, recent research has confirmed *Limnoria* are capable of endogenously producing cellulolytic enzymes (King *et al*., 2010; Kern *et al.,* 2013). Whilst *Limnoria* appear to lack the capability to capture plankton from the water column, the regular grooming of bacterial and fungal growth from the exoskeleton, provides an important supplement to the nitrogen deficient diet associated with wood digestion.

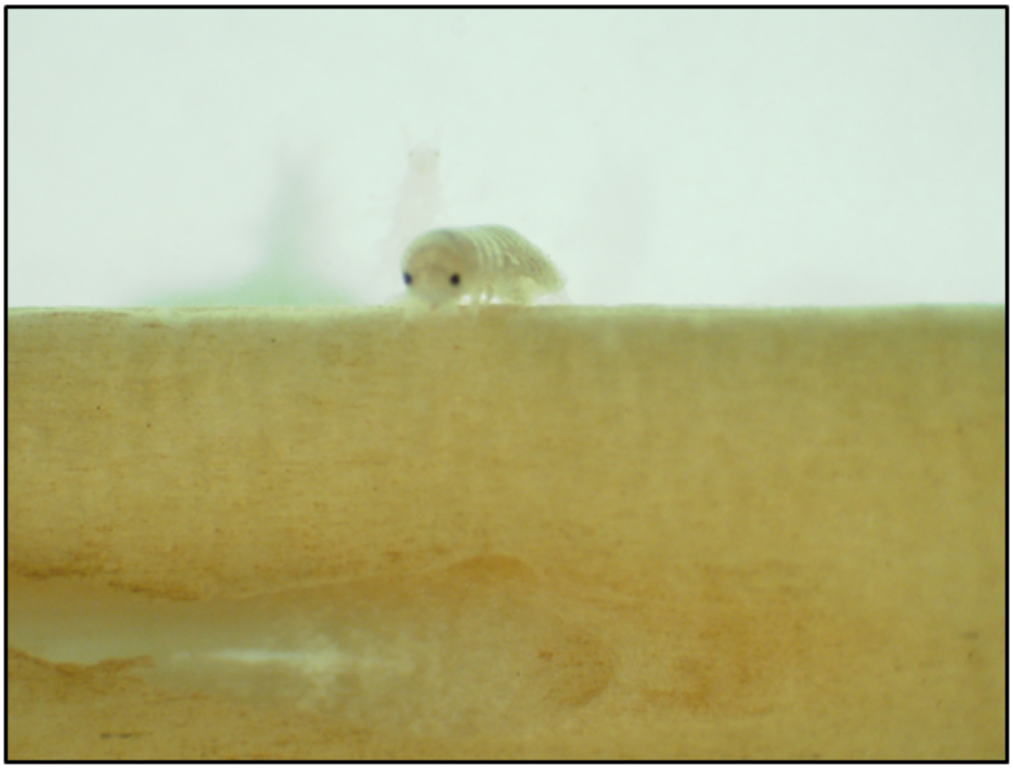

Figure 1.2 The gribble *Limnoria tripunctata*. Image by author.

Figure 1.3 A heavily degraded panel of wood exposed to *Limnoria tripunctata* for a period of one year. Image by author.

The Sphaeromatidae

Relatively little is known about the biology and ecology of the wood boring Sphaeromatidae (Si *et al*., 2000), whose name derives from the ability of the isopod to roll into a ball when disturbed. Commonly referred to as pill bugs, Sphaeromatids have a world-wide distribution and are thought to be more specious than limnoriids, although exact numbers are not known due to the lack of comprehensive surveys available in the literature (Turner, 1971). Only members of the genera Sphaeroma, Cymodoce and Exosphaeroma are known to infest wood, with many genera undertaking a free-living existence (Turner, 1971). Sphaeromatids tunnel by cutting away chunks of wood with their mandibles and typically tunnel across the grain, perpendicular to the surface of the wood (Kuhne, 1971; Eaton & Hale, 1993). The burrows are then enlarged when individuals turn on a longitudinal axis creating a semicircular burrow (Rotramel, 1975). Boring activity decreases drastically after completion of the burrow, which is approximately the size of the organism (Theil, 1999). Populations are typically composed of solitary individuals inhabiting a single burrow, yet during the breeding season, mating pairs are found in the same burrow. The males depart after copulation

and the female retains between 5 – 20 juveniles within the parental burrow (Theil, 1999). Juveniles are afforded extended parental care whilst their exoskeletons harden and they develop the physiological capability of burrowing (Theil, 1999). Once mature, young adults will then migrate to a new substratum (Cragg *et al*., 1999). Evidence suggests that the Sphaeromatids neither ingest nor digest wood particles, instead relying on planktotrophy for nutrition (Rotramel, 1975; Si *et al*., 2002). Whilst the mandibles allow the rasping of wood, the mouth parts are more suited to capturing plankton from the water column. Furthermore, gut morphology compliments the mouth parts and is similar to other terrestrial herbivorous isopods (Si *et al*., 2002). Indeed, *Sphaeroma* have been observed filter-feeding: the pleopods beat to generate a current and the plume setae on the peraeopods filter particulate matter (Cragg & Icely, 1994).

The Cheluridae

The family Cheluridae are the smallest group of marine wood-borering crustaceans, consisting only of the genus *Chelura* Philippi (1839). Only three species exist within this genus: *Chelura terebrans* Philippi, *Chelura insulae* Calman and *Chelura brevicauda* Shiino. Cheluridae are white yellow to pinkish red in colour and are distinguished from other amphipods by the fusion of the final three pleomers (Turner, 1971). Whilst common in temperate, sub-tropical and tropical waters, only *Chelura terebrans* has a worldwide distribution (Eaton & Hale, 1999). Although typically associated with the Limnoriidae – *Chelura* widens the existing tunnels of *Limnoria* and reprocesses faecal pellets – *Chelura* can live and reproduce independently from *Limnoria* (Cragg & Daniel, 1992). Copulation takes place within the tunnels and eggs are retained within the female brood pouch. Development may last between 17 – 42 days depending on temperature and once released sexual maturity is attained within 10 – 12 weeks at 20 ° C (Kühne & Becker, 1964). The migratory phase in *Chelura* is probably similar to that described for *Limnoria* (Becker, 1971).

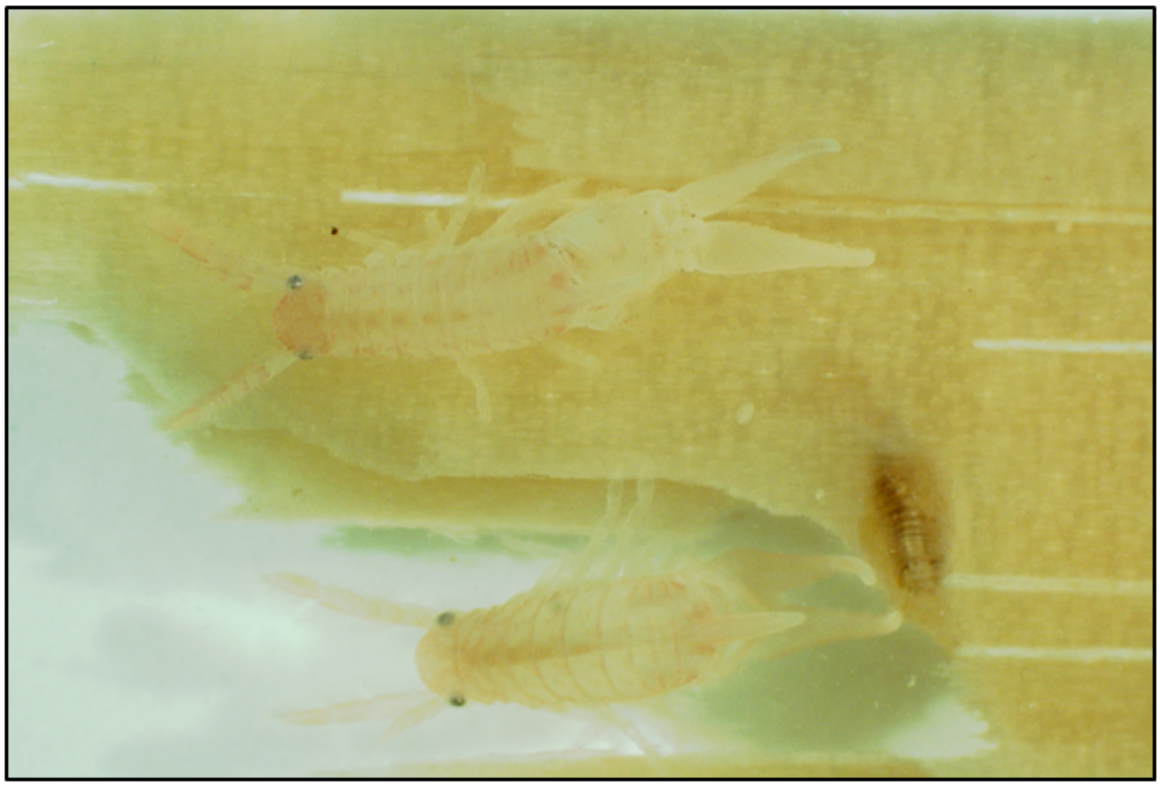

Figure 1.4 *Chelura terebrans* infesting a panel of wood. Image by author.

Wood-boring Bivalvia

The Pholadidae

The Pholadidae (commonly known as piddocks) are divided into three subfamilies, the Phodadinae, Martesiinae and Xylophaginae. However, recent phylogenetic studies suggest elevating the Xylophaginae to the rank of family, or transferring the subfamily from the Pholadidae to the Teredinidae (Distel *et al*., 2011). The Phodadinae are opportunistic borers and can tunnel into a variety of substrata other than wood, including sand, the calcareous shells of other molluscs, stone and certain plastics (Mann & Gallager, 1984). Only two genera from the Martesiinae, *Martesia* and *Lignopholas*, regularly bore into, but do not ingest wood (Mann & Gallager, 1984; Turner and Johnson, in Jones and Eltringham, 1971).

The Xylophaginae form the deep sea, high latitude ecological replacement of the Teredinidae and are obligate wood-borers (Voight, 2007). There are 57 known species of Xylophaginae, which are found primarily in the deep sea extending to depths of over

7000 m, from polar to tropical regions (Knudsen, 1961; Turner, 2002; Voight, 2007; Voight & Segonzac, 2012). The Xylophaginae contain three genera (*Xylophaga*, *Xylopholas* and *Xyloredo*) of which, *Xylophaga* is thought to be the most species rich (Knudsen, 1961; Turner, 2002; Voight, 2007). Relatively little information is available regarding the biology of the Xylophaginae due to the almost inaccessible nature of their deep sea habitat and the patchy distribution of wood on the sea floor (Voight, 2009). It was initially thought that a number of *Xylophaga* species externally brooded their larvae, with the young attaching to the adult shell (Knudsen, 1961; Santhakumaran, 1980; Harvey, 1996; Turner, 2002; Voight, 2007). Yet recent research proposed that all identified young are in fact dwarf males, which would fertilize eggs released by the host female (Haga & Kase, 2013). Indeed, a brooding strategy seems unlikely for organisms which exploit a temporally and spatially unpredictable resource due to the limitations in dispersal potential from a reduced period in the plankton (Voight, 2007). Xylophaginid larvae are known to spend extended periods developing in the plankton. *Xylophaga atlantica* larvae reach the pediveligers stage after 50 days at 12 °C and metamorphose after 57 days (Tyler *et al*., 2007). Xylophaginid larvae are able to delay metamorphosis for up to six months in the absence of wood. This extended period allows larvae to disperse away from the adult population to colonise other wood habitats (Tyler *et al*., 2007). These long-lived larvae are capable of rapid development post-metamorphosis and mature individuals have a high reproductive output – both of which constitute adaptations to their challenging environment and ephemeral niche. Like the Teredinidae, the Xylophaginae are obligate wood-borers which use their ridged shells to excavate into wood, the fragments are subsequently ingested and digested with the aid of cellulolytic and nitrogen-fixing symbionts residing in the host gill (Purchon, 1941; Distel & Roberts, 1997; Voight, 2007).

The Teredinidae

The Teredinidae are characterised by a greatly reduced, calcareous shell and elongated, vermiform (worm like) body. This distinctive anatomy and their tendency to infest wooden sailing vessels gave rise to their common name, the ‘shipworm’ (Turner, 1966). All teredinid larvae begin excavation following settlement upon wood. This burrowing continues as the larva metamorphose and grow. As shipworms derive nutrition from wood (Gallager *et al,*. 1981; Distel *et al*, 2011), they continually tunnel throughout their lives, extending the length of their burrow. Teredinids are the most destructive of the marine organisms and are estimated to cause billions of dollars of damage to submerged

wooden structures per annum (Distel *et al.,* 2011). This damage is often further compounded by costly restoration and the interruption of business (Fernandes & Costa, 1967 cited in Filho *et al*., 2008).

Figure 1.5 The teredinid *Teredo* navalis, extracted from a panel of wood. Image by author.

Shipworms have a world-wide distribution and their range is limited only by temperature, salinity (Borges *et al*,. 2012) and the availability of wood (Turner, 1966). There are currently 68 described species of shipworm (Turner, 1971; Calloway & Turner, 1983; McIntosh, 2012). As the adults spend their entire lives living within the wood into which they burrowed as larvae, a number of mechanisms are necessary for efficient dispersal. The ability to bore into wood means teredinids are pre-adapted to dispersal by rafting in drift-wood. Some rafting voyages may exceed regional scales (> 1000 km) and the extensive distribution of certain species is thought to be due to rafting dispersal (Theil & Gutow, 2005). Dispersal may also be achieved by the larvae, which can be carried over great distances whilst developing in the water column (Scheltema, 1971). In the past, wooden sailing vessels infested with shipworm also acted as a means of dispersal. Indeed, some tropical species have been documented to survive trans-oceanic circumnavigation through freezing waters and still survive to breed (Turner,

1966). Shipworms have also been documented to survive in shipping ballast water and may also disperse by this means (Culha, 2010; Gollasch, 2006).

Teredinids exhibited a range of developmental and reproductive modes. All genera bar *Lyrodus*, *Teredo* and *Zachsia* are broadcast spawners. Typically, broadcast spawners release their gametes into the water column where fertilization takes place. Larvae will then spend an extended period of time developing until they can settle on wood. Short-term brooders fertilize internally and the larvae develop to the veliger stage before they are released by the adult to continue their development in the water column. Long-term brooders also fertilize internally, however the larvae develop to the pediveliger stage and are typically able to settle upon release (Turner, 1966; Nair & Saraswathy, 1971; MacIntosh *et al*., 2012). Direct fertilization or intromission (Fig. 1.5), has been observed for a number of broadcast spawning species (Clapp, 1951; Turner, 1966; Hiroki *et al*., 1994). This 'pseudocopulation' involves the excurrent siphon of a male penetrating the incurrent siphon of a neighbouring female and directly transferring sperm into the infrabranchial cavity. The excurrent siphons of up to six males have been observed penetrating a single female incurrent siphon in mangrove specialist *Nausitora fusticula* (Hiroki *et al.,* 1994). Whilst this behaviour increases reproductive efficiency it is restricted to individuals living within a close proximity to one another (Hiroki *et al*., 1994).

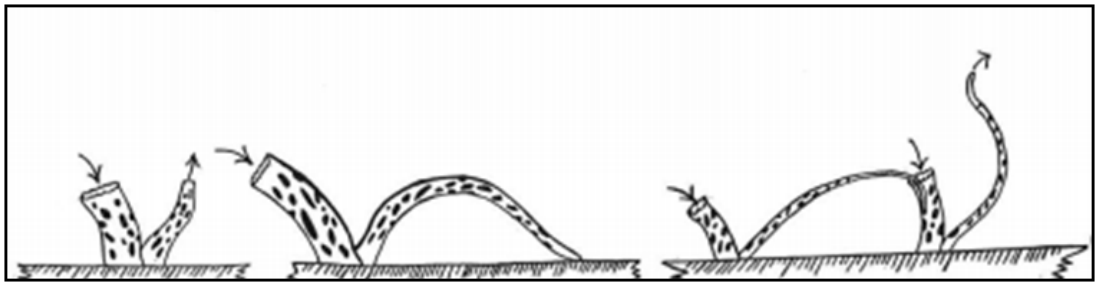

Figure 1.6 Pictogram demonstrating the mating activity of the shipworm *Bankia gouldi*. The excurrent siphon of a male teredinid enters the incurrent siphon of a female in order to transfer spermatozoa. Taken from Clapp (1951).

It is believe the eggs are fertilized in the suprabranchial cavity prior to release into the water column (Turner, 1966). Teredinids are also protandric hermaphrodites capable of

self fertilization (Eckelbarger & Reish, 1972). *Zachsia zenewitschi*, a rare seagrass rhizome-borer, demonstrates the most complex and least understood reproductive strategy among the Teredinidae. Dwarf males, 100 times smaller than the female, attach to a specialised pouch in the female. The males then provide the female with sperm, which is taken into the epibranchial cavity and ensures a high fertilization success. Larvae are brooded to the veliger stage and are then released en masse to continue development in the water column (Turner & Yakovlev, 1982; Yakovlev *et al*., 1998).

The broadcast spawning and brooding teredinids display life history characteristics of r-selection and k-selection respectively. It has been predicted that the broadcast spawning species are more effective at locating new sources of wood, but the brooding species should become strong competitors once established (Cragg, 2007). Indeed, field work has demonstrated the short-term brooders, a strategy effectively balancing fecundity, larval retention and dispersive ability, dominate recruitment (MacIntosh *et al*., 2012). Whilst competition for wood can be significant, 11 different species from several genera have been reported to inhabit a single wooden panel (Cragg, 2007), varying reproductive strategies and modes of larval dispersal allow species to co-exist in sympatry despite competition for a highly limited resource (Hoagland and Turner, 1981). The importance of the xylotrophic contribution to teredinid nutrition has been debated (Turner, 1966; Waterbury *et al*., 1983). Analysis of the carbon isotope ratios between five species of teredinid and their wooden burrows found that teredinids selectively utilize cellulose and that wood was the main carbon source for teredinids (Nishimoto *et al*., 2009). Paalvast & van der Velde (2013) also carried out carbon isotope ratio analysis and suggest *Teredo navalis* derived its carbon predominantly from filter feeding, with $\delta^{13}C$ values an average of 3.3 % higher in the teredinid than that of the wood substrate. However, the authors failed to take into account that $\delta^{13}C$ values of cellulose are 3 % higher than lignin, and 2 % higher than whole wood (Loader *et al*., 2003). Thus $\delta^{13}C$ values are expected to be 3 % higher in the teredinid than that of the wood itself (Nishimoto *et al*., 2009). Investigations have shown that *L. pedicellatus* incorporates ^{14}C-labelled phytoplankton into soft tissues (Pechenik *et al.*, 1979), yet growth rate does not vary between specimens under both plankton deprived and plankton supplied diets (Gallager *et al*., 1981). Growth is also rapid and continuous during the winter, in the absence of phytoplankton (Morton, 1970). Furthermore, maintenance of glycogen reserves in *L. pedicellatus* is entirely dependent on xylotrophy, as individuals removed from their burrow expire shortly after the caeca

empties of wood, despite the provision of concentrated phytoplankton (Lane *et* al., 1952; Turner & Johnson in Jones & Eltringham, 1971). Although wood accounts for the primary carbohydrate source of teredinids it only contains 0.25 % nitrogen, which is believed to be insufficient for shipworm nutrition (Greenfield, 1953; Lasker & Lane, 1953; Turner, 1966; Gallager *et al*., 1981; Nishimoto *et al*,. 2009). This nitrogen deficit was thought to be supplemented by planktotrophy; however, teredinid nitrogen levels are lower than those of other filter-feeding bivalves (Nishimoto *et al.*, 2009). Instead, teredinids derive their nitrogen from the nitrogen-fixing symbionts which are harboured in the host gill tissue (Waterbury *et al*., 1983; Distel *et al*., 1991; Nishimoto *et al.*, 2009). Nitrogen excretion in *T. navalis* is extremely low and it is likely that teredinids are extremely nitrogen conservative (Hammen, 1968; Gallager *et al*., 1981). Whilst planktotrophy does not account for the main sources of carbon or nitrogen in teredinid nutrition, it is still a valuable supplementary source of nitrogen and vitamins (Morton, 1970).

Ecological role of wood-boring bivalves

Teredinid and xylophaginid bivalves play a fundamental role in the nutrient-cycling in marine environments, by processing the organic material trapped in wood matrices through specialised anatomical adaptation and association with symbiotic bacteria (Turner, 1966).

Whilst most commonly located off the mouths of rivers, around wooded coastline and mangrove forest and along shipping routes, wood can be found widely distributed across the sea floor and has been observed in all oceans at all depths (Beinhold, 2013). Indeed, wood may reach abyssal depths in sufficient quantity to support an entire sub-family of the obligate wood borer the Xylophaginae (Turner, 2002). Xylophaginids are considered ‘keystone’ species in wood fall habitats, as they transform the energy stored in wood into nutrients which may then become available to other organisms. Borer activity provides a range of food sources for these organisms including, faecal pellets for detritivores, larvae and adults for predators, carcasses for scavengers, and free swimming larvae and debris for suspension-feeders (Turner, 2002). Furthermore, the littering of wood chips and faecal matter around the wood fall, leads to enhanced respiration rates and the development of anoxic zones in the surrounding sediment. These anoxic zones enable sulphate production by sulphate reducing bacteria, which in turn attract thiothropic chemosynthetic symbioses, such as chemosynthetic mussels from the genus *Idas* (Beinhold *et al*., 2013). Wood falls attract a variety of deep-sea

fauna and become hotspots for diversity (Turner, 2002). The fauna associated with wood fall communities include a number of organisms reported from other deep-sea habitats and thus constitute stepping stones for hydrothermal vent and cold seep communities (Beinhold *et al*., 2013).

Teredinids are the dominant borers of the intertidal wood niche (Cragg, 2007). This is because they can grow to large sizes, some individuals have been recorded to grow over a metre in length (Turner, 1966), tolerate a considerable variation in seawater temperature and salinity (Eckelbarger & Reish, 1972) and have the capacity to produce large numbers of offspring (Sigerfoos, 1908; Turner, 1966). In mangrove ecosystems, teredinids can cause > 90 % weight loss from the trunks of the mangrove *Rhizophora* (Fig. 1.7) and it has been estimated that 50 % of the mangrove wood volume passes through their guts before fragmentation, tidal export or burial takes place (Robertson & Daniel 1989; Cragg, 2007). Furthermore, the large number of teredinids associated with mangrove wood, the production of nitrogen-rich faeces and the turnover of teredinid biomass contributes significantly to the mangrove ecosystem nitrogen budget (Robertson & Daniel 1989).

The labyrinth of tunnels created by teredinids may also provide refuge for cryptofauna. In the Langira mangrove of Indonesia, almost 40 % of the population of the dartfish *Parioglossus interruptus* seek refuge in teredinid tunnels at low-tide (Hendy *et al*., 2013). Not only does this allow the dart fish to avoid being carried away into the open sea by ebbing water or stranding on the mudflat at low tide, it protects individuals from the threat of predation (Hendy *et al*., 2013). Rapid changes in temperature and salinity are also common in mangrove ecosystems and teredinid tunnels shelters the dartfish from desiccation (Hendy *et al*., 2013). Thus, besides their fundamental role in nutrient cycling, wood-boring bivalves may also be considered ecosystem engineers due to their ability to enhance biodiversity by niche creation.

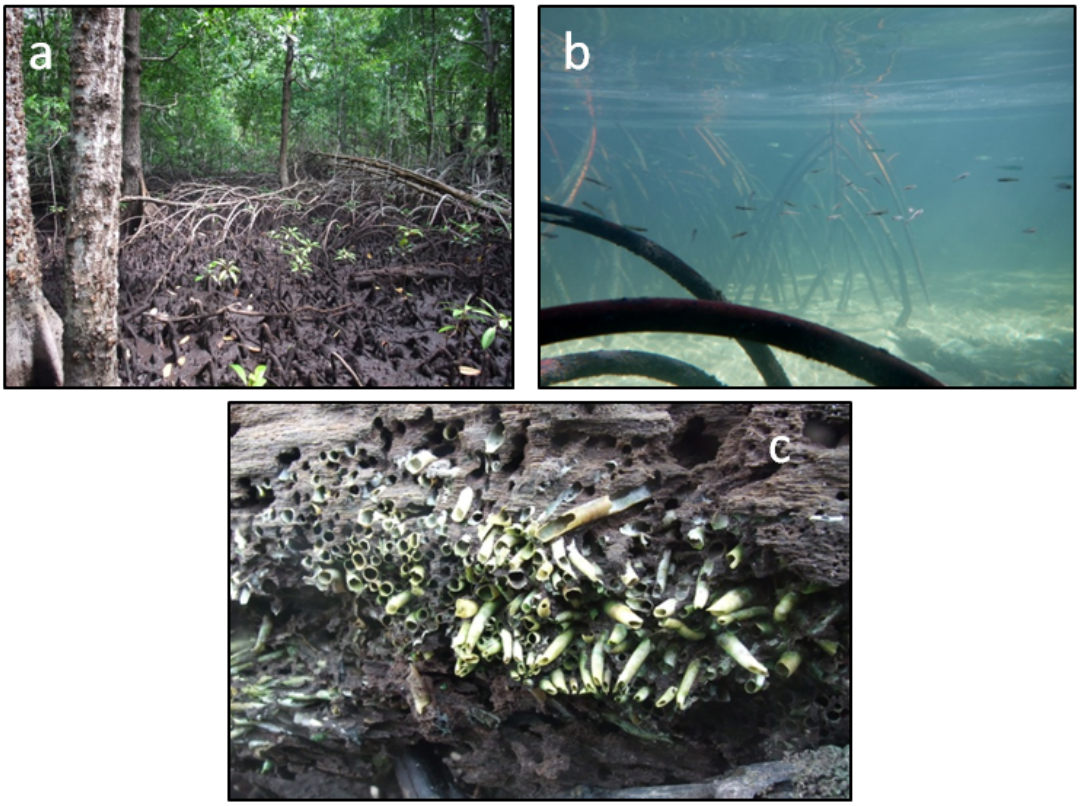

Figure 1.7 Teredinids play a fundamental role in nutrient cycling in mangrove ecosystems. The mangroves of south east Sulawesi, Indonesia at low (a) and high tide (b). *Rhizophora* become infested with teredinids (c). Images courtesy of Laura Michie.

Economic impact of wood-boring bivalves

Despite their ecological importance, the Teredinidae are considered pests and have been labelled 'the termites of the sea' (Turner, 1966). Wood has played a vital role in construction throughout human history, due to its wide availability, good strength-to-weight ratio, lower energy cost compared with alternative materials and its pliability (Cragg *et al*., 1999). Modern construction still uses timber for a variety of marine structures including wharf components such as fenders, piling, decking and curbing, traditional wooden sailing vessels and fisheries and aquaculture equipment. Yet any timber submerged below the water line is at risk from destruction by wood-degrading marine organisms, the most destructive of which are the Teredinidae, which are the dominant borers in coastal and shallow waters (Turner, 1966). Teredinid larvae enter the wood as pediveligers, typically measuring around 300 μm in diameter. The initial larval entry point only slightly enlarges during the growth of the teredinid and as result, detecting infestation is difficult. The teredinids inhalant and exhalent siphons are the

only externally visible sign of infestation (Fig. 1.8). Often these are difficult to spot as the borer may quickly retract the siphons into the burrow upon disturbance (Nair & Saraswathy, 1971). Detection is also compounded by the presence of fouling organisms, which can obscure teredinid damage. Often, infestation is only noticeable upon structural failure of the timber (Bjordal & Gregory, 2011). These organisms can rapidly degrade wood and damage is higher in tropical regions (Southwell and Bultman, 1971).

Figure 1.8 The siphons are often the only external sign of teredinid infestation. Showing the siphons of *Teredo navalis***.** Image by author.

For example, planks of dense timber exposed along the north coast of Papua New Guinea lose two thirds of their weight within four months of exposure (Cragg, 2007) and panels exposed in the Panama Canal, including some hard, tropical wood species, were completely destroyed in only 14 months. Globally, teredinids are estimated to cause billions of Dollars of damage to submerged wooden structures per annum (Distel *et al*., 2011) and the introduction of shipworms into new areas is often followed by rapid and extensive destruction (Carlton & Cohen, 1995). This problem is often further compounded by costly restoration and interruption to business (Fernandes & Costa, 1967 in Filho *et al*., 2008).

Figure 1. 9 These heavily degraded wooden pilings in Venice Lagoon demonstrate the impacts of marine-borers. Image by author.

Teredinids also pose a major threat to sites of marine archaeological heritage. Centuries of human maritime activity have resulted in countless vessels becoming wrecked at sea, the vast majority of which became infested by wood-borers and were eventually destroyed. King Henry VIII's flagship, the Mary Rose, one of the world's most famous and well documented wrecks, sank on the 19th of July 1545 off the coast of Portsmouth and was raised almost five centuries later on the 11th of October 1982 (Fig. 1.10). Whilst two thirds of the vessel was destroyed by borers, the remaining portions became buried under sediment, thus preventing further damage by wood-boring organisms (UNESCO Sources, 2007). Part of the remaining timber still shown signs of infestation and damage from teredinids (Fig. 1.11). Over 19,000 artefacts, including the Mary Rose itself, have been preserved. These have contributed (and indeed, continue to do so) vast amounts of knowledge from ship design through to life during the Tudor period (UNESCO Sources, 2007). This famous warship has captured the public's imagination; an estimated 60 million television viewers watched the raising of the vessel and the Mary Rose museum in the Portsmouth's Historic Dockyard is a popular tourist attraction (UNESCO Sources, 2007). This demonstrates the significant cultural and

historical impacts of underwater archaeological heritage and the importance of protecting sites against borer damage.

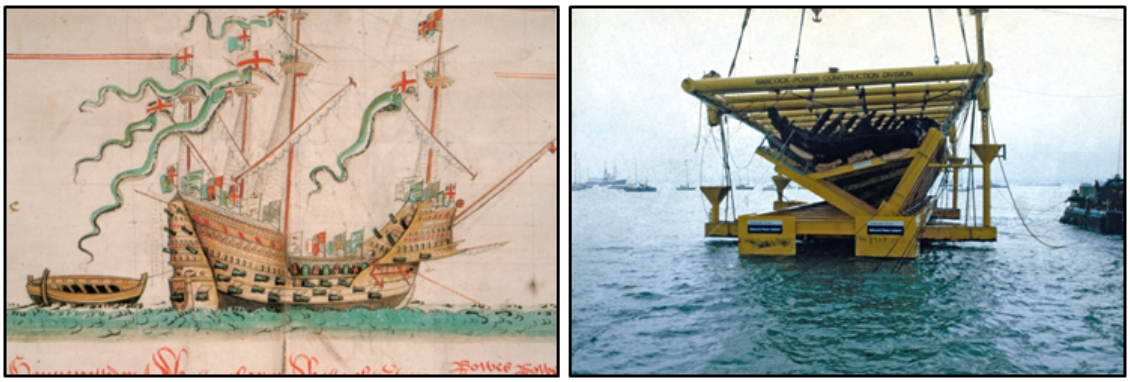

Figure 1.10 An illustration of the Mary Rose taken from the Anthony Roll and the raising of the wreck in 1982. Taken from Marsden *et al*., (2009).

Figure 1.11 The timber of the Mary Rose shows signs of infestation from teredinid wood-borers. Image by author.

The Baltic Sea is one of the few seas in the world which still contains a well preserved collection of submerged archaeological sites, with an estimated 100,000 shipwrecks, 6,000 of which are deemed historically and archaeologically significant (Bjordal & Gregory, 2011). A number of these wrecks have even been discovered standing upright, with masts and rigging intact as if 'set in amber' (Gregory, 2010). Such preservation is only possible because of the low salinities of the Baltic Sea, which largely prohibits teredinid distribution in the region (Gregory, 2010; Bjordal & Gregory, 2011). However, rising sea temperatures and salinities are known to increase both the activity and distribution range of teredinids (Borges *et al*., 2010; Paalvast and van Der Velde, 2011). This constitutes a significant threat to the underwater archaeological heritage in the Baltic and a number of projects are underway to protect the vast number of important sites in the region (Gregory, 2010; Bjordal & Gregory, 2011).

Historical importance of the Teredinidae

Teredinids have had a significant impact on human maritime activity and problems associated with their activity are likely as old as the history of the navigation of the sea (Kofoid and Miller 1927). These wood borers were certainly familiar to the Greeks and Romans, as indicated by the reference to them in the works of Pliny, Ovid, Cicero, Aristotle and were even noted by Homer (Nair & Saraswathy, 1971). Sellius (1733) was the first person to identify teredinids as molluscs and Linnaeus instituted the genus *Teredo,* naming the first species *Teredo navalis.* The ancient Phoenicians, Carthaginians and Romans were known to take measures to protect their vessels from teredinids, such as painting the hulls with tar or using a thin lead-based covering, yet these methods were of limited success (Woods Hole Oceanographic Institution, 1952). Columbus' fourth voyage to the Americas in 1502 came to a disastrous end when all his ships sank due to severe infestation from teredinids, marooning him and his crew on Jamaica for a year. In a letter to King Ferdinand and Queen Isabella of Spain, Columbus describes his ships as "rotten, worm-eaten, more riddled with holes than a honeycombed [SIC]" and "with three pumps, pots and kettles, and with all hands working, they could not keep down the water which came into the ship, and there was no other remedy for the havoc which the worm had wrought. My ship is sinking beneath me" (Columbus, letter from the fourth voyage). Even the safety of a nation has been threatened by the ability of these organisms to rapidly degrade wood. In the 1730s a shipworm epidemic destroyed miles of flood defence structures, including dykes, embankments and sluice gates, along the coast of Holland. These coastal defences were rendered useless and subsequent poor

weather led to severe flooding of large parts of the low-lying lands (Bjordal and Gregory, 2011). This is perhaps the origin of the famous fable where the little Dutch child plugs a hole with his finger. Similarly, the invasion of San Francisco Bay by *Teredo navalis* in 1912 caused areas along the coast to crumble and collapse into the sea (Fig. 1.12), causing over $25 million worth of damage (Kofoid and Miller, 1927), equating to almost $3B dollars today.

Figure 11.2 The invasion of San Francisco Bay by the Teredinid *Teredo navalis* caused extensive damage to submerged wood structures along the coast. Taken from kofoid & Miller, 1927.

Research Aims

This research aimed to address a number of fundamental questions regarding the ability of the teredinids to exploit wood as a food source. Whilst teredinids have been shown to incorporate symbiont fixed nitrogen into their body tissue, it is not known whether they utilize symbiont produced cellulolytic enzymes in order to digest wood. Furthermore, the mechanism transporting these enzymes from the symbionts in the gill to digestive system of the host is yet to be elucidated (Betcher *et al*., 2012; Elshahawi *et al*., 2013). It has previously been suggested that the teredinid *Teredo furcifera* has a specialised duct, called the duct of Deshayes, connecting the gills and digestive system (Nair & Saraswathy, 1971). Yet this was evidenced in the form of a single drawing and has yet to be confirmed despite the large body of research on the Teredinidae (Moraes & Lopes, 2003).

Chapter Two, 'The functional anatomy of *Lyrodus pedicellatus*', assess the anatomical and physiological adaptations which allow *L. pedicellatus* to complete its life cycle on a diet composed solely from wood, as shown by Gallager *et al*. (1981). Furthermore, x-ray scanning micro-computer tomography evidence is used to determine whether a duct like structure, joining the gill to the digestive system, is present in *L. pedicellatus*.

Chapter Three, 'Transcriptomic analysis of the digestive system of *Lyrodus pedicellatus*', sets out to determine the endogenous capability of the teredinid to produce cellulolytic enzymes and the role the major digestive organs play in lignocellulose deconstruction.

As teredinids spend their entire adult lives living within wood, dispersal is achieved primarily by larval dispersal. This free-swimming larval-stage is the most vulnerable stage in the life cycle of teredinids. Thus, preventing settlement and metamorphosis of larvae represents the most logical means of protecting timber from infestation (Turner & Johnson in Jones & Eltringham, 1971). Yet relatively few studies have examined the complete life-cycle of teredinids, particularly the long-term brooding species such as *Lyrodus pedicellatus*. Furthermore, the interactions between the parent and larvae during the brooding period are poorly understood.

Chapter Four, 'Aspects of the life cycle of *Lyrodus pedicellatus*', follows the teredinid from its early life history as a pediveliger, through to settlement, metamorphosis, and

maturity as an adult. This research uses *L. pedicellatus* as a model teredinid species to assess these interactions and gain new insights into the early life history strategy of larvae and their subsequent growth and development to maturity. Attention is also given to larval development during brooding as a number of key questions still exist. These include: whether the adults provide extra embryonic nutrition to developing larvae; how many larvae are brooded at any one moment; are these larvae brooded synchronously or are different developmental stages present?

Teredinid species identification is challenging and much of the early literature is fragmented, published in obscure journals, or of little scientific use (Kofoid & Miller, 1927; Turner, 1966; Borges *et al*., 2012). This led to a high level of synonymy and a taxonomy which existed in a state of chaos. The survey by Turner (1966) bought more order to the classification of the Teredinidae, yet a number of issues with identification and the evolutionarily relationships among the group still persist. Recently, molecular markers have proven a useful tool for phylogenetic analysis (Blaxter *et al*., 1998; Herbert *et al*., 2003). Yet only the research by Santos *et al*. (2005), Distel *et al*. (2011) and Borges *et al*. (2012) has attempted molecular-based phylogenetic analysis of the Teredinidae and of these, only the work by Distel *et al*. (2011) infers a comprehensive taxonomic relationship.

Chapter Five, 'Molecular phylogeny of the Teredinidae' builds on the previous work by Distel *et al*. (2011) to produce the most complete phylogenetic tree of the Teredinidae. Furthermore, this work adopts the integrative taxonomic approach outlined by Borges *et al*. (2012), which greatly aids the identification of this taxonomically challenging group.

Teredinids cause billions of dollars worth of destruction to submerged wooden structures per annum (Distel *et al*., 2011) and the invasion of non-indigenous species is a serious cause for concern. Yet research on teredinid invasions and the early establishment of communities is lacking.

Chapter Six entitled 'The broadcast spawning Caribbean shipworm, *Teredothyra dominicensis* (Bivalvia, Teredinidae), has invaded and become established in the eastern Mediterranean Sea', is the first documented report of a non-indigenous teredinid invasion. Species identification was confirmed using morphological characteristics and molecular markers, which will assist in the future identification and tracking of this invasive species. The chapter provides evidence for species establishment and the

potential invasion vectors are discussed. Fieldwork combined with anatomical and behavioural observations confirm this poorly studied species is a broadcast spawner.

Chapter Two: Functional anatomy of *Lyrodus pedicellatus*

Introduction

Teredinids are some of the most highly adapted bivalves and display more interspecific variation in anatomical form than any other group in the Mollusca (Turner, 1966). This diversity arises primarily from their xylotrepetic (wood-boring, as defined by Distel *et al*. 2011) existence and their capability to derive food from two independent sources: the wood through which they burrow and plankton captured from the water column (Morton, 1970). A brief summary of the typical teredinid body plan (Fig. 2.1), the specialist terminology used in its description and the unique anatomical features of the Teredinidae are outlined below. Particular emphasis is given to the structures relating to the boring and digestion of wood.

General organisation & anatomical terminology

The shell – which is greatly reduced and covers only a small portion of the anterior part of the body (Fig. 1) – is formed from two valves (Fig. 2a) which gape widely both anteriorly and posteriorly allowing projection of the foot and extension of the body respectively (Nair & Saraswathy 1971). The surfaces of the valves are subdivided into three distinct regions: the anterior slope, the median slope and the posterior slope (Fig. 2a). The latter two regions are commonly referred to as the disc and auricle – specialised valve nomenclature of the Teredinidae. The disc is composed of three regions, the anterior, middle and posterior median. Growth lines extend across the outer surface of the auricle and posterior median, appearing as denticles on the middle median, anterior median and anterior slope. The denticulated ridges of the middle and anterior medians form almost perpendicular to one another and are coarser than the finely serrated denticles of the anterior slope (Kofoid & Miller, 1927).

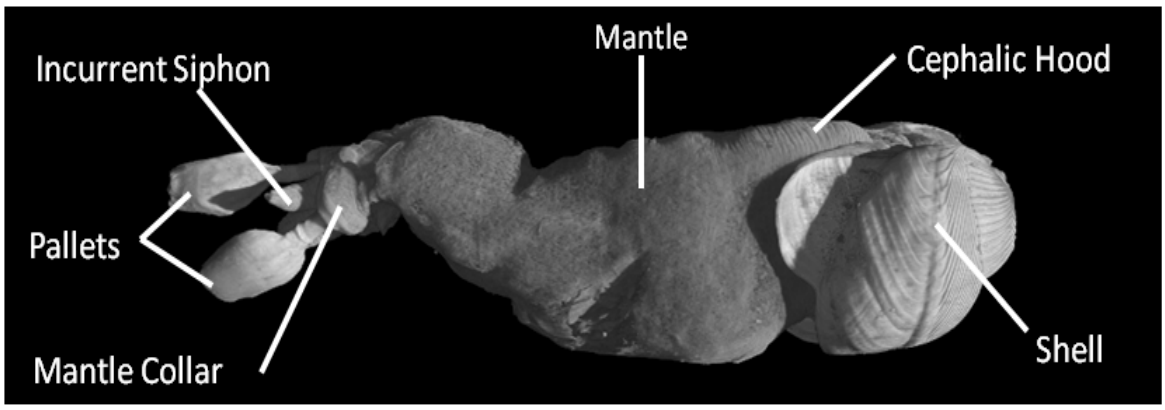

Figure 2.1 A 3-D rendered image of an adult *Lyrodus pedicellatus*. Showing the relative arrangement of the shell, pallets and siphons.

The three distinct regions of the valve are also apparent on its inner surface (Fig. 2.2b). The umbonal and ventral regions are marked by pronounced spherical thickenings which form the umbonal and ventral knob respectively (Nair & Saraswathy, 1971). A small ventral adductor muscle attaches to knobs on opposing valves forming a movable articulation and this is protected by an extension of the mantle tissue called the cephalic hood. The large posterior adductor muscle is antagonistic to the ventral adductor and attaches over almost the entire inner surface of the auricle (Kofoid & Miller, 1927). Stylloid apophyses extend from beneath the umbos to almost half the length of the shell and provide muscular attachment for the foot (Turner, 1966).

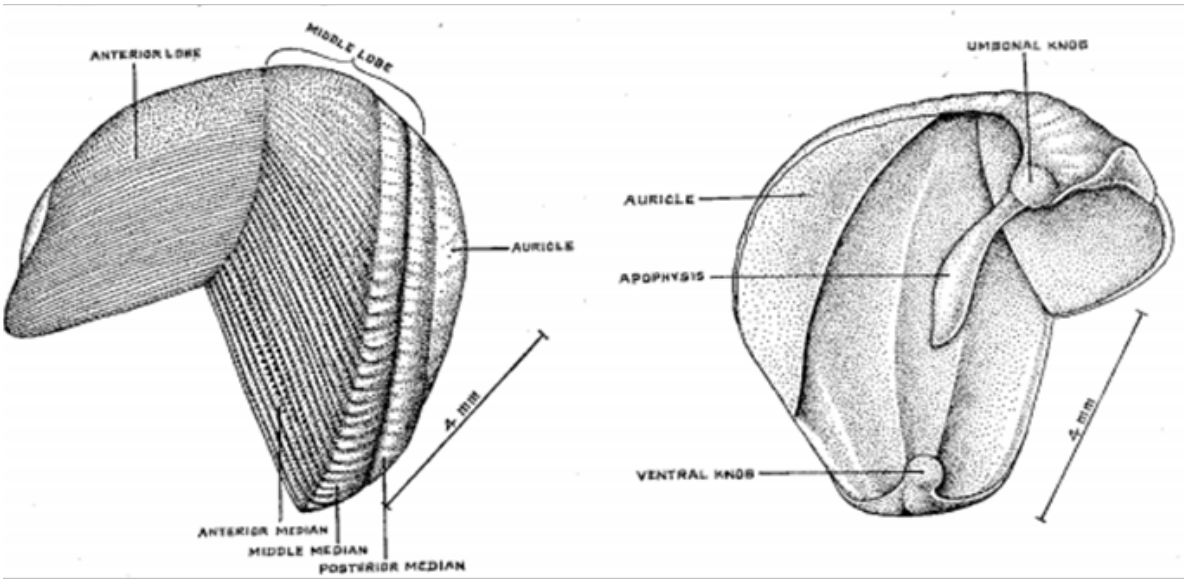

Figure 2.2 A schematic from the right shell features of the shipworm *Nausitora hedleyi* a). The external view of the right valve. b). The internal view of the right valve. Taken from Nair & Saraswathy (1971).

The general organisation of recently metamorphosed individuals is essentially that of a typical bivalve (Sigerfoos, 1908). It is only during development and subsequent growth that the visceral mass migrates and the body elongates (Fig. 2.3). In contrast to all other bivalves, the organ systems of adult teredinids lie predominantly outside of the shell, posterior to the adductor muscle (Sigerfoos, 1908; Distel *et al*., 2011).

The pericardial cavity, which contains the heart and associated vessels, has become considerably elongated and has undergone rotation around the posterior adductor and is thus situated above the intestine (Nair & Saraswathy, 1971). Similarly, the kidney also lies on the upper side of the pericardial cavity. The mouth and anus retain the typical bivalve position: the former lies between the anterior adductor and the foot, whilst the latter is situated dorsally to the posterior adductor muscle (Turner, 1966). Despite the extensive elongation, the digestive system orientation follows the typical bivalve body plan.

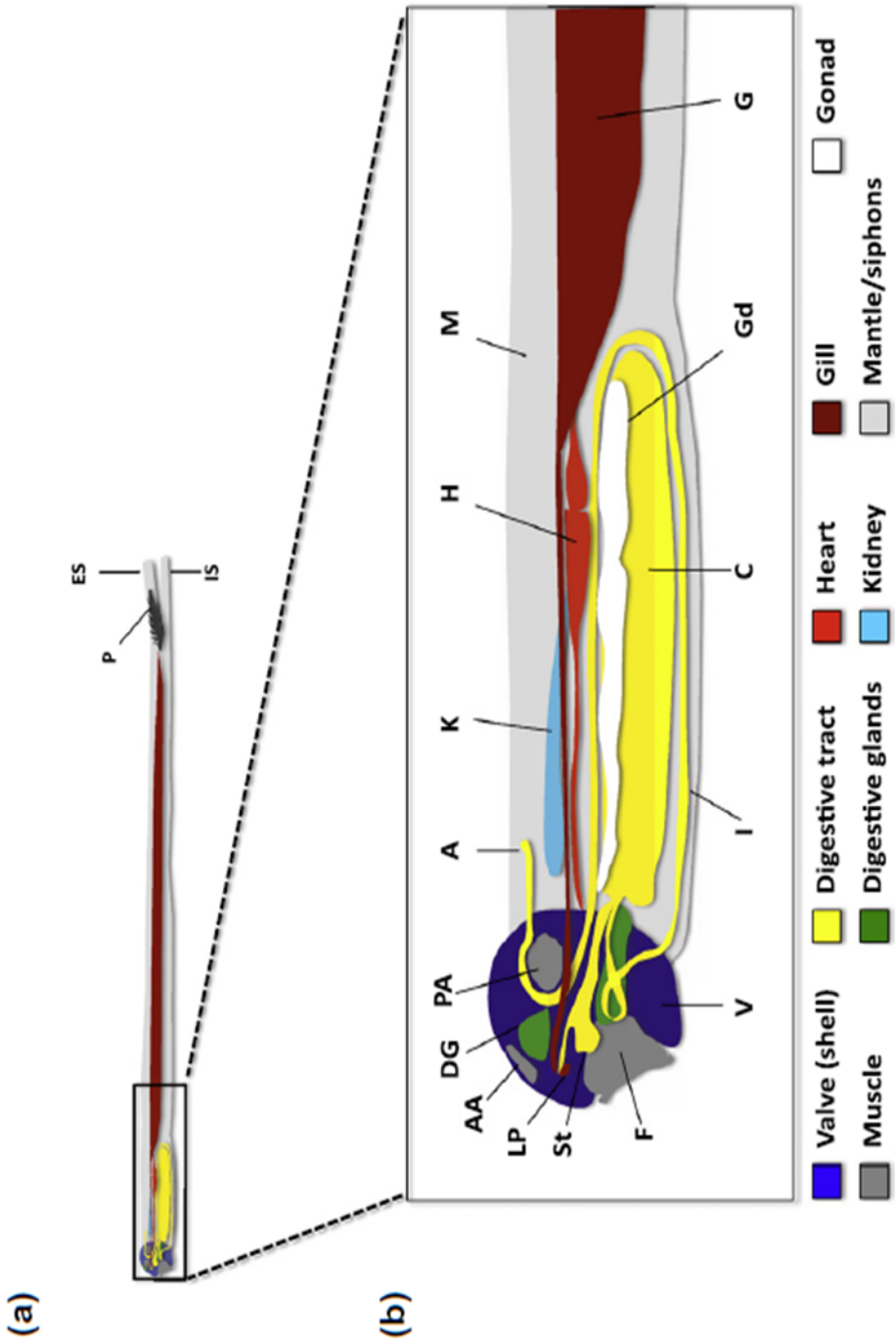

Fig. 2.3. The general anatomical arrangement and nomenclature of the teredinid *Bankia setacea*. Taken from Distel *et al*. (2011).

The nomenclature used in the description of the ctenidia (gills) is adopted from Ridewood (1903) and Atkins (1937). As with many other bivalves, the gills function in both respiration and suspension-feeding, and for the brooding species from the genus *Lyrodus* and *Teredo*, also serve to house developing larvae (Turner, 1971).

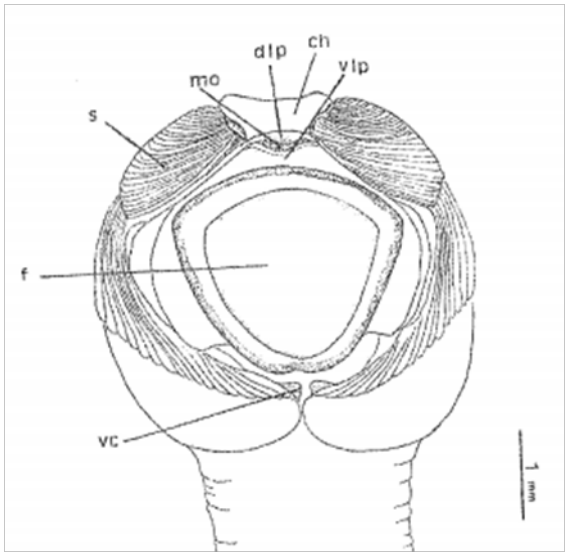

Figure 2.4 Frontal view of the anterior extremity of *Bankia fibriatula*. ch, cephalic hood; dlp. Dorsal labial palp; f, foot sole; mo, mouth; s; shell; vc, ventral condoyle; vlp, ventral labial palp. Taken from Martins-Silva & Narchi (2008).

The gills extend anteriorly from the base of the siphons to the visceral mass (Fig. 2.5), where they are reduced to food grooves, which then connect with the anterior gill and the labial palps (Lopes & Narchi, 1998; Martins-Sliva & Narchi, 2008). The length of the gill varies between species; those of the genus *Teredora* extend from the base of the siphons all the way to the mouth, whereas the gills of *Neoteredo reynei* and *Nausitora dunlopei* are short and truncate (Turner, 1966). The V shaped demibranchs unite to form a marginal groove, dividing the mantle into a ventral and dorsal chamber, known as the infrabranchial and suprabranchial cavity. Water is drawn in through the incurrent siphon, into the infrabranchial cavity and is passed over the gills. Depending on the degree of contraction of the specimen examined, the ctenidium may fold upon itself, simulating a plait (Lopes & Narchi, 1998). At each side of the internal wall of the afferent branchial vein lies the gland of Deshayes, which houses the symbionts in specialised bacteriocytes (Popham & Dickson, 1973, Distel *et al*, 2002; Lechene *et al*., 2007).

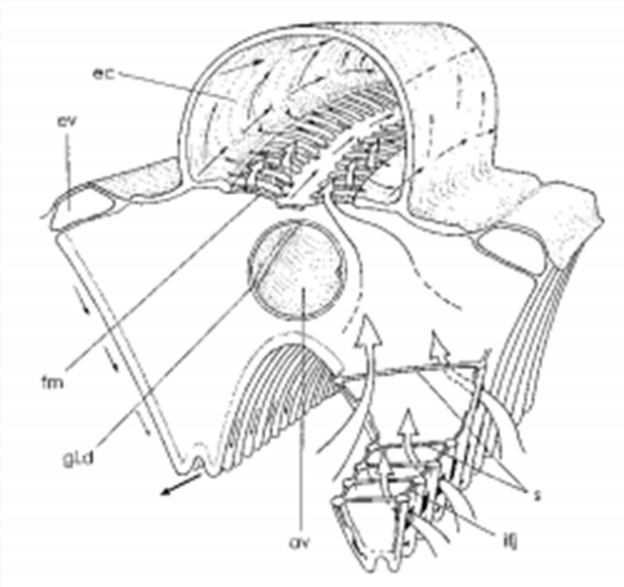

Figure 2.5 A schematic of a section from the posterior ctenidium and respective epibranchial cavity of *Nausitora fusticula*, indicating ciliary current and water flow (small arrows). av, afferent branchial vessel; ec, epibranchial cavity; ev, efferent branchial vessel; fm, free edge of septum; gl.d, gland of Deshayes; ifj, interfilamental junction; s, septum of branchial filament. Taken from Lopes & Narchi (1998).

The nomenclature used in the description of the pallets is adopted from Turner (1966). The pallets are situated at the base of the siphons, either side of the muscular collar. Formed of a stalk and blade (Fig. 2.6 a-b), individual pallets are semi-circular in cross section and complete a conical plug when pressed together, as shown in Figure 2.6c (Turner, 1966; Nair & Saraswathy, 1971). The muscles involved in moving the pallets include the protractors, anterior, median and posterior retractors and the adductor muscles (Lopes & Narchi, 1998). When the individual is disturbed or faces unfavourable environmental conditions, the siphon retractor muscles withdraw the siphons and the pallets are bought together and thrust into the burrow opening by the adductor and protractor muscles respectively (Lopes & Narchi, 1998). Once disturbance ceases, the pallets are withdrawn and parted by the retractor and adductor muscles respectively, thus allowing the siphons to extend (Lopes & Narchi, 1998). Both the pallet protractor and the siphon retractor muscles are attached to the inner lining of the burrow; attachment to this hard substrate facilitates rapid retraction of the siphons and protraction of the pallets into the burrow opening (Lopes & Narchi, 1998). The siphonal musculature is shown in Figure 2.7.

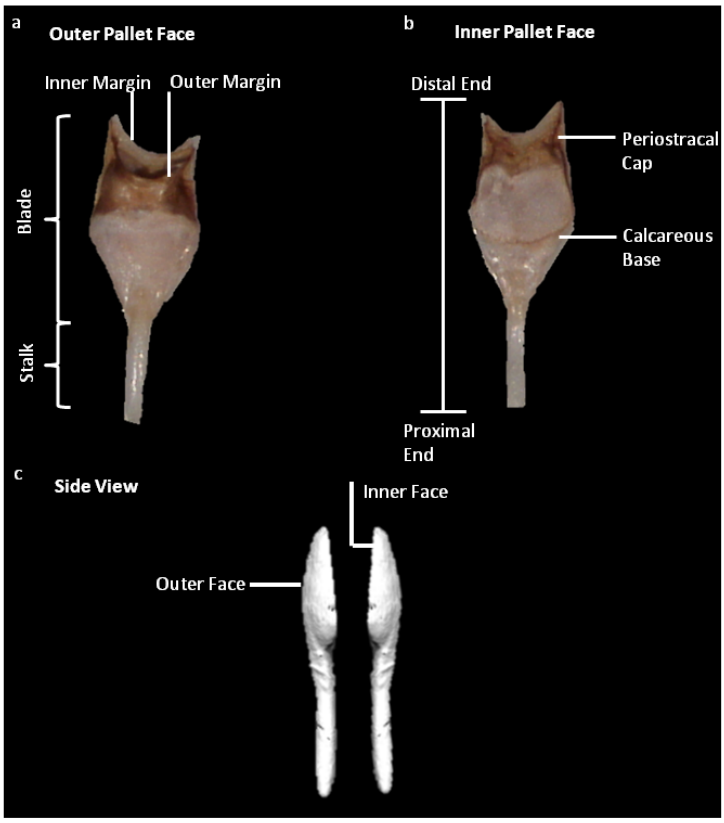

Figure 2.6 The structural features and nomenclature of the pallets from *Lyrdous pedicellatus.* a). The outer face of a pallet. b). the inner face of a pallet. c). a 3-D rendered image showing the side view of opposing pallets.

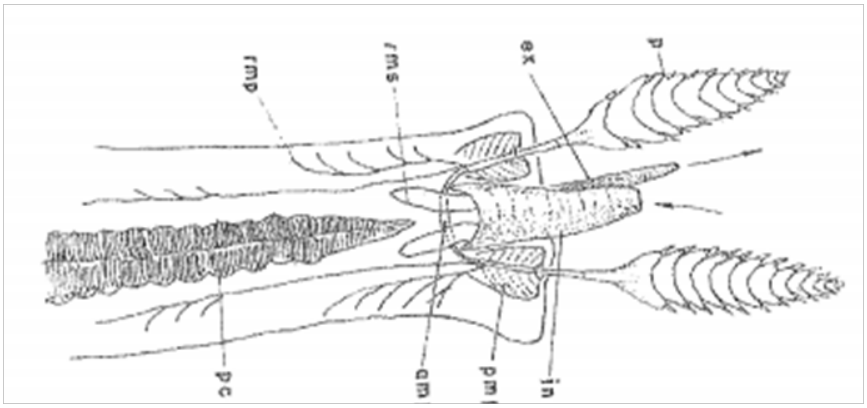

Figure 2.7 Diagrammatic view of the pallet and siphon musculature of *Bankia fibriatula.* amp, adductor muscle of pallet; ex, exhalent siphon; in, inahlent siphon; p, pallet; pc, posterior ctenidia; pmp, protractor muscles of the pallet; rms, retractor muscles of the siphon; rmp, retractor muscles of the pallets. Taken from (Martins-Silva & Narchi, 2008).

Special features of teredinid anatomy

The double-valved shell, from which bivalves derive their name, typically envelops the visceral mass and primarily functions as a protective boundary. The shells of teredinids are greatly reduced, offering limited protection to their elongated, vermiform bodies and the organ systems which predominantly lie posteriorly to the shell adductor muscles. Instead, this highly adapted shell – covered with rows of denticles – functions as a wood-boring tool. Whilst most teredinids derive nutrition from wood, the substrate also serves a protective function, sheltering individuals within from the external environment and predation.

Teredinids also produce a calcareous tube which lines the inside of the burrow. Wood may become heavily degraded by other marine borers such as the crustaceans *Limnoria* and *Chelura*, which cause superficial damage to the surface of the wood potentially exposing Teredinids to the external environment. Thus, the calcareous lining provides additional protection. Furthermore, the smooth surface of the lining protects the soft-bodied teredinid from the rough wood and also serves to limit desiccation (Turner, 1966).

Incurrent and excurrent siphons, the only features of a teredinid externally visible from the wood, protrude from the small opening into which the shipworm initially entered as a larva. Water and any suspended particles are continually drawn in though the siphons and pass across the gills. The siphons may be fully retracted inside the burrow upon disturbance or when faced with unfavourable environmental conditions. In such an instance the pallets, structures which flank the siphons, are then pushed into the burrow entrance, effectively sealing the individual within. These calcareous paddle-like structures are unique to the Teredinidae and are vital to the wood-boring lifestyle. It is only when the siphons are retracted and the pallets are closed together that boring takes place. When boring ceases, the siphons are once again extended and filter-feeding commences. This highly specialised mechanism allows teredinids to continuously feed by alternating between food sources (Morton, 1970).

The wood-storing appendix, the caecum, is another unique anatomical feature of the Teredinidae (Purchon, 1941). This organ is the principle site of lignocellulose degradation and nutrient absorption (Betcher *et al*., 2012) and its relative size is believed to reflect a species dependence on wood as a food source. For example, the caecum is large and conspicuous in facultative xylotrophic species such as *Nausitora hedleyi* and *N. dunlopi*, yet completely lacking in *Kuphus polythalamia*, the only species which does not ingest

wood (Nair & Saraswathy, 1971; Distel *et al*., 2011). The presence of an internal typhlosole, which greatly increases the surface area of the caecum, is considered an adaptation towards a more complete utilization of wood and also indicates a cellulose-dependent diet (Turner, 1966; Distel *et al*., 2011).

Like the caecum, the relative gill size is believed to represent a species reliance on either cellulose or plankton for nutrition. Plankton drawn from the water column are captured by the gills and transported along a food groove towards the labial palps, which direct these particles to the mouth. Thus, gill elongation was initially interpreted as an adaptation to increase filter-feeding capability and was considered symptomatic of planktotrophic-dependent species (Turner, 1966). However, this view has recently been challenged by the discovery of bacterial symbionts residing in the bacteriocytes in a region of the gill known as the gland of Deshayes (Popham & Dickson, 1973), as shown in Figure 2.8 a-d. As these symbionts produce a range of cellulases which are thought to assist the teredinid in the digestion of wood (Waterbury *et al*., 1983; Distel *et al*., 1991), it has been suggested that large gills should be reinterpreted as a greater reliance on xylotrophy, due to the increased volume of intralamellar bacteriocytes which may accommodate more symbionts (Distel *et al*., 2012).

The mechanism by which symbiont-produced cellulolytic enzymes are transported from the bacteriocytes in the gill to the digestive system has yet to be determined. A duct with a close association to the afferent branchial vein, leading from the Gland of Deshayes to the oesophagus (Fig. 2.8 e), has been described in *Teredo furcifera* (Nair & Saraswathy, 1971). This duct is reported to have contained granular spherules which increase in number towards the anterior region of the gill and, due to the absence of cilia in the wall of the duct, are believed to be transported by a mechanism of muscular contraction (Nair & Saraswathy, 1971). Yet this duct has never been described in other members of the *Teredo* genus, or any other teredinid species (Moraes & Lopes, 2003). The question of whether symbiont-derived cellulolytic enzymes are utilized by the shipworm and the means by which these enzymes are delivered to the digestive system remains one of the most fundamental questions yet to be resolved in teredinid biology.

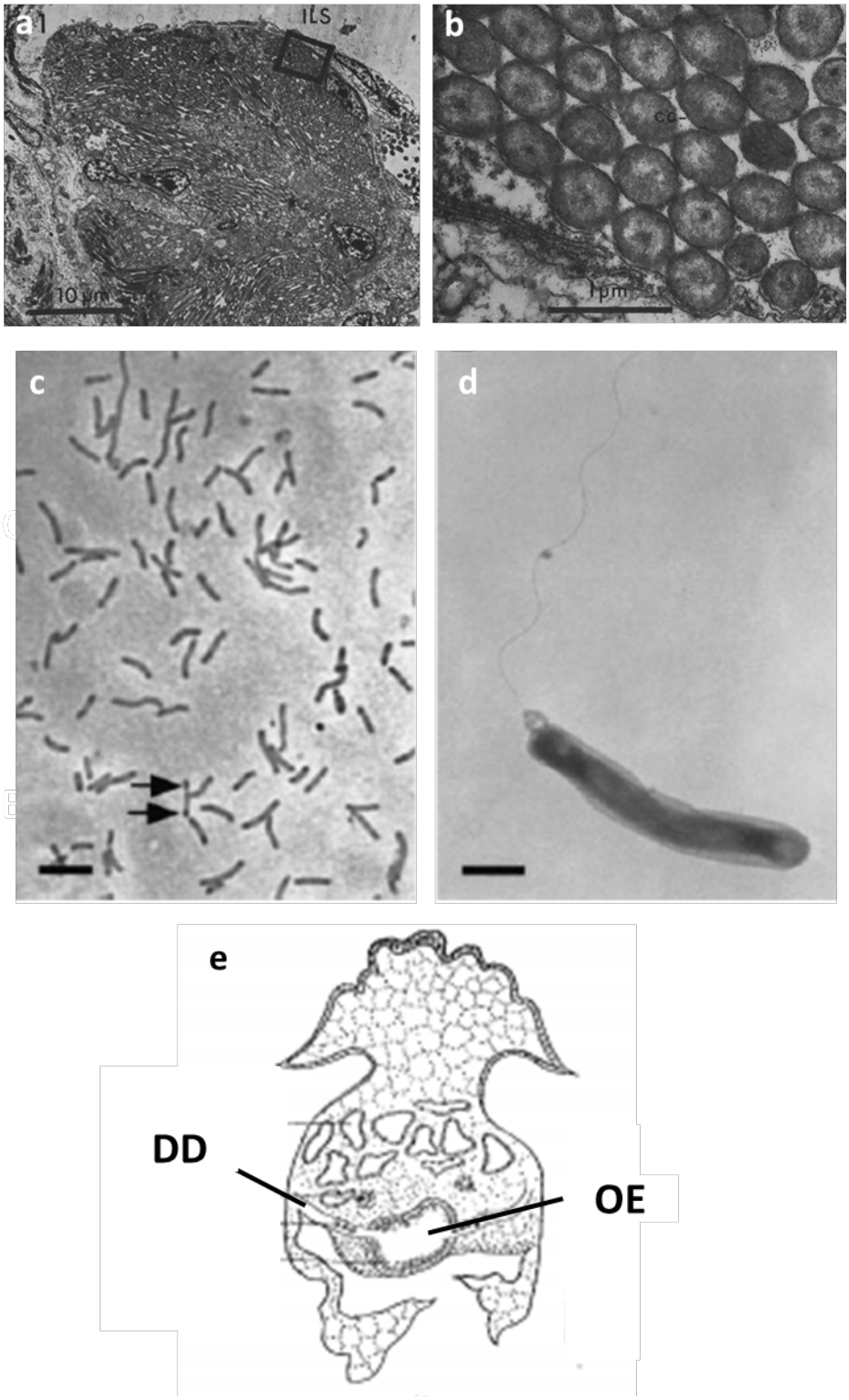

Figure 2.8 The Gland of Deshayes and the symbionts *Teredibacter turnerae,* located in bacteriorcytes on the gill. a-b). Gill lamina of *Bankia australis* containing the symbionts (from Popham & Dickson, 1973). c-d). The symbionts *T. turnerae* (from Distel *et al*,. 2003). e). The duct of Deshayes (DD) , linking the oesophagus (OE) of *Teredo furcifera* (taken from Nair & Saraswathy, 1971).

The boring mechanism

Although the shell has lost its protective function, it has become a highly specialised and extremely effective instrument of excavation (Fig. 2.9). Through the combined action of both the foot - which attaches to the extreme anterior end of the burrow - and the cephalic hood - which is distended with turgour - the valves are held in position and the denticles maintain contact with the wood (Turner, 1966).

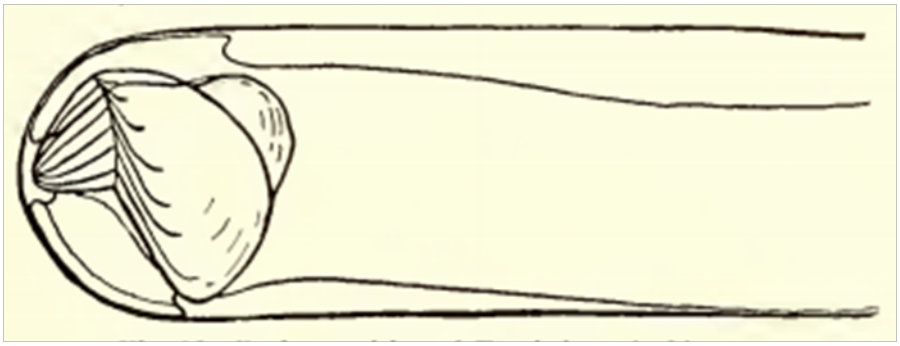

Figure 2.9 The boring position of *Teredo navalis*. The foot is fully extended and attached to the extreme anterior burrow (taken from Kofoid & Miller, 1927).

Contraction of the anterior adductor brings the anterior end of both valves together and spreads the posterior region. The boring 'stroke' is then initiated by contraction of the large posterior adductor, moving the valves through an arc of 20°-30° in an anterior-posterior direction, with both the distal and ventral condyle acting as a hinge (Miller, 1924; Kofoid & Miller, 1927). Upon each stroke of the valves, the foot takes a new hold, advancing approximately 0.5 mm. The foot flattens against the surface of the burrow, extending its margin beyond the gape of the valves. The muscles of the foot then retract the central disc, forming a concave sucker effectively anchoring the organ (Miller, 1924; Kofoid & Miller, 1927).

The anterior slope, covered with finely serrated ridges, extends to the tip of the burrow, excavating particles of wood approximately 0.02 mm in length and breadth. The coarsely denticulate ridges of the anterior median slope serve to enlarge the diameter of the burrow and produce large fragments of wood, varying from 0.3–0.4 mm in length and 0.02–0.08 mm in diameter (Kofoid & Miller, 1927). These particles are swept towards the mouth by cilia on the foot.

The dual feeding mechanism

The particles of wood produced from the mechanical action of the shell are swept towards the mouth by cilia on the base of the foot. These particles are then ingested, passing through the oesophagus and into the stomach (Morton, 1970). A small crystalline style projects into the stomach and is predominantly involved in sorting material, playing a minor role in extracellular digestion when compared to its function in other bivalves (Morton, 1970). Wood particles then accumulate in the caecum (Purchon, 1941).

Besides its wood-storing function, anatomical features suggest the caecum plays an important role in cellulolytic digestion and nutrient absorption. The internal epithelium is lined with microvilli and a large coiled typhlosole extends the entire length of the organ, greatly increasing its internal surface area. Extensive vascularisation is provided by an artery connecting directly from the heart (Bazylinski & Rosenberg, 1983). The digestive gland, which opens into the caecum, is divided into two distinct lobes (Morton, 1970; Lopes *et al*., 1998). The first lobe, which opens into the floor of the caecum via ducts associated with the typhlosole, is capable of taking in small particles of filtered material for intracellular digestion. The second lobe is specialised for wood digestion and opens into the floor of the caecum via a series of ducts (Potts, 1923; Morton, 1970). Reducing sugar assays indicate that the caecum is the primary site of cellulose degradation, with tissue upstream of this organ showing double the cellulolytic activity of tissue downstream (Greenfield & Lane, 1953). Wood particles are then returned from the caecum back to the stomach, before passing through a relatively long intestine with a well-developed typhlosole (Turner, 1966). Waste particles are then ejected from the anal canal, where they progress along the suprabranchial cavity and are expelled from the excurrent siphon.

During filter-feeding, water is drawn in through the incurrent siphon and passes over the ctenidia (gill) in the epibranchial cavity (Figures 2.3 and 2.5). The general teredinid ctenidial arrangement is typically eulamellibranch – derived from the ascending and descending demibranch, forming V-shaped filaments which join together to form a marginal groove (Ridewood, 1903; Sigerfoos, 1908). Cilia on these filaments beat towards the marginal food groove (Fig. 2.1 b-c) whose cilia beat anteriorly, driving particles towards the labial palps (Purchon, 1960). Particles arriving at the labial palps are then processed towards the mouth (Morton, 1970). Parasitic ciliates are abundant in the gills and around the palps.

Aims

The research presented herein assists the transcriptomic analysis of the digestive system described in chapter three by identifying the key anatomical features of the digestive system of *Lyrodus pedicellatus* with a particular focus on how this species exploits lignocellulose. Anatomical examination was undertaken to reveal the process allowing *L. pedicellatus* to continually feed from two distinct food sources and to determine whether this species has a greater dependence on xylotrophy or planktotrophy.

Utilisation of X-ray micro-computed tomography (hereafter referred to as Micro-CT), produced the first volume rendered 3-D reconstruction of a teredinid. This powerful technique allows the virtual dissection of specimens in any plane and builds an unparalleled view of the spatial orientation and anatomy of *L. pedicellatus*. Furthermore, videos created from the 3-D renderings allows the viewer to travel through the anatomy of a shipworm giving further insights into the passage of wood though the teredinids digestive system. This technique was used to determine whether the duct of Deshayes, as detailed in *Teredo furcifera* (Nair and Saraswathy; 1971), is also present in *L. pedicellatus*.

Material and methods

The teredinids used in this research originated from specimens collected Langstone Harbour (Portsmouth) from a piece of Greenhert wood in 2005 and were identified as *L. pedicellatus* based on the pallet features described in Turner (1971).

Electron Microscopy

Samples for observation under the electron microscope were fixed in 4 % v/v glutaraldehyde in a cacodylate buffer (0.2 M sodium cacodylate, 0.3 M sodium chloride, 2 mM calcium chloride) for one hour at room temperature. Samples were then rinsed three times in buffer for ten minutes each. All samples were then post-fixed in 1 % w/v aqueous osmium tetroxide for one hour and rinsed three times in seawater for ten minutes each. Samples were then taken immediately through an ethanol dehydration series, evaporation dried via hexamethyldisilazane (HMDS) and then mounted on aluminium stubs using adhesive carbon tabs. Sputter coating was carried out under an argon atmosphere using a gold and palladium target, at a voltage of 1.4 kV using a current of approximately 18 mA for three minutes. Specimens were examined using a JEOL 6060LV Scanning Electron Microscope operating in secondary electron mode using an accelerating voltage of 18 kV.

Micro-computed tomography

An adult *Lyrodus pedicellatus* specimen was fixed according to the scanning electron microscopy methodology outlined above. The sample was then mounted onto the sample holder and secured using glue (Fig. 2.10 a). Scanning was carried out using a nanofocus X-ray tube in combination with a Photonic Science detector (Fig. 2.10 b), with an exposure time of 1700 ms and a rotation angle of 0.25°, which resulted in a scan time of 75 minutes and an approximate voxel pitch of 0.2 µm. Due to large specimen size, two stacked scans were performed. The dataset was reconstructed using the Octopus software package with beam hardening correction. The two reconstructed volumes were then loaded in VGStudio MAX and stitched into a single stack of cross-sections. All resulting image and video analysis was performed using visualisation software myVGL. Scanning was performed by Jan van den Bulcke at, the Gent University Centre for X-ray Tomography.

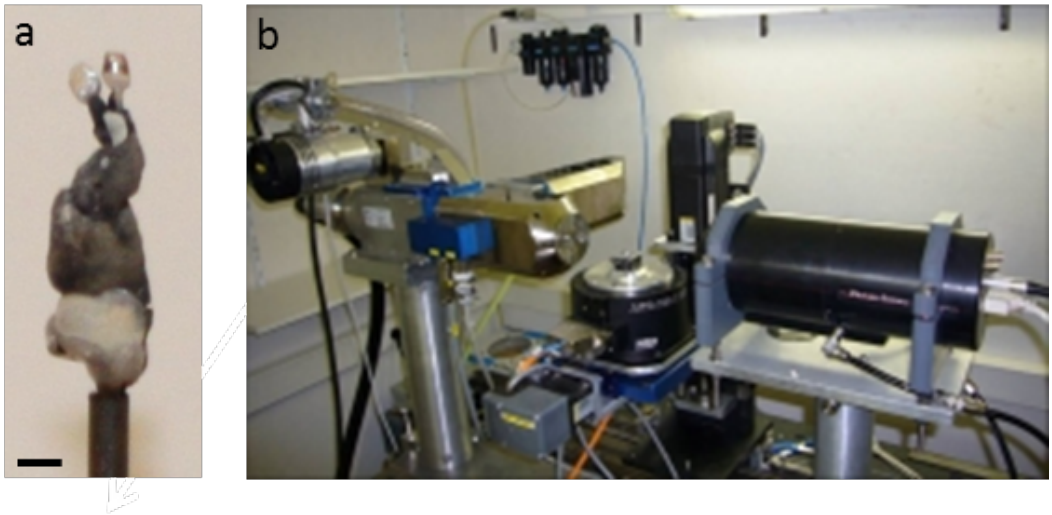

Figure 2.10 a) Mounted adult specimen of the shipworm, *Lyrodus pedicellatus*, for microCT X-ray scanning. b) The micro-computed tomography (MicroCT) scanner at Ghent University Centre for X-ray Tomography. Scale bar represents 0.9 mm. Image courtesy of Jan van den Bulcke, Ghent University.

Results

Shell Structure and the Boring Mechanism

The 3-D structure of the shell valves from *Lyrodus pedicellatus* are shown in Figure 2.11 a–b and demonstrate the relationship between the condyles, chondrophores and apophyses of opposing valves. The ventral regions of the shell valves were overlapping, indicating the specimen was boring when extracted from the wood (Fig. 2.11 a-b). The apophyses are elongated, measuring approximately half the length of the shell valve (Fig. 2.11 a & b). Similarly, the auricle extends to approximately half the width of the shell valve (Fig. 2.11 b, c & d).

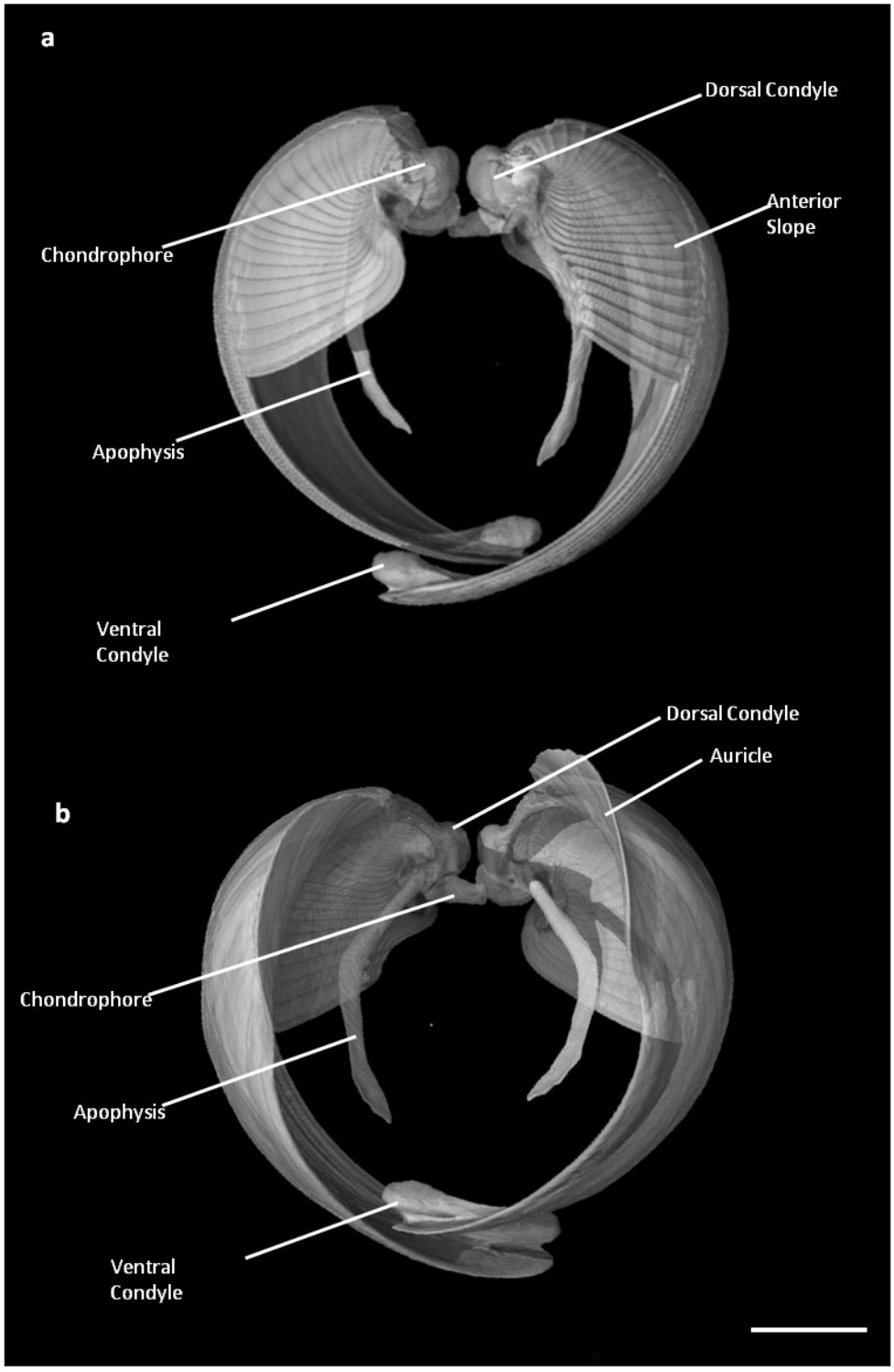

Figure 2.11 A 3-D MicroCT image showing the structural features of the shell valves from *Lyrodus pedicellatus* rendered using myVGL software program. a). Anterior view of the opposing valves showing the large pedal gape. b). Posterior view of opposing valves. Scale bar represents 1 mm.

Fine shell features are shown in Figure 2.12. The ridges of the medial slope were densely packed, measuring approximately 40 µm between the rows (Fig. 2.12 b-c). This compares with a distance of 100 µm between the ridges on the anterior slope (Fig. 2.12 d). Yet the denticles of the anterior slope are more finely serrated, each measuring approximately 5 µm and 5-10 µm in length and width respectively, compared with the larger, blunter denticles on the medial slope, which measured 30-40 µm in length and 30 µm in width. As a result, denticles of the anterior slope are more numerous and compact than those on the medial slope.

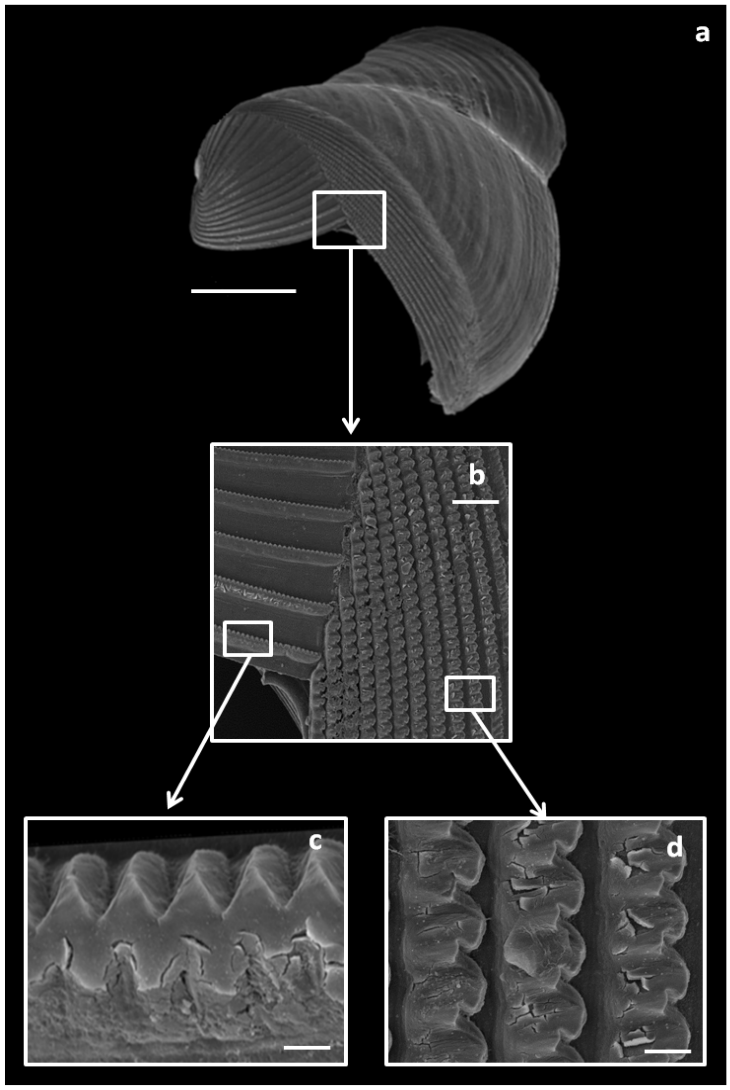

Figure 2.12 An SEM image showing the shell features of *Lyrodus pedicellatus*. a). the external shell valve. b). Magnified view of the anterior and median slope. c). the finely serrated ridges of the anterior slope. d). the coarser denticulations of the median slope. Scale bars for a, b, c and d represent 1 mm, 500 µm, 100 µm and 100 µm respectively.

Suspension-feeding mechanism

Components of the suspension feeding mechanism and associated organs are shown in Figure 2.12. The ctenidia of *L. pedicellatus* are composed solely of the outer demibranch and are generally similar in composition to other teredinids (Fig 2.11 a-b). The right and left V-shaped demibranchs fuse at the medial axis, separating the mantle cavity into the suprabranchial and infrabranchial cavity. Water is drawn into the infrabranchial cavity via the incurrent siphon, where it passes across the ctenidia (Fig. 2.11 a). Particles are then drawn by ciliary motion towards the apex of the demibranch (Fig 2.11 b). The apex of each V-shaped demibranch forms a ciliated tract, known as the marginal groove or food groove (Fig. 2.11 c). These grooves measure 50 - 60 μm in depth, becoming shallower towards the anterior gill. Particles are then swept along the marginal groove in a posterior to anterior direction. The anterior gill is greatly reduced, formed only of the marginal groove, and connects with the labial palps (Fig. 2.11 d). The labial palps are greatly reduced and are formed of eight filaments (Fig. 2.11 e). A number of ciliated parasites were found on the ctenidia and palps (Fig. 2.11 f). All particles arriving at the palps are then directed towards the mouth (Fig. 2.12 a). Excavated particles of wood are directed to the mouth by cilia, which line the surface of the foot (Fig. 2.12 b-c).

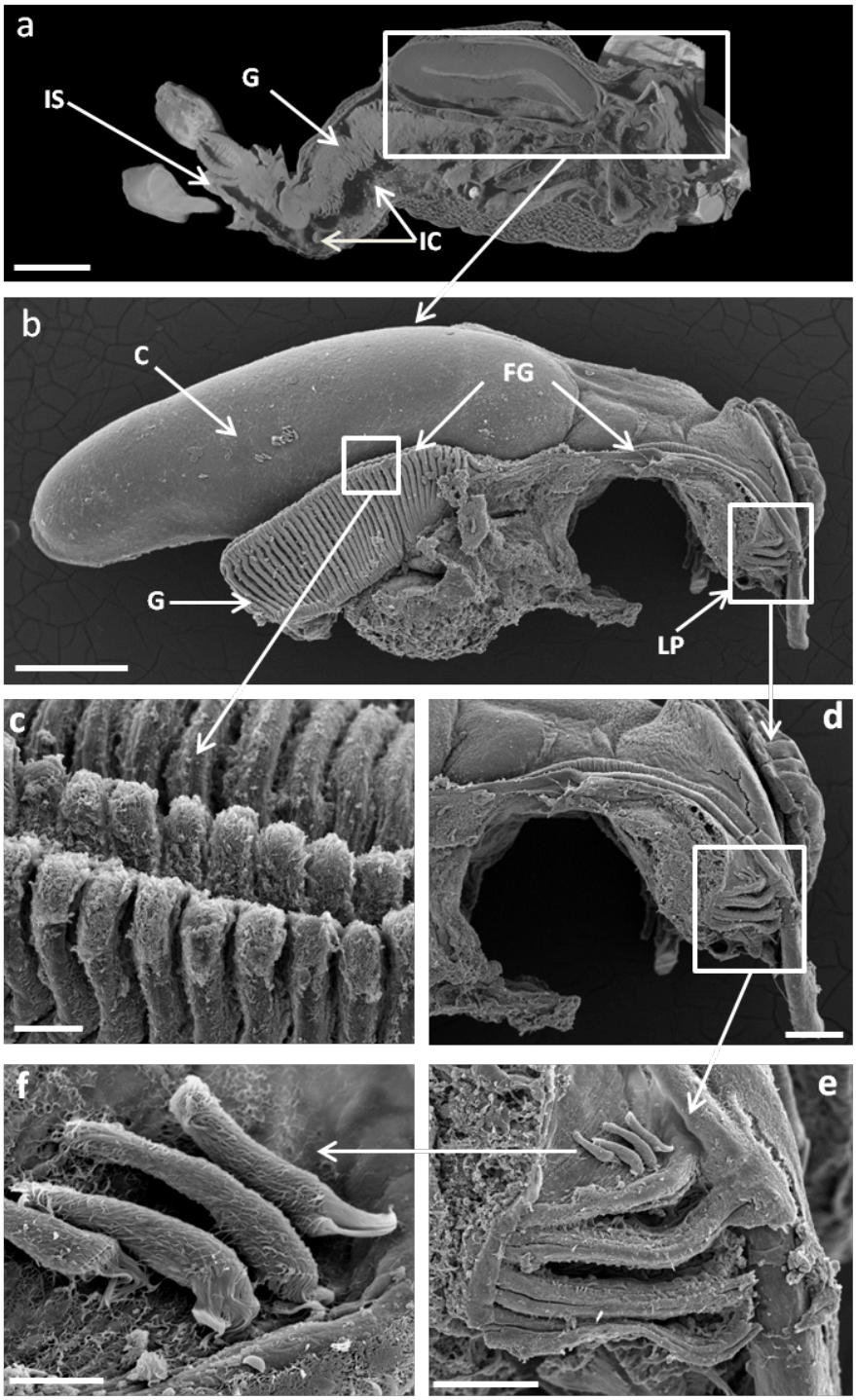

Figure 2.13 Anatomical arrangement of the suspension-feeding mechanisms from the shipworm *Lyrodus pedicellatus*. a) Micro-computed tomography image dissected on myVGL shows incurrent siphon leading to the infrabhanchial cavity (IC), the ctenidial arrangement and organisation of the digestive system. b) The gill (G) arrangement and connection between the connective region between the anterior gill and the labial palps (LP). c) Filtered particles are transported along the food groove (FG) and along to (d) the labial palps (LP) for further processing. e) ciliated parasites may be located on the labial palps (LP). Scale bars for a, b, c, d, e and f represent 1 mm, 500 µm, 50 µm, 200 µm, 100 µm and 10 µm respectively.

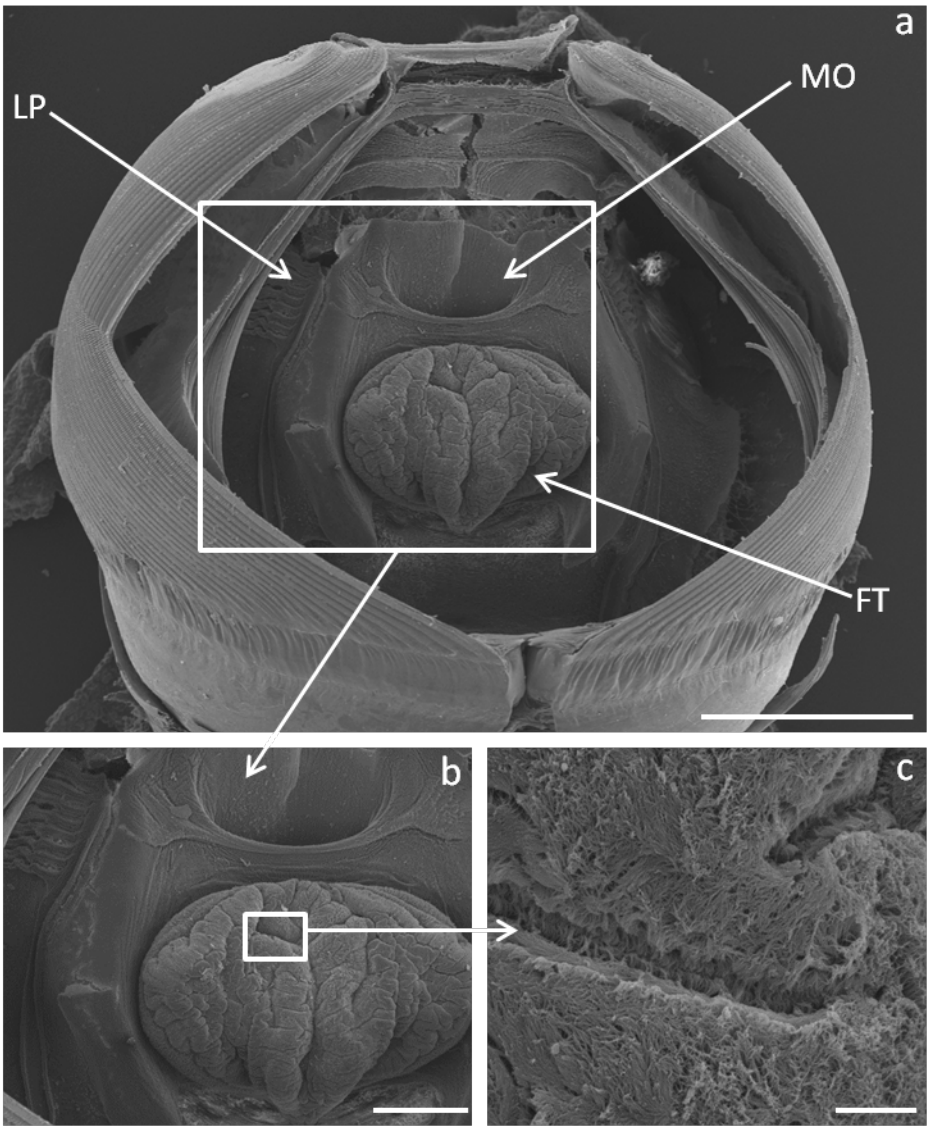

Figure 2.14 a) Anatomical arrangement of the labial palps, mouth and foot enclosed within the shell valves (a). b) Enhanced view of the interaction between labial palps and the foot, with the mouth. c) Cilia on the surface of the foot, responsible for generating currents towards the mouth. Scale bars for a, c and c represent 1 mm, 500 µm and 20 µm respectively.

Digestive organs

A microCT 3-D rendering of an adult *L. pedicellatus* was digitally dissected, showing the anatomical arrangement of the mid-sagittal plane (Fig. 2.13).

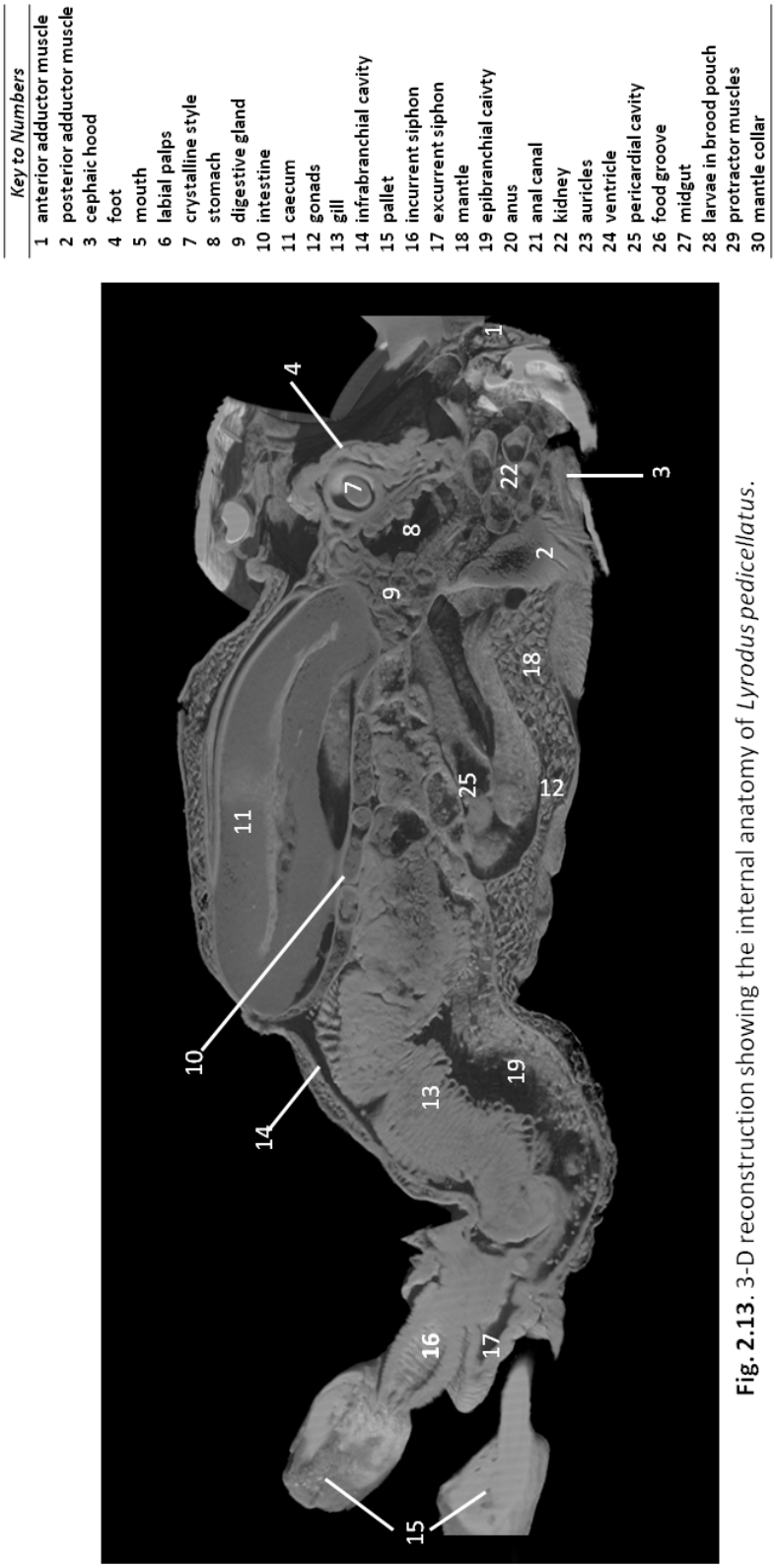

Fig. 2.13. 3-D reconstruction showing the internal anatomy of *Lyrodus pedicellatus*.

Anterior-posterior, dorso-ventral and lateral-medial sections of the digestive organs, the crystalline style, digestive gland, stomach, caecum and intestine are shown in figures 2.14 - 16. The crystalline style (Fig. 2.14 a-d), lies within the foot and has a close association with the stomach (Fig. 2.14 a and d). The stomach is elongated and leads to the caecum (Fig. 2.14 a and c). The digestive diverticula (Fig. 2.15 a-d), which surrounds the anterior region of the caeca, is formed of two distinct regions: the first region opens into the caeca via a flare of the typhlosole (Fig. 2.15 a and d), whilst the second opens at its base (Fig. 2.15 d). This corroborates findings of Lazier (1924) and Morton (1970). The caecum is large and conspicuous in *L. pedicellatus*, extending to approximately 40 % of the total length of the specimen examined (Fig. 2.16 a-d). The luminal surface area is greatly increased by the presence of a coiled typhlosole which extends along the length of the organ (Fig. 2.16 a and c). The intestine, originating from an opening in the stomach, extends along the length of the caecum, loops back over the top of the organ, continues towards the posterior adductor muscle and then doubles back upon itself before finally emptying into the anal canal (Fig. 2.16 b and d). Individual pellets of waste, called frass, were observed in the posterior regions of the intestine, travelling towards the anal canal for expulsion from the animal (Fig. 2.16 a and b).

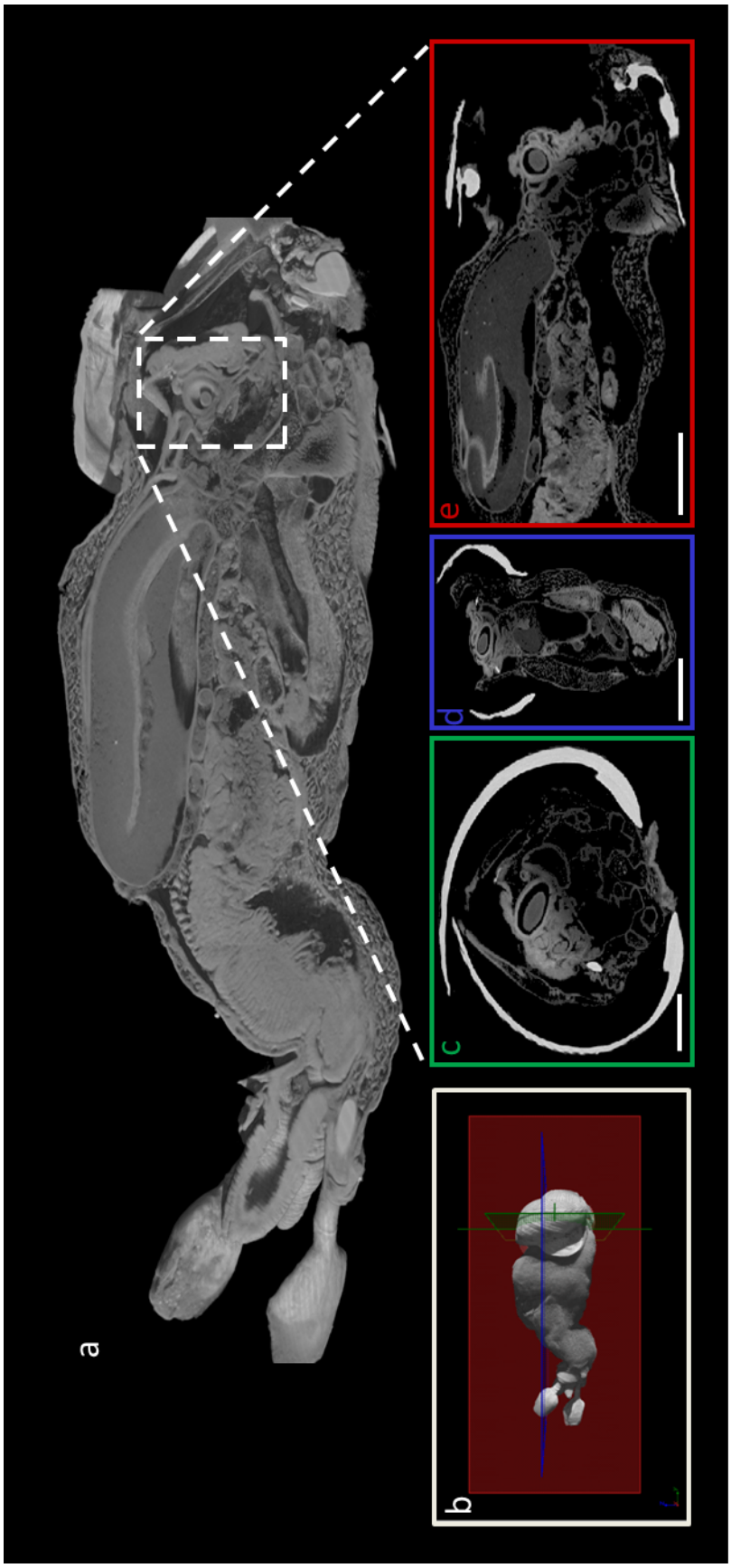

Fig. 2.14. The anatomy of the digestive tract of *Lyrodus pedicellatus* as imaged by microCT. a) a 3-D model of *L. pedicellatus* dissected through the lateral-medial axis. Region containing the crystalline style highlighted. b) the planes of dissection orientated as follows: anterior-posterior dissection shown coloured green and plane visualised in image c; (image c) dorso-ventral dissection shown coloured blue and plane visualised in image d; and d) lateral-medial dissection shown coloured red and plane visualised in image e. Scale bar represents 100 µm.

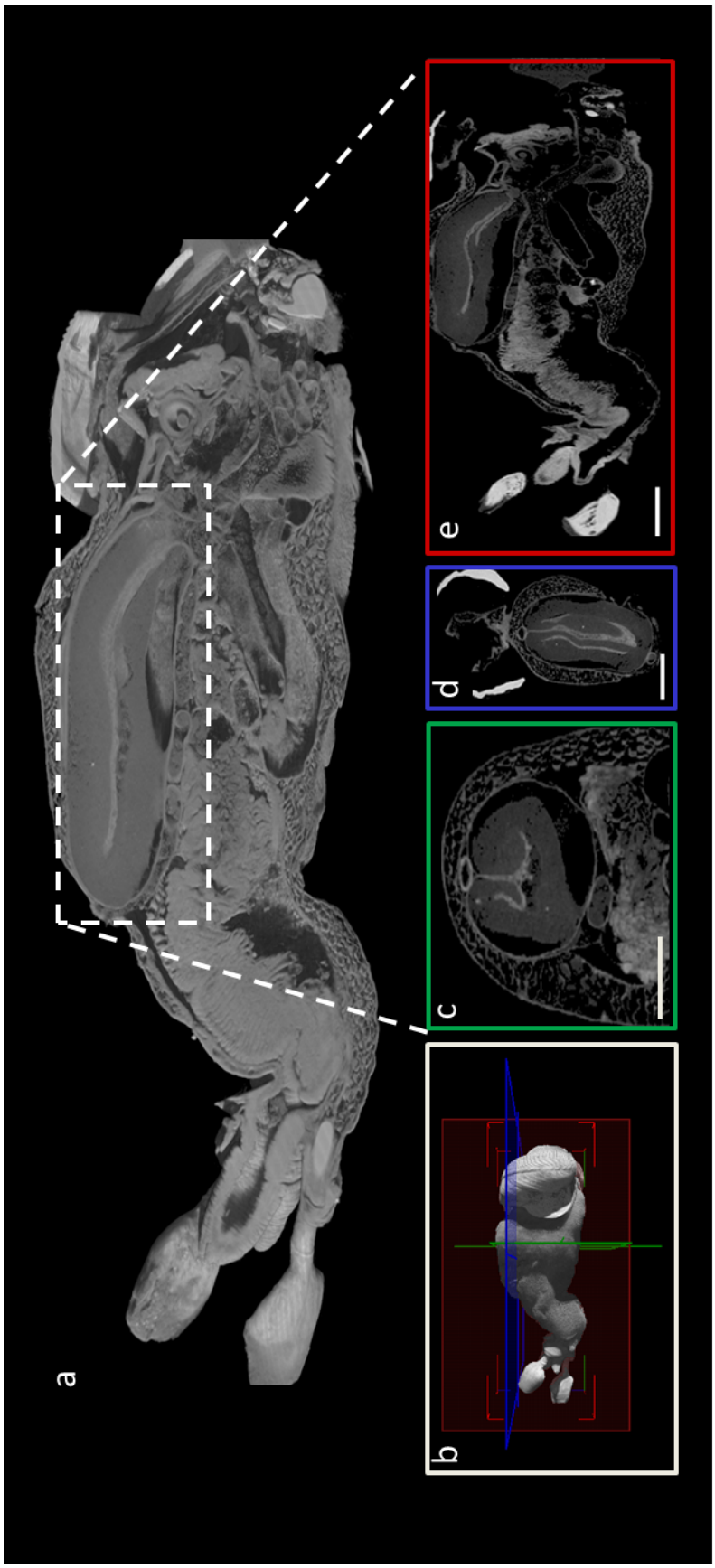

Fig. 2.15 The anatomy of the digestive tract of *Lyrodus pedicellatus* as imaged by microCT. a) a 3-D model of *L. pedicellatus* dissected through the lateral-medial axis. Region containing the caecum highlighted. b) the planes of dissection orientated as follows: anterior-posterior dissection shown coloured green and plane visualised in image c; (image c) dorso-ventral dissection shown coloured blue and plane visualised in image d; and d) lateral-medial dissection shown coloured red and plane visualised in image e. Scale bar represents 100 µm.

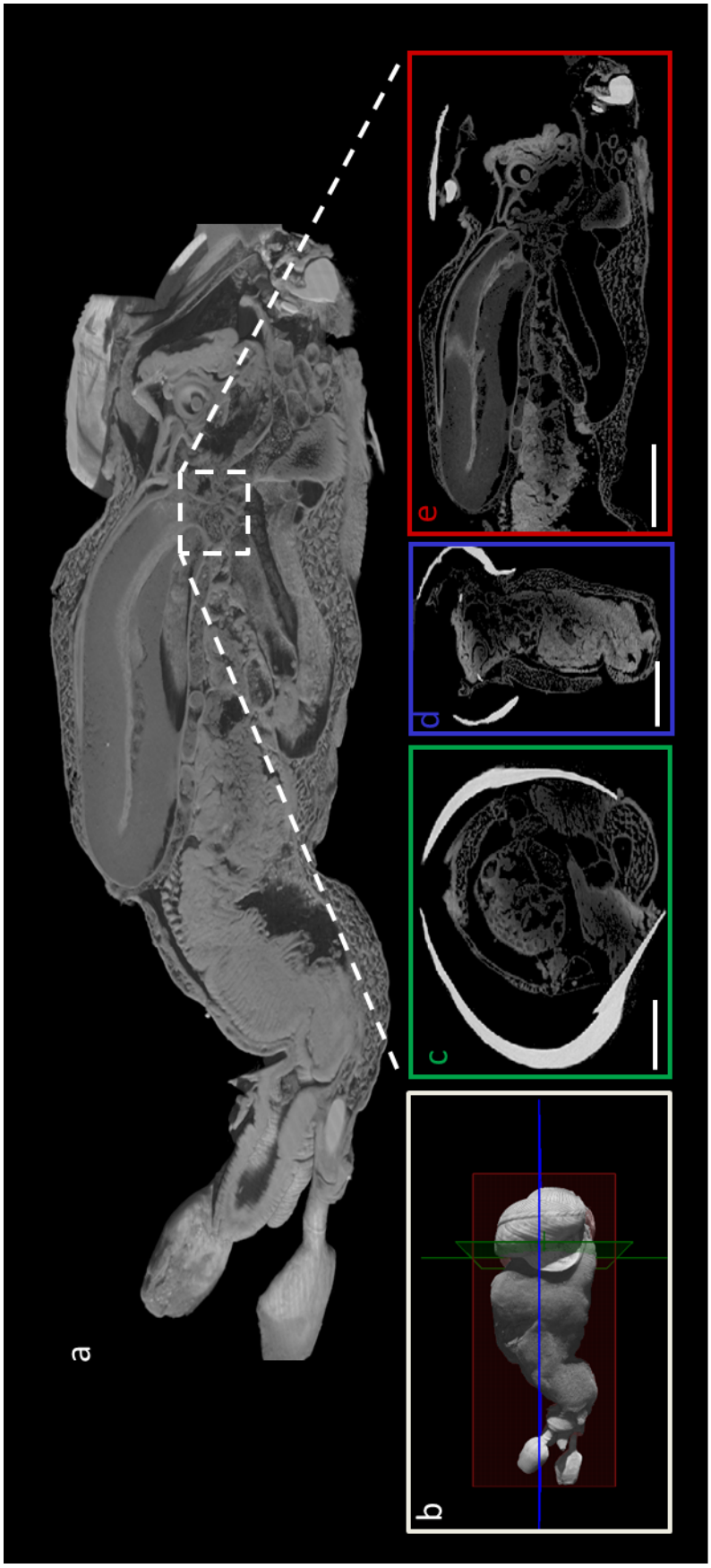

Fig. 2.16. The anatomy of the digestive tract of *Lyrodus pedicellatus* as imaged by microCT. a) a 3-D model of *L. pedicellatus* dissected through the lateral-medial axis. Region containing the digestive gland highlighted. b) the planes of dissection orientated as follows: anterior-posterior dissection shown coloured green and plane visualised in image c; (image c) dorso-ventral dissection shown coloured blue and plane visualised in image d; and d) lateral-medial dissection shown coloured red and plane visualised in image e. Scale bar represents 100 µm.

Micro-CT Anatomy

The following section describes the anatomical arrangement of sections taken from the 3-D virtual rendering of an adult *Lyrodus pedicellatus* specimen, along the anterior-posterior axis. The accompanying media file is compiled from a total of 1246 sections taken along the entire length of the teredinid - again, along the anterior-posterior axis - to create a video which scans through the specimen. The sectioned images and their relative position to the accompanying video are provided as a measure of time (minutes and second) from the start of the video.

Fig. 2.17 a (video 0 minutes and 8 seconds). The right and left shell valves are joined by the anterior adductor muscle.

Fig. 2.17 b (video 0 minutes and 11 seconds). Ventral condyles from both the left and right valve are shown, along with the connective ligament between the chondrophores on opposing valves. Denticulated ridges formed across the medial slope are visible.

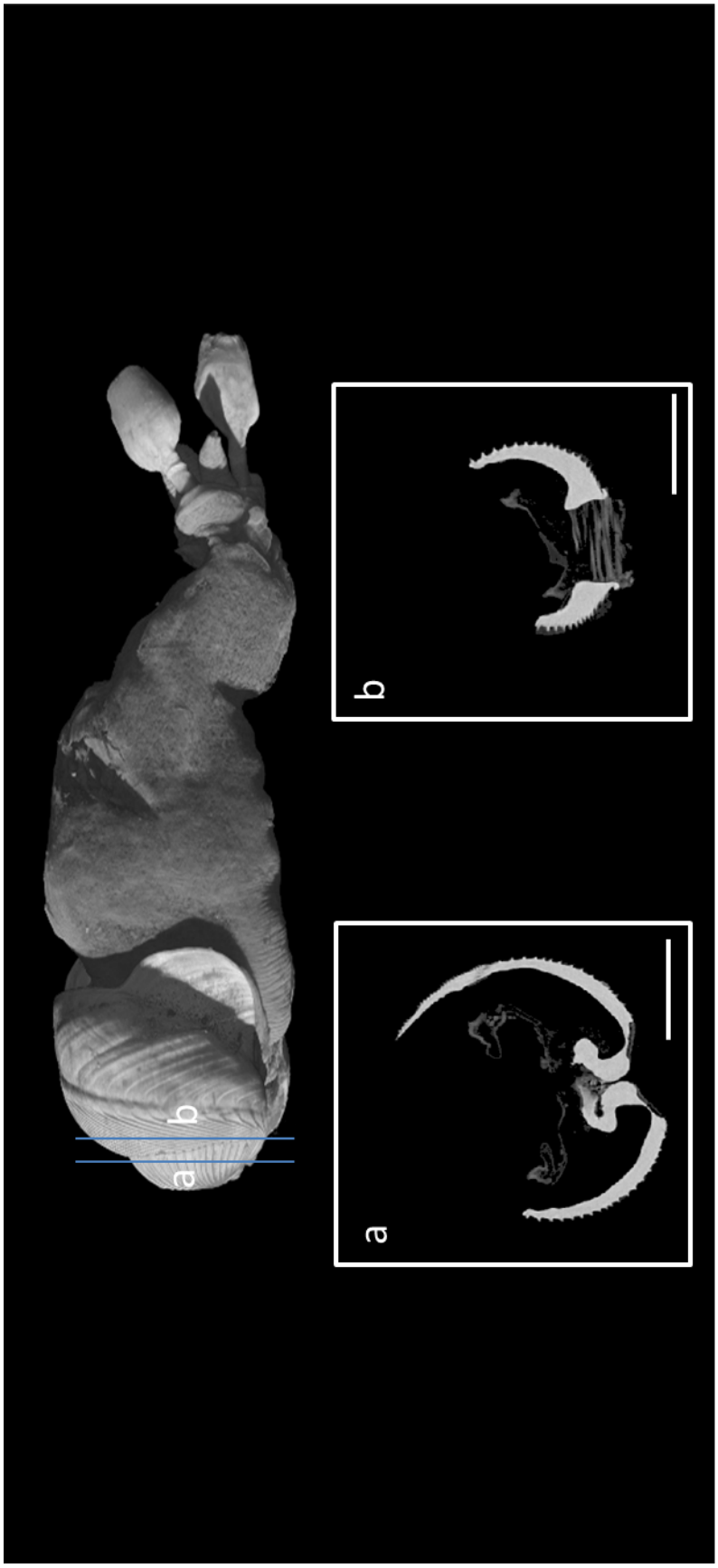

Fig. 2.17. 3-D rendered models of the digestive anatomy of *Lyrodus pedicellatus*. a) condyles visible, opposing chondrophores linked by ligament. b) anterior adductor muscle. Scale bar 0.03 mm.

Fig. 2.17 c (video 0 minutes and 18 seconds). The lobed kidney is clearly visible. The small, silt-like opening of the mouth forms ventrally of the foot.

Fig. 2.17 d (video 0 minutes and 22 seconds). The thickening of the right valve forms the dorsal condyle. The sole of the foot emergences, along with the crystalline style which is found embedded within the foot. The base of both the right and left apophysis are visible and demonstrate the relation to the foot musculature is apparent. The oesophagus lies dorsal to the foot and begins to open into the stomach.

Fig. 2.17 e (video 0 minutes and 25 seconds). The pear-shaped crystalline style sac and its position relative to the stomach – located dorsally to the style – are fully revealed. The shell valves are shown to fully envelop the visceral mass within. The kidney is situated dorsal to the stomach.

Fig. 2.17 f (video 0 minutes and 30 seconds). The intestine loops over the posterior adductor muscle and opens into the anal canal. The stomach opens into the intestine, which is characterised by a large typhlosole.

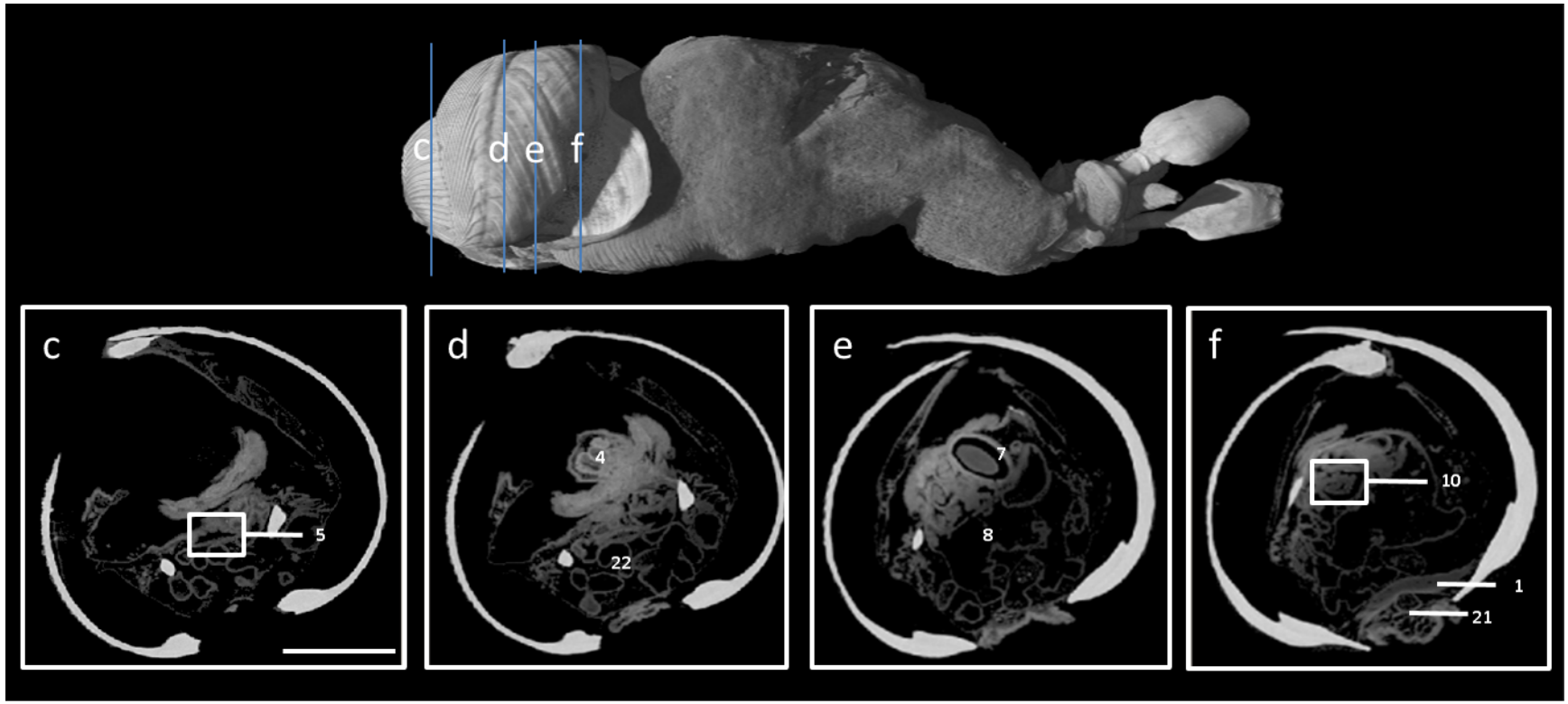

Fig.2. 17 3-D rendered models of the digestive anatomy of *Lyrodus pedicellatus*. c) opening of the mouth below the foot, leads directly to oesophagus d) foot, kidney and stalk of apophysis present e). relationship between crystalline style and stomach. f). typhlosole of intestine and stomach visible, anal canal loops under anterior adductor muscle. Scale bar 0.03 mm.

Fig. 2.17 g (video 0 minutes and 32 seconds). The full cross-section of the large, posterior adductor muscle is now visible, joining the two opposing valves. The stomach can now be seen in relation to the intestine and the digestive diverticula.

Fig. 2.17 h (video 0 minutes and 33 seconds). Posterior to the posterior adductor muscle, the anal canal continues to run dorsal to the kidney. The caecum begins to emerge and is enveloped by the digestive diverticula. The pericardial cavity lies dorsal to the digestive diverticula and ventral to the kidney.

Fig. 2.17 i (video 0 minutes and 45 seconds). The intestine is now shown to loop around the caecum, with the intestine running in the anterior to posterior axis located ventral to the caecum, whilst the returning intestine is dorsal to the caecum. The large, twin-coiled typhlosole greatly increases the internal surface area of the caecum. The gonads are located dorsal to the caecum. The pericardium cavity, which contains both the auricle and ventricle, is situated dorsally to the caecum, which is ventral to the pericardium cavity, containing both the auricle and ventricle.

Fig. 2.17 j (video 0 minutes and 55 seconds). A thick mantle, the granular appearance indicative of calcium deposits, surrounds the viscera. The gonads continue along the base of the caecum. Large afferent and efferent blood vessels extend away from the pericardial cavity in a dorso-ventral direction. The presence of what appears to be a large kidney stone is present in a compartment of the kidney.

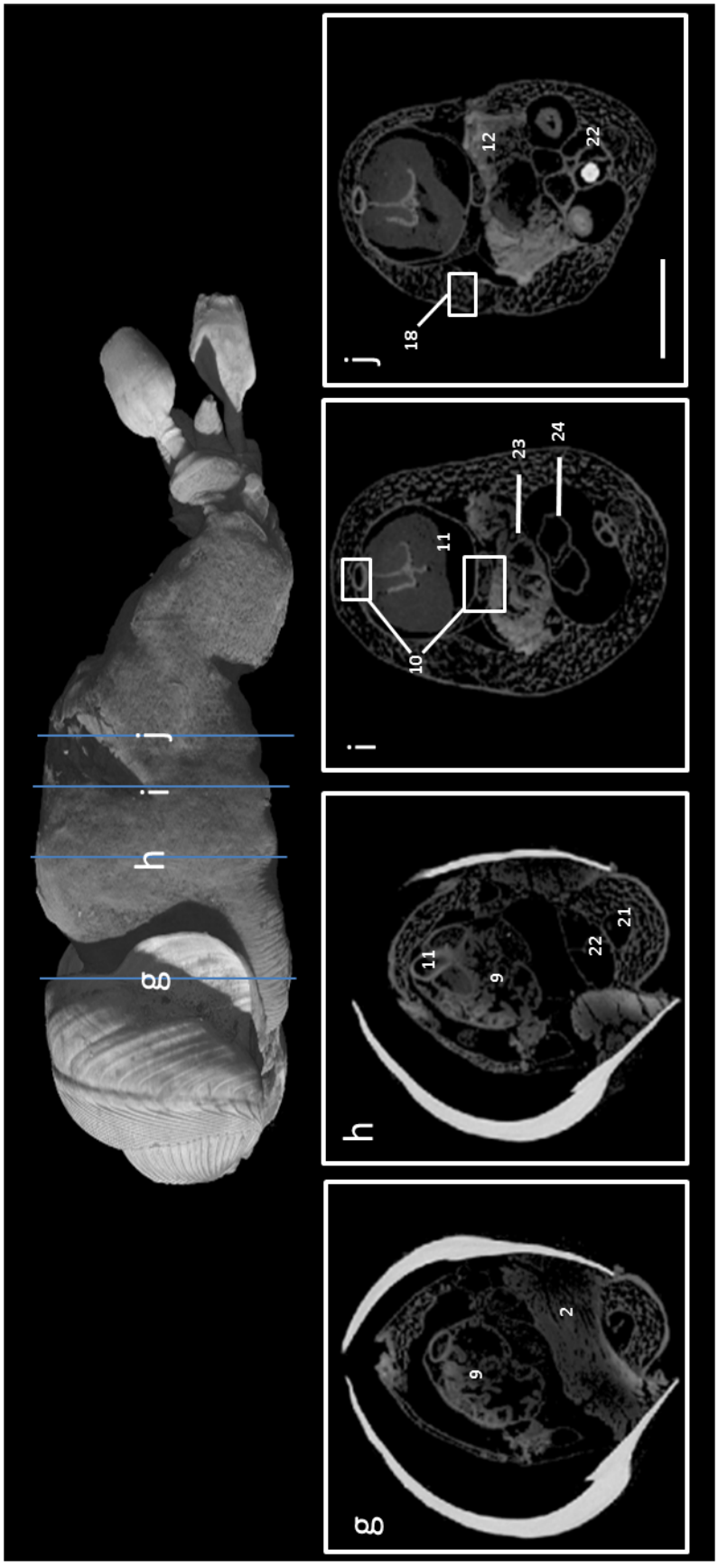

Fig. 2.17. 3-D rendered models of the digestive anatomy of *Lyrodus pedicellatus*. g) the relationship between the digestive diverticula and the caecum. j) The intestine wraps around the caecum and the atrium and ventricle of heart visible. h) stomach visible, thick posterior adductor attaches between opposing shell valves i). showing the mantle cavity, gonad and a kidney stone. Scale bar 0.03 mm.

Fig. 2.17 k (video 1 minutes and 4 seconds). Homorrhabdic and eulamellibranch ctenidia separate the mantle into the infrabranchial and suprabranchial cavities, which lie ventrally and dorsally to the ctenidia respectively. Parasitic cilia attach to the gill and membrane of the suprabranchial cavity. A particle, possibly consisting of a waste pellet, is also visible in the suprabranchial cavity. A fragment of the white-calcareous burrow lining, secreted by teredinid, is visible on the outside of the mantle cavity.

Fig. 2.17 l (video 1 minutes and 13 seconds). Specialised brood pouches containing veliger and pediveliger larvae present on the ctenidia.

Fig. 17 m (video 1 minutes and 33 seconds). Pallet stalks and the connective adductor muscle are visible.

Fig. 17 m (video 1 minutes and 44 seconds). The incurrent and excurrent siphons are visible, the former characterised by the present of five, tentacle-like sensory structures. Internal pallet structure is visible and shows the calcareous deposits.

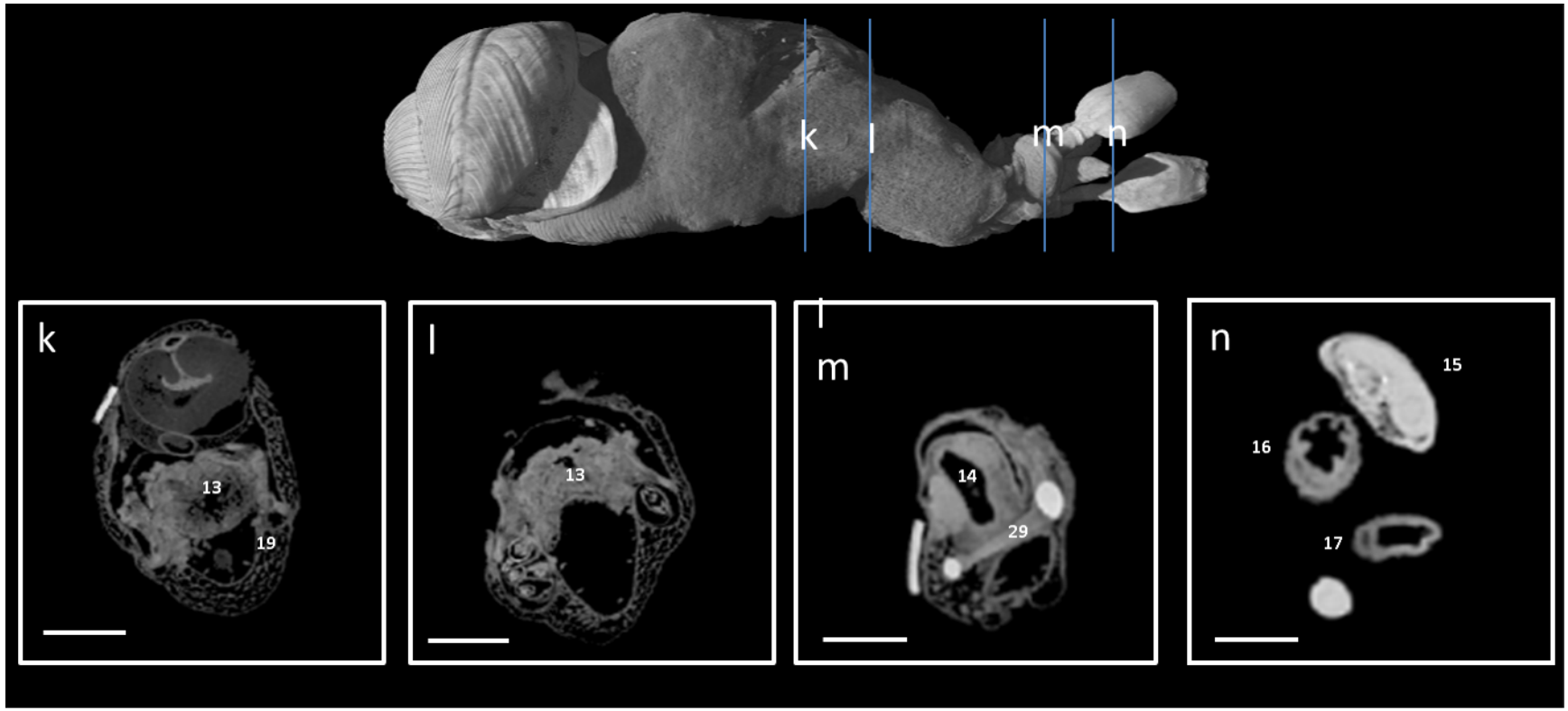

Fig. 2.17. 3-D rendered models of the digestive anatomy of *Lyrodus pedicellatus*. k) ctenidial – caecal arrangement l). the ctenidia and suprabranchial cavity. m) opposing pallet stalk and abductor muscle n). the incurrent and excurrent siphons in relation to the pallets. Scale bar 0.03 mm..

Duct of Deshayes

The mouth, oesophagus and opening to the stomach are shown in Figure 2.18. It was not possible to locate a duct connecting the gills and digestive system. Examination of the entrance of the mouth (Fig. 2.18 a & b), the opening of the oesophagus into the stomach (Fig. 2.18 c & d) and the entire length of the stomach (Fig. 2.18 e) also failed to reveal any duct or opening, or any associated vessel with the ctenidia.

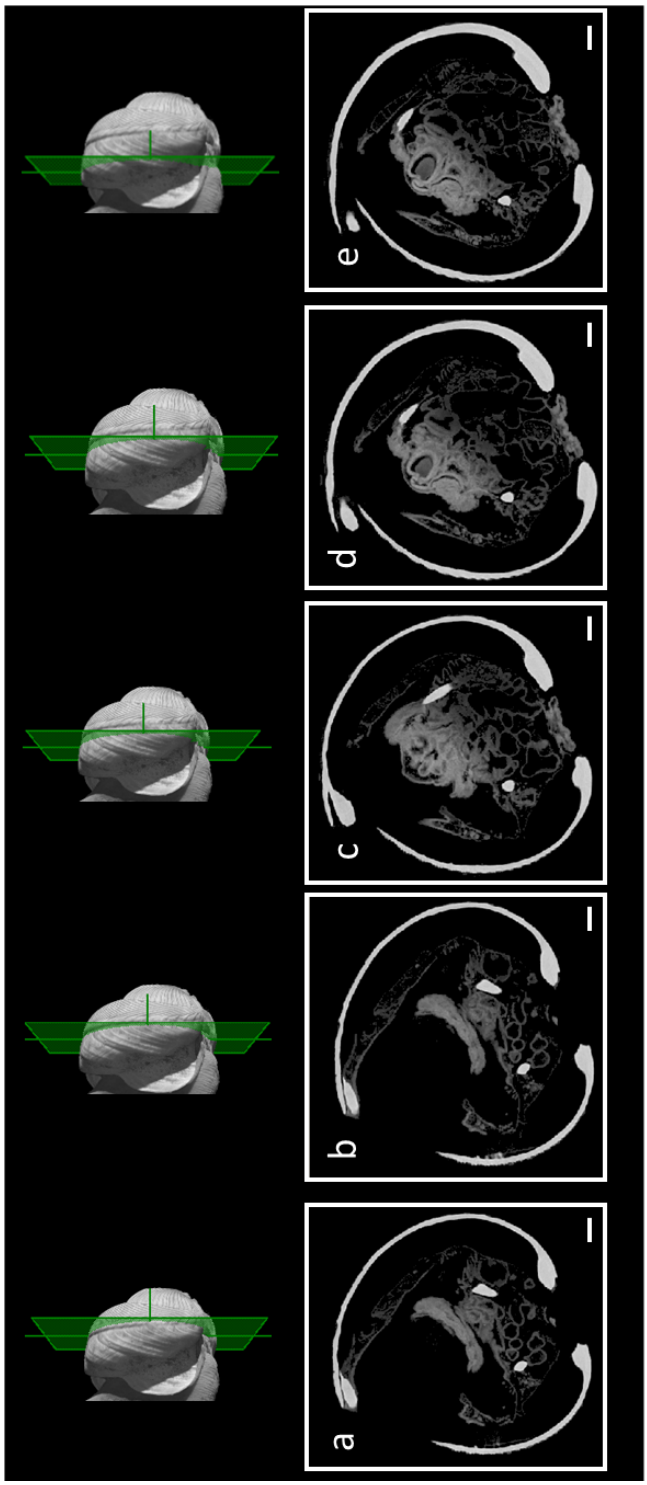

Fig. 2.18. 3-D rendered models of the mouth opening, oesophagus and stomach of *Lyrodus pedicellatus*. a) the opening to the mouth. b) inside the mouth and the beginning of the oesophagus. c) elongation of oesophagus. d) opening of the stomach. e) the elongation of the stomach. Scale bar 0.03 mm.

Discussion

The duct of Deshayes

It was not possible to accurately visualise the region containing the gland of Deshayes and the associated afferent branchial vessel. This was due to limitations in the resolution of the micro-CT 3-D rendering of *L. pedicellatus*, the ctenidial contraction of the specimen examined – resulting in inconsistent orientation of ctenidial tissue – and the presence of a large larval brood, which altered the ctenidial structure. Yet visualisation of the mouth and oesophagus failed to reveal any duct or opening, or any association with structures related to the gill. Although numerous anatomical investigations of the Teredinidae are described in the literature, the 'duct of Deshayes', a structure linking the resident symbionts of the gland of Deshayes with the hosts' digestive system, has only been described in *Teredo furcifera* (Nair & Saraswathy, 1971).

Further work should aim to examine the early life-history stages of *L. pedicellatus* to definitively clarify whether the 'duct of Deshayes' exists in this species, or, indeed, within the Teredinidae. By examining larval and juvenile individuals – post-metamorphic yet pre-sexual maturation – the problems associated with the structural changes of the ctenidia during brooding would be avoided. Furthermore, the respiratory and digestive systems of juvenile specimens would not have undergone the extensive growth and elongation of adults, thus making the potential identification of this duct more feasible.

Anatomical adaptations towards xylotrophy

A number of key anatomical features suggest *L. pedicellatus* has a greater reliance on xylotrophy than planktotrophy. Whilst the filter-feeding mechanism is clearly functional, the reduced capacity of the ctenidia, as evidenced by the abundance of larvae retained within brood pouches on the gill, and small labial palps suggest planktotrophy is of limited importance in *L. pedicellatus*. Early investigations on the anatomy and life history strategy of the Teredinidae perceived long ctenidia as an adaptation towards efficient filter-feeding (Ridewood, 1903; Turner, 1966; Nair & Saraswathy, 1971). Indeed the ctenidia of species from the genus *Teredora* and *Uperotus* extend the entire length of the body, from the base of the siphons to the mouth (Turner, 1966). These species are thought to rely almost entirely on plankton for nutrition. However, this interpretation was challenged by the recent discovery of bacterial symbionts which are located in a specialised region of the ctenidia (Popham & Dickson, 1973) and are thought to produce cellulolytic enzymes which aid the host in lignocellulose digestion (Waterbury *et al.*, 1983; Distel *et al.*, 1991).

As increased ctenidial capacity would also support a larger symbiont population, it has been suggested that large gills should be reinterpreted as an adaptation towards xylotrophy (Distel *et al*., 2011). In order to determine a species reliance on either planktotrophy or xylotrophy, future studies should draw anatomical information from multiple characteristics, including size of the intestine, the specialisation of both the digestive gland and caecum, sorting ability of the palps, size and function of the gill and the volume of bacteriocytes in relation to gill size.

Whilst the ctenidia of *L. pedicellatus* are relatively large, occupying approximately 50 % of the total body length, the internal surface area is greatly reduced by the presence of larvae enclosed in specialised brood pouches. Post-metamorphosis, the larvae of *L. pedicellatus* develop rapidly into sexually-mature adults gravid with larvae (Isham & Tierney 1952; Turner & Johnson, 1971). Larval retention over the winter is common, Indeed, the author has observed year-round brooding in *L. pedicellatus,* with winter larval retention. Thus, the majority of this species' life-cycle is spent with a greatly reduced capacity for filter-feeding due to its advanced parental care. As brooding does not interfere with the region of the ctenidia containing the bacterial symbionts, the relatively large ctenidia of this species should be considered an adaptation towards xylotrophy and increased reproductive output.

The size and function of the labial palps are also considered as an indication of dietary preference. Species with large and highly developed labial palps, such as *Nototeredo norvagica*, are considered planktotrophs (Purchon, 1941). The labial palps of *L. pedicellatus* are greatly reduced, inconspicuous and display limited processing ability (Morton, 1970). Particles are supplied to the labial palps via the marginal groove: as such, the depth and capacity of the marginal groove should be considered as an additional factor in determining a species' filter-feeding ability (Moraes & Lopes, 2003). The marginal groove of *L. pedicellatus* is shallow, thus limiting the amount of filtered particles which may reach the mouth.

The caecum, the primary site of lignocellulose digestion and nutrient absorption (Betcher *et al*., 2013), is large and conspicuous and its surface area is greatly expanded by the presence of an elaborate, coiled typhlosole. The digestive diverticulum is composed of two distinct regions, one of which is believed to function specifically in lignocellulose digestion and is present only in xylotroph-dependent species (Potts, 1923; Morton, 1970). The significantly elongated stomach, which extends beyond the posterior adductor muscle,

combined with the relatively long intestine, are further adaptations towards efficient lignocellulose digestion. This is supported by the production of compact faecal pellets, which Turner (1966) associated with a more complete utilisation of wood.

Shell morphology and the boring mechanism

The 3-D rendering and high magnification images of the shell valves provide new insights into the shell morphology and the boring mechanism. For instance, the 3-D reconstruction of the shell shows the valves in a resting position, with the ventral valves overlapping by approximately 30 – 40 degrees. This would provide a greater arc of movement during the boring 'stroke', ensuring increased surface contact between the valve ridges and the burrow lining, thus increasing abrasion efficiency during burrowing. The long apophyses and broad auricle provide extensive muscular attachment for the foot and posterior adductor muscle respectively, the primary muscles involved in the boring process. Examination of the denticulated ridges demonstrates the varying function of the shell regions, with the fine, saw-like projections on the anterior slope used for cutting into the wood, whilst the blunt denticles of the anterior-median are used for grinding and enlarging the burrow (Kofoid & Miller, 1927).

Summary

1. To the author's knowledge, the research presented herein constitutes the first morphological investigation of a bivalve using X-ray scanning micro-computed tomography.

2. This technique produced 3-D renderings at a resolution of 2 μm which allowed detailed non-invasive examination of the teredinid, *Lyrodus pedicellatus,* and proved a promising technique for further anatomical studies.

3. Anatomical examination revealed the presence of an extensive larval brood maintained on the gills of the parents. A reduction in the surface area of the gill would limit the adult's ability to draw in water and capture plankton.

4. Whilst the capacity to feed on plankton was reduced, the digestive system displayed adaptations highly specialised towards wood-digestion. These include an elongated stomach, a specialised digestive gland, a large caecum with an internal typhlosole and an intestine containing faecal pellets.

5. Micro-CT analysis failed to elucidate the presence of a duct connecting the gland of Deshayes to the oesophagus, as described in *T. furcifera* (Nair & Saraswathy, 1971).

6. 3-D rendering of the shell, combined with scanning electron microscopy, provided new insights into the teredinid boring mechanism.

Chapter Three: Transcriptomic analysis of the digestive system of *Lyrodus pedicellatus* suggests an endogenous capability to deconstruct lignocellulose

Introduction

How do Teredinids Digest Wood?

Teredinids are the principle degraders of large woody biomass in marine ecosystems and play a fundamental role in the carbon cycle. Yet given their ecological importance, relatively little is known about how teredinids enzymatically degrade wood and exploit the high energy content of lignocellulose.

The teredinids ability to digest wood is believed to be enhanced by endosymbionts which produce lignocelluloses-degrading enzymes and have the ability to fix nitrogen, thus supplementing a diet composed mainly of carbohydrates (Waterbury *et al*., 1983; Distel *et al*., 1991). These symbionts are found in a region of the host gill known as the Gland of Deshayes, residing in specialised cells called bacteriocytes (Popham & Dickson, 1973). The symbiont population was initially thought to consist of a single bacterium, *Teredinibacter turnerae* (Waterbury *et al*., 1983; Distel *et al*., 1991). However, recent reports show that individual specimens of *L. pedicellatus* harbour multiple genetically distinct yet closely related bacteria, suggesting that the endosymbiont populations are complex and dynamic (Distel *et al*., 2002; Luyten *et al*., 2006). At present, *T. turnerae* remains the only member of this symbiotic consortium which has been successfully isolated and cultured (Luyten *et al*., 2006). The complete genome of *T. turnerae* revealed a multitude of genes predicted to have functionality in degrading plant polysaccharides (Yang *et al*,. 2009). Yet it is not known whether these symbiont produced enzymes are utilized by the host and the mechanism by which they are transported from the gill to the digestive system.

Whilst the gill endosymbionts have been well characterised (Distel *et al*., 1991; Luyten *et al*., 2006), microbial distribution in the teredinid digestive system remains poorly understood (Betcher *et al.*, 2012). Morphologically diverse microbial communities of high population density have been found in the intestines of five teredinid species – including *L. pedicellatus* – and are mainly confined to the food mass (Betcher *et al*., 2012). Anatomical

examination of the intestines revealed the absence of structures typically associated with organisms reliant on fermentation; nonetheless, this microbial community may still play a fundamental role in lignocellulose degradation (Betcher *et al.*, 2012). The large size of the caecum (Turner, 1966), as noted in the previous anatomical chapter, and the availability of soluble polysaccharides (Greenfield & Lane, 1953) are conditions likely to support a considerable microbial population, yet an extremely low abundance of bacteria was detected in the caecum (Betcher *et al.*, 2012).

This low microbial population density of the teredinid digestive system – particularly in the caecum, the principle site of lignocelluloses degradation and nutrient absorption - suggests observed cellulolytic activity may be due to endogenously-encoded cellulases from the genome of the host (Betcher *et al.*, 2012). Indeed, a number of invertebrates are known to encode enzymes capable of cellulose degradation (Smant *et al*., 1998; Watanabe & Tokuda, 1998; King *et al.*, 2010). The lignocellulolytic activity observed in the shipworm is likely to be a dual system similar to that of higher termites (Warnecke *et al*., 2007), utilizing enzymes which are both endogenously produced and derived from symbiotic bacterium.

Despite the evidence suggesting shipworm produce cellulases endogenously, investigations have predominantly focused on the symbionts. A single investigation on the shipworm's capacity to produce cellulases has been conducted by Honien *et al*. (2012), with transcriptomic analysis revealing sequences with predicted functionality of β-glucanases and β-glucosidases. Yet this research offers limited insight into teredinid digestion as whole specimens of *Teredo navalis* were sequenced. As a result, it was not possible to determine where these cellulose degrading enzymes were produced and where the major sites of enzyme production lie within the Teredinidae. Furthermore, no information was provided regarding the functionality of specific digestive organs or their levels of enzymatic activity.

Biomass Recalcitrance and the Structure of Lignocellulose

The plant cell wall is a complex macromolecular structure composed of three main polymers – cellulose, hemicellulose and lignin, which are collectively termed lignocellulose. Cellulose consists of repeating glucose units joined with β-1, 4 glycosidic bonds arranged in long chains (Klemm *et al.,* 2005). Parallel chains form hydrogen bonds with neighbouring chains to create a crystalline microfibril network of high tensile strength, acting as a scaffold for the plant cell wall (Sommerville, 2006). Lignocellulose

degradation is further complicated by the presence of two cellulose crystal polymorphs in the plant cell wall (O'Sullivan, 1997). Hemicellulosic polysaccharides, which include xylans, xyloglucans, mannans and glucomannans, interact with cellulose fibres to further increase the strength of the cell wall (Scheller & Ulvskov, 2010). The cellulose-hemicelluloses scaffold is filled with pectins, a family of covalently-linked, galacturonic acid-rich plant cell wall polysaccharides which are believed to regulate intracellular adhesion and function as a cement-like substance in the plant cell wall (Mohnen, 2008). The crystalline microfibril network is embedded in lignin matrix which is covalently bonded to hemicelluloses, affording further mechanical strength to the plant cell wall (Lewis & Yamamoto, 1990). The low solubility, crystalline nature and complex chemical and structural interactions between lignocelluloses endow plant cell walls with a high resistance to microbial degradation and enzymatic deconstruction, known as 'biomass recalcitrance' (Himmel *et al.,* 2007).

Enzymatic Deconstruction of Lignocellulose

A range of enzymes hydrolyse complex polysaccharides including polysaccharide lysases, carbohydrate esterases and most notably glycoside hydrolases, hereby referred to as GHs (Lovasseur *et al.,* 2013). GHs are classified according to their amino acid sequences, structural homology and substrate specificities (Henrissat & Davies, 1997; Cantarel *et al.,* 2009) and are provided with the Enzyme Commission (EC) number EC 3.2.1.-, based on the enzyme nomenclature guidelines from the International Union of Biochemistry and Molecular Biology (IUBMB). The GH classification system is available on the Carbohydrate-Active Enzyme (CAZy) server (http://www.cazy.org) and, at the time of writing, details over 150323 modules, assigned into 132 GH families representing 14 clans. Cellulolytic activity has been identified in 18 GH families (1, 3, 5, 6, 7, 8, 9, 12, 16, 17, 30, 44, 45, 48, 51, 74, 116 and 124). However, many GH families are functionally heterogeneous, displaying overlapping substrate specificities as well as sites and modes of substrate cleavage (Henrissat & Davies, 1997).

The traditional model of cellulose hydrolysis to glucose requires a multi-component enzyme system comprised of at least three types of cellulolytic enzyme: endoglucanases (EC 3.2.1.4) randomly cleave internal glycosidic bonds within the amorphous regions of the cellulose, creating new chain ends for the attachment and detachment of cellobiohydrolases; cellobiohydrolases (EC 3.2.1.91) cleave the ends of the cellulose chain exposed by endoglucanases, resulting in cellodextrin or cellobiose; and β-glucosidases (cellobiases , EC 3.2.1.21), which hydrolyse these exocellulase products into individual

monosaccharides. Additionally, there are a number of ancillary enzymes that attack hemicelluloses, for example β-xylosidases, α-d-glucuronidases, α-l-arabinofuranosidases, β-mannanases and xylanases (Shallom & Shallom, 2003). The enzymatic deconstruction of cellulose is shown in Figure 3.1.

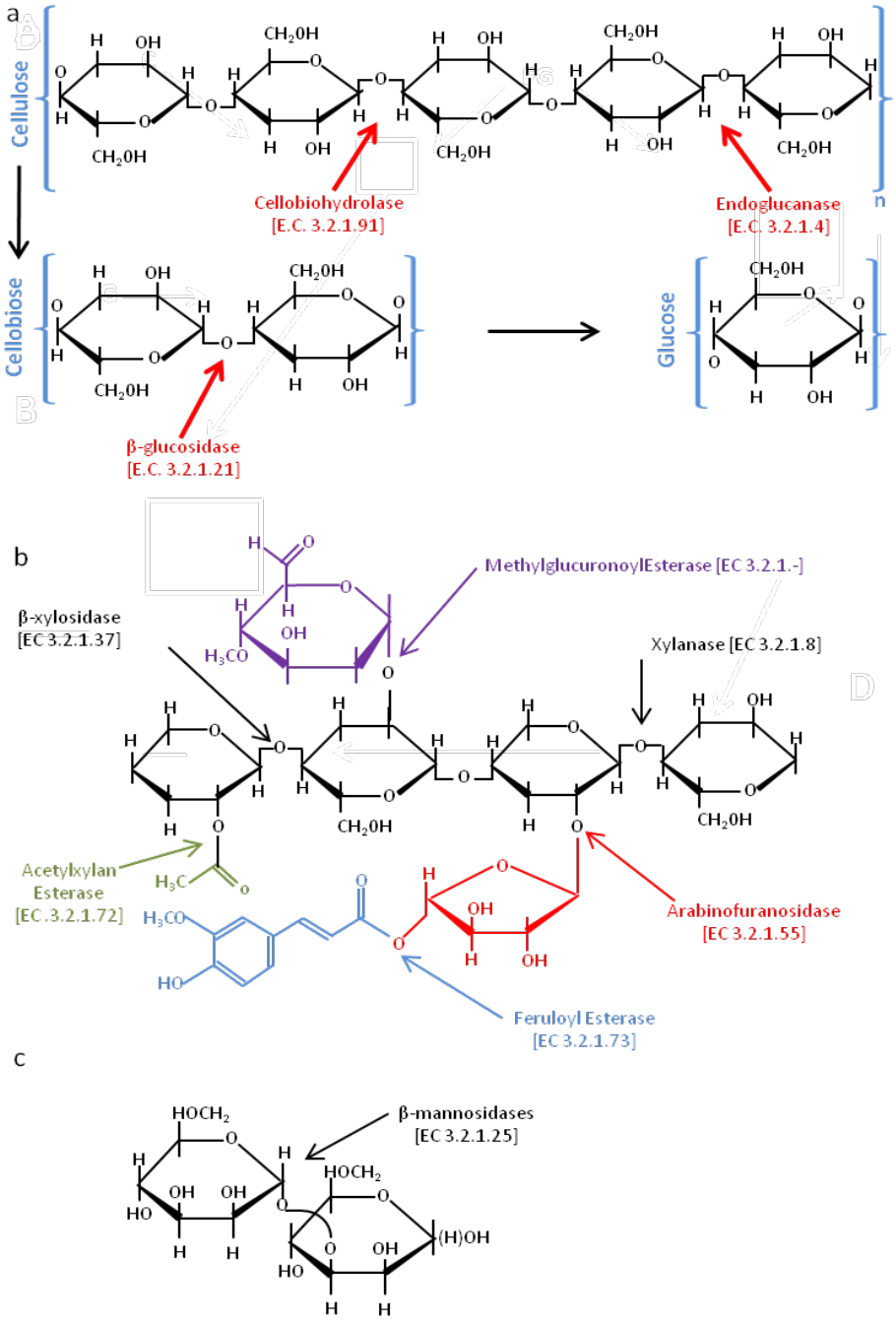

Figure 3.1 The enzymatic deconstruction of cellulose and hemicellulose. Enzymatic components, including the designated EC number, required for the breakdown of cellulose into (a) cellobiose and glucose, (b) hypothetical xylan and (c) mannan. Image modified from Yang *et al*., 2009.

The typical endoglucanases or cellobiohydrolases produced by microorganisms consist of three functional domains: the catalytic domain (CD), a carbohydrate-binding module (CBM) and a flexible linker, which connects the two regions (Wang *et al*., 2013). CBMs promote the association between enzyme and substrate by targeting specific polysaccharide polymers, thus increasing regional enzyme concentrations and catalysis rate. A number of CBMs also disrupt the structural integrity of the polysaccharide matrix, increasing CD-accessibility to potential sites of hydrolysis (Boraston *et al*., 2004; Arantes & Sadler, 2010). Like the GHs, CBMs are divided into families based on amino acid sequence homology. To date 30437 modules have been identified, belonging to 67 families (http://www.cazy.org). In addition to GH and CBM activities, carbohydrate esterases (CE) and polysaccharide lyases (PL) are also believed to play a role in complex polysaccharide degradation (Yang *et al*., 2009).

Research Outline

This research undertakes a transcriptomic analysis of the digestive system of *L. pedicellatus* in order to identify the endogenous capacity of the shipworm to enzymatically deconstruct lignocellulose. Individual digestive organs will be isolated and analysed, providing information on the specific functioning of the teredinid digestive system and levels of transcriptomic activity per organ. The caecum, proposed as the major site for enzyme production and cellulolytic deconstruction (Betcher *et al*., 2012), is of particular interest. Transcriptomic analysis will also offer insights into the host-symbiont relationship and how the dual-enzyme system overcomes the significant challenge of converting recalcitrant plant polysaccharides into monomeric sugars. Not only will this resolve the mechanism by which teredinids exploit lignocellulose as an energy source, it may also identify novel cellulases with potential application in the biofuel industry.

Material & Methods

RNA Extraction

Thirty specimens of *L. pedicellatus* were extracted from experimental lamellar panels (Fig. 3.2), taken from the cultures maintained at the Intstitute of Marine Science, University of Portsmouth. The digestive tissues (caecum, digestive gland, gill and intestine) were excised and separately placed in 800 µL Trizol® (Invitrogen) on ice. Sample tissues were homogenised using Teflon pestles, vortexed for 10 seconds and then left to incubate at room temperature for five minutes to permit complete dissociation of nucleoprotein complexes.

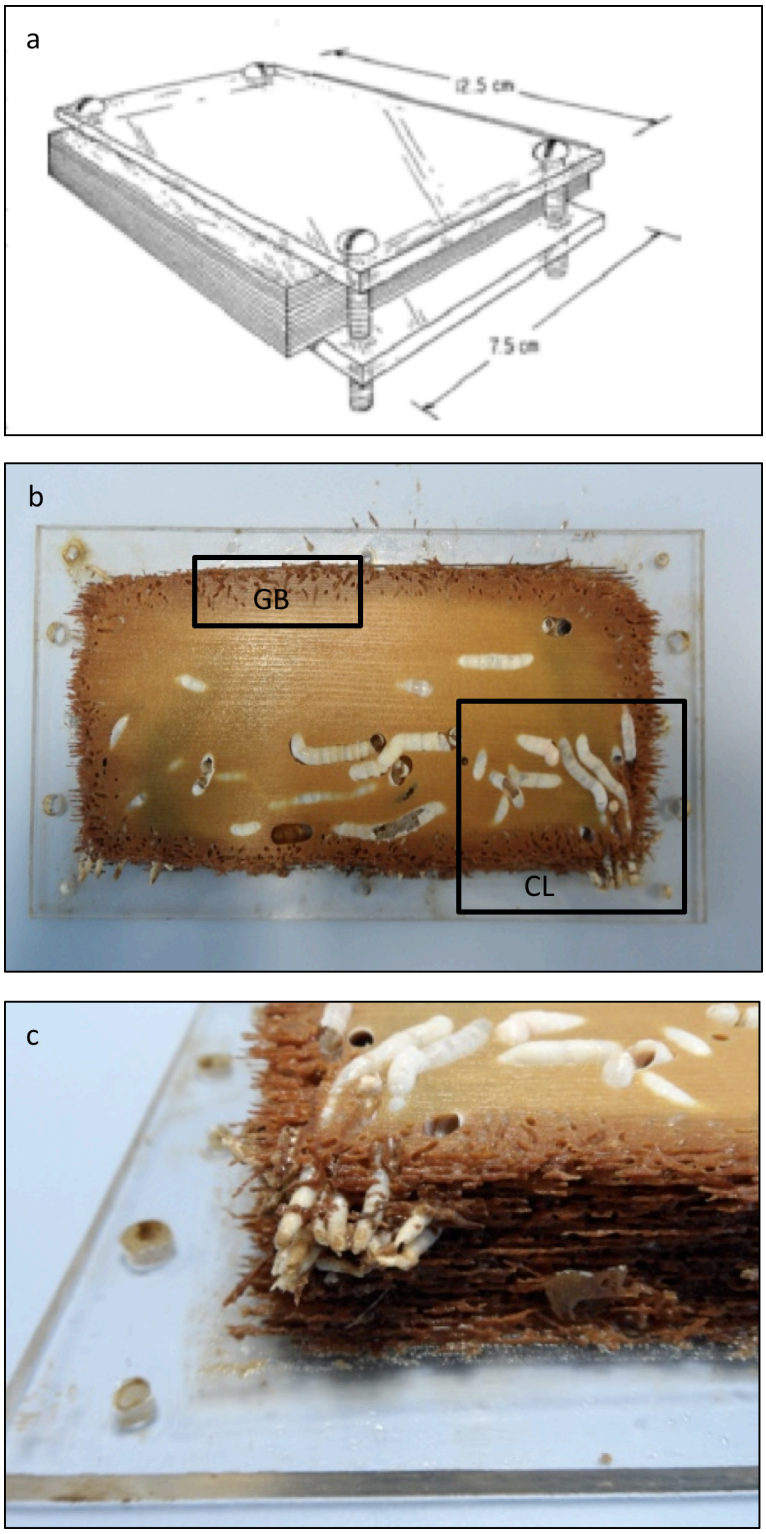

Figure 3.2 Experimental design of a wooden panel composed of thin wood laminae sheets compressed between two pieces of Plexiglas. a) Image taken from Manyak (1982). b-c) Showing teredinid infestation of experimental wooden panels. GB, gribble burrow; CL, calcareous lining formed by teredinids.

A 200 µL aliquot of chloroform was added to the homogenate, which was shaken vigorously and then left to incubate at room temperature for three minutes. Samples were centrifuged at 12,000 × g for 15 minutes at 4 °C. The aqueous phase was removed and transferred to a new microcentrifuge tube and 200 µg RNase-free glycogen was added to each sample to aid precipitation. A 400 µL aliquot of isopropanol was added and samples were mixed by gently inverting the microcentrifuge tubes, which were then left to incubate at room temperature for ten minutes. Samples were then centrifuged at 12,000 × g for ten minutes at 4 °C. The resulting RNA pellet was isolated by removing the supernatant and was then washed with 800 µL of chilled 70 % v/v ethanol before centrifugation at 14,000 × g for four minutes at 4°C. The RNA pellet was then air-dried for ten minutes before re-suspension in 123 µL RNase-free water.

To confirm the integrity of the RNA, a 3 µL aliquot of each sample was mixed with 1 µL of 5 × Orange G dye, 1 µL of dH_2O and the product was loaded onto a 1 % w/v agarose gel (containing 0.5 g agarose dissolved in 50 mL 1 × TBE buffer and 3 µL 10 mg/mL ethidium bromide) and electrophoresed at 120 V for fifteen minutes. RNA was then visualised under UV excitation.

rRNA Depletion and Clean-up

DNA and divalent cations were removed from samples using the Turbo DNA-free™ Kit (Invitrogen), following the manufacturers protocol. For the caecum and gill samples, probes were combined from both the RiboZero™ Magnetic Gold Kit (Human/Mouse/Rat) and RiboZero™ Magnetic Gold Kit (Bacteria) to deplete ribosomal RNA and isolate RNA molecules. For the digestive gland sample, pure PolyA mRNA was isolated using the Oligotex mRNA Mini Kit (QIAgen) following the manufacturer's protocol. Samples were then cleaned and concentrated using the RNA Clean and Concentrator™-5 (Zymo Research), following the manufacturers protocol. The concentrations and quality of RNA were assessed using both the Agilent 2200 Tapestation System and the Qubit® 2.0 Fluorometer (Life Technologies).

Whole Transcriptome Library

RNA samples were fragmented with RNase III, cleaned and hybridized prior to reverse transcription. The resulting cDNA libraries were prepared, purified and amplified following the manufacturer's protocol (Ion Total RNA-Seq Kit, Life Technologies™). The

quality and quantity of the amplified DNA samples were assessed using both the Agilent 2200 Tapestation System and Qubit® 2.0 Fluorometer (Life Technologies).

Sequencing & Assembly

DNA fragments were attached to the surface of Ion Sphere™ particles (ISPs) and amplified following the manufacturer's protocol (Ion Torrent OneTouch template Kit, Life Technologies). Sequencing was carried out using the Ion Sequencing Kit, according to the Ion Torrent user guide. Following amplification, samples were washed according to the Ion Template Solution Kit protocol (Life Technologies), mixed with sequencing reagents (Ion Sequencing Reagent Kit) and template ISPs were loaded onto a 318 chip for sequencing with the Ion Torrent Personal Genome Machine™ (Life Technologies). For the caecum sample, amplification and sequencing was repeated and the raw reads were pooled.

The raw reads of all three libraries (caecum, digestive gland and gill) were pooled and assembled into 33, 9352 total contiguous (hereby referred to as contigs) consensus sequences using the MIRA assembly software package. The raw reads of individual libraries were then re-mapped onto these contiguous (contigs) sequences respectively with the BWA mapping software to obtain read counts for each contig. The top 1000 contigs with the highest total counts of all three libraries were subsequently annotated using the Blast2GO software package. Contigs were ranked according to transcript abundance (measured by the number of mapped reads), with the contig composed of the largest number ranked 1st, and so on.

Sequencing was carried out at the University of York with the assistance of Dr Deborah Rathbone and the sequence libraries were annotated by Dr Yi Li and Dr Zhesi He from the Centre for Novel Agricultural Products (CNAP), also at the University of York.

Analysis

Sequences of interest were further analysed using a number of comparison tools. The program ExPASy was used to translate nucleotide sequences into protein sequences (Artimo *et al*., 2012). These were then aligned and compared with previously banked sequences using the Basic Local Alignment Search Tool, hereafter referred to as BLAST (Mount, 2007), the protein homology/analogy recognition engine PHYRE (Kelley & Sternberg, 2009) and the structure homology modelling program Swiss Model (Arnold *et al*., 2007).

Results

Sequencing

RNA was isolated from the digestive gland, caecum and gill of the shipworm *Lyrodus pedicellatus* as shown in Figure 3.3.

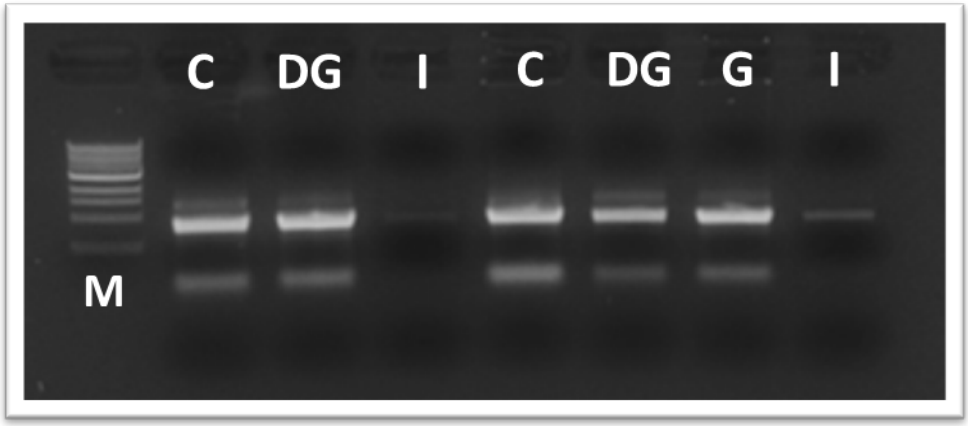

Figure 3.3 Purified RNA from the caecum (C), digestive gland (DG), intestine (I) and gill (G) of *L. pedicellatus,* electrophoresed and shown on a 1 % agarose gel. 1M denotes the 100 bp gel marker.

Quantities of RNA isolated from the intestine (I) were of insufficient concentration for downstream processing (Fig. 3.3). For the first run of the digestive gland and gill samples, there was total coverage of 88 % of addressable wells on the 318 chip (9,957,745 out of the 11,306,333 of available wells). Of the loaded ISPs, 96 % (9,535,911) were template bearing, yet 27 % of these were polyclonal and 8 % were either of low quality or contained primer dimer. This left a final library read of 6,148,062. A total number of 6,145,827 reads were generated equating to 856.64 Mbp (695 Mbp for the digestive gland and 153 Mbp for the first gill sample). The longest read length was 384 bp with a mean length of 139 bp. A summary of the ISP and the sequence run data for the digestive gland and first caecum sample, including the total number of template attached to ISP's, the ISP coverage on the 318 Ion Torrent chip and a breakdown of the sequence data is shown in Figure 3.4a.

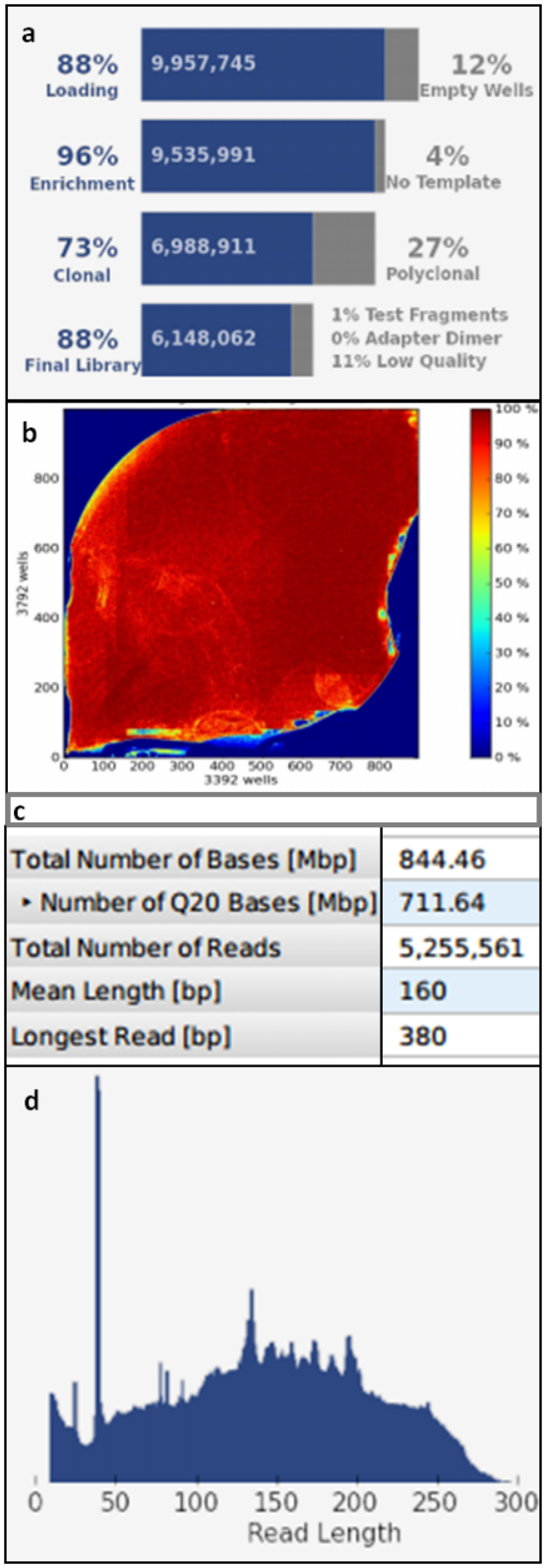

Figure 3.4a Ion Sphere Particle (ISP) and sequencing summary for the second caecum and gill samples. a-b) the sequence load quality and quantity and ISP coverage of the 318 Ion Torrent Sequencing chip. c – d) the EST library properties, including total number of bases analysed and reads produced and the mean and longest mean sequence length (BP).

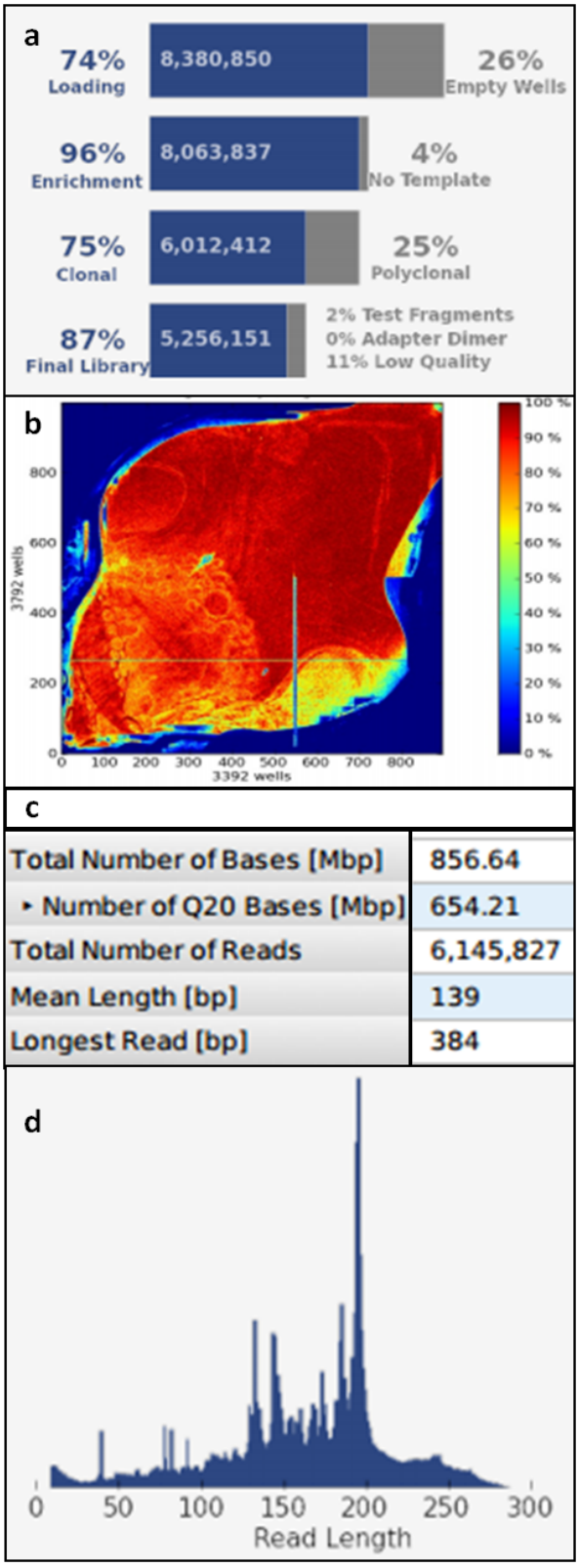

Figure 3.4b Ion Sphere Particle (ISP) and sequencing summary for the digestive gland and first caecum samples. a-b) the sequence load quality and quantity and ISP coverage of the 318 Ion Torrent Sequencing chip. c – d) the EST library properties, including total number of bases analysed and reads produced and the mean and longest mean sequence length (BP).

For the second run of the caecum and gill samples, there was total coverage of 74 % of addressable wells on the 318 chip (8,380,850 out of 11,308,321 of available wells). Of the loaded ISPs, 96 % (7,932,275) were template bearing, yet 26 % of these were polyclonal and 8 % were either of low quality or contained primer dimer. This left a total final library read of 5,256,151. A total number of 5,255,561 reads were generated equating to 844.46 Mbp (561 Mbp for the caecum and 278 Mbp for the second gill sample). The longest read length was 380 bp with a mean length of 168 bp. A summary of the ISP and the sequence run data the gill and second caecum sample, including the total number of template attached to ISP's, the ISP coverage on the 318 Ion Torrent chip and a breakdown of the sequence data is shown in Figure 3.4b. ISP data and the sequence run summary for the gill and second caecum sample are shown in Figure 3.5b. Due to low coverage during the first sequence run, gill reads were repeated during the second run and both sets of sequence reads were pooled into one data set.

Transcriptome Analysis

Tables 3.1, 3.2 and 3.3 detail the top twenty most abundantly expressed transcripts for each tissue as identified by BLAST analysis. Details include the GenBank accession number, E-value, the read abundance based on the number of ESTs and the percentage with which these read accounts for the entire transcription. Ribosomal transcripts dominated the top 20 most expressed transcripts in the caecum and gill, accounting for 7 out of 20 of the top transcripts (50.8 % of top 20 total reads) in the caecum and 8 out of 20 of the top transcripts (42.4 % of top 20 total reads) in the gill. This compares with only two ribosomal transcripts in the digestive gland, accounting for 1.6 % of the total top 20 reads. BLAST searches for unannotated sequences revealed no significant similarities. Unannotated sequences accounted for 1, 3 and 2 reads out of 20 top reads in the digestive gland, caecum and gill, respectively. These corresponded to 1.0 %, 6.7 % and 1.3 % of the top 20 total reads, respectively.

	Annotation	Organism	GenBank	E-Value	Reads	%
1	Hypothetical protein	*B. taurus*	DAA15227	1.73E-18	11741	1.88
2	Uncharacterized protein	*G. max*	XP_003542272	7.12E-07	11219	1.79
3	Unnamed protein product	*M. fascicularis*	BAE89779	3.20E-22	8005	1.28
4	Myosinase-1-like	*M. rotunda*	XM_003705406	0.001	6477	1.04
5	No significant similarity				6328	1.02
6	18s ribosomal RNA gene	*P. amurensis*	EF035108.1	9.00E-62	5691	0.91
7	Hypothetical protein	*C. gigas*	EKC19484	2.91E-137	5374	0.86
8	Collagen alpha-4(vi) chain	*C. gigas*	EKC19483	0.00E+00	5164	0.83
9	Unknown	*Z. mays*	ACR38454	4.98E-22	5146	0.83
10	Collagen alpha-5 (vi) chain	*C. gigas*	EKC40283	1.96E-92	4897	0.79
11	Collagen alpha-4 (vi) chain	*C gigas*	EKC40282	0.00E+00	4654	0.75
12	18s ribosomal RNA gene	*P. amurensis*	EF035108.1	2.00E-61	4273	0.69
13	Thioester-containing protein	*C. farreri*	ADA77515	0.00E+00	4069	0.65
14	Hypothetical protein	*B. floridae*	XP_00263630	4.39E-15	3904	0.63
15	Uncharacterized protein	*G. max*	XP_00354272	1.23E-08	3834	0.62
16	Collagen alpha-4(vi) chain	*C. gigas*	EKC40282	1.49E-116	3681	0.59
17	Exoglucanase xynx	*C. gigas*	EKC38981	1.13E-67	3300	0.53
18	Hypothetical protein	*Acinetobacter sp.*	ZP_0914523	9.61E-21	3184	0.51
19	Cytochrome b	*S. scabra*	YP_00657415	2.27E-111	3007	0.48
20	Collagen alpha-1 chain	*C. gigas*	EKC40282	3.34E-39	2817	0.45
		Total Transcript %				**17.2**

Table 3.1. The top twenty most abundantly represented ESTs from the digestive gland of *Lyrodus pedicellatus*. The combined top twenty reads are expressed as a % of the overall transcriptome.

	Annotation	Organism	GenBank	E-Value	Reads	%
1	18s Ribosomal RNA Gene	*P. amurensis*	EF035108.1	9.00E-62	208846	16.5
	18s Ribosomal RNA Gene	*P. amurensis*	EF035108.1	5.00E-60	194974	15.4
3	18s Ribosomal RNA Gene	*P. amurensis*	EF035108.1	2.00E-61	136213	10.7
4	protein	*S. purpuratus*	XP_785151.3	2.00E-05	91395	7.20
5	18s Ribosomal RNA Gene	*P. amurensis*	EF035108.1	4.00E-60	69305	5.46
6	No significant similarity				62793	4.95
7	Uncharacterized protein	*S. harrisii*	XP_0036447.1	2.28E-08	38297	3.02
8	No significant similarity				32426	1.15
9	18s Ribosomal RNA Gene	*P. amurensis*	EF035108.1	2.00E-60	14536	1.15
10	proteasome maturation protein	*N. vectensis*	XP_0016785.1	4.02E-25	13358	1.05
11	pol-like protein	*D. pseudobscura*	XP_0021676.1	1.61E-08	12603	0.99
12	18s Ribosomal RNA Gene	*P. amurensis*	EF035108.1	4.00E-60	12403	0.98
13	BRAFLDRAFT_129679	*B. floridae*	XP_0023630.1	4.39E-15	11780	0.93
14	H1 transcribed RNA sequence	*B. siamensis*	GAGS018003.1	8.00E-21	11052	0.87
15	regulator of sigma e activity	*T. turnerae*	YP_00307759.1	9.94E-26	9578	0.75
16	cell wall-associated hydrolase	*B. multivorans*	dbj|BAG4932.1	4.65E-26	8373	0.66
17	No significant similarity				8189	0.65
18	antisense-ribosomal RNA protein	*A. capsulatus*	gb|EGC42647.1	4.30E-09	8133	0.64
19	uncharacterized protein	*S. harrisii*	gi|395504206	8.78E-06	7960	0.63
20	uncharacterized protein	*S.harrisii*	gi|395504206	5.60E-05	7415	0.58
		Total Transcript %				**75.59**

Table 3.2 The top twenty most abundantly represented ESTs from the caecum of *Lyrodus pedicellatus*. The combined top twenty reads are expressed as a % of the overall transcriptome.

	Annotation	Organism	GenBank	E-Value	Reads	%
1	18s Ribosomal RNA Gene	*P. amurensis*	EF035108.1	9.00E-62	52854	12.03
2	18s Ribosomal RNA Gene	*P. amurensis*	EF035108.1	2.00E-61	47387	10.79
3	Uncharacterized protein	*G. max*	XP_0035427	7.40E-07	31708	7.22
4	18s Ribosomal RNA Gene	*P. amurensis*	EF035108.1	9.00E-60	24369	5.55
5	18s Ribosomal RNA Gene	*P. amurensis*	EF035108.1	4.00E-60	20967	4.77
6	18s Ribosomal RNA Gene	*P. a amurensis*	EF035108.1	2.00E-60	19877	4.53
7	18s Ribosomal RNA Gene	*P. amurensis*	EF035108.1	5.00E-60	11368	2.59
8	18s Ribosomal RNA Gene	*P. amurensis*	EF035108.1	3.00E-62	6534	1.49
9	Uncharacterized protein	*S. harrisii*	XP_0037567	2.28E-08	6052	1.38
10	sjchgc01393 protein	*Z. mays*	ACR38454	4.98E-22	4435	1.01
11	BRAFLDRAFT_129679	*B. floridae*	XP_00260330	4.39E-15	4297	0.98
12	No Significant Similarity				3487	0.79
13	18s Ribosomal RNA Gene	*P. amurensis*	EF035108.1	2.00E-60	2849	0.65
14	pol-like protein	*D. pseudoobscura*	XP_00213766	1.61E-08	2842	0.65
15	predicted protein	*N. vectensis*	XP_00162709	9.12E-09	2833	0.65
16	Ch308 microsatellite sequence	*C. hongkongensis*	HM461241.1	4.00E-35	2816	0.64
17	proteasome maturation protein	*N. vectensis*	XP_00163775	4.02E-25	2544	0.58
18	OXYTRI_13058	*O. trifallax*	EJY66653	1.86E-46	2431	0.55
19	No Significant Similarity				2366	0.54
20	protein	*O. trifallax*	EJY65597	1.36E-24	2105	0.48
		Total Transcript %				**57.85**

Table 3.3 The top twenty most abundantly represented ESTs from the gill of *Lyrodus pedicellatus*. The combined top twenty reads are expressed as a % of the overall transcriptome.

The digestive gland transcriptome analysis produced a total of 6,233,660 read counts, of which 32,955 – representing 5.3 % of the total count - were predicted to encode catalytic domains of glycoside hydrolase families (GHs). BLAST and PHYRE analysis, as shown in figures 3.6 and 3.7 respectively, identifies a total of 26 GH sequences within the top 1000 transcripts produced by the digestive gland. These include sequences representing nine different GH family domains (GH families 1, 2, 5, 9, 10, 13, 16, 18 and 45) following the CAZy nomenclature for carbohydrate-active enzymes. Eight out of the 25 (GHs 1, 9, 10,

13, and 18) were found in the top 100 most abundant transcripts and two of these (GH 1 and 9) were found in the top 20 most abundant transcripts. A comparison between GHs from both the symbiont and the host digestive gland are shown in Figures 3.5 and 3.6.

No.	Description	GH Family	Max score	Query cover	E value	Max I.D	Accession
6	lactase [*S. purpuratus*]	GH1	703	99%	0	55%	XP_79769.2
19	Exoglucanase xynX [*C. gigas*]	GH10/CBM4-9	138	94%	6.00E-33	31%	EKC38981.1
35	alpha-amylase [*C. fluminea*]	GH13	758	85%	0	77%	AAO17927.2
37	cellulase [*C. japonica*]	GH9	407	94%	3.00E-133	52%	BAF38757.1
58	cellulase [*C. japonica*]	GH9	498	97%	1.00E-161	56%	BAF38757.1
64	Putative chitinase 3 [*C. gigas*]	GH18	537	94%	4.00E-176	74%	EKC38803.1
76	cellulase [*C. japonica*]	GH9	446	95%	5.00E-148	53%	BAF38757.1
78	endoglucanase [*M. yessoensis*]	GH9	244	99%	5.00E-72	42%	BAH85844.1
107	endo-1,4-beta-glucanase [*C. japonica*]	GH45	199	89%	4.00E-61	59%	BAH23794.1
167	Exoglucanase xynX [*C. gigas*]	GH10/CBM4-9	362	98%	4.00E-110	35%	EKC38981.1
169	Chitotriosidase-1 [*C. gigas*]	CBM14	121	57%	7.00E-28	38%	EKC38802.1
181	Processive-cellulase [*S. cyanosphaera*]	GH9	110	95%	2.00E-26	47%	YP_007174.1
200	cellulase [*C. aponica*]	GH9	407	100%	3.00E-134	55%	BAF38757.1
253	Mannan endo-1,4-beta-mannosidase	GH5	370	97%	5.00E-123	49%	Q8WPJ2.1
300	cellulase [*C. japonica*]	GH9	404	100%	1.00E-132	57%	BAF38757.1
346	Beta-mannosidase [*C. gigas*]	GH2	447	96%	7.00E-149	47%	EKC29480.1
377	endo-1,4-beta-xylanase [*C. japonica*]	GH10/CBM4-9	1002	99%	0	59%	BAH84829.1
392	endoglucanase [*M. yessoensis*]	GH10	147	90%	7.00E-39	52%	BAH85844.1
397	Exoglucanase/xylanase [*S. davawensis*]	GH10	391	63%	3.00E-129	23%	YP_0079292.1
431	Endoglucanase [*C. gigas*]	GH45	78.6	100%	1.00E-15	62%	EKC38125.1
457	beta-glucan recognition protein [*T. literata*]	GH16	595	96%	0	67%	AEE89455.1
474	endo-1,4-beta-glucanase	GH9	114	86%	8.00E-28	23%	XP_0025114.1
499	endo-1,4-beta-glucanase precursor [*G. max*]	GH10	109	70%	7.00E-29	51%	ABC70312.1
510	endo-1,4-beta-glucanase [*C. japonica*]	GH10	204	81%	2.00E-62	51%	BAH23793.1
523	alpha-amylase [*B. germanica*]	GH13	258	93%	2.00E-80	51%	ABC68516.1
532	alpha-amylase [*B. germanica*]	GH13	258	93%	2.00E-80	51%	ABC68516.1

Table 3.4 GH and CBM families identified within the digestive gland transcriptomic data. Sequences identified using Basic Local Alignment Search Tool (BLAST) and include the predicted function and GH family classification, the query coverage of analysed sequence and the E-value and maximum identity.

	PDB Molecule/Superfamily	PDB Title/Family	Confidence %	Coverage %	I.D. %
6	beta-glucosidase	beta-glucosidase	100	39	47
19	endo-1,4-beta-xylanase y	endo-1,4-beta-d-3 xylanase cbm22	100	80	21
35	alpha-amylase 1	alpha-amylase	100	86	53
37	endo/exocellulase e4	endo/exocellulase	100	89	41
58	endoglucanase 9g	endoglucanase 9g	100	47	41
64	acidic mammalian chitinase	chitinase	100	94	50
76	endo/exocellulase e4	endo/exocellulase	100	90	45
78	endo/exocellulase e5	endo/exocellulase	100	96	38
107	Barwin-like endoglucanases	Eng V-like	100	89	58
167	endo-1,4-beta-xylanase	endo-1,4-beta-d-3 xylanase cbm22	100	77	20
169	Chitin-binding proteins	Tachycitin	99.5	18	31
181	endo/exocellulase e4	endo/exocellulase	99.8	94	44
253	beta-1,4-mannanase	beta-1,4-mannanase	100	94	47
300	endoglucanase 9g	endoglucanase 9g	100	97	35
346	beta-mannosidase	beta-mannosidase	100	94	31
377	endo-1,4-beta-xylanase	endo-1,4-beta-d-3 xylanase cbm22	100	54	19
392	endoglucanase 9g	endoglucanase 9g	99.8	18	56
397	endo-beta-1,4-xylanase	xylanase10c	100	73	23
457	endo-1,3-b-glucanase	endo-1,3-b-glucanase	100	62	34
474	endo/exocellulase e4	endo/exocellulase	100	97	39
510	Barwin-like endoglucanases	Eng V-like	100	77	44

Table 3.5 GHFs identified within the digestive gland transcriptomic data. Sequences identified using PHYRE by comparing predicted structural homology with known enzyme structure on the Protein Data Bank (PDB). Table includes data on PDB family, the coverage of analysed sequence and confidence of identity (%).

The caecum transcriptome analysis produced a total of 1,269,434 read counts, 865 of which were predicted to encode for catalytic domains of GH families (representing 0.1 % of the total count). A total of 22 GH domains were found in the top 1000 transcripts, including the sequences of eight different GH family domains (GH families 1, 2, 5, 9, 10, 13, 18 and 45) following the CAZy nomenclature for carbohydrate-active enzymes. However, these were weakly expressed as only GH1 appeared within the top 300 most abundantly expressed transcripts (at position 276). Analysis of the gill revealed transcripts for four GHs (one GH10 and three GH9 enzymes), yet these were based on a single read count for each and were outside the top 700 most abundantly expressed transcripts.

For the digestive gland, the GH transcripts are dominated by GH families 1, 9 and 10, which account for 70 % of total GHs (20.2 %, 33.1 % and 16.7 %, respectively). GH families 13, 18 and 45 accounted for just fewer than 25 % of the total GH transcripts (8.3 %, 8.0 % and 8.4 %, respectively). The GH family's 2, 5 and 16 account for 1.9 %, 2.4 % and 1.6 %, respectively, of the remaining GH transcripts. Similarly, the caecum GH transcripts are also dominated by GH 1 and 9, both of which comprise over 80 % of the total GH read counts (34.6 % and 47.1 %, respectively). GH 13 and 45 account for 13.4 % (6.0 % and 7.4 %, respectively), with GH 2 (0.2 %), 5 (1.2 %), 10 (0.9 %) and 18 (2.5 %) comprising the remaining read counts. The GH transcripts expressed in the gill account for <0.01 % of the total read counts and were of insufficient significance for further analysis.

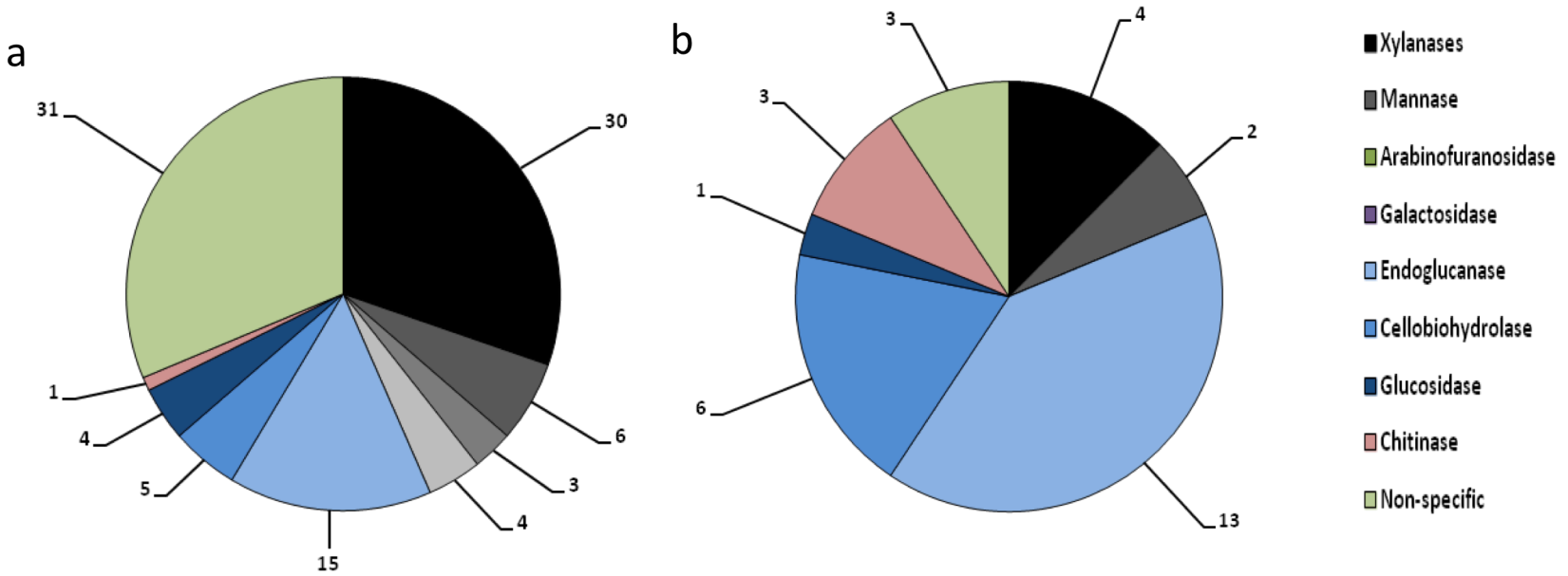

Fig. 3.5. Prevalence of GH domains as a function of substrate specificity. a). GHs from the genome of the bacterial symbiont *Teredinibacter turnerae* taken from Yang *et al*. (2009). b). GHs from the digestive gland transcriptome of *Lyrodus pedicellatus*. GH domains are sorted by known substrate specificity and are presented as the total number of GHs from the bacterial symbiont and the host digestive gland respectively. Substrate specificities are coded as follows: black = xylanases (GH families 5, 7, 8, 10, 11 and 43); dark grey = mannanases (GH families 2, 5 and 26); arabinofuranosidases (GH families 3, 27, 43, 51 and 62); white = galactosidases (GH families 1, 2, 5, 16, 28, 35, 43, 53); light blue = endoglucanases (GH families 1, 3, 5, 9, 12, 16, 44, 45, 51 and 74); dark blue = cellobiohydrolases (GH families 5, 7, 9, 74 and 94); navy blue = glucosidases (GH families (GH families 1, 3, 5, 9, 13 and 31) ; red = chitinase (GH families 18); green = GHs with no known specificity towards lignocellulolytic deconstruction.

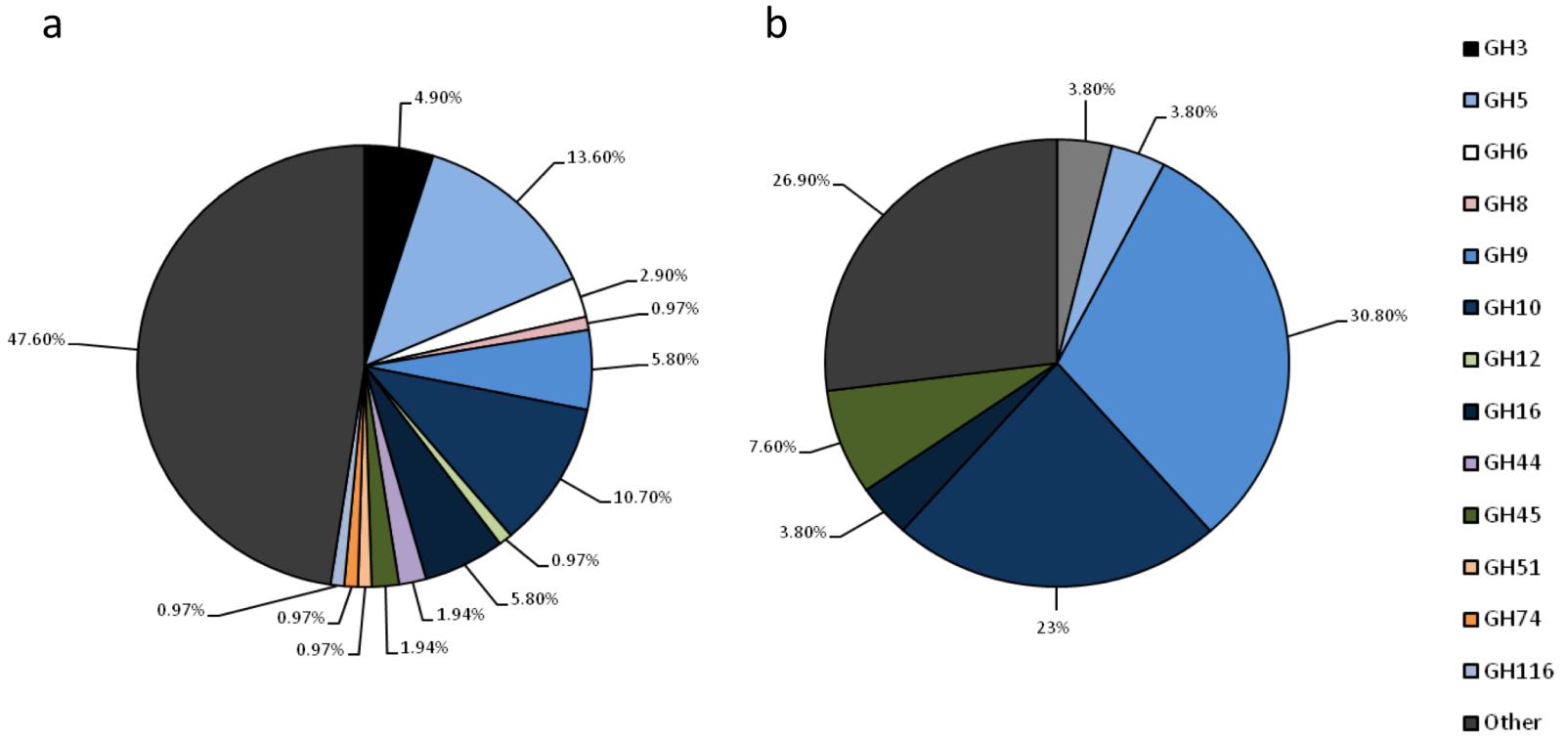

Fig. 3.6 Abundance of GHFs with known activity towards cellulose. a). GHFs from the genome of the bacterial symbiont *Teredinibacter turnerae* taken from Yang *et al*. (2009). b). GHFs from the digestive gland transcriptome of *Lyrodus pedicellatus*.

Discussion

Of the four digestive tissues samples, only the intestine failed to produce sufficient quantities of RNA for further downstream processing. The top twenty most abundant transcripts from the gill and caecum dominated the transcriptome of those organs, accounting for 58 % and 76 % of the total transcriptome respectively. This contrasts with the digestive gland, in which the top 20 transcripts only accounted for 17 % of the overall transcriptome. The greater transcriptomic diversity seen in the digestive gland in comparison to both the gill and caecum tissue may be explained by the differences in rRNA extraction, with the former technique using polyA extraction compared with rRNA depletion in the latter. Of the transcripts involved in GH (glycoside hydrolase) production, the caecum produced very low numbers of GHs, totalling 0.7 % of the entire transcriptome. The most highly-expressed GH from this tissue, ranked at position 276, produced only 299 reads. As the primary site of both digestion and nutrient absorption, it was predicted that the caecum might play a fundamental role in the endogenous production of enzymes with cellulolytic capabilities (Betcher *et al.*, 2012). However, this view is not supported by the transcriptomic data set, which suggests the caecum is not a site of GH transcription and plays a limited role in cellulolytic enzyme production. The digestive gland, which has a close association with the caecum, is thought to play a role in both xylotrophy and planktotrophy (Morton, 1970). Transcriptomic analysis of the digestive gland revealed a range of endogenously-produced enzymes with predicted cellulolytic function (GH families 1, 2, 5, 9, 10, 13, 16, 18, 45) accounting for 5 % of the total transcriptome, and a number of GHs ranked in the top 100 most highly-expressed transcripts. Analysis of the gill failed to reveal a single endogenously-encoded cellulolytic enzyme. As such, further discussion of these results concentrates solely on the digestive gland, which appears to play a fundamental role in wood digestion for the shipworm.

GH 13 amylase and GH 16 & 18 chitinases

Transcriptomic analysis revealed the presence of a number of GHs from families whose members play no active role in cellulose deconstruction. Putative GH family (GHF) 13 α-amylases (EC 3.2.1.1) ranked at positions 33, 521 and 530 of the top one thousand transcripts. This amylolytic enzyme depolymerises starch into glucose by hydrolysing the α-glucosidic linkages and is found in many phyla of the animal kingdom (Svensson, 1994; Janeček, 1997).

The 62nd most abundant contig (contiguous sequence) was predicted by BLAST, PHYRE and Swiss Model to be a GHF 18 chitinase (EC 3.2.1.14). The *T. turnerae* genome also

revealed the presence of a chitinase (EC 3.2.1.14) from GHF 18, with associated CBMs 2, 5 and 10. Generally, members of this family bind to insoluble chitin, the major structural component of arthropod exoskeletons and the fungal cell wall, hydrolysing the β-1, 4-linkages and producing chitobiose (Li & Greene, 2010). An invertebrate chitin-binding protein assigned to CBM family 14 was identified as the 169th most highly expressed transcript. This CBM lacks association with catalytic activity from the enzyme, yet may independently function to degrade insoluble chitin (Tjoelker *et al.*, 2000; Huang *et al.*, 2012). Chitinases do not bind to or show activity with other polysaccharides such as cellulose, mannan, xylan or laminarin (Kawabata *et al.*, 1996; Huang *et al.*, 2012). It is therefore unlikely that the chitinase and chitin CBM play an active role in cellulolytic deconstruction, yet the high expression of this enzyme suggests an important role.

There are a number of plausible explanations for the production of chitinases. Chitinolytic enzymes are used by a range of organisms as antimicrobial defence molecules against fungal pathogens (Kawabata *et al.*, 1996; Dahiya *et al.*, 2010) and a large diversity of fungi and many species are found colonizing wood in marine environments (Richards *et al.*, 2012). A number of these species are also cellulolytic (Hyde *et al.*, 1998). It is therefore possible that teredinids produce chitinases to deter competition from fungi for glucose-rich cellulose. Finally, cellulose-degrading soil microbes are known to degrade chitin and utilize it as a nitrogen source to supplement their nitrogen-deficient diet (Reguera & Leschine, 2001). Whilst teredinids derive most of their nitrogen from the resident symbionts (Lechene *et al*., 2007; Nishimoto *et al.*, 2009), it would seem advantageous to exploit the nitrogen present in the chitin of marine fungi, which may enter the digestive system either on the surface of wood or during filter feeding.

GH 2 & 5 mannanases

Due to the structural complexity of hemicellulose, which may include a variety of polysaccharides such as xylose, galactose, mannose, glucose and arabinose, a range of enzyme systems are required for its deconstruction (Moreira & Filho, 2008). Transcriptomic analysis revealed the presence of two hemicellulolytic enzymes, a GHF 5 mannan endo-β-1, 4-mannosidase (EC 3.2.1.78) and a GHF 2 β-mannosidase (EC 3.2.1.25), at positions 251 and 344 respectively. β-mannanases randomly hydrolyse the internal β-1, 4-mannosidic linkages of mannan polysaccharides, one of the major constituent groups of hemicelluloses in the plant cell wall, yielding mannotriose and mannobiose (Shallom & Shallom, 2003; Moreira & Filho, 2008). These short β-1, 4-manno-oligomers are further depolymerised by β-mannosidases to D-mannose. β-mannanases have been isolated from the crystalline style and digestive gland of the blue mussel, *Mytilus edulis*, and the characterisation of this enzyme revealed active degradation of galactomannans but no specificity towards xylan or cellulose (Xu *et al.*, 2002; Larsson *et al.*, 2006). *T. turnerae* also produced a range of mannanases including β-mannanases [GH 26 (EC 3.2.1.32) and GH 5 (EC 3.2.1.-)], β-mannosidase (GH 5, EC 3.2.1.25), and a range of other hemicellulose-degrading enzymes such as galactosidases, arabinofuranosidases and xlyosidases. Hemicellulose distribution varies between softwoods (gymnosperms) and hardwoods (angiosperms), with softwoods composed of galactoglucomannan, in a 3:1:1 ratio of mannose/glucose/galactose, and glucomannan, with a 3:1 ratio of mannose/glucose (Puls, 1997). As the teredinids in this investigation were fed exclusively on Scots Pine (*Pinus sylvestris*), a gymnosperm, it is possible that the enzyme production reflects the high mannan content of the substrate wood and only a partial representation of the endogenous hemicellulolytic capability of shipworm.

GHF 10 xylanases

Xylanases (EC 3.2.1.8) belonging to GHF 10 ranked at positions 17, 165, 375 and 395 of the top one thousand transcripts. Comparisons from BLAST, PHYRE and Swiss Model all predict endo-1, 4-β-xylanase activity, yet BLAST and PHYRE differ regarding the species of the CBM present, with the former predicting CBM 4-9 and the latter CBM 22. Generally, xylanases attack the backbone of xylan, the internal 1, 4-bonds, thereby producing several xylo-oligomers of varying length. It has been shown that most GHF 10 xylanases attack the xylosidic linkage on the non-reducing end of the substrate residue and are capable of hydrolysing the β-glycosides of xylobiose and xylotriose (Biely *et al*., 1997;

Collins *et al*., 2005). However, this family does not exclusively exhibit activity on xylan and has been shown to hydrolyse cellulose substrates, particularly aryl-cellobiosides (Biely *et al*., 1997).

As well as endo-1, 4-β-xylanase (EC 3.2.1.8), the complete depolymerisation of xylan also requires β-D- xylosidases (EC 3.2.1.37), which cleave xylose monomers from xylo-oligosaccharides. Enzymes that catalyse the removal of xylan side-groups, such as acetylxylan esterases (EC 3.1.1.72), α-L-arabinofuranosidases (EC.3.2.1.55) and α-D-glucuronidases (EC 3.2.1.139), are also required (Collins *et al*., 2005). These enzymes were not detected in *L. pedicellatus* transcripts. However, the *T. turnerae* genome revealed a large set of genes from a range of GHFs (5, 8, 10, 11, 12, 39, 43, 52 and 74), including acetylxylan esterases (EC 3.1.1.72), arabinofuranosidases (EC.3.2.1.55), α-D-glucuronidases (EC 3.2.1.139), endo-1, 4-β-xylanase (EC 3.2.1.8) and xylosidases (EC 3.2.1.37), with predicted xylanase activity (Yang *et* al., 2009). Whilst *L. pedicellatus* is only likely to partially depolymerise xylans, the combined enzymatic activity of both the shipworm and *T. turnerae* would appear sufficient.

The contig ranked 455th was predicted to belong to GHF 16, with BLAST predicting a β-glucan recognition protein, whereas PHYRE and Swiss Model predict endo-1, 3-β glucanase (EC 3.2.1.39) activity. β-glucan recognition proteins have a strong affinity for β-glucan, the major component of the fungal cell wall, and are associated with pathogen defence systems. Interaction between the two stimulates a protein cascade immune response, protecting the host from invading pathogens (Pebery *et al.*, 1990; Janeway, 1992; Ochiai & Ashida, 2000; Brown & Gordon, 2005). Similarly 1, 3-β-glucanases are also associated with pathogen defence and catalyze the hydrolysis of the 1, 3-β-glucosidic linkages of β-glucan, hydrolyzing the fungal cell wall and resulting in cell lysis (Pitson *et al.*, 1993; Hong & Meng, 2003).

GHF 9 glucanases

The most abundantly represented GHs belonged to GHF 9, which accounted for half the total number of glycoside hydrolases from the digestive gland. These were found throughout the 500 transcripts (only one appeared outside the top 500 at position 508), with four in the top 100 transcripts. These were predicted to function as endoglucanases (EC 3.2.1.4) by BLAST comparison. However, PHYRE and Swiss Model analyses predict endo/exo-glucanase activity for a number of these transcripts (37, 58, 76, 78, 181, 392 and 474). Whilst endoglucanases randomly cleave the cellulose chain and produce new

reducing ends, endo/exo-glucanases, which are termed processive endoglucanses, act both as endoglucanases and exoglucanases (Sakon *et al*., 1997). These processive endoglucanases bind strongly to the cellulose and slide along the chain from the non-reducing to the reducing end in a processive action, releasing mainly cellobiose units (Sakon *et al*., 1997).

The teredinid system appears to lack a classic exoglucanase (EC. 3.2.1.94), considered one of the three general categories of enzymes required for the complete depolymerisation of lignocelluloses (Himmel *et al.*, 2007). However, it has recently been shown that a number of invertebrates, including the bivalve *Corbicula japonica*, can degrade particulate lignocelluloses in the absence of exocellulases (Watanabe & Tokuda, 2001; Nakashima *et al*., 2002; Sakamoto *et al*., 2007). In the instance of the termite *Coptotermes formosanus*, the lack of exocellulase is compensated by the physical degradation of wood by the termite's mandibles. The wood is crushed into tiny particles 20-50 μm in size, thus increasing the surface area available for cellulolytic enzymes (Watanabe & Tokuda, 2001; Nakashima *et al*., 2002). Similarly, teredinids mechanically grind wood into particles 10 μm in size (Miller, 1924), which greatly increases the surface area of wood exposed to cellulolytic enzymes. A range of microorganisms are capable of cellulolytic deconstruction without an obvious exoglucanase, including the marine bacterium *Saccharophagus degradans*, which is a close relative of *T. turnerae* (Wilson, 2008; Watson *et al*., 2009; Distel *et al*., 2009). This microorganism has a dual-enzyme mechanism for the degradation of cellulose, relying on a processive endoglucanase in the absence of an exoglucanase (Wilson, 2008; Watson *et al*., 2009). Thus, the combined mechanical degradation of wood along with the presence of an endo/exo-cellulose may adequately overcome the lack of a classical exoglucanase in the teredinid system. In comparison, the bacterial symbiont also produces a wide range of endoglucanases from GHFs 5, 9, 16, 44 and 45 and three exoglucanases, two from GHF 6 and one from GHF 94 (Yang *et al*., 2009). This also includes a multifunctional cellulase, displaying both endo- and exo-glucanase properties (Ekborg *et al*., 2007).

The final component of cellulose degradation requires the action of a β-glucosidase (EC. 3.2.1.21), which hydrolyses the oligosaccharides produced by the cellulases into glucose. Bioinformatic analysis suggests that the 6th most abundant digestive gland contig is a GHF 1 glucosidase. BLAST analysis predicts lactase activity for this protein, whilst both PHYRE and Swiss Model predict glucosidase activity. β–glucosidase activity has been previously detected in the digestive tissue of the shipworm *Bankia gouldi*, with reducing

sugar assays showing the hydrolysis of cellobiose and other oligosaccharides into glucose (Dean, 1978). Thus, in correspondence with transcriptomic evidence, it would appear likely that shipworms can endogenously produce glucosidases. A total of five putative GHF 3 glucosidases have also been identified in the symbiont genome (Yang *et al*., 2009).

Summary

This research has produced preliminary data regarding the capability of the shipworm, *L. pedicellatus*, to enzymatically deconstruct lignocellulose without the aid of the cellulolytic symbiont, *T. turnerae*. Transcriptomic analysis suggests that in the absence of a classical cellobiohydrolase, shipworm utilize endoglucanases and processive endoglucanases to produce cellobiose units. This is further assisted by the grinding action of the teredinid shell, which fracture the crystalline matrix and increases the surface area of wood particles to enzymatic deconstruction. Furthermore, this research reveals that the digestive gland plays a fundamental role in cellulolytic enzyme production with limited contribution from the caecum. In light of these findings, the current view on the role of the caecum as the main site of enzyme production needs to be reconsidered. The findings suggest that the digestive gland produces cellulases which are likely secreted into the caecum, where wood digestion and nutrient absorption take place.

Chapter Four: Aspects of the life history strategy of the long-term brooding teredinid *Lyrodus pedicellatus.*

Introduction

Despite the economic and ecological importance of the Teredinidae, few studies have examined the early life history stages encompassing larval development, spawning, settlement, metamorphosis and growth (Turner & Johnson in Jones & Eltringham, 1971). This is perplexing as these stages represent the most vulnerable in the life-cycle of teredinids and their understanding is crucial for developing methods of borer control and timber protection (Turner, 1966). This difficulty is further compounded by species misidentification within these few studies (Turner & Johnson, 1971). These include the works of Hatschek (1880), Isham and Tierney (1953) and Lane *et al.* (1954), who incorrectly describe larval development of *Teredo navalis*, *Lyrodus pedicellatus* and *L. pedicellatus* whom Turner (1966) subsequently changed to *L. pedicellatus, T. bartschi* and *T. navalis*, respectively.

Larval Development and Metamorphosis

Only a single study has observed larval development for a long-term brooding teredinid (*L. pedicellatus*), yet its significance has remained largely unnoticed due to the age and obscurity of the manuscript and the fact the species was misidentified. A number of studies have described embryology for short-term brooding and broadcast spawning species and Figure 4.1 demonstrates typical teredinid development. Development of the egg is rapid post-fertilization and appears similar for most species (Turner, 1966). The first, second and third cell cleavages typically occur within two hours and the blastula, free swimming blastula, trochophore and straight-hinged veliger stage are reached within 3, 5, 12 and 24 hours respectively (Nair, 1956; Turner & Johnson in Jones & Eltringham, 1971). Development to the pediveliger stage varies between species and is strongly influenced by temperature: *Bankia carinata* may reach settlement competency after 17 days (Nair, 1956), whereas *Bankia fimbriatula* takes approximately 40 days (Turner & Johnson in Jones & Eltringham, 1971). Typically, larval maturity is reached within three to four weeks in oviparous and short-term brooding teredinids (Loosanoff & Davis, 1963; Turner, 1966).

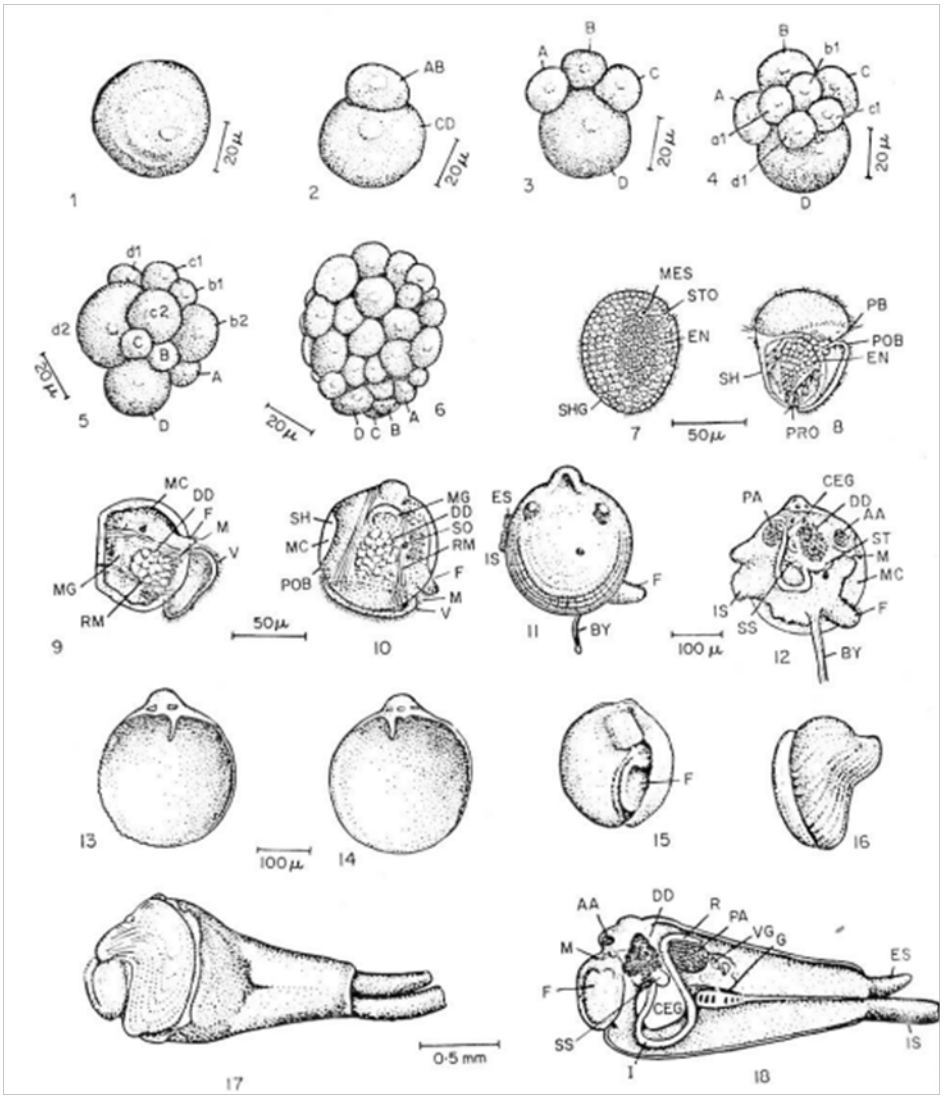

Figure 4.1 Developmental stages of the broadcast spawning teredinid *Bankia carinata*. 1) surface view of a ripe ovum; 2) two-celled stage; 3) four-celled stage; 4) eight-celled stage; 5) twelve-celled stage; 6) gastrulation; 7) eleven hour larva; 8) trochophore larva; 9) early veliger; 10) eleven day-old veliger larva; 11) fifteen day-old veliger; 13 – 14) right and left shell valves of a larva attached to wood; 15) settled larva removed from wood; 16) shell from a 2 mm long specimen; 17) 2 mm long specimen; 18) 2 mm long specimen with shell and mantle removed. AA, anterior adductor; BY, byssus thread; CEG, caecum; DD, digestive diverticula; ES, excurrent siphon; EN, endoderm; F, foot; G, gill; I, intestine; IS, incurrent siphon; M, mouth; MC, mantle cavity; MES, mesodermal cells; MG, midgut; PA, posterior adductor; PB, pre-oral band of cilia; POB, post-oral band of cilia; R, rectum; RM, retractor muscle; SH, shell; SHG, shell gland; SO, sense organ; SS, style sac; ST, stomach; STO, stomadaeal invagination; V, velum, VG, visceral ganglion. Taken from Nair & Saraswathy (1971).

Like all other brooding teredinids, adult *L. pedicellatus* fertilize internally and retain the young in specialised brood pouches located on the gill. Brooded bivalve larvae are typically provided with large eggs which subsequently fuel the formation of a large prodissoconch I shell, with limited growth during the prodissoconch II phase. Yet the shells of brooded teredinids display features typically associated with planktotrophic larvae: veligers are provisioned with small eggs, develop a prodissoconch I of 100 µm or less and undertake significant growth during the prodissoconch II phase (Cragg *et al*., 2009). It has been suggested that these small eggs are insufficient for providing the necessary energy to fuel such extensive prodissoconch II growth (Cragg *et al*., 2009). Instead, brooded teredinids are believed to derive this surplus nourishment by ingesting glycogen-forming cells within the brood pouch (Calloway, 1982), a type of parental care known as matrotrophy.

It is likely that the embryology and larval development of *L. pedicellatus* is similar to that of broadcast spawning and short-term brooding species. The larvae of *L. pedicellatus* are released at the pediveliger stage and measure 360 µm in length and 325 µm in width (Coe, 1941) - the largest known pediveliger dimensions among the Teredinidae (Turner & Johnson in Jones & Eltringham, 1971). Upon release, pediveligers begin actively swimming and crawling, as shown in Figure 4.2a. These pediveligers display a number of modifications typical of brooded bivalve larvae including the loss of the pre-oral cilia on the velum (Stanton, 2012), the larval feeding, swimming and respiratory organ. This is of critical importance with regard to the dispersal and survival of this species during the free-swimming period. The lack of the pre-oral cilia suggests individuals are incapable of planktotrophy within brood pouches and once in the water column. Indeed, research on free-swimming larvae found that ^{14}C-labelled phytoplankton is not incorporated into tissue (Gallager *et al*., 1981), adding further weight to the argument that the development of *L. pedicellatus* is supplemented by maternally derived nutrition.

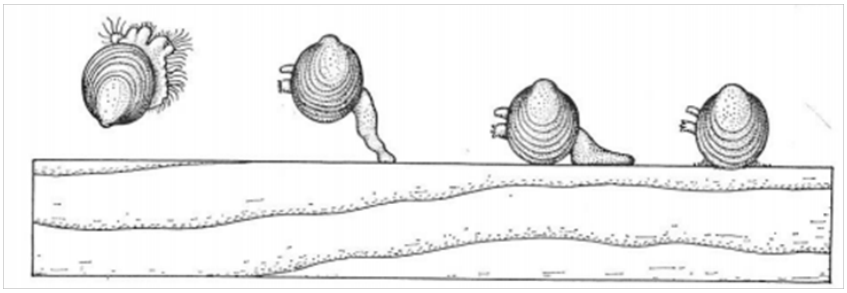

Figure 4.2a Diagrammatic sketch of *Lyrodus pedicellatus* larval pediveliger free-swimming, crawling and boring stage. Image taken from Nair & Saraswathy (1971).

The presence of wood triggers metamorphosis and in its absence, *L. pedicellatus* larvae have a limited free-swimming period in which to locate a suitable substrate for settlement. As the larvae are incapable of planktotrophy during the free-swimming period they must rely on stored reserves provided by the parent (Pechenik *et al*., 1978), which are believed to last for between four and seven days before the larvae expire (Turner & Johnson, 1971). The duration of the free-swimming stage determines dispersal potential: species with a long free-swimming developmental period have a large distribution range in comparison to those with short free-swimming periods (MacIntosh *et al*., 2012).

The fully developed pediveligers of *L. pedicellatus* are capable of settlement within hours after release from the parent and have even been observed settling immediately after spawning (Turner & Johnson, 1971; Coe, 1941). As wood is a spatially and temporally unpredictable resource in marine environments (Romey *et al*., 1994) this strategy maximises the potential for larvae to locate wood by typically settling on parental timber, thus ensuring the survival of future generations (Turner, 1966). Whilst limiting dispersal potential, this allows *L. pedicellatus* to dominate local populations and out-compete species with long planktotrophic development stages (Pechenik *et al*., 1978).

Larval settlement follows a typical pattern among the Teredinidae as demonstrated by Figures 4.2 b-c. Approximately two to three days post-settlement, larvae excavate a small opening roughly equal to the depth and width of the shell (Coe, 1941). During metamorphosis the major biological systems *e.g.*, the feeding, respiratory and excretory systems, undergo considerable morphological transformation (Turner, 1976). The loss of the velum, which is absorbed soon after attachment (Sigerfoos, 1908) requires rapid development of the siphons and ctenidia to provide alternative means for respiration. Continual borrowing requires changes in foot musculature and rapid growth of the calcareous features (Lane & Tierney, 1952; Turner, 1976). The larvae begin to secrete a calcareous cap, complete with a small aperture allowing extension of the siphons (Fig. 2c). This cap serves to protect the larvae, extends into the burrow to form the initial lining and provides a site of attachment for the pallets (Turner, 1976).

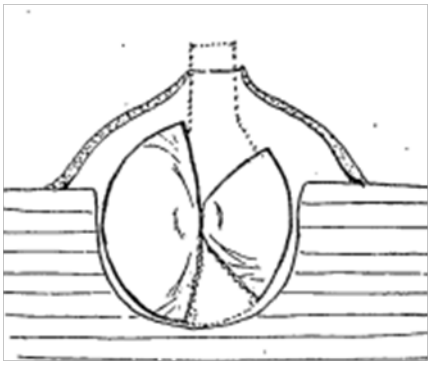

Figure 4.2b. Diagrammatic sketch showing a metamorphosing teredinid pediveliger forming a calcareous cap over its burrow. Image taken from Rancurel (1951).

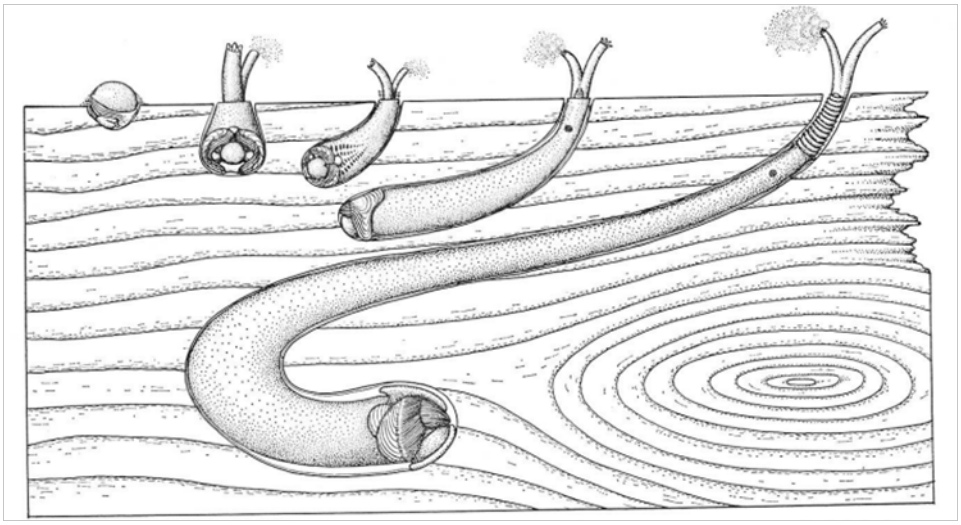

Figure 4.2c. Diagrammatic sketch showing teredinid growth over time. Image taken from Nair & Saraswathy (1971).

As the larvae continue to burrow into wood, the shell thickens and lays down rows of dermal denticles – a marker for metamorphosis. The body continues to elongate and will protrude from the valves after approximately one week. The gills and siphon develop and become more visible and the pallets grow in length and breadth (Isham & Tierney, 1953; Nair & Saraswathy, 1971). Beyond metamorphosis, growth produces little change in form, bar elongation and the continued growth of calcareous structures (Isham & Tierney, 1953).

Maturity and Growth

Numerous studies have been undertaken on the growth rates of teredinids as this directly relates to the speed at which timber is destroyed (Nair & Saraswathy, 1971). A number of factors affect growth rate, including abiotic conditions such as seawater temperature, salinity and the natural durability of wood (Grave, 1928; Eckelbarger & Reish, 1972; Southwell & Bultman, 1971). Crowding also affects growth as individuals which settle on small or heavily infested wood may become stenomorphic (dwarfed) due to the lack of sufficient space and nutrition for growth (Bartsch, 1923). Whilst stenomorphs may complete full life cycles, become sexually mature and live as long as normal individuals, they are unable to increase in length and diameter. Indeed, Clapp (1952) observed stenomorphs that achieve an initial growth of 10 mm after two weeks, yet remain unchanged after a further ten month period.

Often, growth rate values for the same species vary significantly between studies: *Bankia setacea* has been recorded as reaching total body lengths as variable as 38 mm and 610 mm after a five month period, representing growth rates of 0.28 mm and 4.35 mm per day^{-1} respectively (Johnson & Miller, 1935; Quale, 1959). Whilst the growth rates of whole individuals are fairly well documented, growth rates of the calcareous structures in relation to body length are poorly understood. Only three studies have looked at shell and pallet growth in early ontogeny, none of which include a long-term brooding species.

Teredinids may reach sexual maturity shortly after larval settlement, often at relatively small sizes (Nair & Saraswathy, 1971). Whilst the short-term brooding species *Teredo navalis* has been reported to reach sexual maturity six weeks after metamorphosis at sizes ranging between 10 and 12 mm (Coe, 1933), 15 and 20 mm (Bulatov, 1941) and 38 mm (Grave, 1928), it is not known how rapidly long-term brooding species develop and the minimum body size at which they can attain sexual maturity. *L. pedicellatus* is known to be capable of producing full broods of fully developed pediveligers, which are competent upon release, approximately ten weeks after metamorphosis (Turner & Johnson in Jones & Eltringham, 1971). Assuming larval developmental times are similar to non-brooded larvae (the pediveliger stage is reached approximately three to four weeks - Turner, 1966), individuals would have to develop rapidly and produce ripe gonads within weeks of metamorphosis (Gallager *et al*., 1981). Although broadcast spawning species are estimated to produce and release vast numbers of eggs – *Psiloteredo megatora* is believed to release 100 million eggs in a single spawning (Sigerfoos, 1908), data on the fecundity of brooding species is limited and reproductive output is unknown. Furthermore some long-term

brooders such as *L. pedicellatus* are known to contain larvae at various developmental stages during brooding (Turner, 1966), but the size and frequency of these different cohorts also remains unknown.

Aims

This study aimed to develop a greater understanding of the early life history strategy of the long-term brooding teredinid *Lyrodus pedicellatus* by examining settlement, metamorphosis and development through to maturity. Direct observation of the larval behaviour and settlement rates provided insights into the success of the extended parental care for this species. The measurement of growth rates aimed to determin whether there were shifts in dietry preference throughout ontogeny when species became sexually mature, and the fecundity of individuals in relation to size. Finally, the relationship between the parent and larva were examined during brooding in order to examine whether matrotrophy was present.

Materials & methods

Specimen Acquisition & Culturing

Specimens of *Lyrodus pedicellatus* were obtained from an infested pier composed of greenheart (*Chlorocardium* sp.) in Langstone Harbour, Eastney, UK. Populations of the crustacean borers *Chelura* and *Limnoria* were initially found to co-inhabit the timber infested with *L. pedicellatus*. In order to maintain a teredinid-specific culture, the gribbles were coerced into abandoning the timber by lowering the oxygen content of the water. The timber was then placed into a separate tank of seawater. All specimens were maintained in the aquaria at The Institute of Marine Sciences, University of Portsmouth. The culturing set-up is shown in Figure 4.3a. Housing tanks were temperature controlled, measuring 100 cm × 100 cm × 50 cm and contained approximately 50l of filtered seawater,. Seawater was pumped directly from Langstone Harbour at a flow-though rate of approximately 10L $Hour^{-1}$. The temperature was maintained using an Aquael Thermo-Precision electronic heater with the ATC-800+ microcomputer temperature controller. Air was bubbled through the water, keeping the tank well oxygenated and preventing stagnation. Perspex lids covered the tanks in order to minimise water loss and maintain salinity levels. Spawning conditions were maintained year-round by elevating the seawater temperature above 15 °C. Wooden panels were regularly supplied to tanks thus providing new substrates for larval settlement.

Figure 4.3a The teredinid cultures and experimental set-up maintained at the Institute of Marine Sciences, University of Portsmouth.

Wooden Panels

Wood Pre-treatment

All panels were vacuum impregnated in filtered seawater until the wood was waterlogged. Panels were then submerged in a flow-through tank at ambient temperature for a minimum period of one month, prior to borer larvae exposure.

Lamellar panels

Sheets of pine laminate (sapwood, 1mm in thickness) were assembled into panels (measuring 15 cm × 10 cm × 2.5 cm), encased between blocks of transparent Perspex (measuring 12.5 cm × 7.5 cm × 0.5 cm) and fixed in place with stainless steel screws. The design was modified from that of Manyak (1982). Lamellar panels are shown in Figure 3.2.

Standard panels

Panels were cut from pine sapwood, measuring 15 cm × 10 cm × 2.5 cm.

Larval Detection

Larval release was monitored using a modified box filter, as outlined by Raskoff *et al.,* (2003) and Stanton (unpublished Ph.D thesis). The box filter mechanism is described in Figure 4.3b. Air passed into the filter through narrow tubing and was allowed to escape through broader tubing, situated higher than the inflow tubing. Outflow tubing was then connected to a container sealed with 63 µm plankton mesh. Water was drawn across slats on the lateral surface of the box filter, through the tubing and then expelled out the mesh. Airflow was regulated to a rate sufficient to entrain the free-swimming pediveligers, yet gentle enough so as to leave circulating larvae intact. Larvae drawn in though slats, were then impelled through the outflow tubing where they were trapped between the incoming current and plankton mesh. The box filter was monitored daily for teredinid larvae. Captured larvae were released back into separate tanks containing un-infested panels allowing settlement and metamorphosis to occur.

Teredinid Extraction from Timber

Wooden panels were carefully split open using a hammer and chisel. Upon removal of the calcareous lining, teredinids were extracted using a fine paint brush. Teredinids were removed from lamellar panels by removal of the Perspex sections and the peeling apart of laminar sheets to reveal the teredinid borings. Upon removal of the calcareous lining, teredinids were extracted using a fine paint brush.

Photomicroscopy & Image Analysis

Specimens were photographed under the microscope using a JVC KY-F 1030U digital camera with accompanying KY0Link image capture program. All images were taken using a 1 mm graticule. Anatomical measurements were made using the image analysis program ImageJ.

Specimen Dissection

The calcareous structures (shell valves and pallets) were excised using fine dissecting tweezers and forceps. Larval broods were removed from the parental gill using a fine paint-brush.

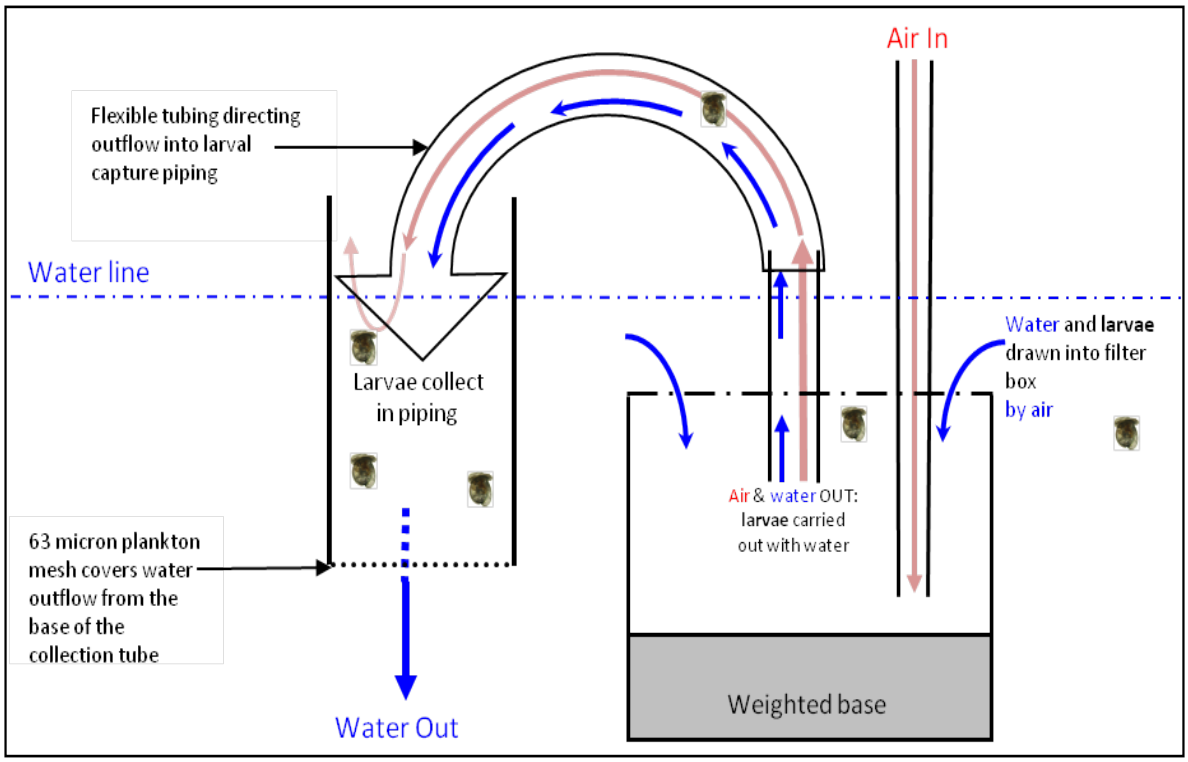

Figure 4.3b A box filter modified to capture larval pediveligers upon release from the adult. Air is pumped into the filter, drawing water (and larvae) through slits located on the lid of the box. Both air and water are then forced through an outflow and into an adjacent filter. Plankton mesh retains larvae, whilst water and air escape through the base of the secondary filter. Image modified from Stanton (Ph.D Thesis, 2012), box filter design from Raskoff *et al.,* (2003).

Settlement Experiment

Blocks of pine, measuring 2.5 × 2.5 × 2.5 cm, were placed into tanks containing spawning *L. pedicellatus*. After a 24 hour period, these blocks were then transferred to a separate tank. Blocks were then removed from the tank at fortnightly intervals and placed in fixative (see Materials and methods in Electron Microscopy, Chapter Two). The larval settlement rate was determined by counting the number of bore holes on the exposed surfaces. Individuals were then extracted from the wood (see Materials and methods in Teredinid Extraction from Timber, this chapter) and their total body length and calcareous structures were photographed and measured.

Results

Brood Abundance

A typical adult specimen and the size distribution of brooded larvae are shown in Figures 4.4a and 4.4b respectively. A total of 69 gravid individuals and their larval brood were measured and the results are shown in Figure 4.5. The smallest and largest gravid specimens measured 4.43 mm and 40 mm in length, brooding 16 and 804 larvae respectively. The smallest and largest clutch contained eight and 1092 larvae, from specimens measuring 5.16 mm and 24.8 mm respectively. The average specimen measured 14 mm in total body length and produced a brood of 222 larvae.

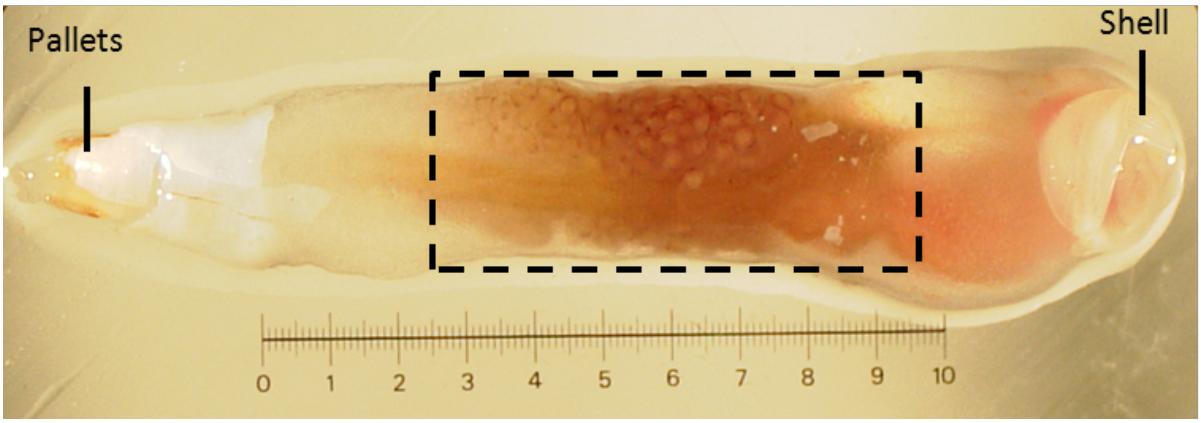

Fig. 4a. A gravid adult *Lyrodus pedicellatus*. Variation of larval developmental stages visible on the gill, with the developed pediveliger located towards the anterior (shell region) and the veligers located posteriorly (towards the pallets). Dashed area outlines the region of the gill in which larvae are brooded. Scale bar = 1 mm.

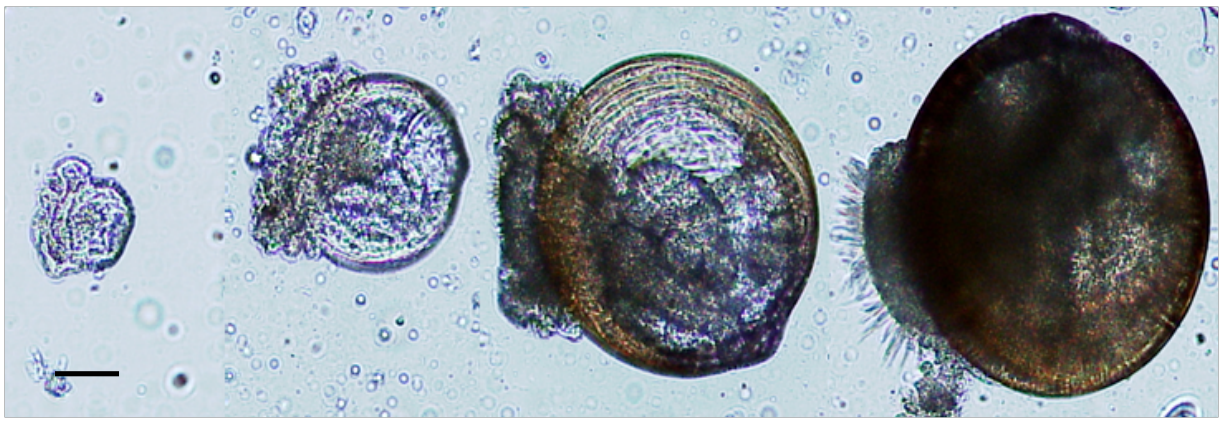

Figure 4.4b. Larval developmental stages of *Lyrodus pedicellatus*. From left to right: early D-shaped veliger; advanced veliger with velum extended; early stage pediveliger with velum extended; advanced staged pediveliger, velum fully extended. Scale bar = 100 µm.

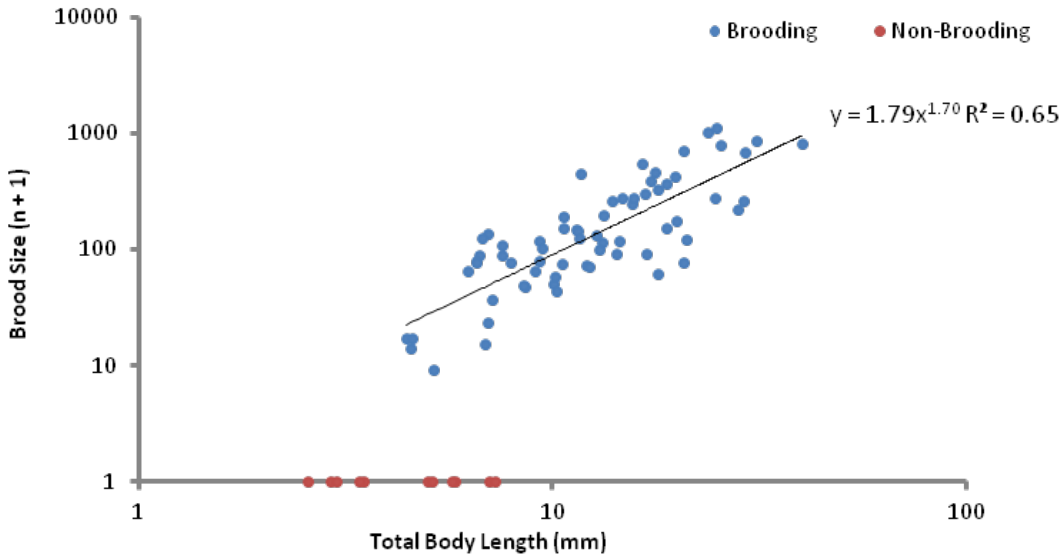

Figure 4.5 Brood abundance in relation to adult body length. Logarithmic plot with both the X & Y axis transformed to n + 1 in order to allow plotting of non-brooding animals.

A total number of 1484 larvae from 12 brooding adults were measured and the larval dimensions are shown in Figures 4.6a-c. Adults varied from 7 mm to 40 mm in length. Larval shell length typically varied from veligers measuring 0.05 mm to pediveligers measuring 0.36 mm. The smallest larval veliger measured 0.04 mm in shell length and width, whilst the largest pediveliger measured 0.37 mm in length and 0.32 mm in width. The average larval dimensions measured 0.27 mm in length and 0.22 mm in width. It is apparent from the historgram observatsion that a number of specimens contain at least two size cohorts of larvae, yet further statistical analysis is required. Larvae from the cohort size measuring up to 0.05 mm in diameter were the lowest in abundance accounting for 3.1 % of the total brood. Conversely, larvae from the size range measuring between 0.30 mm

and 0.35 mm were the highest in abundance on average, constituting 31.5 % of the total brood.

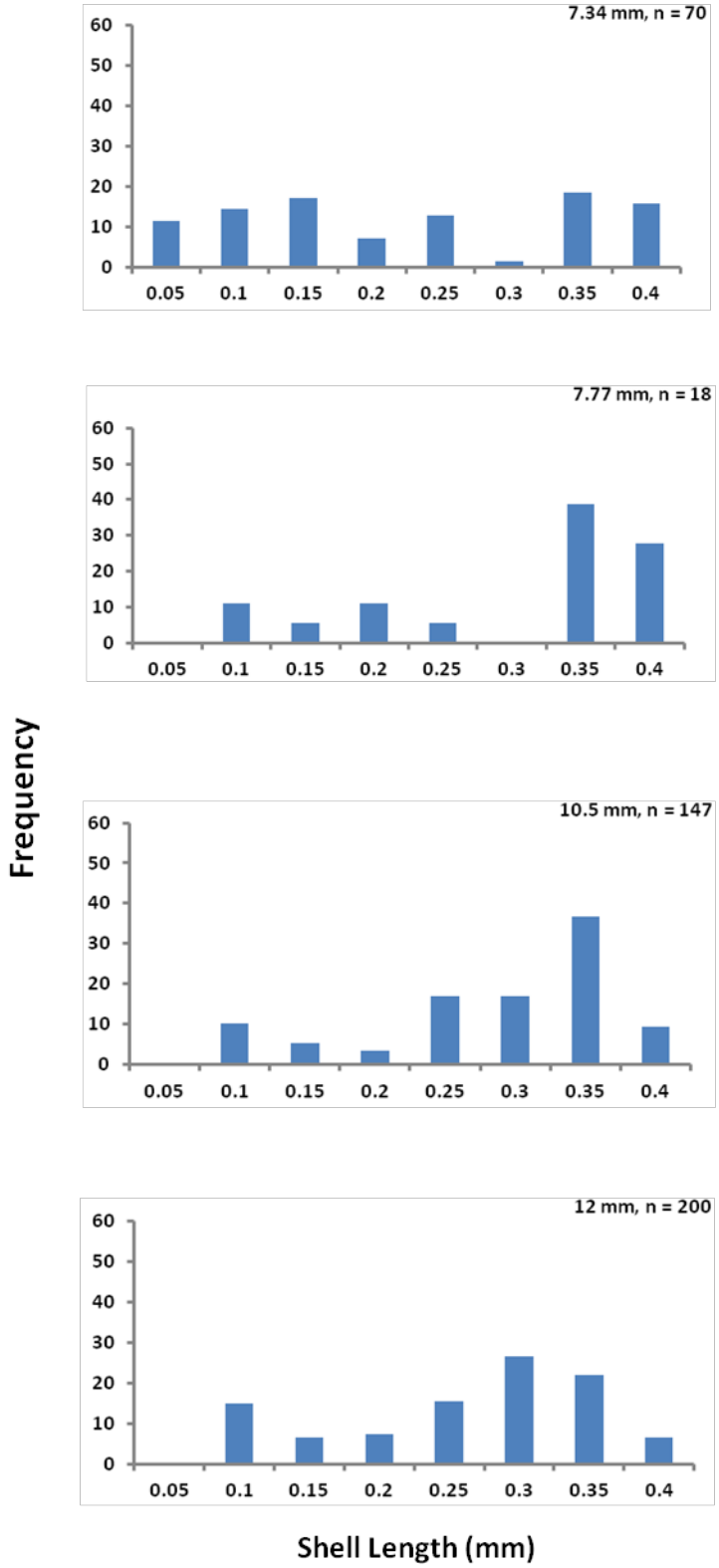

Figure 4.6.a Size frequency distribution of brooded larvae retained in individual adults *Lyrodus pedicellatus* specimens. Adult body length and larval sample size shown in top right of each graph.

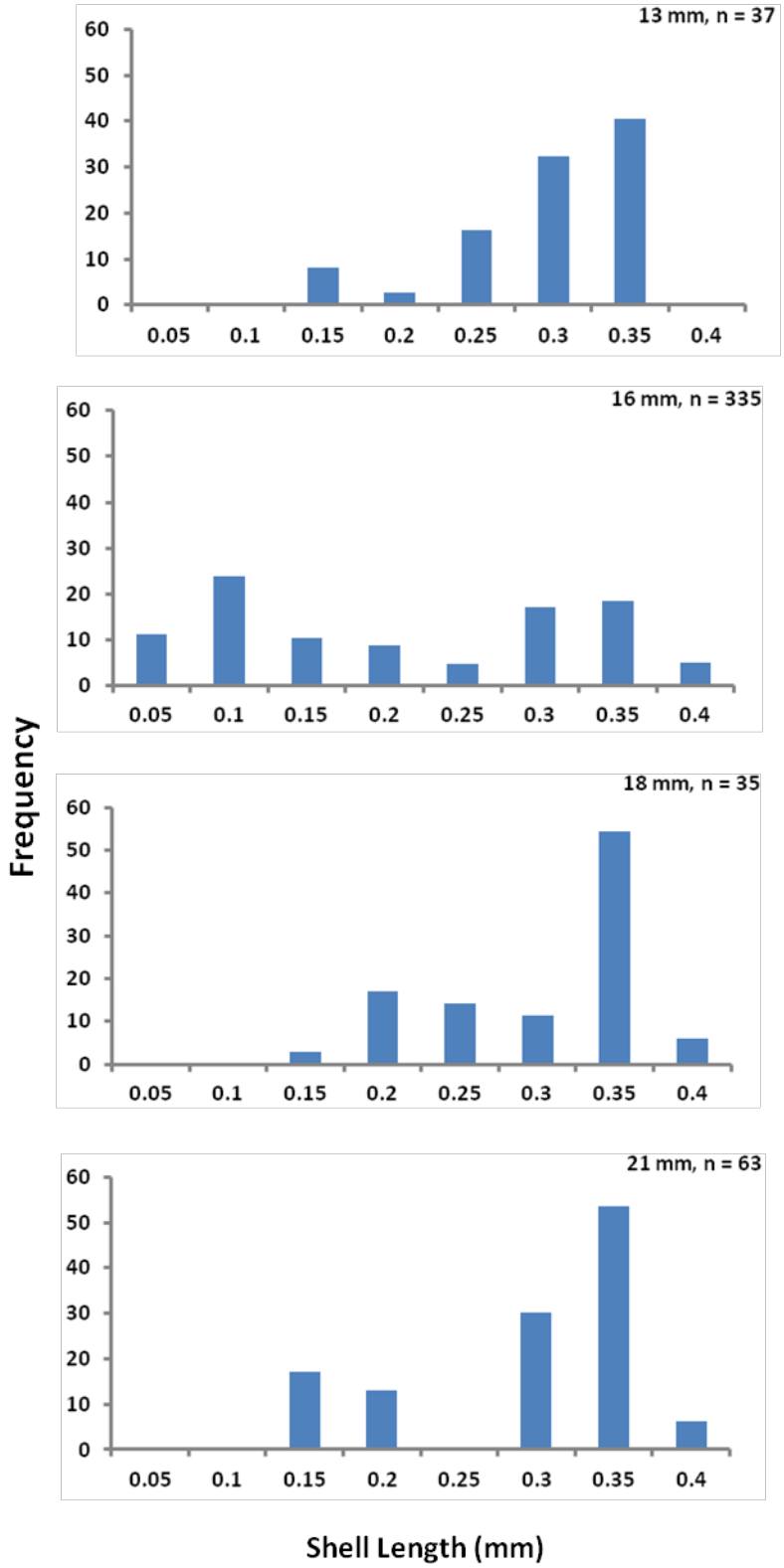

Figure 4.6.b Size frequency distribution of brooded larvae retained in individual adults *Lyrodus pedicellatus* specimens. Adult body length and larval sample size shown in top right of each graph.

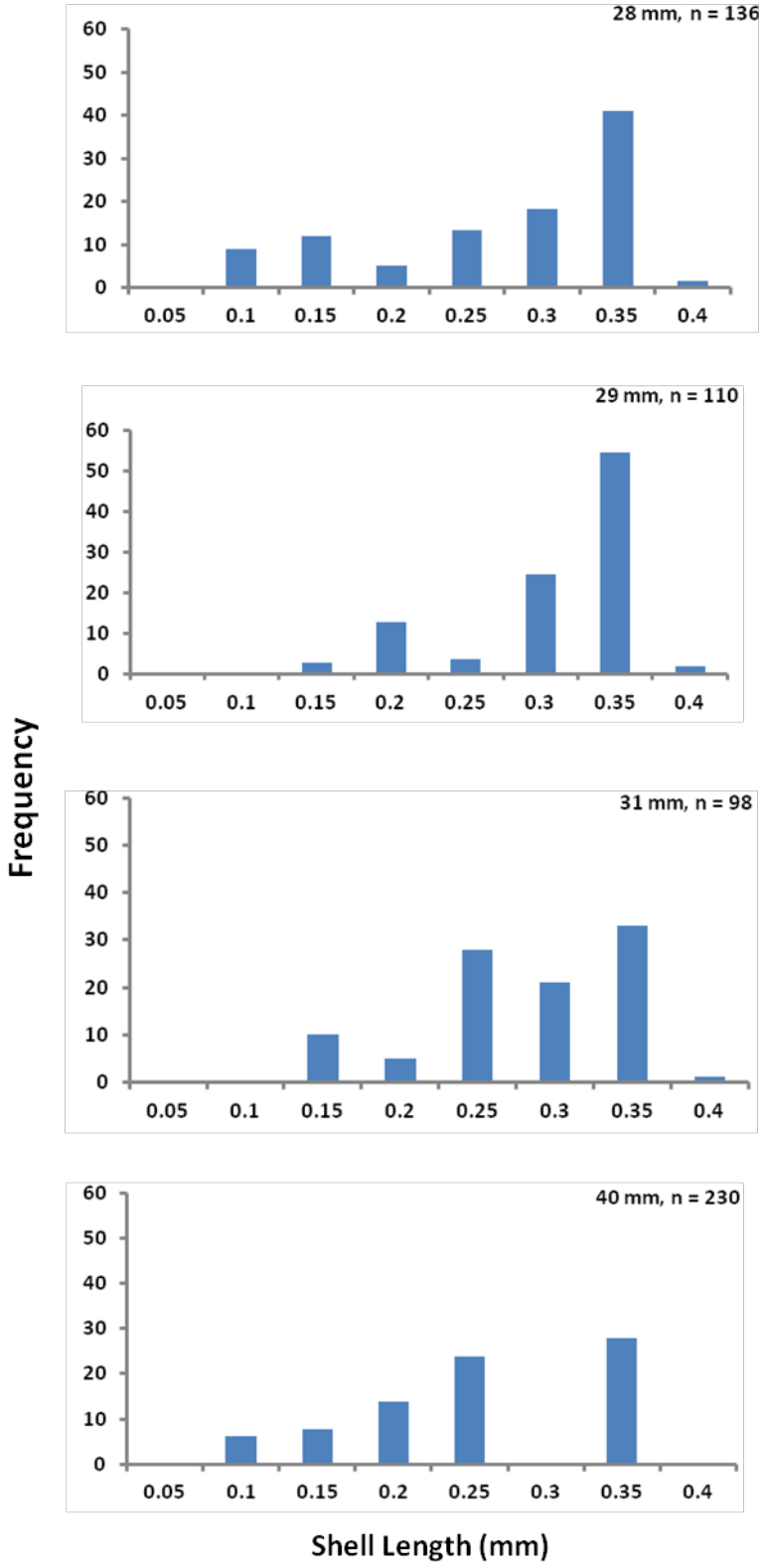

Figure 4.6.c Size frequency distribution of brooded larvae retained in individual adults *Lyrodus pedicellatus* specimens. Adult body length and larval sample size shown in top right of each graph.

Larval Settlement

Figure 4.7a shows larval release from the excurrent siphon of the adult and Figure 4.7b shows larvae swimming, crawling and beginning to burrow into wood. Figure 4.8 details the settlement preferences of free-swimming larvae, between the upper and lateral surfaces and spring and summer growth lines, with the summer wood showing the typical wider growth lines compared with the narrower winter growth lines. Larval settlement on the upper surface of experimental panels was approximately twice that of the lateral surfaces (P Value = 0.00, Paired-T-test). The highest and lowest total larval settlement on the upper surface was 283 and 133 larvae respectively, compared with 127 and 74 larvae on the lateral surface. This trend is reflected in the frequency of larvae per cm^{-2}, with an average of 34.6 larvae on settling on the upper surface compared with an average of 17.7 larvae on the lateral surface. The highest and lowest larval settlement frequencies on the upper surface measured 45.9 cm^{-2} and 23.3 cm^{-2} respectively, compared with 30.06 cm^{-2} and 13.91 cm^{-2} respectively for the lateral surface. An average of 595.5 larvae settled per block, across all exposed surfaces.

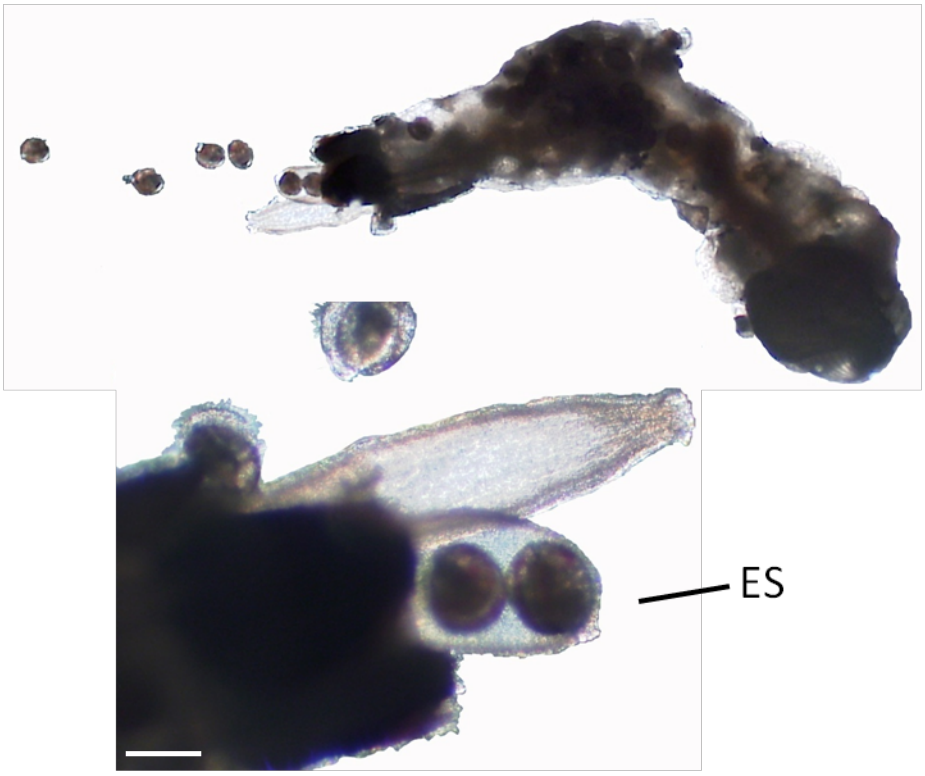

Figure 4.7.a The release of larval pediveligers from the exhalent siphon (ES) of *Lyrodus pedicellatus*. Scale bar represents 0.5 mm.

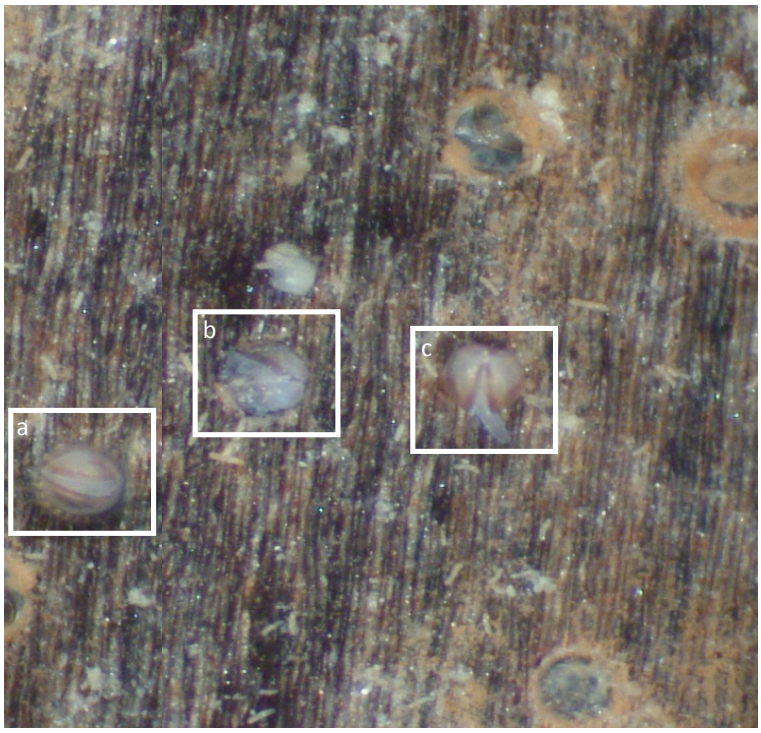

Figure 4.7.b Larval pediveligers begin to settle and metamorphose. a) velum (swimming organ) extended. b) a larva begins burrowing into the wood. c) a larva uses it foot to crawl across the surface of the wood.

Larvae demonstrated approximately a two-fold preference for settlement on spring wood as opposed to summer wood ($P = < 0.001$, two-way ANOVA), with an average larval settlement of 32.4 larvae per cm^2 on spring growth compared with 14.4 larvae cm^{-2} on summer growth. The highest settlement frequencies for both spring and summer growth were 63.9 larvae cm^{-2} and 37.3 larvae cm^{-2} respectively. The lowest settlement frequencies for both spring and summer growth were 21.8 larvae cm^{-2} and 6.9 larvae cm^{-2} respectively.

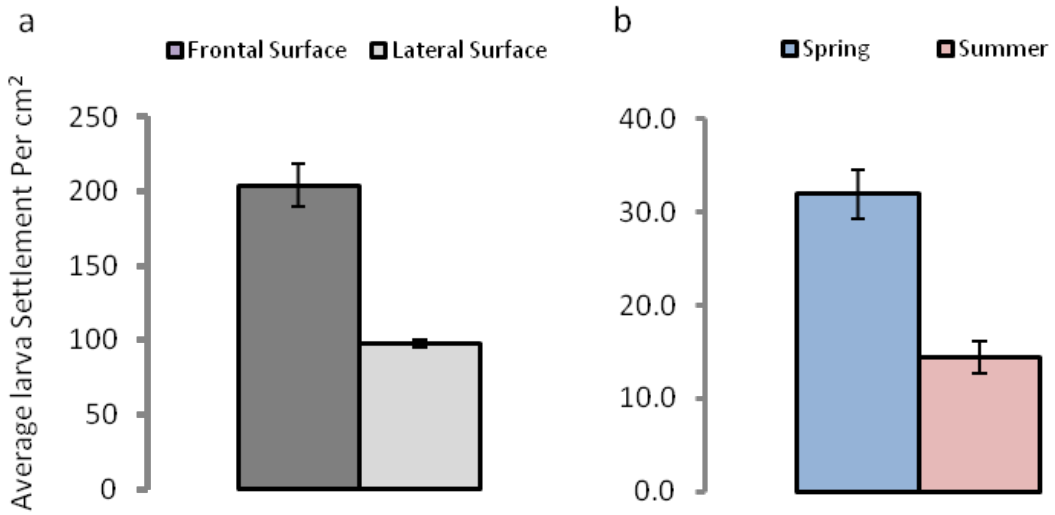

Figure 4.8 The settlement preference of *Lyrodus pedicellatus* larval pediveligers. a) the surface settlement preference; b) growth ring preference.

Teredinid Growth Rates

The typical developmental stages of *L. pedicellatus* are shown in Figure 4.9, from juvenile specimens extracted from wood 20 days post-metamorphosis to fully developed adults gravid with larvae, extracted 241 days post-metamorphosis.

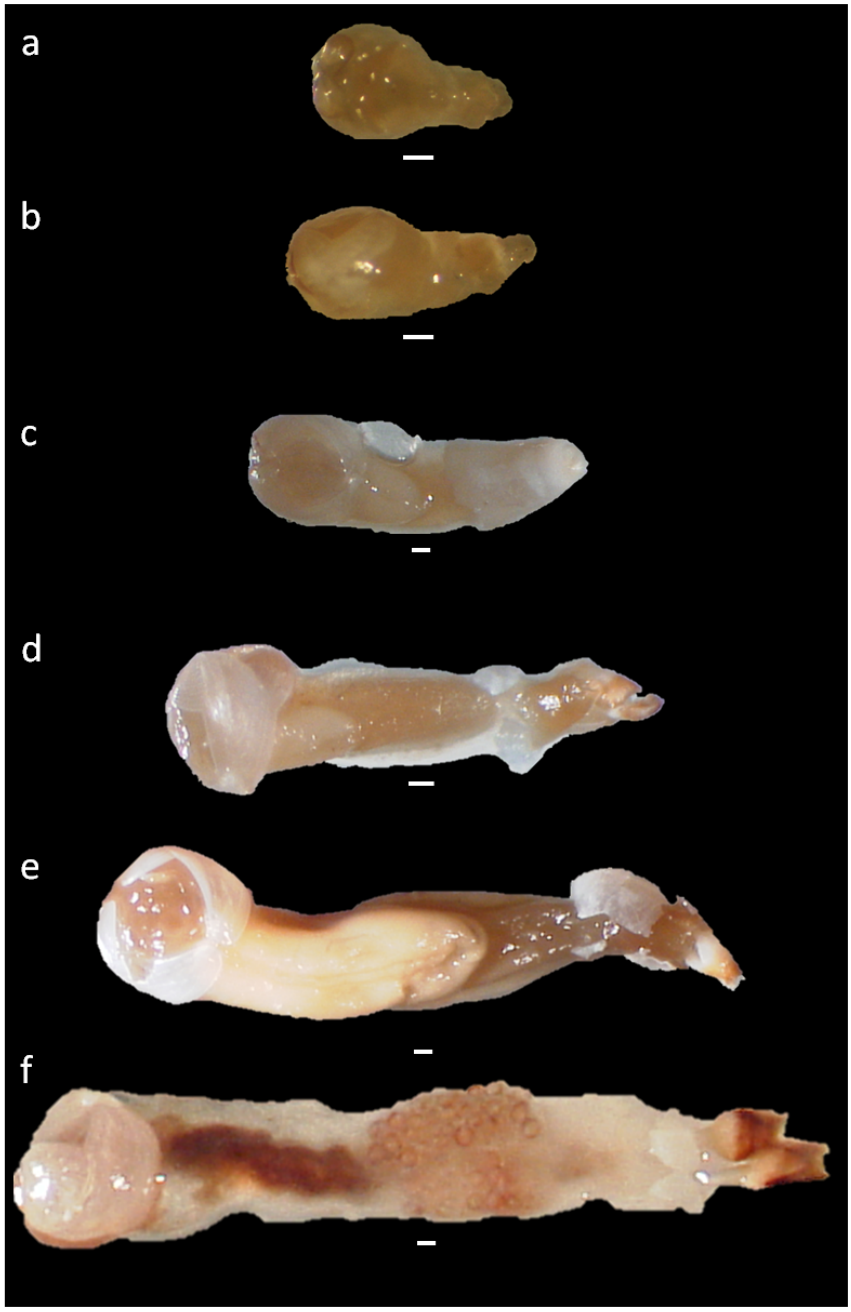

Figure 4.9 Specimens of *Lyrodus pedicellatus* throughout various developmental stages of the life cycle: a) 21 days post-larval settlement; b) 34 days post-larval settlement; c) 48 days post-larval settlement; d) 62 days post-larval settlement; e) 180 days post-larval settlement; f) 271 days post-larval settlement. Scale bar represents 1 mm.

Figure 4.10 shows the growth rates and development of the calcareous structures over time. The largest individuals sampled 20, 34, 48, 60, 182 and 271 days after larval settlement measured 3.5 mm, 3.27 mm, 6.6 mm, 10.25 mm, 19.3 mm and 29.87 mm in body length respectively, representing growth rates of 0.175 mm, 0.096 mm, 0.014 mm, 0.165 mm, 0.107 mm and 0.11 mm per day. Conversely, the smallest individuals after 20, 34, 48, 60, 182 and 271 days after larval settlement measured 0.61 mm, 0.79 mm, 1.13

mm, 1.2 mm, 3.35 mm and 8.30 mm in body length respectively, representing growth rates of 0.03 mm, 0.023 mm, 0.024 mm, 0.02 mm, 0.018 mm and 0.31 mm per day. The average body lengths were 1.53 mm, 1.58 mm, 2.84 mm, 4.26 mm, 10.30 mm and 13.94 mm, representing average growth rates of 0.077 mm, 0.064 mm, 0.059 mm, 0.069 mm, 0.057 mm and 0.051 mm per day, after 20, 34, 48, 60, 182 and 271 days respectively.

The largest pallets sampled 20, 34, 48, 60, 182 and 271 days after larval settlement measured 0.62 mm, 0.76 mm, 0.92 mm, 1.76 mm, 2.2 mm and 2.43 mm in length and 0.32 mm, 0.47 mm, 0.46 mm, 0.73 mm, 0.84 mm and 0.85 mm in width. Conversely, the smallest pallets sampled 20, 34, 48, 60, 182 and 271 days after larval settlement measured 0.17 mm, 0.16 mm, 0.28 mm, 0.30 mm, 1.38 mm and 1.67 mm in length and 0.13 mm, 0.15 mm, 0.17 mm, 0.14 mm, 0.44m, 0.51 mm respectively. The average pallet size sampled 20, 34, 48, 60, 182 and 271 days after larval settlement measured 0.31 mm, 0.38 mm, 0.53 mm, 0.85 mm, 1.74 mm and 2.0 mm in length and 0.2 mm, 0.24 mm, 0.30 mm, 0.45 mm, 0.63 mm and 0.74 mm respectively.

The largest shells sampled 20, 34, 48, 60, 182 and 271 days after larval settlement measured 1.33 mm, 1.69 mm, 1.52 mm, 2.31 mm, 2.38 mm and 2.84 mm in length and 0.42 mm, 0.45 mm, 0.69 mm, 0.72 mm, 1.26 mm and 1.82 mm in width. Conversely, the smallest shells sampled 20, 34, 48, 60, 182 and 271 days after larval settlement measured 1.17 mm, 1.37 mm, 1.89 mm, 1.76 mm, 2.42 mm and 2.46 mm in length and 0.27 mm, 0.37 mm, 0.59 mm, 0.54 mm, 1.2 mm, 1.56 mm respectively. The average shell size sampled 20, 34, 48, 60, 182 and 271 days after larval settlement measured 0.79 mm, 0.83 mm, 1.1 mm, 1.30 mm, 1.85 mm and 2.22 mm in length and 0.65 mm, 0.67 mm, 0.91 mm, 1.08 mm, 1.83 mm and 2.11 mm respectively.

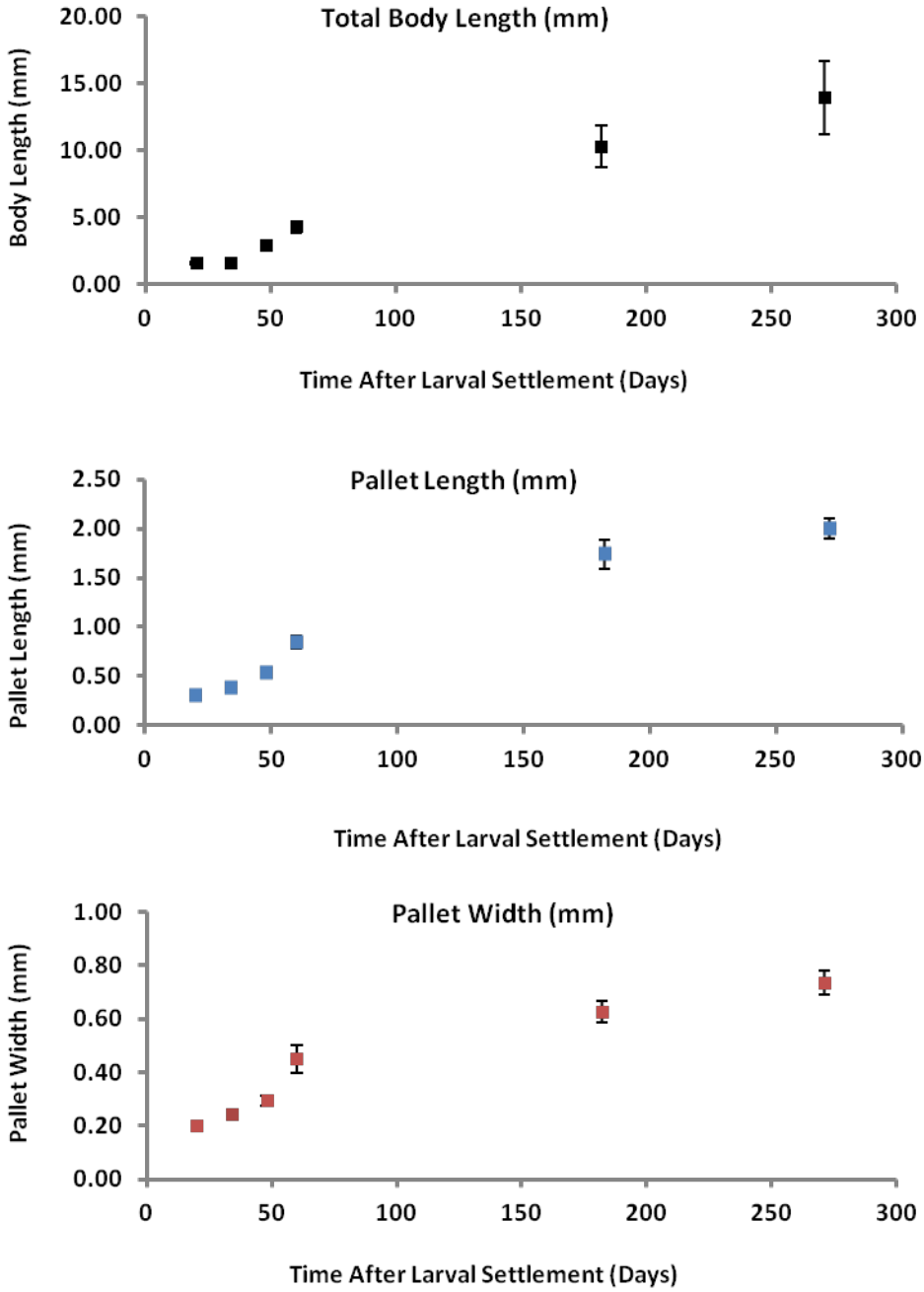

Figure 4.10 Dimensions of *Lyrodus pedicellatus* throughout various developmental stages of the life cycle: a) 21 days post-larval settlement; b) 34 days post-larval settlement; c) 48 days post-larval settlement; d) 62 days post-larval settlement; e) 180 days post-larval settlement; f) 271 days post-larval settlement. Mean ± SE.

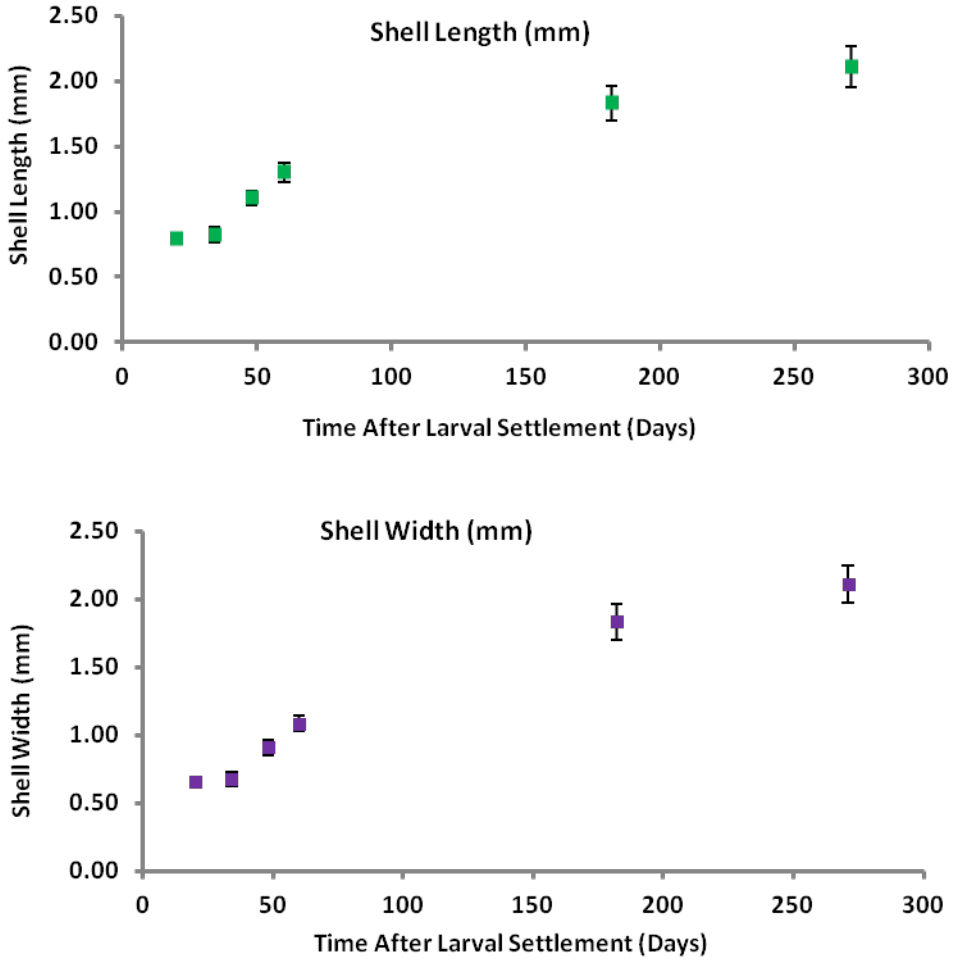

Figure 4.10 Dimensions of *Lyrodus pedicellatus* throughout various developmental stages of the life cycle: a) 21 days post-larval settlement; b) 34 days post-larval settlement; c) 48 days post-larval settlement; d) 62 days post-larval settlement; e) 180 days post-larval settlement; f) 271 days post-larval settlement. Mean ± SE.

Adult Calcareous Structures

The development of the calcareous structures in relation to body length is shown in Figures 4.11 a -b. The data obtained from the metamorphosing, juvenile and adult individuals from the settlement and growth experiment were similar to the data obtained for the adult specimens. The shells and pallets increased in dimension as the animal increased in total body length. Whereas the shell valves only increased slightly more in length than width, the pallets increased much more rapidly in length than width and were typically twice as long as they were wide. These trends continue throughout ontogeny.

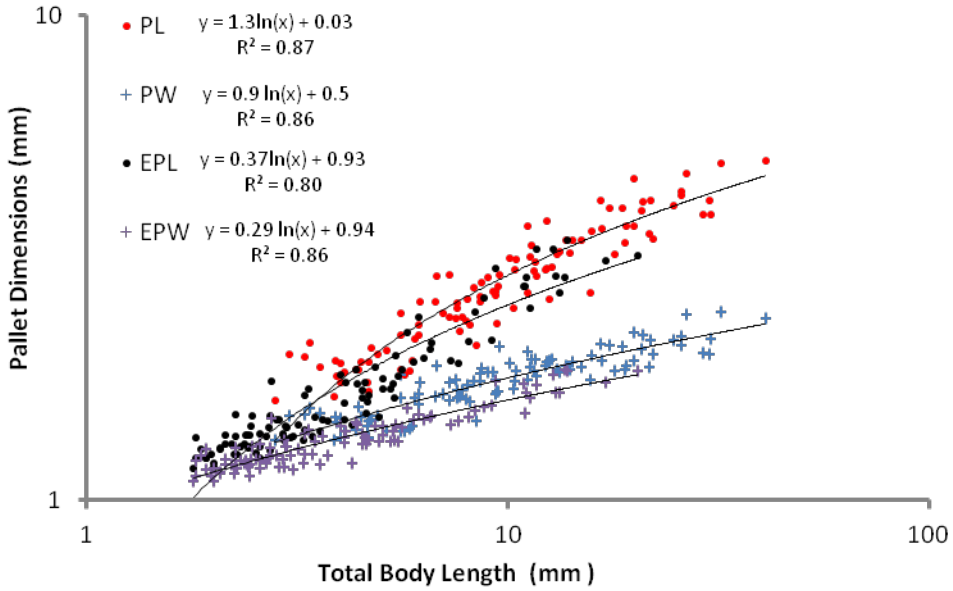

Figure 4.11.a Development of pallets in relation to body length of *Lyrodus pedicellatus* throughout ontogeny. PL and PW), pallet length and width of mature specimens; PW), pallet width of mature specimens; EPL and EPW), pallet length and width of post-metamorphic individuals from the settlement and growth experiment.

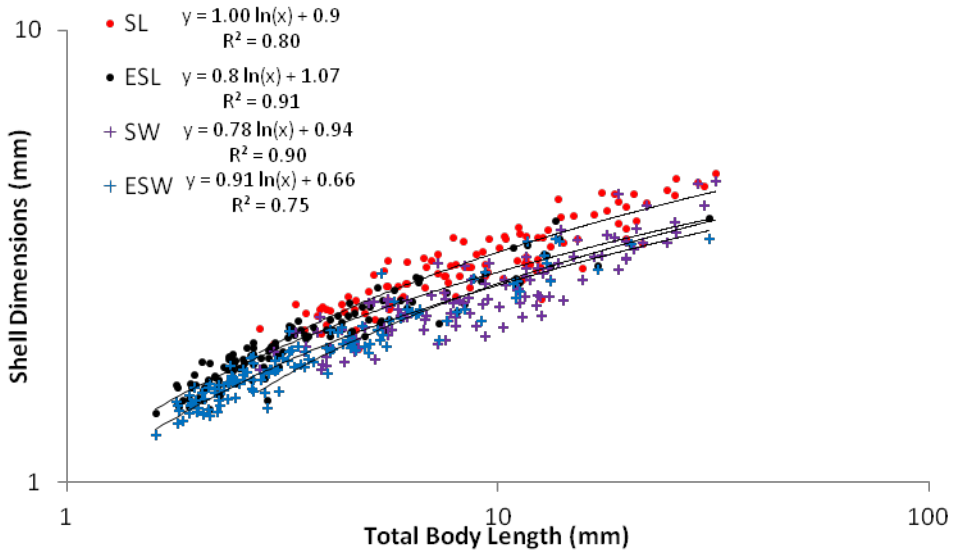

Figure 4.11.b Development of shell valves in relation to body length of *Lyrodus pedicellatus* throughout ontogeny. SL and SW), shell length and width of mature specimens; EPL and EPW), pallet length and width of post-metamorphic individuals from the settlement and growth experiment.

A measurement of pallet dimensions throughout ontogeny is shown in Figure 4.12 a comparison between pallet and shell diameter of *L. pedicellatus* and *Nototeredo norvagica* is shown in Figure 4.12 b. A total of 407 individual pallets were measured. Pallet length proved an excellent predictor of pallet width. Comparison of calcareous structures of *Lyrodus pedicellatus* and *Nototeredo norvagica* revealed that the pallets of *N. norvagica* grew far greater in width than those of *L. pedicellatus,* increasing more rapidly in diameter than the shell valves. However the ratio of shell diameter to pallet width shifts at larger sizes in *L. pedicellatus*, with shell diameter (and therefore tunnel width) growing faster than the burrow opening, as defined by pallet width.

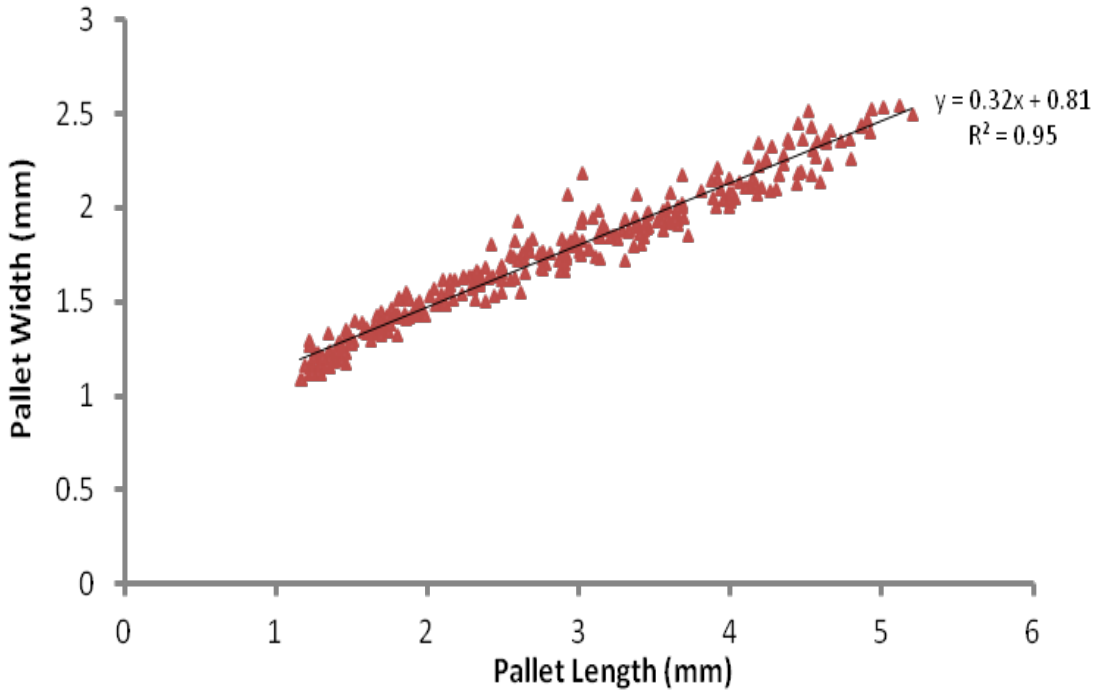

Figure 4.12.a Pallet dimensions of *Lyrodus pedicellatus* throughout ontogeny.

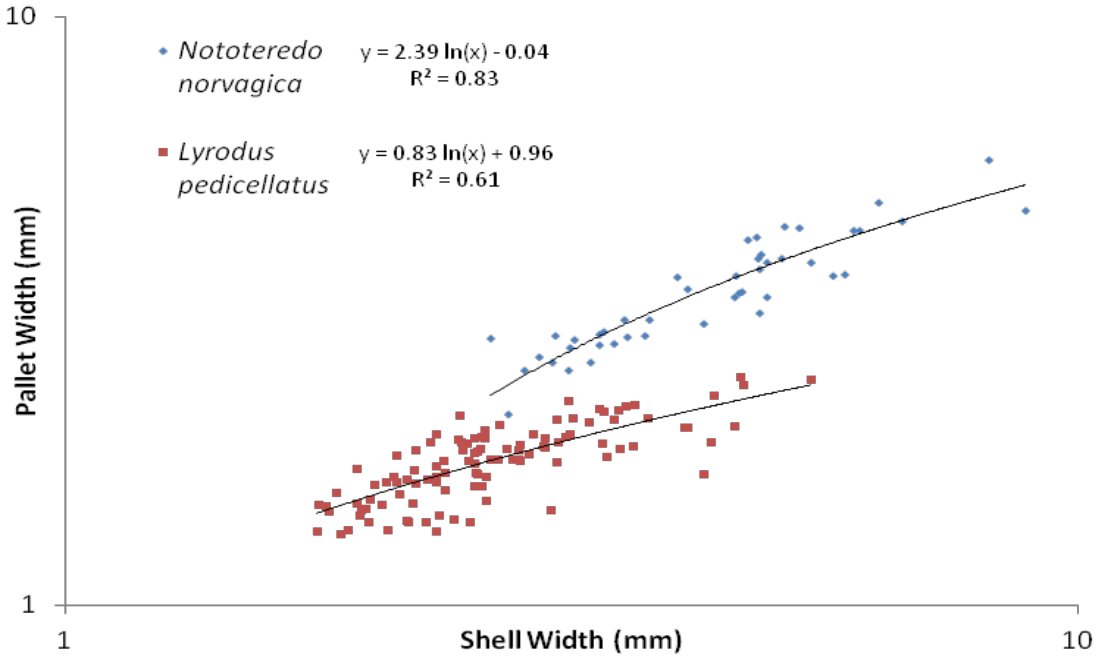

Figure 4.12.b A comparison between the shell and pallet widths of the teredinids *Nototeredo norvagica* (blue) and *Lyrodus pedicellatus* (red).

Evidence for matrotrophy

Figure 4.13a shows the brooded larvae of *L. pedicellatus* on the parental gill. Figures 4.13 b-c show each individual larva encapsulated in a thin, membranous pouch. Cells can be seen budding-off from the inner surface of these pouches (Fig. 4.13 c-d) Figure 14e shows a fully developed larval pediveliger with a hypertrophied velum absent of the pre-oral cilia and reduced post-oral cilia. A unique, epaulette-like cilial structure is seen on the lateral surface of the hypertrophied velum (Fig. 4.13 d-e).

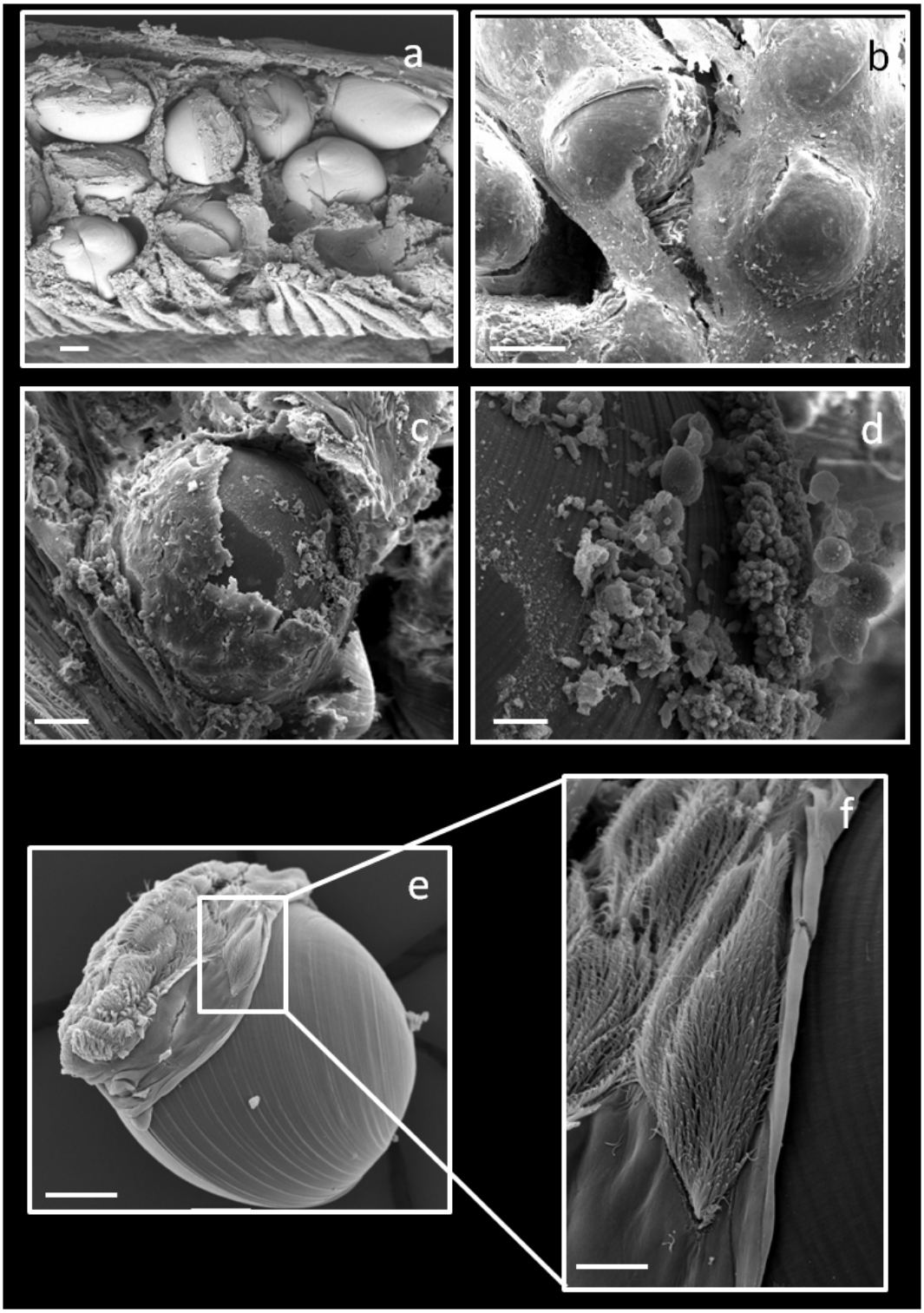

Figure 4.13 A scanning electron microscope image showing the larval pediveligers of *Lyrodus pedicellatus*. a) larval pediveligers on the adult gill with the brood pouch covering removed; b) larval pediveligers wrapped in a thin membranous brood pouch; c) cells budding off from the inner lining of the brood pouch; d) magnified image of budding cells; e) brooded pediveliger with hypertrophied velum showing specialised cilia structure; f) specialised structure magnified . Scale bars for a, b, c, d, e and f represents 100 µm, 100 µm, 50 µm, 10 µm, 100 µm, 20 µm respectively.

Discussion

Larval Release & Settlement

The larval settlement results indicate that *L. pedicellatus* larvae have a strong preference for settling on softer spring growth and upper-facing surfaces of wooden panels as opposed to harder summer growth and lateral surfaces. Settlement on softer substrate may provide larvae with a competitive advantage by allowing them to enter the safety of the wood more quickly, thus limiting exposure to predation and any potential changes in current, which could carry individuals away. Furthermore, burrowing rates would be more rapid in softer timber, thus increasing the volume of wood available to individuals for nutrition. This should allow for an increase in the early growth rate and allow larvae to establish, thus offering a competitive advantage over other individuals.

The intensity of larval settlement, with up to 658 larval boreholes recorded in blocks measuring 2.5 cm^3, demonstrates the huge potential for destruction by long-term brooding species. Adult *L. pedicellatus* brood larvae to the advanced pediveliger stage and these larvae are capable of settlement within hours of release from the parent and have even been observed to begin boring immediately after release (Coe, 1941). This long-term brooding strategy protects the larvae during the most vulnerable period of the life cycle and bypasses many of the threats faced by broadcast spawning and short-term brooding species, such as starvation and predation. Furthermore settlement shortly after release maximises the potential of larvae to locate wood - which is a scarce and patchy resource in marine environments, thus increasing the likelihood of offspring survival (MacIntosh, 2012). Indeed, larvae often settle and bore into the same timber from which their parents originate (Turner & Johnson in Jones & Eltringham, 1971). The high settlement and survival rates presented herein demonstrate the success of this advanced parental care, which provides a developmental 'head start' over broadcast spawners and short-term brooders and allows individuals to dominate and monopolise timber.

Growth & Maturity

The results revealed that *Lyrodus pedicellatus* achieves maturity and may brood fully developed pediveligers at a body size of as small as 4.43 mm in length. This is far smaller than any other documented broadcast spawning or brooding teredinid. Indeed, the previous smallest size at which individuals reached maturity has been measured as 10 mm in the

brooding species *L. mediolobata* (Edmondson, 1942), 10 - 12 mm for *Teredo navalis* (Coe, 1933) and 12 mm in the broadcast spawning *Bankia campanellata* (Nagahushanam, 1959).

Teredinid growth rates are known to be strongly influenced by seawater temperature, with growth rates accelerating as the temperature increases (Eckelbarger & Reish, 1972). The results presented herein show an average growth rate of 0.13 mm in length per day^{-1} for *L. pedicellatus* during the autumn and winter months with an average seawater temperature of 9.8 °C, decreasing to a low of 4.8 °C in January (temperatures taken from www.chimet.co.uk, which records seawater temperatures for Chichester Harbour). Whilst the results presented herein agree with those of Eckelbarger and Reish (1972), who calculated an average growth of 0.124 mm per day between 14 °C and 16 °C, the species optimal growth rate is underestimated. Indeed, the fastest growth rate recorded for *L. pedicellatus* was 0.55 mm per day when maintained at a temperature of 28 °C (Gallager *et al*., 1981), thus specimens from this survey are probably capable of increased growth rates at a higher temperature.

It has been previously observed that *L. pedicellatus* may begin brooding ten weeks after metamorphosis in seawater temperatures of 28 °C (Turner & Johnson in Jones & Eltringham, 1971). Based on growth rates measured herein, *L. pedicellatus* is predicted to reach maturity and begin brooding larvae approximately 34 days after metamorphosis, a rate twice as fast as previous research suggests. Assuming larval developmental times are consistent throughout the genera (approximately three to four weeks for broadcast spawning species - Turner, 1966), *L. pedicellatus* must reach sexual maturity rapidly following metamorphosis.

An individual measuring approximately 24.8 mm in total length was found brooding over 1000 larvae, and specimens measuring 10 mm in length brooded an average of 157 larvae. Larval analysis, which comprised of analysing veligers and pediveligers, did not include trochophores or very early stage veligers yet to secrete a shell due to the difficulties in dissection and handling of minute, fragile specimens. Nevertheless, cohort analysis suggests at least three distinct larval clutches occupying distinct regions of the gill at any one time. This sequential brooding suggests multiple fertilization events and allows adults to regularly release competent pediveligers. Wood is a spatially and temporally unpredictable resource; the high population densities, rapid growth and maturation and the ability to sequentially produce and release large numbers of advanced pediveligers at

relatively small body sizes allow *L. pedicellatus* to maximise its exploitation of this resource.

Calcareous Structures

The shell valves of *L. pedicellatus* grow throughout ontogeny and are approximately equal in both length and width. In comparison the pallets also increase in size throughout ontogeny, yet growth in length is more pronounced than width. Analysis of these calcareous structures may reveal insights into species reliance on either planktotrophy or xylotrophy (Cragg *et al*., 2009). Pallet width defines the opening of the respiratory current and thus volume of water accessible to the individual for suspension-feeding. Shell width correlates with the area of denticulated surface in contact with the anterior burrow and thus indicates the degree to which individuals may exploit wood.

The shell and pallet diameter of *L. pedicellatus* were compared with *Nototeredo norvagica*, a species thought to rely more on planktotrophy than xylotrophy due to a number of anatomical features *i.e.*, the presence of a simple caeca, truncate gills, a pronounced marginal groove and the most complex labial palps of the Teredinidae (Purcheon, 1941; Turner, 1966; Nair & Saraswathy, 1971). The shell valves of *L. pedicellatus* were approximately 1.5-fold broader than the pallets throughout ontogeny, compared with 1.2-fold broader in *N. norvagica*. Whereas shell diameter increased more rapidly in *L. pedicellatus*, pallet diameter increased more rapidly in *N. norvagica*. Indeed, shells with a diameter of 5 mm in *L. pedicellatus* had pallets which were 40 % slimmer than those of *N. norvagica* with a similar shell diameter. This indicates limited access to the water column, thus a reduced dependency on planktotrophy for nutrition. Conversely, a larger shell diameter should abrade more wood, allowing a greater volume of cellulose to pass through the digestive system.

The reduced capacity to draw plankton from the water column and the increased surface area of the shell valves, which should facilitate greater wood consumption, suggests xylotrophy drives growth of the calcareous features in *L. pedicellatus*.

Whilst the pallets are still considered a principle diagnostic feature, identification is challenging due to the variability of these calcareous structures (Turner, 1966; Borges *et al*., 2012). Research by Cragg *et al*. (2009) remarked on the need to measure a large number of pallets across various developmental stages to increase the security of identification based on these calcareous structures. The pallet morphology results presented herein map the variation of 405 pallets from newly settled individuals through to

mature adults of *L. pedicellatus*, thus assisting future identification of this species. This is of particular importance to the taxonomy and identification of this species as it demonstrates the greatest variability in pallet characteristics of any teredinid. Indeed, this has resulted in numerous misidentifications and synonymy throughout the literature (Turner, 1971). Furthermore two cryptic species which are morphologically indistinguishable from *L. pedicellatus* are known to exist (Calloway & Turner, 1983; Borges *et al*., 2012), thus highlighting the necessity of a robust model for the pallet-based identification of *L. pedicellatus*.

Parent-larval interaction during brooding and the evidence for matrotrophy

It is unlikely that short-term brooding teredinids demonstrate matrotrophy, as evidenced by the ability of fertilized *Teredo navalis* eggs to successfully develop to the pediveliger stage and undergo metamorphosis once stripped from the parental gill (Loosanoff & Davis, 1963). Thus, the eggs must provide sufficient energy for development to the veliger stage, at which point the larvae is capable of planktotrophy.

Yet a small body of evidence suggests that long-term brooding species may provide their larvae with extra-embryonic nutrition. The small eggs of brooding teredinids appear insufficient to fuel prodissoconch II growth based on the extensive growth of the shell during this developmental stage (Jablonski & Lutz, 1983; Cragg *et* al., 2009) and Calloway (1982) briefly noted that the larvae of some brooding species appear to ingest glycogen-forming cells originating from the parent. However, no further evidence was provided by Calloway (1982) and this research has not been continued by others.

The pallet dimensions of *L. pedicellatus* relative to shell diameter (as mentioned above) remain slim throughout the species life-cycle. This limits the volume of water which may be drawn into the adult's body cavity. The sheer number of brooded larvae, which take up a significant proportion of the gill area, would also limit the parent's ability to draw in water and then process the suspended particles. Furthermore, the larvae do not appear to have contact with the water column as they are completely encapsulated by a thin, membranous, brood pouch lining. Finally, the larval velum has no clearly defined post-oral cilia and reduced pre-oral cilia and is therefore poorly equipped for the opposed-band feeding mechanism described by Strathman & Grunbaum (2006). The evidence therefore suggests that a limited volume of water enters the gills, the larvae do not come into contact with the water, and the larval velum is not capable of capturing plankton.

Indeed, free swimming *L. pedicellatus* larvae do not incorporate ^{14}C labelled plankton into their body tissue (Mann & Gallager, 1981) and the entire life-cycle of this species may be complete in the absence of plankton (Gallager *et al*., 1981). This strongly suggests that larval growth is supplemented with extra-embryonic nutrition (i.e. nutrition not derived from the egg). SEM images presented herein, appear to show larvae ingesting cells which bud from the inner surface of the brood pouch. Furthermore, the hypertrophied velum included a unique epaulette-like cilial structure, with a possible function of brushing these budding cells towards the mouth for ingestion. Indeed, this structure is likely an adaptation which allows feeding within the confined space of the brood pouch.

Summary

1. The larvae of *L. pedicellatus* settle at rates averaging 38 larvae per 1 cm^3 block and preferentially settle on softer spring wood as opposed to the harder summer wood (2:1 ratio). This may allow individuals to enter the protection of the wood more rapidly due to an increased boring rate, thus limiting exposure to predation and changing environmental conditions.

2. *L. pedicellatus* may attain sexual maturity 34 days after settlement, far more rapidly than previously suggested.

3. Research presented herein provides the first known study of brood size and abundance.

4. Individuals may become gravid and brood pediveliger larvae at 4.43 mm in total body length.

5. Broods contain at least three cohorts of larvae at various developmental stages, suggesting multiple fertilizations.

6. Comparison of the shell and pallet dimensions between *L. pedicellatus* and the suspension-feeding species *Nototeredo norvagica* indicate that *L. pedicellatus* has a greater dependence on xylotrophy and a limited capability for planktotrophy.
7. The mapping of pallet variation throughout ontogeny provides a comparison model for a more assured means of pallet-based identification of *L. pedicellatus*.

8. The larvae have no contact with the water column and lack the typical cilial feeding mechanism. Therefore, it is unlikely that larvae derive nutrition from the plankton.

9. A specialised cilial structure on the velum may allow larvae to feed upon cells which bud from the inner surface of the brood pouch.

Chapter Five: Molecular Phylogeny of the Teredinidae

Introduction

Xylotrophic (wood-eating) and xylotrepetic (wood-boring) bivalves are currently found in only two families, the Pholadidae and the Teredinidae (Turner, 1971). The Pholadidae (commonly known as piddocks) typically occur in shallow, brackish to marine waters and have a wide distribution throughout temperate and tropical regions (Turner & Johnson in Jones & Eltringham, 1971). They are opportunistic borers, burrowing into a variety of substratae other than wood including sand, calcareous shells of other molluscs, stone and certain plastics (Mann & Gallager, 1984). The xylophaginid subfamily are the only known pholads capable of ingesting wood and, whilst they have been reported in shallow waters (Santhakumaran, 1980), they are typically limited to deep marine waters between 100-7500 m (Turner, 2002; Voight & Segonzac, 2012). In contrast to the Pholadidae, all known teredinids – with the possible exceptions of the mud-boring Kuphinae and seagrass-boring Zachsia – are obligate wood-borers and possess the ability to digest wood (Turner, 1966; Turner & Yakovlev; 1981; Distel *et al.*, 2011).

Several anatomical adaptations facilitate this xylotrophic and xylotrepetic lifestyle. These include: the possession of greatly reduced, albeit highly adapted, shells; elongated vermiform (worm-like) bodies; and a pair of calcareous pallets, structures which flank the siphons and are used to plug the entrance to the burrow if the animal is either disturbed or faces unfavourable environmental conditions (Nair & Saraswathy, 1971). Due to these unique anatomical characteristics and specialised lifestyle, the Teredinidae represent some of the most highly adapted Bivalvia and exhibit more variations in morphology than any other group of molluscs (Turner, 1988). Consequently species identification is challenging, and the difficulties of selecting homologous traits among the group mean few phylogenetic surveys have been attempted (Turner, 1966; Santos *et al*., 2005; Distel *et al.*, 2011).

Teredinid Identification

Bivalve identification is typically based on shell features; however, the shells of teredinids fail to display sufficient interspecific variation to be used as a diagnostic feature. Instead, the interspecific variation demonstrated by the pallets provides taxonomists with a means for identification (Turner 1971; Nair & Saraswathy, 1971). However, pallet features may vary during development (Fuller *et al.*, 1989; Tan *et al*., 1993) and are susceptible to alteration by: weathering and erosion through constant contact with the burrow lining and

the opposing pallet; attack from predators; discolouration and erosion from chemicals in the water or tannins in the wood; and the effect of overcrowding, which may lead to malformation (Turner, 1966). Indeed, the opposing pallets from a single pair may be so dissimilar as to be mistaken for separate species (Turner, 1966).

Species identification based on pallet features is more assured if the variation in pallet morphology is characterised by a large number of individuals across a range of developmental stages (Cragg *et al*., 2009). However, this variation has only been documented for four species – *Psiloteredo senegalensis*, *Teredo bartschi*, *Bankia gouldi* and *Teredo navalis* (Monod, 1952; Fuller *et al.*, 1989; Tan *et al*., 1993; Cragg *et al*., 2009) - and this lack of information renders identification challenging (Nair & Saraswathy, 1971). For example, the pallets of species from the genus *Lyrodus* are particularly variable (as shown in Fig. 5.1) and this has resulted in a total of 34 synonyms for the species *L. pedicellatus* alone (Turner, 1966 & 1971). In addition to the poor documentation of pallet variation, many descriptions are based on mature specimens with fully developed pallets. This creates ambiguity in identifying young specimens which is further compounded by the similarities in pallets of a number of species, such as *Lyrodus pedicellatus* and *Bankia carinata*, which are similar in appearance during their early development (Turner, 1966). Misidentification by non-specialists using general keys may result in these errors becoming perpetuated throughout the literature (Borges *et al*., 2012).

Figure 5.1 Variation in pallet morphology of *Lyrodus pedicellatus* specimens cultured at the Institute of Marine Sciences. Scale bar 1 mm.

Certain morphological characteristics may also be used to aid identification, the most notable of which are the siphonal features. Variations in siphonal length, the degree of

separation between incurrent and excurrent siphon, pigmentation and the number of papillae are known to differ to a degree among certain species (Roch, 1940; Turner, 1966). Characterising these features would prove valuable for field identification as specimens could be studied *in situ* without the necessity of extracting the teredinid from its burrow. However, the siphonal characteristics have only been described for a small number of species (Roch, 1940; Turner & Johnson in Jones & Eltringham, 1971; Moraes & Lopes, 2003) and the degree of genetic, ontogenic and regional variation and the influence ecological conditions may have on these features has yet to be documented (Turner, 1966). As such, siphonal characters offer limited value to species identification.

Teredinid Phylogeny

Species identification is therefore challenging due to the poor documentation of the variation in principal diagnostic characters. Difficulties in identification were further compounded by the fragmentary nature of teredinid literature, the description of new species based on few or incomplete specimens and the poor understanding of teredinid biogeography and dispersal. This resulted in over 200 synonyms and a taxonomy which existed in a state of "chaos" (Turner, 1966; Nair & Saraswathy, 1971).

The first systematic taxonomic survey of the Teredinidae (Turner, 1966) organised species into three subfamilies composed of six groups (as shown in Table 5.1), based on the structure and growth of the pallets, anatomical characters and species life history strategies: the *Kuphinae*, containing the mud-boring genus *Kuphus* (group I); the *Teredininae*, which includes the genera *Bactronophorus*, *Neoteredo*, *Dicyathifer*, *Teredothyra* (group II), *Teredora*, *Psiloteredo*, *Uperotus* (group III) and *Lyrodus* and *Teredo* (group IV); the four *Bankiinae* genera - *Nototeredo* (group V), *Spathoteredo*, *Nausitora* and *Bankia* (group VI). Accordingly, the 227 existing synonyms were condensed into 66 well-described species, representing a considerable milestone in the teredinid literature. Since this survey two further species have been described, bringing the total number of species to 68 (Turner, 1966; Turner & Yakovlev, 1982; Macintosh, 2012).

Subfamily	Group	Genus
Kuphinae	I	***Kuphus*** **(Guettard, 1770)**
Teredinidae	II	***Bactronophorus*** **(Tapparone-Canefri 1877)**
		Neoteredo **(Bartschi, 1920)**
		Dicyathifer **(Iredale, 1932)**
		Teredothyra **(Bartschi, 1920)**
	III	***Teredora*** **(Bartschi, 1920)**
		Psiloteredo **(Bartschi, 1920)**
		Uperotus **(Guettard, 1770)**
	IV	***Lyrodus*** **(Gould, 1870)**
		Teredo **(Linaeus, 1758)**
Bankiinae	V	***Nototeredo*** **(Bartschi, 1920)**
		Spathoteredo **(Moll, 1928)**
	VI	***Nausitora*** **(Wright, 1864)**
		Bankia **(Grey, 1842)**

Table 5.1 The Teredinidae as grouped by Turner (1966). Groups are based on pallet morphology, anatomical characters and breeding strategy.

More recently, the emergence of genomic approaches towards phylogeny have challenged traditional models and offered new insights into taxonomic relationships across the Animal Kingdom, which have become widely accepted in the literature (Field *et al*., 1988; Blaxter *et al*., 1998; Herbert *et al*., 2003; Miller, 2007**;** Bourlat *et al*., 2008). This powerful tool for taxon diagnosis has also been successfully utilised for the Bivalvia (Adamkewicz *et al*., 1997; Steiner & Hammer, 2000; Plazzi *et al*, 2010). Furthermore, molecular identification offers a streamlined means of species identification and has proven useful for detecting cryptic species, clarifying problems associated with synonymy, improving traceability of invasive species and assisting in the identification of early life history stages and incomplete specimens (Herbert & Gregory, 2005; Borges *et al*., 2012). This is of particular relevance when considering the difficulties associated with teredinid extraction, as the removal of whole specimens from heavily infested wood is often challenging. Yet despite the advantages of molecular-based phylogenetics and given both the economic and

environmental importance of the Teredinidae, few molecular-based studies have been undertaken.

The first phylogenetic study assessed four species (*Neoteredo reynei*, *Bankia fimbriatula*, *Nausitora fusticula* and *Psiloteredo healdi*) from two subfamilies (Teredinidae and Bankiinae) using the small mitochondrial 16S subunit and found that the genetic distances did not support classification of these species into separate sub-families (Santos *et al*., 2005). Distel *et al.* (2011) produced the first phylogenetic tree of the Teredinidae based on the small and large nuclear subunit rRNA genes in order to determine the origins of xylotrophy in the Bivalvia. This study included 16 teredinid species representing all groups defined by Turner (Turner, 1966), with the exception of *Nototeredo* from group V (Distel *et al*., 2011). The data indicated that the Pholadidae and sub-families of the Teredinidae (Bankiinae and Teredininae) are not monophyletic and that the principal traits for their taxonomic diagnosis are phylogenetically misleading (Distel *et al*., 2011). Whilst providing valuable insights into the origin of xylotrophy in the Bivalvia, this study only used nuclear markers for phylogenetic analysis (Distel *et al*., 2011), even though a fragment of the mitochondrially-encoded cytochrome C oxidase subunit I (COI-5P) has been accepted as the standardised marker in animal species identification (Herbert *et al*., 2003; Miller, 2007).

The most recent molecular phylogenetic study of the Teredinidae used an integrative taxonomic approach, combining nuclear and mitochondrial markers with biogeographical data and pallet morphologies, to examine European teredinid distribution (Borges *et al*., 2012). The analysis of multiple characteristics employed in taxon diagnosis and species identification is termed ‘integrative taxonomy’ and is considered the most robust technique for species identification (Herbert & Gregory, 2005; Schlick-Steiner *et al*., 2009; Padial *et al*., 2010).

Adopting the integrative approach outlined by Borges *et al*. (2012), this study builds upon the phylogenetic survey by Distel *et al*. (2011) by producing sequence data for additional species not included in previous works. Furthermore, research presented herein produces the first phylogenetic survey of the Teredinidae based on mitochondrial markers, thus offering a greater resolution in species delimitation. The sequence data are combined with biogeographical information on species collection, pallet morphologies and other anatomical characteristics, thus improving the taxonomic resolution of species within this

complex group. Moreover, COI-5P and 18S sequences will be uploaded to the GenBank, thus further assisting future species identification.

Materials and methods

Sample Collection

Teredinid sample collection details are outlined in Table 5.2.

Specimen	Location	Collector
Neoteredo reynei	Cartagena, Columbia	Michael Ahrens
Teredothyra dominicensis	Carlisle Bay, Barbados/ Kaş , Turkey	Melanie Crockett/Reuben Shipway
Psiloteredo megatora	Strömstad, Sweden	Christin Appelqvist
Nototeredo norvagica	Kas, Turkey/ Samos, Greece	Reuben Shipway
Lyrodus pedicellatus	Samos, Greece/ Langstone Harbour, UK	
Teredo sommersi		
Dicyathifer manni		
Teredo mindanensis		
Teredo furcifera		
Lyrodus bipartitus	Takang Besi Archipelago, Indonesia	Ian Hendy
Spathoteredo obtusa		
Teredo clappi		
Lyrodus turnerae		
Lyrodus massa		

Table 5.2 Details of teredinid specimens collected for sequencing, including sample locations and specimen collector.

Identification & Morphometry

Calcareous structures were photographed using a stereo microscope. Images were captured using a JVC KY-F 1030U digital camera with accompanying KY0Link image capture program. Identification was based on species descriptions and pallet characteristics provided by Turner (1971).

Molecular Identification

DNA was extracted from siphonal tissue and associated musculature. Total genomic DNA was extracted using DNeasy Blood & Tissue kit (Qiagen), deviating from the manufacturer's protocol as follows: tissue was lysed overnight at 56 °C and DNA was eluted from the spin column using molecular grade water (2 × 70 µL washes) as opposed

to elution buffer. Concentration, yield and purity of DNA were determined by UV spectrophotometry, with 1 absorption unit at 260 nm approximately equal to 50 ng/µL dsDNA). When necessary, DNA template was diluted using molecular grade water to a concentration of 10-20 ng/µL.

A 658 bp fragment from the 5' end of the cytochrome oxidase subunit I (COI-5P) was amplified using the primer pair LCO1490 (forward 5' GGT CAA CAA ATC ATA AAG ATA TTG G 3') and HCO2198 (reverse 5' TAA ACT TCA GGG TGA CCA AAA AAT CA 3') (Folmer *et al.*, 1994). Amplifications were performed in 25 µL reactions, with each reaction containing (stock concentrations in parentheses): 2.5 µL 10 × PCR buffer, 2.5 µL $MgCl_2$ (25 mM), 0.25 µL dNTP mixture (10 mM each), 0.5 µL of each primer (10 mM), 0.25 µL Taq Polymerase (5 U/µL), 1-2 µL DNA template (10-20 ng/µL) and brought to volume with molecular grade water. The PCR protocol was as follows: an initial cycle of 94 °C for 90 s, 45 °C for 90 s and 72 °C for 60 s, followed by 35 cycles of 94 °C for 30 s, 51°C for 90 s and 72°C for 60 s, with a final extension of 72 °C for five minutes.

A small fragment of the 18S rRNA gene, approximately 345bp, was amplified using the primer pair SSU_FO4 (5'-GCTTGTCTCAAAGATTAAGCC-3') and SSU_R22 (5'-GCCTGCTGCCTTCCTTGGA-3') (Blaxter et al., 1998). Amplifications were performed in 25 µL reactions, with each reaction containing (stock concentrations in parentheses): 2.5 µL 10 × PCR buffer, 2.5 µL $MgCl_2$ (25 mM), 0.25 µL dNTP mixture (10 mM each), 0.5 µL of each primer (10 mM), 0.25 µL Taq Polymerase (5 U/µL), 1-2 µL DNA template (10-20 ng/µL) and bought to volume with molecular grade water. The PCR protocol was as follows: an initial cycle of 2 min at 95 °C, followed by 35 cycles of 1 min at 95 °C, 45 s at 57 °C, 3 min at 72 °C and a final extension of 10 min at 72 °C. A 6 µL aliquot of PCR product was then electrophoresed in a 2 % agarose gel. Amplified products were purified using a NucleoSpin Gel and PCR Clean-up kit (Macherey-Nagel, Duren, Germany) according to the manufacturer's guidelines. All PCR products (COI-5P and 18S) products were sequenced by Source Bioscience.

Data Analysis

COI-5P and 18S sequences were edited and aligned using MEGA 5.1 (Tamura *et al.,* 2011). Sequences were uploaded onto GenBank. Edited sequences were compared with those on the GenBank database to confirm species identity and ensure that endosymbiont bacteria or other contaminant had not been co-amplified in error. Sequences were aligned using Clustal W (Tamura *et al.,* 2011) and COI sequences were translated to check for the

presence of frameshift mutations, stop codons or unusually divergent amino acid profiles. Sequences consisting of 658bp and 345bp for COI and 18S, respectively, were used for phylogenetic inference using Neighbour-joining (NJ). Neighbour-joining trees for both COI and 18S sequences were constructed using the Kimura 2-parameter model (K2P) with the programme MEGA 5.1. Selected GenBank sequences were used to compare with our data set and to be used as outgroups.

Results

Morphological identification of specimens

Specimens could be identified to a species level based on the following morphological characteristics and pallets features. Pallet characteristics match descriptions by Turner (1971), with text in bold offering new observations and additional features.

Figure 5.2a *Lyrodus pedicellatus* (Quatrefages, 1849)

Pallet description: pallets non-segmented, formed of a single calcareous base and tipped with a golden brown-black periostracum which is highly variable in shape and often worn away in older specimens; typical periostracum end in a U-shape with lateral horns at the distal margin; distal region of calcareous blade is conical; blade distally sheathes the stalk.

Figure 5.2b *Lyrodus bipartitus* Jeffreys 1860

Pallet description: pallets similar to that of *L. pedicellatus*, yet differs with regards to periostracum morphology; periostracum features a deep, longitudinal furrow on outer face.

Figure 5. 2c *Lyrodus turnerae* MacIntosh 2012

Pallet description: calcareous base rounded and compact; conical cup-shaped periostracum, varying from golden brown to black in colour, inserted into and contiguous with the calcareous base; periostracum descends into base forming a V-shape.

Figure 5.2d *Lyrodus massa* Lamy 1923

Pallet description: triangular calcareous base with a conical cup-shaped periostracum, varying from golden brown to black in colour, inserted into calcareous base.

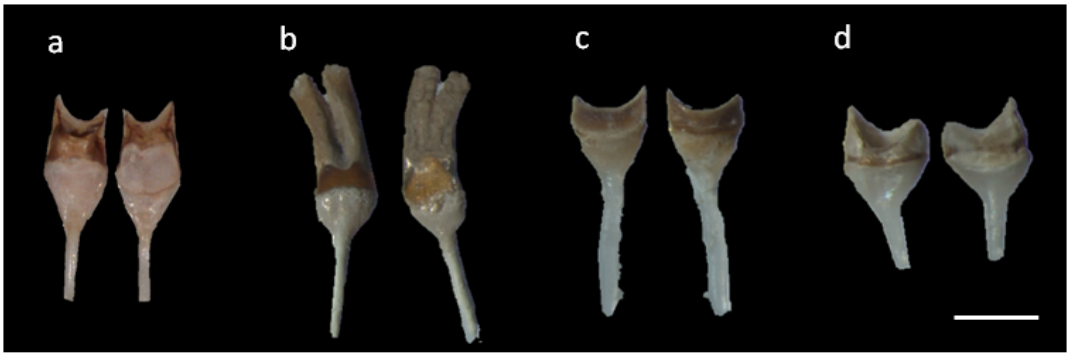

Figure 5.2 Inner and outer face of pallet pairs from species of the genus *Lyrodus* a). *L. pedicellatus;* b) *L. bipartitus*; c). *L. turnerae;* d). *L. massa*; Scale bar 5 mm. All species bar *L. pedicellatus* were collected from Indonesia as detail in Table 5.2.

Figure 5.3a *Teredo sommersi* Clapp, 1924

Pallet description: stalk straight and thick, typically equal to or shorter in length than the blade; distal end slightly of the blade is concave, more so on the outer margin than the inner margin; distal blade covered in red-brown periostracum.

Figure 5.3b *Teredo clappi* Bartsch, 1923

Pallet description: stalk is distally swollen and typically longer than the blade; the proximal stalk is enveloped by the periostracum; the inner and outer distal margin of blade is slightly concave and a small cleft often forms in the distal margin of younger specimens; slight thumbnail-like depression on inner face of blade.

Figure 5.3c *Teredo furcifera* von Martens, 1894

Pallet description: pallets non-segmented, blade formed of one piece with a traversed ridge at its mid-point; periostracum varies from light to dark brown in colour and forms deep U/V shape which is more pronounced on the outer margin than the inner.

Figure 5.3d *Teredo mindanensis* Bartsch 1923

Pallet description: the blade is triangular shaped and hollow through to the stalk; periostracum yellow-brown in colour; the stalk is short and forms a knob at proximal end.

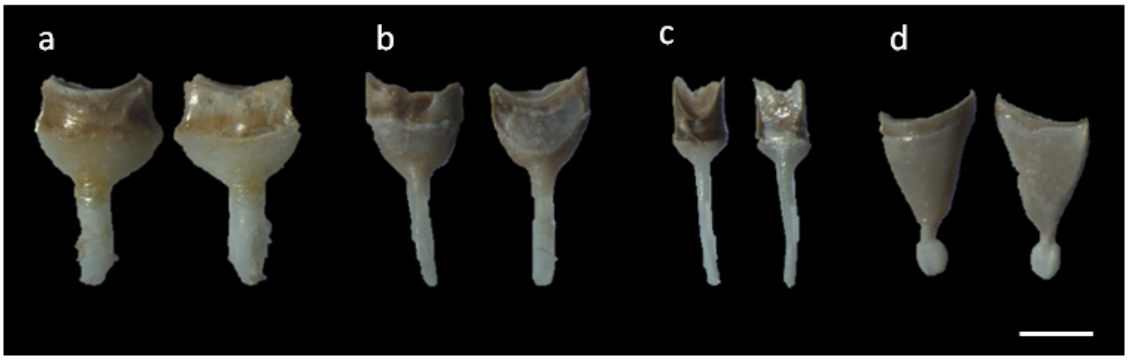

Figure 5.3 Inner and outer face of pallet pairs from species of the genus *Teredo*. a). *T. sommersi*; b). *T. clappi*; c). *T. furcifera*; d). *T. mindanensis*. Scale bar 5 mm. All species collected from Indonesia as detail in Table 5.2.

Figure 5.4a *Dicyathifer manni* Wright 1866

Pallet description: the blade is as wide as it is long and forms a U-shape on the distal margin of the inner face whilst appearing flat on the inner face; pallet divided by a medial ridge forming a double cup.

Figure 5.4b *Spathoteredo obtusa* (Sivickis 1928)

Pallet description: pallets segments and fused; a thin, brown coloured incrustation with fine papillae cover the outer surface; **blade extends entire length of calcareous blade on inner surface**.

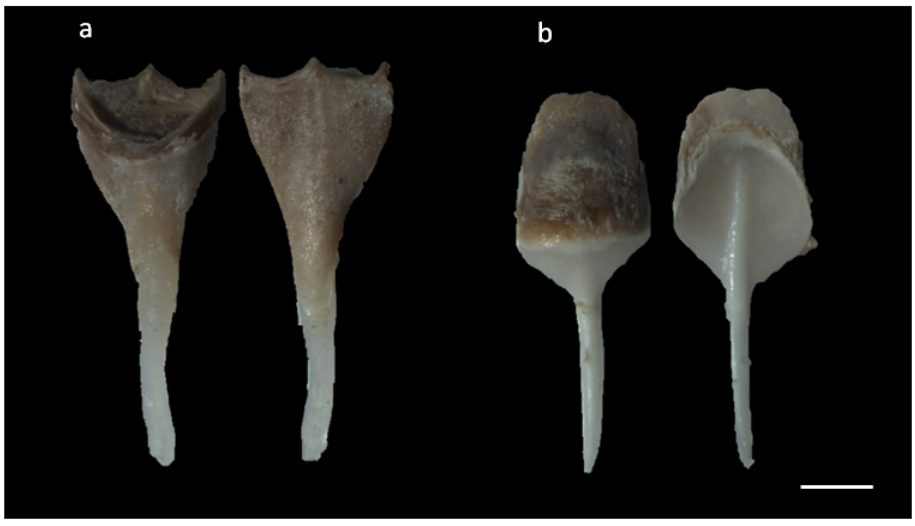

Figure 5.4. Inner and outer face of pallet pairs from a) *Dicyathifer manni* and b) *Spathoteredo obtusa*. Scale bar 5 mm. All species collected from Indonesia as detail in Table 5.2.

Figure 5.5a *Teredothyra dominicensis* Bartsch, 1921

Pallet description: pallets are non-segmented and longer than wide throughout ontogeny; calcareous portion of the blade is sub-divided into two cups and separated by a medial septum; the distal margin of blade is concave, more so on the outer margin than the inner margin; the stalk thick and extends into blade; both the blade and stalk are predominantly hollow throughout. **The posterior region of calcareous burrow thickens and bifurcates around siphons and this lining may extend a number of centimetres from the wood substrate** (Fig. 5.6a).

Figure 5.5b *Nototeredo norvagica* (Spengler, 1792)

Pallet description: pallets composed of fused segments which are tightly compacted; the stalk extends entire length of blade with rib-like elements radiating from it; the blade paddle-like, broadest distally and tapering proximally; a yellow-brown periostracum covers entire surface of blade in younger specimens and is often worn away in older specimens; a subtle, thumbnail-like depression is present on the outer face. The posterior region of calcareous burrow is concamerated (Fig. 5.6b). **The siphon papillae are short, truncate and non-pigmented** (Fig. 5.7a).

Figure 5.5c *Psiloteredo megatora* Hanley, 1848

Pallet description: pallets are non-segmented and almost entirely calcareous; the perimeter of blade covered in clear periostracum which is often worn away in older specimens; periostracum is more visible on the outer face; outer face characterised by moderate to deep, thumbnail-like depression; finger-like projections extend outward from depression and are often lost in older specimens; pallets of older specimens become more paddle-like; **distal region of stalk is triangular and extends almost along the entire length of the blade on the outer face**. The posterior region of calcareous burrow is concamerated (Fig. 5.6b). **The siphon papillae are long, finger-like and non-pigmented** (Fig. 5.7b).

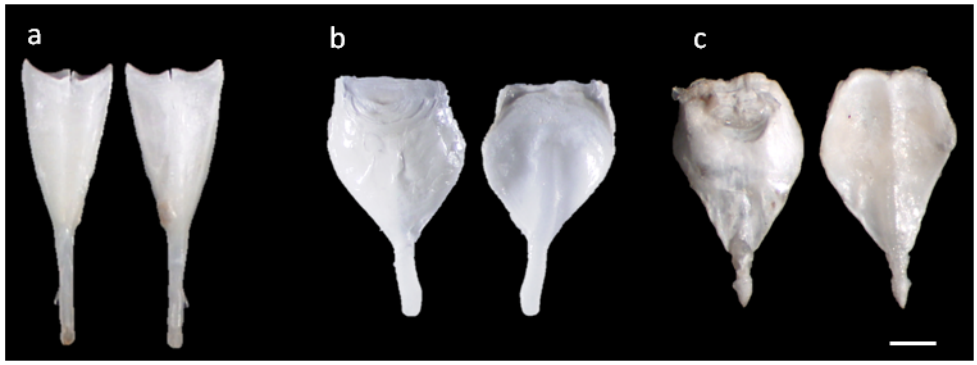

Figure 5.5 Inner and outer face of pallet pairs from three species. a) *Teredothyra dominicensis*; b) *Nototeredo norvagica* and c) *Psiloteredo megatora.* Detailing the pointed and round stalks (St) of specimens b and c. Scale bar 1 mm. All specimens collected in European waters as outlined in Table 5.2.

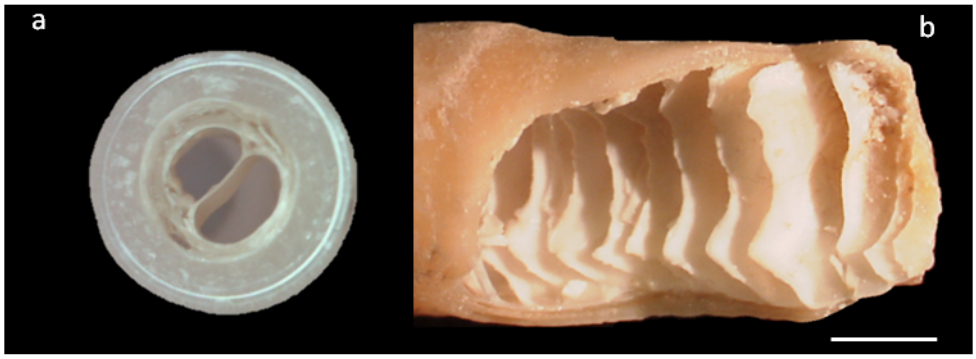

Figure 5.6 Calcareous burrow lining features. a) Posterior region of the calcareous burrow lining of *Teredothyra dominicensis*, showing the septum separating incurrent and excurrent siphons; b) showing concamerations in the burrow lining of *Nototeredo norvagica*. Scale bar 1 cm.

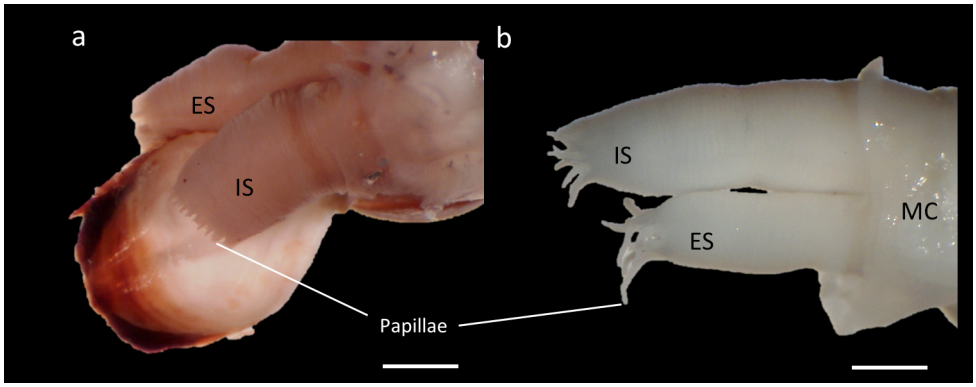

Figure 5.7 Siphonal features. The siphons of a) *Nototeredo norvagica* and b) *Psiloteredo megatora* . IS, incurrent siphon; ES, excurrent siphon; MC, mantle collar. Scale bar 1 cm.

Figure 5.8 *Neoteredo reynei* Bartsch, 1920

Pallet description: pallets large and paddle shaped; slight thumbnail-like depression on distal outer face, more apparent in young specimens; some pallets display digitiform projections with calcareous encrustations; dorsal lappets, found at the posterior region anteriorly of the siphons, are a diagnostic feature of the species.

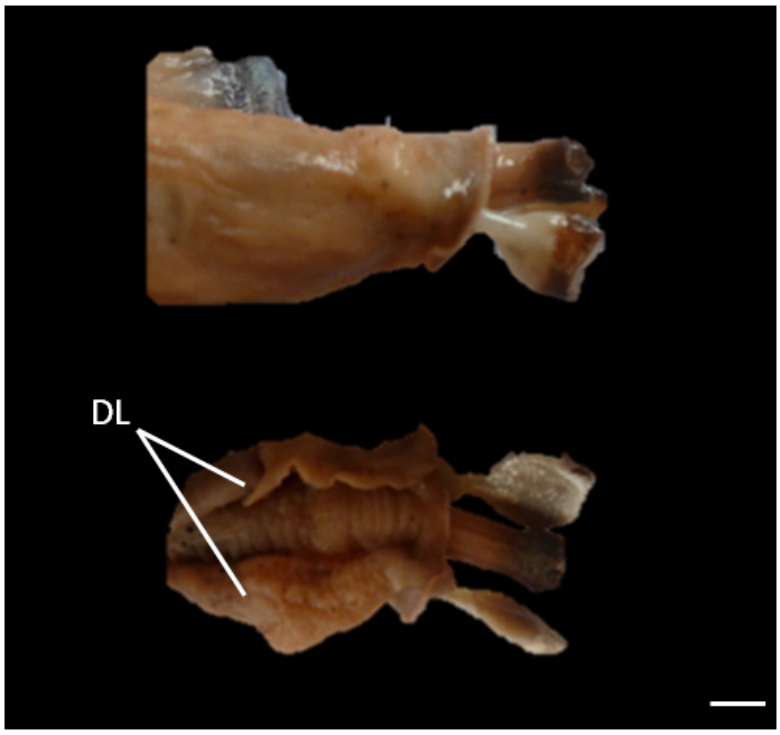

Fig 5.8. Pallet, siphonal and dorsal lappet (DL) morphology of *Neoteredo reynei* from Colombia. Images courtesy of Michael Ahrens, Universidad de Bogotá. Scale bar 1 cm. Specimen collected from Colombia as detail in Table 5.2.

Basic Local Alignment Search Tool (BLAST) Analysis of COI-5P and 18S Sequences

All sequences were confirmed to a taxonomic level (group Teredinidae) by comparing homologies using the basic local alignment search tool (BLAST) from GenBank, thus ruling out the possibility of analysing bacterial sequences. A number of sequences were confirmed to species level when compared with known teredinid sequences previously deposited within GenBank.

Table 5.3a details the BLAST analysis of 18S sequences from this survey with those of deposited teredinid sequences on GenBank and includes the closest species match, the E-value and maximum % ID. The 18S sequences for *Neoteredo reynei*, *Teredothyra dominicensis*, *Nototeredo norvagica*, *Lyrodus pedicellatus* and *Spathoteredo obtusa* all showed a 100 % match with sequences from the corresponding species previously deposited in GenBank. *Dicyathifer manni* was also positively identified, showing a 99 % match. BLAST comparisons of sequences for *Teredo clappi, Teredo sommersi* and *Teredo furcifera* match with a sequence for *Teredo navalis* – the only 18S *Teredo* sequence currently deposited with GenBank - with 99 %, 99 % and 100 % identity respectively. The sequence for *Lyrodus* sp. possessed 100 % identity with the GenBank sequence for *Lyrodus massa*, and the sequence for *Lyrodus massa* possessed 99 % identity with the GenBank sequence for *Teredo navalis*. The sequence for *Psiloteredo megatora* from this survey showed a 99 % match to the closest related species on GenBank, *Dicyathifer manni*.

Table 5.3b details the BLAST analysis of COI-5P sequences from this survey with those of deposited teredinid sequences on GenBank and includes the closest species match, the E-value and maximum % ID. Sequence analysis for *Teredothyra dominicensis*, *Nototeredo norvagica* and *Lyrodus pedicellatus* possessed 99 %, 100 % and 100 % identity with their corresponding sequences on GenBank. The species *Neoteredo reynei*, *Psiloteredo megatora*, *Teredo sommersi*, *Teredo mindanensis*, *Teredo clappi*, *Lyrodus bipartitus* and *Lyrodus turnerae* displayed highest similarity with *Lyrodus pedicellatus*, possessing between 79 % and 91 % maximum identity. COI-5P sequences for *Dicyathifer manni* most closely matched those of *Nototerdo norvagica*, with 81 % maximum identity.

18S								
Specimen	Closest GenBank Match	BP	Max Score	Total Score	Query Coverage	E-Value	Max I.D.	Accession
Neoteredo reynei	*Neoteredo reynei*	337	648	648	100%	0	100%	gi|338163524|JF899217.1
Teredothyra dominicensis	*Teredothyra dominicensis*	345	550	550	100%	2.00E-153	100%	gi|442535622|KC158222.1
Psiloteredo megatora	*Dicyathifer manni*	345	640	640	100%	2.00E-180	99%	gi|338163515|JF899208.1
Nototeredo norvagica	*Nototeredo norvagica*	345	542	542	85%	5.00E-151	100%	gi|442535610|KC158210.1
Lyrodus pedicellatus	*Lyrodus pedicellatus*	345	664	664	100%	0	100%	gi|159025819|AM774540.1
Teredo sommersi	*Teredo navalis*	345	658	658	100%	0	99%	gi|338163529|JF899222.1
Dicyathifer manni	*Dicyathifer manni*	345	656	656	100%	0	99%	gi|338163515|JF899208.1
Teredo mindanensis	*Lyrodus massa*	345	650	650	100%	0	99%	gi|338163519|JF899212.1
Teredo furcifera	*Teredo navalis*	345	664	664	100%	0	100%	gi|338163529|JF899222.1
Lyrodus bipartitus	*Lyrodus pedicellatus*	345	664	664	100%	0	100%	gi|338163518|JF899211.1
Spathoteredo obtusa	*Spathoteredo obtusa*	345	664	664	100%	0	100%	gi|338163528|JF899221.1
Teredo clappi	*Teredo navalis*	345	658	658	100%	0	99%	gi|338163529|JF899222.1
Lyrodus turnerae	*Lyrodus massa*	345	700	700	99%	0	100%	gi|338163519|JF899212.1
Lyrodus massa	*Teredo navalis*	362	685	685	99%	0	99%	gi|338163529|JF899222.1

COI-5P								
Specimen	GenBank Match	BP	Max Score	Total Score	Query Coverage	E-Value	Max I.D.	Accession
Neoteredo reynei	*Lyrodus pedicellatus*	639	490	490	91%	5.00E-135	81%	gi|442535639|KC157922.1
Teredothyra dominicensis	*Teredothyra dominicensis*	601	1150	1150	100%	0	99%	gi|442535680|KC157943.1
Psiloteredo megatora	*Lyrodus pedicellatus*	628	421	421	93%	3.00E-114	79%	gi|442535639|KC157922.1
Nototeredo norvagica	*Nototeredo norvagica*	658	542	542	85%	5.00E-151	100%	gi|442535610|KC158210.1
Lyrodus pedicellatus	*Lyrodus pedicellatus*	658	1265	1265	100%	0	100%	gi|442535639|KC157922.1
Teredo sommersi	*Lyrodus pedicellatus*	628	573	573	95%	6.00E-160	83%	gi|442535639|KC157922.1
Dicyathifer manni	*Nototeredo norvagica*	633	519	519	97%	1.00E-143	81%	gi|442535657|KC157931.1
Teredo mindanensis	*Lyrodus pedicellatus*	642	477	477	86%	5.00E-131	81%	gi|442535639|KC157922.1
Teredo furcifera	NA	NA	NA	NA	NA	NA	NA	NA
Lyrodus bipartitus	*Lyrodus pedicellatus*	555	600	600	98%	4.00E-168	86%	gi|442535639|KC157922.1
Spathoteredo obtusa	NA	NA	NA	NA	NA	NA	NA	NA
Teredo clappi	*Lyrodus pedicellatus*	639	206	206	35%	2.00E-49	82%	gi|442535627|KC157916.1
Lyrodus turnerae	*Lyrodus pedicellatus*	627	575	575	94%	2.00E-160	83%	gi|442535639|KC157922.1
Lyrodus massa	NA	NA	NA	NA	NA	NA	NA	NA

Table 5.3 Basic Local Alignment Search Tool (BLAST) analysis of both the 18S and COI-5P sequences from all teredinid specimens analysed. Data includes the closest sequence match on GenBank and its accession details, the number of base pairs (BP) compared, the E-value and the maximum percentage identity.

Phylograms Inferred from 18s and COI-5P Sequences

The 18S and COI-5P trees are shown in figures 5.10a and 5.10b respectively. The 18S tree contained a greater number of species than the COI-5P tree, thus topologies between the two trees differed slightly. For the COI-5P tree *N. norvagica*, *N. reynei*, *D. manni, P. megatora*, *T. sommersi* and *L. bipartitus* all clustered in a monophyletic group with either sequences of the same species from GenBank or when multiple sequences from the same species were aligned. For the 18S tree, specimens of *N. reynei*, *N. norvagica*, *D. manni, S. obtusa* and *L. bipartitus* all clustered in a monophyletic group with either sequences of the same species from GenBank or when multiple sequences from the same species were aligned. However, resolution was not sufficient to clearly separate the genera *Teredo* and *Lyrodus*. Tree topologies showed no variation based on the evolutionary model or tree-building method.

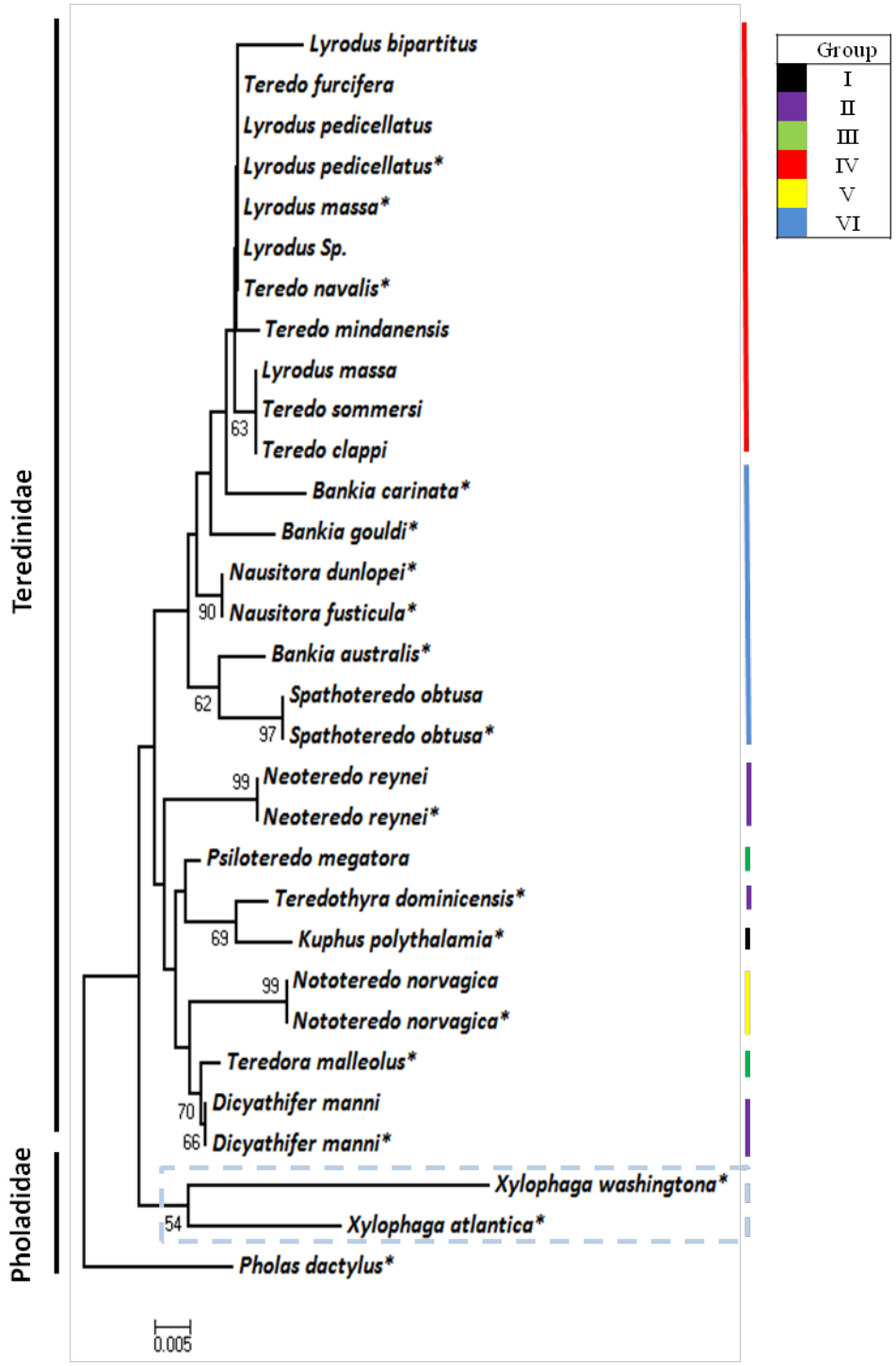

Figure 5.10 a. Phylogenetic hypothesis for teredinid bivalves and related taxa using the 18S sequences. Phylogram inferred by neighbour-joining of partial sequences for the small subunit nuclear rRNA gene. Boot strap proportions > 50 % indicated at associated nodes. The closely related *Pholas dactylus* is rooted as an outgroup. Taxa displayed within dashed box are Xylophagidae. Asterisks denote sequences from GenBank. Coloured bars correspond to the teredinid group defined by Turner (1966) as follows: group I (black); group II (purple); group III (green); group IV (red); group V (yellow); group 6 (blue).

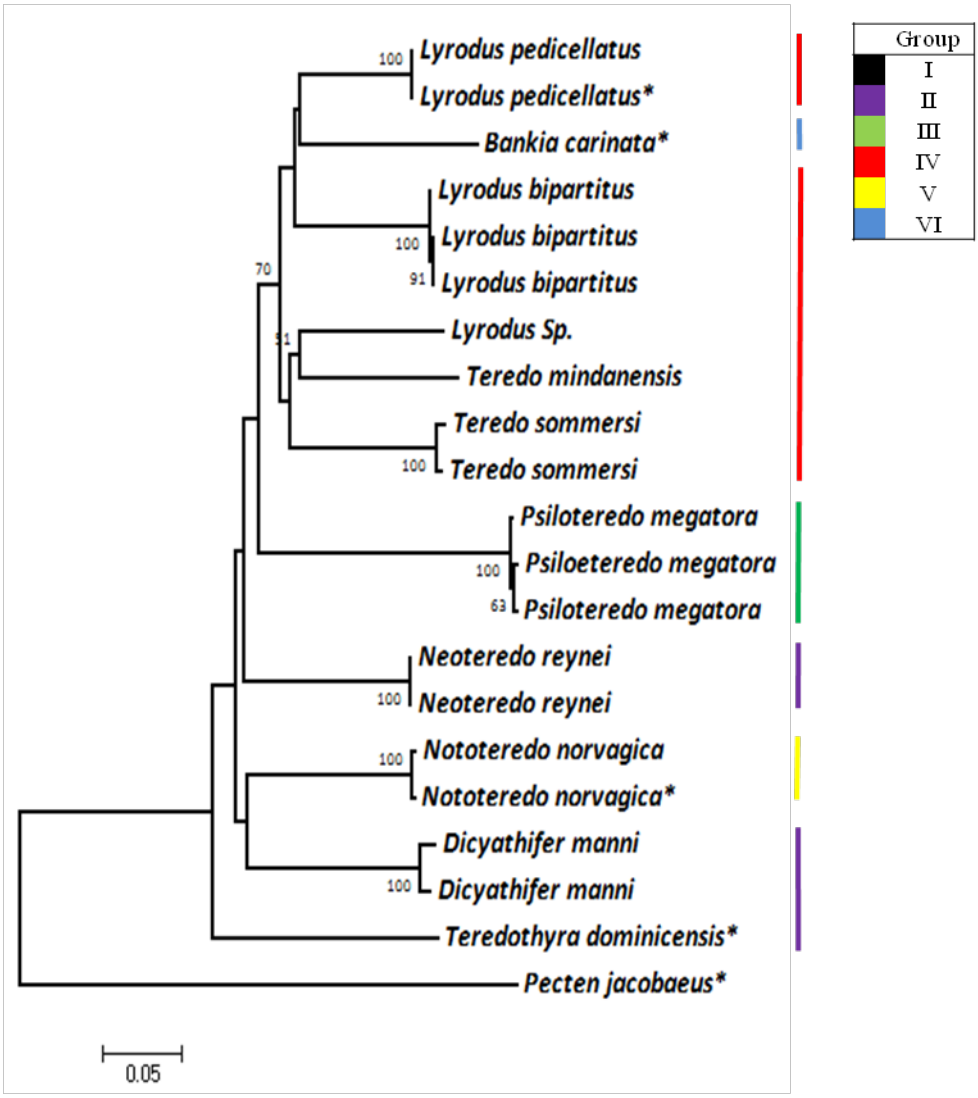

Figure 5.10 b. Phylogenetic hypothesis for teredinid bivalves and related taxa using COI-5P sequences. Phylogram inferred by neighbour-joining (NJ) of partial sequences for the cytochrome oxidase COI-5P gene of the mitochondria. Boot strap proportions > 50 % indicated at associated nodes. The closely related *Pecten jacobaeus* is rooted as an outgroup. Asterisks denote sequences from GenBank. Coloured bars correspond to the teredinid group defined by Turner (1966) as follows: group I (black); group II (purple); group III (green); group IV (red); group V (yellow); group 6 (blue).

Pairwise Distance Analysis for the 18S Region

The pairwise distance between all 18S samples analysed, including the comparative teredinid sequences from GenBank, are displayed in Table 5.4a. All sampled specimens were significantly different to the outgroup species *Pholas dactylus*, with an average pairwise distance of 4.8 %. The average pairwise distances between *Xylophaga washingtona* and *Kuphus polythalamia* when compared to all the sampled species were 8.7 % and 5.9 % respectively. The 18S sequences of the specimens *Nototeredo norvagica*, *Neoteredo reynei*, *Dicyathifer manni*, *Spathoteredo obtusa* and *Lyrodus pedicellatus* were indistinguishable from existing 18S sequences of the same species available on GenBank (0 % distance). Species within the *Bankia*, *Teredo* and *Lyrodus* genus showed an average interspecific divergence of 3.3 %, 0.3 % and 0.8 % respectively. The average interspecific pairwise distance was 0.5 % between the genera *Lyrodus* and *Teredo,* 2.3 % between *Bankia* and *Lyrodus* and 2.4 % between *Bankia* and *Teredo*. The two *L. massa* sequences were identical, yet showed a 0.6 % divergence with the *L. massa* sequence available on GenBank. The *L. massa* GenBank sequence showed no divergence from the *L. turnerae* sequence. The *Lyrodus* genus shows an average interspecific divergence of 0.8 %, and no intraspecific divergence between *L. pedicellatus* and *L. bipartitus*.

	Taxon	Average Pairwise Distance (%) Between Species																																				
		1	2	3	4	5	6	7	8	9	10	11	12	13	14	15	16	17	18	19	20	21	22	23	24	25	26	27	28	29	30	31	32	33	34	35	36	37
1	*Corbula contracta* *																																					
2	*Xylophaga washingtona*	6.2																																				
3	*Kuphus polythalamia* *	4.3	8.6																																			
4	*Teredothyra dominicensis*	4.3	8.3	1.5																																		
5	*Nototeredo norvagica*	6.5	10.5	7.1	6.4																																	
6	*Nototeredo norvagica**	6.8	10.9	7.4	6.6	0.0																																
7	*Psiloteredo megatora*	4.3	8.3	4.5	3.9	1.7	1.8																															
8	*Neoteredo reynei**	4.3	10.1	3.5	3.9	7.1	7.4	4.3																														
9	*Neoteredo reynei*	3.9	9.3	3.3	3.6	6.4	6.6	3.9	0.0																													
10	*Dicyathifer manni**	4.0	8.3	4.8	4.2	1.7	1.8	0.6	3.9	3.6																												
11	*Dicyathifer manni*	4.0	8.3	4.8	4.2	2.1	2.1	0.9	3.9	3.6	0.0																											
12	*Dicyathifer manni*	4.0	8.3	4.8	4.2	2.1	2.1	0.9	3.9	3.6	0.0	0.0																										
13	*Teredora malleolus*	5.2	9.2	6.1	5.5	3.1	3.2	1.8	5.3	4.8	1.2	1.5	1.5																									
14	*Nausitora fusticula**	4.6	9.1	5.5	4.9	3.5	3.6	1.5	4.6	4.3	1.8	2.1	2.1	2.4																								
15	*Nausitora dunlopei**	4.6	9.0	5.5	4.8	3.5	3.6	1.5	4.6	4.2	1.8	2.1	2.1	2.4	0.0																							
16	*Spathoteredo obtusa**	5.6	9.7	6.1	5.5	3.9	4.0	2.7	6.0	5.5	3.0	3.3	3.3	2.4	2.1	2.1																						
17	*Spathoteredo obtusa*	5.6	9.7	6.1	5.5	3.9	4.0	2.7	6.0	5.5	3.0	3.3	3.3	2.4	2.1	2.1	0.0																					
18	*Spathoteredo obtusa*	5.6	9.7	6.1	5.5	3.9	4.0	2.7	6.0	5.5	3.0	3.3	3.3	2.4	2.1	2.1	0.0	0.0																				
19	*Bankia gouldi**	6.2	9.6	7.3	7.0	4.9	5.1	3.0	7.3	6.7	3.0	3.3	3.3	2.4	2.1	2.1	2.4	2.4	2.4																			
20	*Bankia australis**	5.6	9.6	6.7	6.1	5.3	5.4	3.0	6.0	5.5	3.3	3.6	3.6	2.7	1.8	1.8	1.5	1.5	1.5	2.7																		
21	*Bankia carinata**	5.9	9.3	7.4	6.7	4.2	4.3	3.3	6.3	5.8	3.3	3.6	3.6	3.9	2.4	2.4	4.2	4.2	4.2	3.3	3.9																	
22	*Teredo clappi*	4.3	8.0	6.1	5.5	4.2	4.3	2.4	5.3	4.8	2.4	2.7	2.7	3.0	1.2	1.2	2.1	2.1	2.1	2.1	1.8	2.1																
23	*Teredo mindanensis*	4.6	8.3	6.4	5.8	4.2	4.3	2.4	5.6	5.2	2.4	2.7	2.7	3.0	1.2	1.2	2.7	2.7	2.7	2.1	2.4	2.1	0.6															
24	*Teredo mindanensis*	4.9	8.7	6.1	6.1	4.6	4.7	2.7	5.3	4.9	2.7	3.0	3.0	3.3	1.5	1.5	3.0	3.0	3.0	2.4	2.7	2.4	0.9	0.3														
25	*Teredo furcifera*	4.3	8.0	6.1	5.5	3.8	4.0	2.1	5.3	4.9	2.1	2.4	2.4	2.7	0.9	0.9	2.4	2.4	2.4	1.8	2.1	1.8	0.3	0.3	0.6													
26	*Teredo furcifera*	4.3	8.0	6.1	5.5	3.8	4.0	2.1	5.3	4.9	2.1	2.4	2.4	2.7	0.9	0.9	2.4	2.4	2.4	1.8	2.1	1.8	0.3	0.3	0.6	0.0												
27	*Teredo sommersi*	4.3	8.0	6.1	5.5	4.2	4.3	2.4	5.3	4.8	2.4	2.7	2.7	3.0	1.2	1.2	2.1	2.1	2.1	2.1	1.8	2.1	0.0	0.6	0.9	0.3	0.3											
28	*Teredo sommersi*	4.3	8.0	6.1	5.5	4.2	4.3	2.4	5.3	4.8	2.4	2.7	2.7	3.0	1.2	1.2	2.1	2.1	2.1	2.1	1.8	2.1	0.0	0.6	0.9	0.3	0.3	0.0										
29	*Teredo sommersi*	4.3	8.0	6.1	5.5	4.2	4.3	2.4	5.3	4.8	2.4	2.7	2.7	3.0	1.2	1.2	2.1	2.1	2.1	2.1	1.8	2.1	0.0	0.6	0.9	0.3	0.3	0.0	0.0									
30	*Teredo navalis**	4.3	8.0	6.1	5.5	3.8	4.0	2.1	5.3	4.8	2.1	2.4	2.4	2.7	0.9	0.9	2.4	2.4	2.4	1.8	2.1	1.8	0.3	0.3	0.6	0.0	0.0	0.3	0.3	0.3								
31	*Lyrodus pedicellatus*	4.3	8.0	6.1	5.5	3.8	4.0	2.1	5.3	4.8	2.1	2.4	2.4	2.7	0.9	0.9	2.4	2.4	2.4	1.8	2.1	1.8	0.3	0.3	0.6	0.0	0.0	0.3	0.3	0.3	0.0							
32	*Lyrodus pedicellatus**	4.3	8.0	6.1	5.5	3.8	4.0	2.1	5.3	4.8	2.1	2.4	2.4	2.7	0.9	0.9	2.4	2.4	2.4	1.8	2.1	1.8	0.3	0.3	0.6	0.0	0.0	0.3	0.3	0.3	0.0	0.0						
33	*Lyrodus massa**	4.6	8.3	6.4	5.8	4.2	4.3	2.4	5.6	5.2	2.4	2.7	2.7	3.0	1.2	1.2	2.7	2.7	2.7	2.1	2.4	2.1	0.6	0.0	0.3	0.3	0.3	0.6	0.6	0.6	0.3	0.3	0.3					
34	*Lyrodus massa*	4.3	8.0	6.1	5.5	4.2	4.3	2.4	5.3	4.8	2.4	2.7	2.7	3.0	1.2	1.2	2.1	2.1	2.1	2.1	1.8	2.1	0.0	0.6	0.9	0.3	0.3	0.0	0.0	0.0	0.3	0.3	0.3	0.6				
35	*Lyrodus massa*	4.8	8.9	6.8	6.1	4.7	4.9	2.6	5.4	5.4	2.6	3.0	3.0	3.3	1.3	1.3	2.3	2.3	2.3	2.3	2.0	2.3	0.0	0.6	1.0	0.3	0.3	0.0	0.0	0.0	0.3	0.3	0.3	0.6	0.0			
36	*Lyrodus turnerae*	4.6	8.3	6.4	5.8	4.2	4.3	2.4	5.6	5.2	2.4	2.7	2.7	3.0	1.2	1.2	2.7	2.7	2.7	2.1	2.4	2.1	0.6	0.0	0.3	0.3	0.3	0.6	0.6	0.6	0.3	0.3	0.3	0.0	0.6	0.6		
37	*Lyrodus bipartitus*	5.3	8.1	7.1	6.8	5.3	5.5	3.3	6.7	6.1	3.0	3.6	3.6	3.9	2.1	2.1	3.6	3.6	3.6	3.0	3.3	3.0	1.5	0.9	1.2	1.2	1.2	1.5	1.5	1.5	1.2	1.2	1.2	1.2	1.5	1.6	1.2	
38	*Lyrodus bipartitus*	5.3	8.1	7.1	6.8	5.3	5.5	3.3	6.7	6.1	3.0	3.6	3.6	3.9	2.1	2.1	3.6	3.6	3.6	3.0	3.3	3.0	1.5	0.9	1.2	1.2	1.2	1.5	1.5	1.5	1.2	1.2	1.2	1.2	1.5	1.6	1.2	0.0
39	*Lyrodus bipartitus*	5.3	8.1	7.1	6.8	5.3	5.5	3.3	6.7	6.1	3.0	3.6	3.6	3.9	2.1	2.1	3.6	3.6	3.6	3.0	3.3	3.0	1.5	0.9	1.2	1.2	1.2	1.5	1.5	1.5	1.2	1.2	1.2	1.2	1.5	1.6	1.2	0.0

Table 5.4a. Pairwise 18S rRNA sequence divergence for teredinid groups using K2P distances (%). Asterisks denotes sequences obtained from GenBank.

Pairwise Distance Analysis for the COI-5P Region

The pairwise distance between all COI-5P samples analysed, including the comparative teredinid sequences from GenBank, are displayed in Table 5.4b. All teredinid sequences were significantly different from that of the outgroup species *Pecten jacobaeus*, with an average pairwise distance of 59.6 %. COI-5P sequences of the specimens *Nototeredo norvagica* and *Lyrodus pedicellatus* corresponded with existing COI-5P sequences on GenBank, with a pairwise distance of 0.5 % and 0 % respectively. Sequence comparison between matching species of *Neoteredo reynei*, *Dicyathifer manni*, *Psiloteredo megatora*, *Teredo sommersi* and *Lyrodus bipartitus* displayed an average pairwise distance ranging between 0.2 % and 1.7 %. The average interspecific pairwise distance was 19.5 % between the genera *Lyrodus* and *Teredo,* 20.3 % between *Bankia* and *Lyrodus* and 22.5 % between *Bankia* and *Teredo*. Species within the *Teredo* and *Lyrodus* genera showed an average interspecific divergence of 13.9 % and 16.3 % respectively.

Taxon	Average Pairwise Distance (%) Between Species																			
	1	2	3	4	5	6	7	8	9	10	11	12	13	14	15	16	17	18	19	20
1 *Pecten jacobaeus*																				
2 *Teredothyra dominicensis**	59.4																			
3 *Neoteredo reynei*	57.5	28.9																		
4 *Neoteredo reynei*	57.9	29.2	0.2																	
5 *Nototeredo norvagica**	58.3	25.8	23.9	24.2																
6 *Nototeredo norvagica*	58.3	25.8	23.7	23.9	0.5															
7 *Psiloteredo megatora*	65.0	34.9	29.0	29.2	26.5	26.7														
8 *Psiloteredo megatora*	65.0	34.9	29.0	29.2	26.5	26.7	0.3													
9 *Psiloteredo megatora*	64.5	34.6	28.7	29.0	26.2	26.5	0.7	0.3												
10 *Dicyathifer manni*	58.3	30.5	20.6	20.9	22.1	21.8	28.4	28.4	28.1											
11 *Dicyathifer manni*	57.9	31.3	20.2	20.4	22.4	22.1	28.1	28.1	27.8	1.7										
12 *Bankia carinata**	63.4	32.6	24.5	24.3	27.3	27.3	29.3	29.3	29.0	28.2	27.9									
13 *Teredo sommersi*	63.3	26.0	23.0	22.8	25.3	25.0	28.0	28.0	27.7	25.4	25.1	22.4								
14 *Teredo sommersi*	63.7	25.5	22.0	21.8	24.8	24.5	27.4	27.4	27.2	24.6	24.4	22.4	1.0							
15 *Teredo mindanensis*	60.9	29.4	26.2	26.2	27.3	27.3	30.5	30.5	30.2	29.6	28.7	22.6	20.2	20.4						
16 *Lyrodus pedicellatus*	59.0	26.7	22.0	22.2	22.3	21.9	25.2	25.2	25.0	24.1	23.6	18.6	19.1	18.7	21.2					
17 *Lyrodus pedicellatus**	59.0	26.7	22.0	22.2	22.3	21.9	25.2	25.2	25.0	24.1	23.6	18.6	19.1	18.7	21.2	0.0				
18 *Lyrodus massa*	59.9	29.5	22.1	21.8	26.2	25.9	28.2	28.2	27.9	26.8	26.5	23.0	19.1	19.1	19.3	18.9	18.9			
19 *Lyrodus bipartitus*	53.5	26.9	23.0	23.0	23.6	23.3	27.9	27.9	27.9	25.1	25.1	20.7	20.2	19.9	19.5	15.8	15.8	19.2		
20 *Lyrodus bipartitus*	53.5	26.9	23.0	23.0	23.6	23.3	27.9	27.9	27.9	25.1	25.1	20.7	20.2	19.9	19.5	15.8	15.8	19.2	0.4	
21 *Lyrodus bipartitus*	53.9	26.6	22.5	22.5	23.6	23.3	27.6	27.6	27.6	25.1	25.1	20.4	19.9	19.7	19.0	15.6	15.6	19.0	0.4	0.4

Table 5.4b. Pairwise COI-5P sequence divergence for teredinid groups using K2P distances (%). Asterisks denotes sequences obtained from GenBank.

Discussion

The 18S sequences were successfully obtained for 15 species of teredinid, including eight species which had not previously been sequenced. These were combined with the 16 sequences for teredinids available on GenBank, including eight species which were not obtained in this research. Of these GenBank sequences, six were used to identify individuals in this research. However, the GenBank sequence for *Lyrodus massa* did not group with sequences for *L. massa* from this research (average pairwise distance of 0.6 %), instead grouping with the sequence for *Lyrodus* sp. (pairwise distance of 0 %) it is possible that the sequence identified as *Lyrodus* sp. in this survey represents *L. turnerae*. As the sequence for *L. massa* was submitted to GenBank prior to the first species description for *L. turnerae* by MacIntosh (2012), and as the pallet morphology between the two species is similar, it is possible that the GenBank *L. massa* sequence is a misidentification of *L. turnerae*. The pallets from both the potential *L. turnerae* specimen and *L. massa* from this survey were identified by MacIntosh (personal communication), and it is possible that these sequences represent the true sequences for these species. Alternatively, *Lyrodus* sp. may represent a cryptic species of *L. massa*; the *Lyrodus* genera contains many cryptic species, including *L. massa and L. singaporeana*, which may only be differentiated upon examination of brooding strategy (Turner & Calloway, 1987). As the research which contributed the *L. massa* sequence to GenBank (Distel *et al*., 2011) did not include pallet images or morphological descriptions, it was not possible to compare the pallets and verify species identification. This highlights the need for an integrative approach, including details of the pallet morphology along with the molecular sequences, in order to accurately identify species from this taxonomically challenging group.

The only previous large-scale molecular phylogenetic survey of the Teredinidae focused on the small, nuclear rRNA genes (Distel *et al*., 2011) and did not include mitochondrial sequences due to the difficulties in obtaining COI-5P sequences for the Teredinidae (Distel, personal communication). This difficulty is evidenced by the small number of COI-5P sequences for the Teredinidae available on GenBank. At the time of writing, the COI-5P sequences for only four species (*Teredothyra dominicensis*, *Nototeredo norvagica*, *Bankia carinata* and *Lyrodus pedicellatus*) have been submitted, thus limiting comparisons. Nevertheless, these deposited sequences were used to positively identify the matching species in this research. The COI-5P sequences for ten species of teredinid were obtained, including six species which had not been previously sequenced.

Despite the low interspecific divergence of the 18S sequences most species could be grouped, though resolution was insufficient to fully distinguish between the *Teredo* and *Lyrodus* genera. This is in contrast to the COI-5P sequences where all species were sorted into distinct lineages, including both *Teredo* and *Lyrodus*. As COI-5P sequences for *Spathoteredo obtusa*, *Teredo furcifera* and *Lyrodus massa* were not obtained, it was not possible to directly compare tree topologies between COI-5P and 18S markers. This was further compounded by the limited number of COI-5P teredinid sequences available on GenBank for comparison. Indeed, of the Phylograms from this survey, the 18S tree contained twice as many sequences compared with the COI-5P tree (22 Vs 11).

The subfamilies of the Teredininae are primarily distinguished by pallet characteristics, with those of the Bankiinae showing segmentation whilst the pallets of the Teredininae and Kuphinae are fused (Turner, 1966). Yet *Bankia carinata* and *Kuphus polythalamia* fall within the radiation of the Teredininae in the phylogram presented herein, thus corroborating previous phylogenetic works (Santos *et al*., 2005; Distel *et al*., 2011). These findings challenge the traditional taxonomic view of the Teredinidae and the monophyletic subfamilies and suggest that unsegmented pallets are ancestral within the Teredinidae, with segmented pallets first emerging within the Bankiinae and then disappearing in *Lyrodus* and *Teredo* (Distel *et al*., 2011). The pallets of *B. carinata* only become segmented in mature adults (Turner, 1966): therefore, this shift from pallet segmentation may be interpreted as an example of neoteny – the retention of juvenile characteristics in mature adults (Distel *et al.,* 2012). This view is supported by the position of *Bankia carinata* as the most basal member of the larviparous Teredinidae in the 18S tree. All teredinids are broadcast spawners, bar *Teredo, Lyrodus* and *Zachsia* which brood their young (Turner, 1966). Thus, the emergence of brooding may have driven the loss of pallet segmentation. It has been proposed that larvae are less likely to become trapped between unsegmented pallets, which could hinder the adult's ability to seal its burrow whilst also damaging larvae (Distel *et al*., 2011).

The teredinid groups inferred by the 18S phylogram largely corroborate previous phylogenetic arrangement by Distel *et al*. (2011), with *Dicyathifer manni*, *Teredora malleolus*, *Kuphus polythalamia* and *Teredothyra dominicensis* as the most basal members, *Spathoteredo obtusa*, *Nausitora* and *Bankia* comprising the centre of the phylogram and *Lyrodus* and *Teredo* as the higher members. Group II, as defined by Turner (1966), is predicted to be polyphyletic in the phylogram presented herein. This difference is due to the inclusion of both *Teredora* and *Psiloteredo* genera in comparison to just Teredo in

previous phylogenetic works. Group I, which contains the single Genus *Kuphus* comprised of the single species, *K. polythalamia* is monospecific; groups II and III are polyphyletic and groups IV and VI are monophyletic. The COI-5P phylogram generally supports the 18S tree yet there are a few of notable differences. The COI-5P phylogram places *Bankia carinata* amongst the *Lyrodus* and *Teredo* genera, thus group IV is shown to be polyphyletic. For the COI-5P tree, *Teredothyra dominicensis* is placed as the most basal member of the group compared with *Dicyathifer manni* in the 18S tree. This may be explained by the use of the different outgroups *Pholas dactylus* and *Pecten jacobaeus* for the 18S and COI-5P tree respectively. Furthermore, the COI-5P tree did not contain any members of the Pholadidae, which is a closely related 'sister' taxa to the Teredinidae and may influence phylogram composition. Finally, the total number of sequences used to build the two trees differ, with the 18S tree containing twice as many species than the COI-5P tree.

The acquisition of sequences from *Nototeredo norvagica* and *Psiloteredo megatora* assists in distinguishing between two species which are commonly mistaken for one another due to their occurrence in the same regions and because of the similarity of their pallets. Indeed, a major review by Nair and Saraswathy (1971) includes a figure detailing the range of variation in the pallets of *Nototeredo norvagica*; however, a number of these pallets have the characteristic, deep, thumbnail-like depression and pointed stalk of *Psiloteredo megatora,* thus are probably misidentified. As pallet features are very similar between these species, the identification of other distinguishable characters is of importance. Examination of siphon characters revealed distinct differences between the two species, with the siphons of *P. megatora* showing long flamboyant papillae, compared with the short and truncated papillae on the siphons of *N. norvagica*. These distinguishable siphonal characteristics combined with the molecular sequences will allow for a more accurate distinction between these two species.

Summary

Research presented herein provides the first mitochondrial-based phylogenetic tree of the Teredinidae and includes all known groups (as defined by Tuner, 1966) bar *Kuphus*, whose only member – *Kuphus polythalamia* – is extremely rare and has only been described from preserved specimens (Distel *et al*., 2011). Furthermore the nuclear-based phylogenetic analysis builds upon previous efforts, with sequences from species representing all six major groups of the Teredinidae, including the previously unsequenced *Nototeredo*. The results identify a potential species misidentification in the literature, thus highlighting the

necessity to include morphological and anatomical descriptions along with sequence data. This research corroborates previous works by Santos *et al*. (2005) and Distel *et al*. (2011) in concluding that Turner's (1966) division of the six Teredinidae groups into three subfamilies (Kuphinae, Teredinidae and Bankiinae) is not supported by molecular data. Providing sequences from a number of previously unpublished species (eight 18S and six COI-5P species) greatly increases both the taxonomic resolution and confidence in identification of this taxonomically challenging family. Furthermore, this research has potential applications for identifying cryptic species, incomplete specimens or individuals with damaged pallets; assisting larval identification or the identification of poorly documented life history and developmental stages; and improving the traceability of species recently introduced into new areas and monitoring their distribution.

Chapter Six: The broadcast spawning Caribbean shipworm, *Teredothyra dominicensis* (Bivalvia, Teredinidae), has invaded and become established in the eastern Mediterranean Sea.

Introduction

Xylotrophy has evolved in a range of invertebrates to exploit the wood entering the sea via rivers and mangroves. More recently, human activity has provided new niches for xylotrophs, including boats, piers, and sea defences. Teredinids, commonly referred to as shipworms, are the principal consumers of wood in the marine environment. These highly specialised bivalves are characterised by elongated bodies and a greatly reduced shell, adaptations which facilitate their wood-boring life style. Adult shipworms are confined to the timber into which they burrowed as newly metamorphosed larvae: continued burrowing gradually destroys this habitat, thus there are strong selection pressure for the evolution of life history strategies that maximise dispersal.

Teredinids readily colonise driftwood and are thus pre-adapted for dispersal by rafting (Theil & Gutow, 2005). The rafting voyages of floating timber may extend beyond regional scales *i.e.*, greater than 1000 km (Donlan & Nelson, 2003), and the extensive distribution of some teredinids have resulted from rafting (Edmondson, 1962). Dispersal may also be achieved during the larval stage; generally, species with a longer planktotrophic stage have a larger dispersal potential. Species with planktonic larvae may be carried along the coasts of continents and even trans-oceanically (Scheltema, 1971) and the adults and larvae of several species are thought to be highly adapted to an oceanic existence, which greatly extends the distribution range (Edmondson, 1962).

Human maritime activity is also believed to have contributed towards the cosmopolitan distribution of certain species. Wooden sailing vessels can become regularly colonised by shipworm (Woods Hole Oceanographic Institution, 1952; Turner, 1966) which are then transported beyond their natural distribution range (Carlton, 1999). Furthermore, tropical species have been known to survive freezing temperatures during transit (Turner, 1966). The decline in traffic of seafaring wooden vessels has limited this means of dispersal, though the established distributions of teredinids may still reflect the influence of this former means of dispersal. Modern shipping, particularly the

transportation of ballast water, has provided a new vector by which they may now spread. Larvae of the shipworm *Teredo navalis* have been discovered in ballast water and it is likely that larvae from other teredinids are present in ship ballast water across the globe (Gollasch, 2002; Carlton, 1999).

Teredinids display one of three developmental modes: broadcast spawners with planktotrophic larvae and short-term brooders and long-term brooders. Broadcast spawners release large quantities of eggs in a single spawning (Sigerfoos, 1908), yet parental investment is limited and larvae spend an extended period of time (20-25 days) developing in the water column (Turner, 1966). Broadcast spawners have an extensive distribution range, yet only a fraction of the spawned eggs will survive to become successful larvae (Scheltema, 1971). Both short-term and long-term brooders fertilize internally with larvae developing in specialised brood pouches on the parental gill. The former release larvae at the straight-hinged, veliger stage and development continues in the water column for between 10 and 15 days (Calloway & Turner, 1988), whilst the latter release competent pediveligers which are capable of settling immediately (Cragg *et al*., 2009). The long-term brooders have a higher likelihood of geographical larval retention and re-recruitment and are therefore often localised (Strathman *et al*., 2002). Indeed, successive generations may remain in the same piece of wood. Short-term brooders are believed to represent the optimum strategy for dispersal and are geographically widespread (McIntosh *et al.,* 2012). However, species representing all strategies have become successfully distributed across the globe (Turner, 1966).

Reproductive mode may be determined by examination of teredinid spermatozoa, as the ratio between the axial rod length and sperm body length is higher in sperm of external fertilizers than internal fertilizers (Popham, 1974). Furthermore, broodings species may be identified by the presence of larvae in the gill (Turner, 1966). Morphologically identical (cryptic) species may sometimes be distinguished when the developmental mode is examined. For example, *Lyrodus floridanus* is morphologically identical to *L. pedicellatus*, but can differentiated on the basis of brooding larvae to the D-shaped veliger stage, whereas *L. pedicellatus* releases advanced pediveligers (Calloway & Turner, 1984).

Typically, bivalve identification is based on shell characteristics; yet the shells of teredinids are taxonomically uninformative (Turner, 1966). Instead, interspecific variations in pallet features, the calcareous structures which plug the entrance to the

burrow, are used (Turner, 1971). Recently, morphological identification has been integrated with molecular techniques (16S rRNA, COI-5P subunit and 18S ribosomal markers) to improve the taxonomic resolution within the Teredinidae (Santos *et al.,* 2005; Borges *et al.,* 2012).

This research reports the establishment of a substantial population of a Caribbean teredinid, *Teredothyra dominicensis*, in the eastern Mediterranean Sea. Integrative taxonomy, including DNA barcoding, nuclear locus sequencing, morphological and morphometric examination, was used to confirm the identity and increase the taxonomic resolution of this species. As previous descriptions of the reproductive mode and larval development type of *T. dominicensis* were based on a small number of poorly preserved specimens (Turner, 1966), investigations were undertaken to clarify these characteristics in order to predict the ability of this invasive species to establish and disperse throughout the region.

Teredinids are estimated to cause over one billion Dollars worth of damage to submerged wooden structures per annum and the introduction of shipworms into new areas is often followed by rapid and extensive destruction (Turner, 1966; Cohen & Carlton, 1995; Distel *et al.*, 2011). This can be further compounded by costly restoration and the interruption of business (Fernandes & Costa, 1967 cited in Filho *et al*., 2008). As the most effective means for wood protection such as treatment with chromated copper arsenate (CCA) are now heavily restricted (see, for example, EU Commission Directive, 2003), the spread of shipworms is still a major economic issue.

The appearance of *T. dominicensis* in the Mediterranean is of particular concern as tropical teredinid species are more destructive than their temperate counterparts (Castagna, 1961; Southwell & Bultman). As the Mediterranean is gradually increasing in both temperature and salinity due to global warming (Giorgi & Lionello, 2008; Giannakopoulos *et al.*, 2009; Coma *et al.*, 2009) - factors which are known to increase distribution range (Borges *et al.*, 2010), boring activity (Paalvast & van der Velde, 2011) and speed at which teredinids reach sexual maturity (Ibrahim, 1981), their potential for further spread will continue to increase.

Materials and methods

Sample Collection & Rearing

Sample collection was carried out in Kaş in southern Turkey, during August 2010 and June 2011. Infested wood was recovered from the shipwreck, Uluburun III, located approximately 36 metres below mean sea level. Wooden panels of *Pinus sylvestris* (2.5 cm × 10 cm × 20 cm) were also attached to the mast of the wreck during August 2010 for retrieval and analysis the following year. Caribbean specimens were collected in Carlisle Bay, Barbados, from wooden panels exposed over a 6 month period at 15 metres below mean sea level. Aegean sampling was conducted during SCUBA dive surveys.

Specimens of *T. dominicensis* were reared in the aquaria at the Institute of Marine Sciences, University of Portsmouth, for one year. The seawater was maintained on a flow-through system at 25 °C and a salinity of 33 Practical Salinity Units (PSU). A larval capture device (Raskoff *et al.*, 2003) was installed to monitor gamete and larval release.

Identification & Morphometry

Calcareous structures were photographed using a stereo microscope. Images were captured using the JVC KY-F 1030U digital camera with accompanying KY0Link image capture program. Pallets and shells were measured using the image analysis programme, ImageJ. Pallet dimensions were measured from the base of the stalk to the tip of the blade to give the length, and across the broadest section of the blade to give width. Identification was based on species descriptions and pallet characteristics provided by Turner (1971).

Molecular Identification

DNA was extracted from siphonal tissue and associated musculature. Total genomic DNA was extracted using DNeasy Blood & Tissue kit (Qiagen), deviating from the manufacturer's protocol as follows: tissue was lysed overnight at 56 °C and DNA was eluted from the spin column using molecular grade water (2 × 70 µL washes) as opposed to elution buffer. Concentration, yield and purity of DNA were determined by UV spectrophotometry, with 1 absorption unit at 260 nm approximately equal to 50

ng/µL dsDNA). When necessary, DNA template was diluted using molecular grade water to a concentration of 10-20 ng/µL.

A 658 bp fragment from the 5' end of the cytochrome oxidase subunit I (COI-5P) was amplified using the primer pair LCO1490 (forward 5' GGT CAA CAA ATC ATA AAG ATA TTG G 3') and HCO2198 (reverse 5' TAA ACT TCA GGG TGA CCA AAA AAT CA 3') (Folmer *et al.*, 1994). Amplifications were performed in 25 µL reactions, with each reaction containing (stock concentrations in parentheses): 2.5 µL 10 × PCR buffer, 2.5 µL $MgCl_2$ (25 mM), 0.25 µL dNTP mixture (10 mM each), 0.5 µL of each primer (10 mM), 0.25 µL Taq Polymerase (5 U/µL), 1-2 µL DNA template (10-20 ng/µL) and brought to volume with molecular grade water. The PCR protocol was as follows: an initial cycle of 94 °C for 90 s, 45 °C for 90 s and 72 °C for 60 s, followed by 35 cycles of 94 °C for 30 s, 51°C for 90 s and 72°C for 60 s, with a final extension of 72 °C for five minutes.

A small fragment of the 18S rRNA gene, approximately 345bp, was amplified using the primer pair SSU_FO4 (5'-GCTTGTCTCAAAGATTAAGCC-3') and SSU_R22 (5'-GCCTGCTGCCTTCCTTGGA-3') (Blaxter *et al*., 1998). Amplifications were performed in 25 µL reactions, with each reaction containing (stock concentrations in parentheses): 2.5 µL 10 × PCR buffer, 2.5 µL $MgCl_2$ (25 mM), 0.25 µL dNTP mixture (10 mM each), 0.5 µL of each primer (10 mM), 0.25 µL Taq Polymerase (5 U/µL), 1-2 µL DNA template (10-20 ng/µL) and bought to volume with molecular grade water. The PCR protocol was as follows: an initial cycle of 2 min at 95 °C, followed by 35 cycles of 1 min at 95 °C, 45 s at 57 °C, 3 min at 72 °C and a final extension of 10 min at 72 °C.

A 6 µL aliquot of PCR product was then electrophoresed in a 2 % agarose gel. Amplified products were purified using a NucleoSpin Gel and PCR Clean-up kit (Macherey-Nagel, Duren, Germany) according to the manufacturer's guidelines. All PCR products (COI-5P and 18S) products were sequenced by Source Bioscience.

Data Analysis

COI-5P and 18S sequences were edited and aligned using MEGA 5.1 (Tamura *el al.,* 2011). Sequences were uploaded onto GenBank (accession numbers will be provided upon acceptance of paper). Edited sequences were compared with those on the GenBank database to confirm species identity and ensure that endosymbiont bacteria or other contaminant had not been co-amplified in error. Sequences were aligned using

Clustal W (Tamura *et al.,* 2011) and COI sequences were translated to check for the presence of frameshift mutations, stop codons or unusually divergent amino acid profiles. Sequences consisting of 658bp and 345bp for COI and 18S, respectively, were used for phylogenetic inference using Neighbour-joining (NJ). Neighbour joining trees for both COI and 18S sequences were constructed using the Kimura 2-parameter model (K2P) with the programme MEGA 5.1. Selected GenBank sequences were used to compare with our data set and to be used as outgroups.

Electron Microscopy

Samples for observation under the electron microscope were fixed in 4 % v/v glutaraldehyde in a cacodylate buffer (0.2 M sodium cacodylate, 0.3 M sodium chloride, 2 mM calcium chloride) for one hour at room temperature. Samples were then rinsed three times in buffer for ten minutes each. All samples were then post-fixed in 1 % w/v osmium tetroxide for one hour and rinsed three times in seawater for ten minutes each. Samples were then taken immediately through an ethanol dehydration series, evaporation dried via hexamethyldisilazane (HMDS) and then mounted on aluminium stubs. Sputter coating was carried out under an argon atmosphere using a gold and palladium target, at a voltage of 1.4 kV using a current of approximately 18 mA for three minutes. Specimens were examined using a JEOL 6060LV Scanning Electron Microscope operating in secondary electron mode using an accelerating voltage of 18 kV.

Results

Identification

Three species of teredinid, *Lyrodus pedicellatus* (Quatrefages)*, Nototeredo norvagica* (Spengler) and *Teredothyra dominicensis* (Bartsch), were identified from sampling sites in the Mediterranean. Specimens were predominantly acquired from a shipwreck off the coast of Kaş, in which *T. dominicensis* was the dominant species present (93 out of 104 specimens). Wooden panels placed at the wreck site and recovered the following year were colonised exclusively by *T. dominicensis*. A single specimen of this species was also found in a piece of driftwood recovered off the coast of Fourni Island (Greece). *T. dominicensis* was the only species found in wooden panels placed off the Barbadian coast.

The pallets were identified as *T. dominicensis* (Fig. 6.1a) using both the original description of pallet features by Bartsch (1922) and the key in Turner (1971). Pallets collected from Caribbean specimens were indistinguishable from those collected in the Mediterranean and Aegean Seas and the shifts in pallet proportions during ontogeny between the Mediterranean and Caribbean specimens (Fig. 6.1b) were also indistinguishable (GLM P = 0.954).

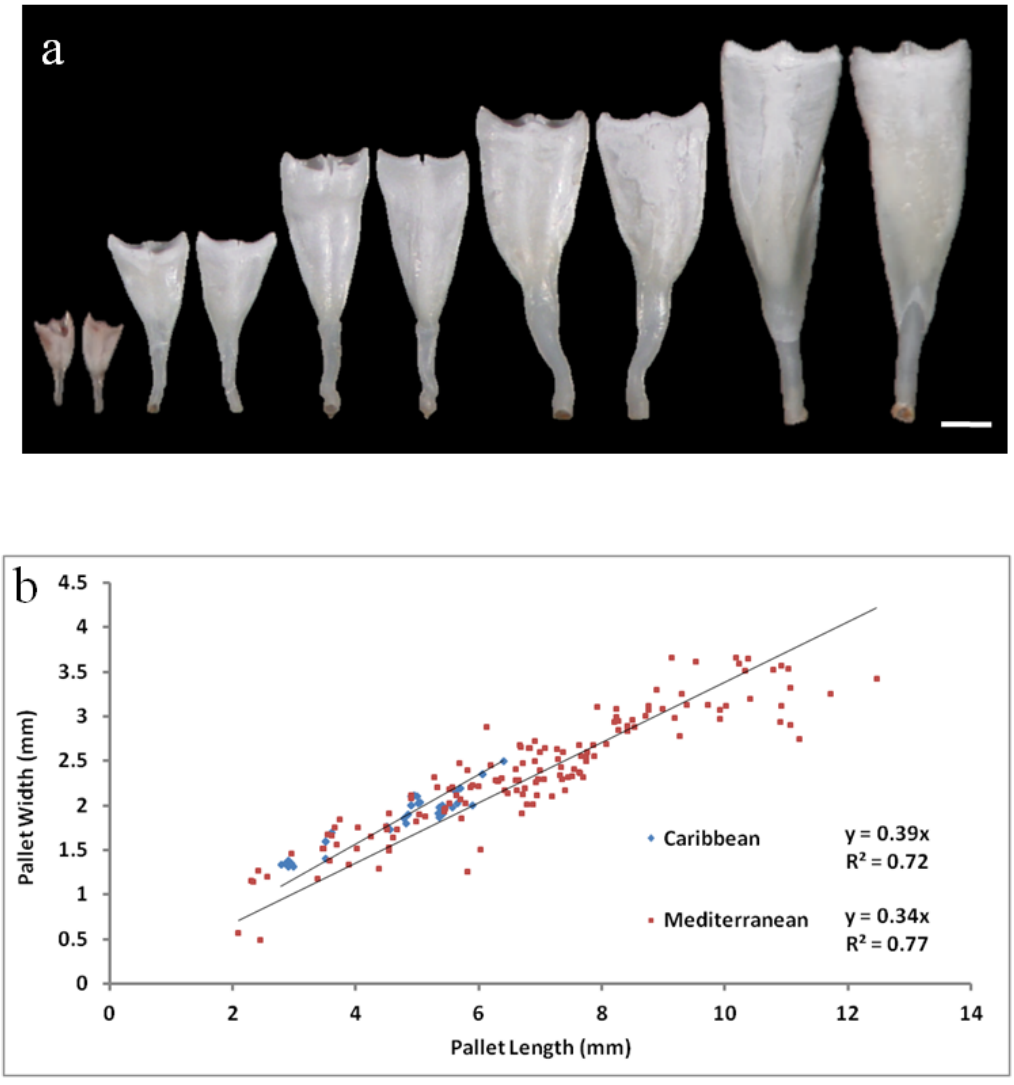

Figure 6.1 Variation in pallet characteristics of *Teredothyra dominicensis*. a). Inner and outer pallet face of pallet pairs taken from specimens extracted from panels placed at the Uluburun III wreck site. Scale bar 1 mm. b). Variation in pallet proportions of Caribbean and Mediterranean specimens of *Teredothyra dominicensis* during growth.

COI-5P and 18s Sequences of Sampled Teredinids

A total of nine COI-5P sequences were obtained for *T. dominicensis* (seven Mediterranean specimens, one Caribbean and one Aegean specimen) all of which were free from stop codons or indels. A BLAST comparison of all sequences with those already published for *T. dominicensis* in GenBank revealed a 99 % or more maximum identity (Borges *et al.*, 2012). Both nucleotide and amino acid sequences aligned unambiguously with those from other teredinids. An average intraspecific divergence of 0.78 % was observed between specimens of *T. dominicensis* obtained in this survey. These diverged by an average of 0.43 % with COI-5P sequences from *T. dominicensis* uploaded on GenBank (Borges *et al.*, 2012). The Caribbean specimen diverged by an average of 0.43 % with specimens obtained from the Mediterranean, 0 % with specimens on GenBank (Borges *et al.*, 2012) and 1.7 % with the Aegean specimen. The *T. dominicensis* specimen from the Aegean Sea matched the specimens located in the Mediterranean from this survey (average pairwise distance of 1.81%) and also with other *T. dominicensis* specimens uploaded onto GenBank (Borges *et al.,* 2012). The average pairwise distances between *T. dominicensis* and *Lyrodus pedicellatu*s, *Nototeredo norvagica* and *Bankia carinata* were 29.6 %, 26.2 % and 33.7 %, respectively.

Thirteen 18S sequences, all free from indels, were obtained for *T. dominicensis* (nine of which were from Mediterranean specimens, three from Caribbean specimens and one from the Aegean Sea). A BLAST comparison of the sequences in GenBank from the Mediterranean, Aegean and Caribbean specimens revealed a 99-100% maximum identity with sequences previously published for *T. dominicensis* (Distel *et al.,* 2011; Borges *et al.*, 2012). Pairwise comparison revealed 0% divergence between all *T. dominicensis* specimens from this study (Mediterranean, Aegean and Caribbean) and these showed 0% divergence with published sequences of *T. dominicensis* from both the Mediterranean (Borges *et al*., 2012) and Netherlands Antilles (Distel *et al.,* 2011). The pairwise distances between *T. dominicensis* and *Lyrodus pedicellatu*s, *Nototeredo norvagica* and *Bankia carinata* were 3.6 %, 4.0 % and 4.0 %, respectively. Although the 18S alignment was more conserved than the COI, the phylogenetic tree topologies were analogous. As tree topologies of COI-5P sequences of nucleotides and amino acid were identical, only the nucleotide tree is shown here. The tree building method used for COI-5P and 18S sequences was Neighbour-Joining (NJ), the most common method used, to allow comparison with other studies. The neighbour-joining phylogenetic trees

for COI and 18s sequences are shown in Figures 6.2 a-b and all pairwise comparisons are shown in Table 6.1a. GenBank accession numbers and species location are given in Table 6.1b.

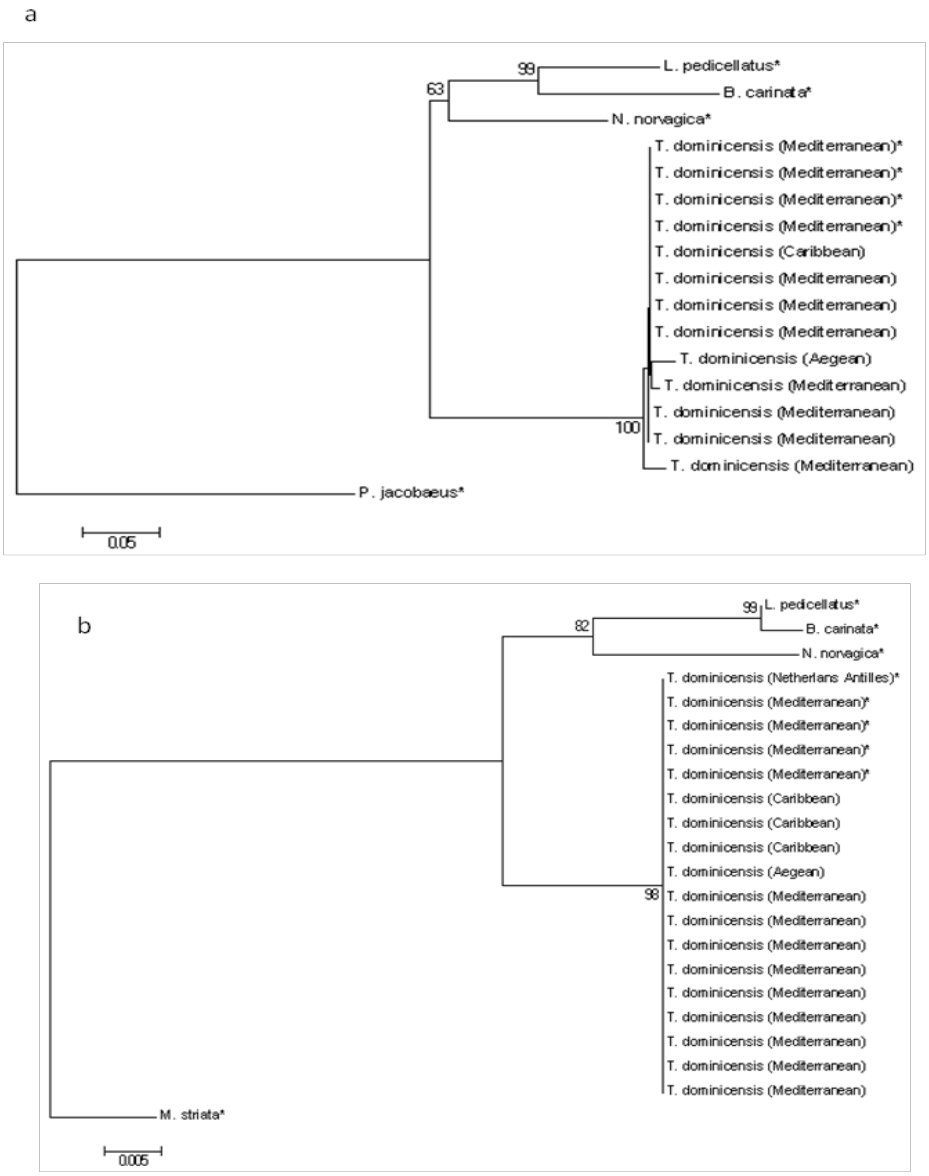

Figure 6.2 Molecular identification of *Teredothyra dominicensis* based on COI-5P and 18S sequences. a). Neighbour-joining nucleotide tree based on the partial sequences of the cytochrome c subunit I gene (COI-5P). Asterisks indicate sequences obtained from GenBank. b). Neighbour-joining tree based on the partial sequences of the 18S rRNA gene obtained from Mediterranean, Aegean and Caribbean specimens of *T. dominicensis*. Asterisks indicate sequences obtained from GenBank. Phylogenetic trees include the teredinids *Lyrodus pedicellatus*, *Nototeredo norvagica* and *Bankia carinata*. The bivalves *Pecten jacobaeus* and *Martesia striata* are used as outgroups in the COI-5P and 18S tree, respectively.

Taxon	Average Pairwise Distance (%)					
	Within Species	Between Species				
		1	2	3	4	5
1 *T. dominicensis* Mediterranean	0.78/0.0					
2 *T. dominicensis* Mediterranean*	0.0/0.0	0.43/0.0				
3 *T. dominicensis* Caribbean	N/A	0.43/0.0	0.0/0.0			
4 *Lyrodus pedicellatus**	N/A	29.6/3.6	26.0/3.6	29.2/3.6		
5 *Nototeredo norvagica**	N/A	26.2/4.0	29.2/4.0	26.0/4.0	23.5/3.6	
6 *Bankia carinata**	N/A	33.7/4.0	32.2/4.0	33.1/4.0	28.6/3.1	19.6/3.4

Species (No. of specimens)	Location	GenBank Accession Details		
		Accession No. COI	Accession No. 18S	Source
Teredothyra dominicensis (9)	Kaş, Turkey			This study
Teredothyra dominicensis (4)	Kaş, Turkey	KC157940-KC157943	KC158219-KC158222	Borges *et al.*, 2012
Teredothyra dominicensis (1)	Fourni, Greece			This study
Teredothyra dominicensis (1)	Carlisle Bay, Barbados			This study
Teredothyra dominicensis (1)	Netherlands Antilles		JF899225	This study
Nototeredo norvagica (1)	Mersin Bay, Turkey	KC157926	KC158207	Distel *et al.*, 2011
Lyrodus pedicellatus (1)	Berder, France	KC157937	KC158216	Borges *et al.*, 2012
Bankia carinata (1)	Mersin Bay, Turkey			Borges *et al.*, 2012
Martesia striata (1)	Indonesia		JF899213	Distel *et al.*, 2011
Pecten jacobaeus (1)	Ankara, Turkey	JQ623969		Keskin, unpublished

Table 6.1. Pairwise comparison and GenBank details for both the COI-5P and 18S sequencing. a) Pairwise COI-5P nucleotide (black) and 18S rRNA sequence (blue) divergence for teredinid groups using K2P distances (%). N/A., not applicable, denotes group with only a single specimen. Asterisks denote sequences obtained from GenBank. 6.1b) Sequence details including specimen location, GenBank accession number and source of the sequence.

Evidence of Life History Strategies

Spermatozoa were located in a mass aggregation, or spermatozeugmata. All spermatozoa had an elongated pyramidal acrosome, approximately 1.7 µm long, with a distinct and prominent axial rod (Fig. 6.3a). This axial rod lies in a canal which is formed by invaginations of the acrosomal vesicle. The mid-piece (measuring 1.3 µm in length) is typical of bivalve sperm morphology and at its base consists of four spherical mitochondria and a flagellum. Dimensions of the axial rod to sperm body length are shown in Figure 6.4a.

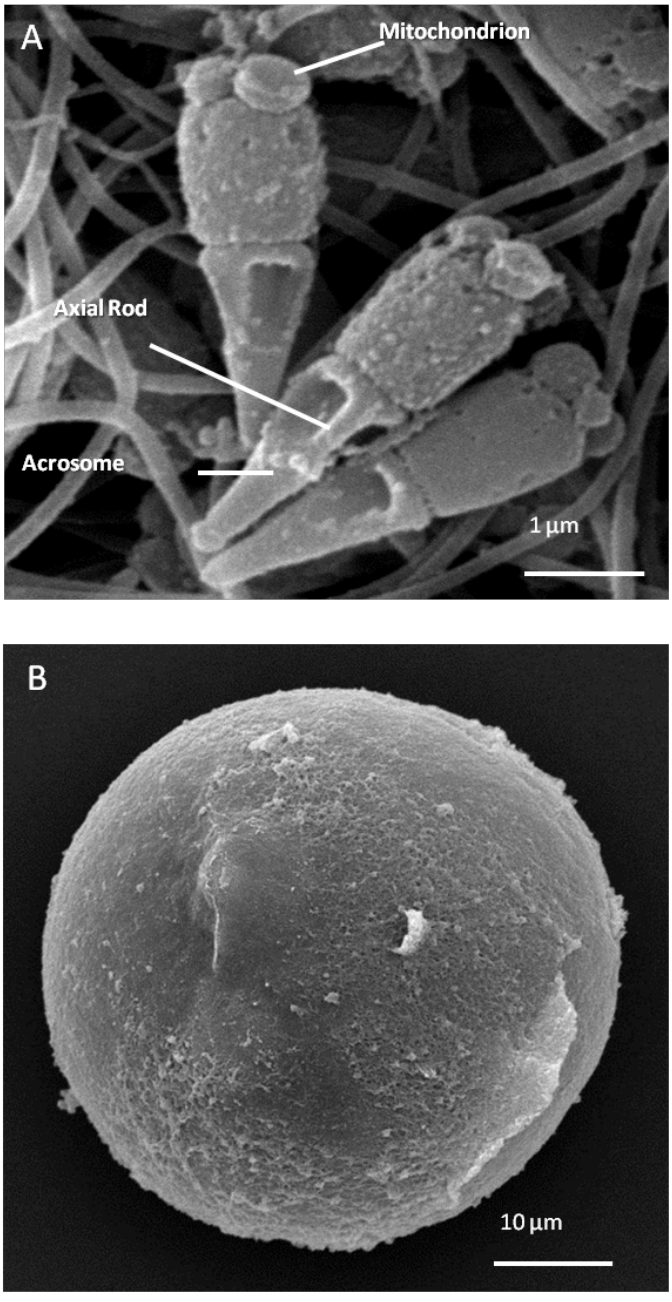

Figure 6.3 The gametes of *Teredothyra dominicensis.* a) Spermatozoa features. b) a free spawned egg. Scale bars represent 1 µm and 10 µm respectively.

The larval capture device installed in the aquaria did not detect any larvae during the entire period in which *T. dominicensis* was cultured. Following extraction from wooden panels reared specimens began to spawn, releasing a continuous and uninterrupted stream of unfertilized eggs which ranged from 48-52 µm in diameter (Fig. 6.3b). Egg dimensions for *T. dominicensis* are comparable with other known broadcast spawning teredinids and pholads (Fig. 6.4b). No brooded larvae or associated brooding structures were found in any of the 96 dissected specimens. Specimens obtained from wooden panels showed large variation in total body length (Fig. 6.5), with individuals as small as 1.3 cm and as large as 31.2 cm.

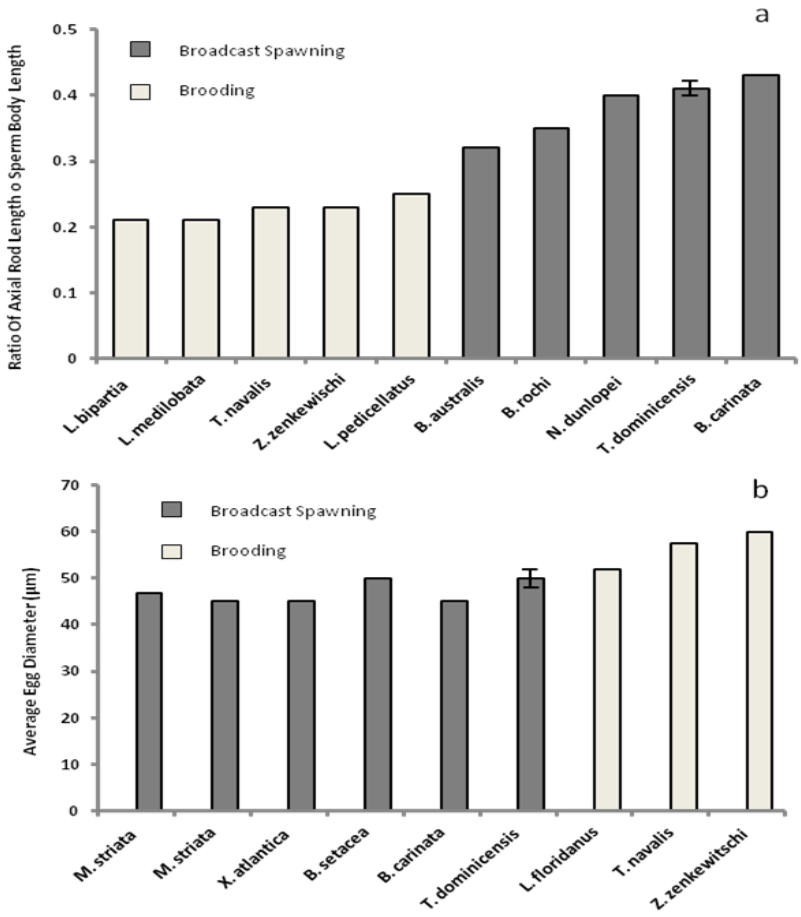

Figure 6.4 Correlation of gamete features with life history characteristics in the Teredinidae. a) Ratio of axial rod length to sperm body length (mean ± SE) of internally and externally fertilizing teredinids. Data for *Lyrodus bipartita, L. medilobata, L. pedicellatus, Teredo navalis, Zachsia zenkewitschi, Bankia australis, B. rochi, B. carinata* and *Nausitora dunlopei* were taken from Popham (1974). b). Egg size (mean ± SE) of broadcast spawning and brooding teredinids and pholads. Data for *Martesia striata* (Boyle & Turner, 1976), *Xylophagia atlantica* (Culliney & Turner, 1976*), Bankia setacia* (Townsley & Lee, 1967), *Bankia carinata*

(Nair & Saraswathy, 1956), *Lyrodus floridanus* (Calloway & Turner, 1983) *Teredo navalis* (Costello *et al.,* 1957) and *Zachsia zenkewitschi* (Yakovlev, *et al.,* 1998).

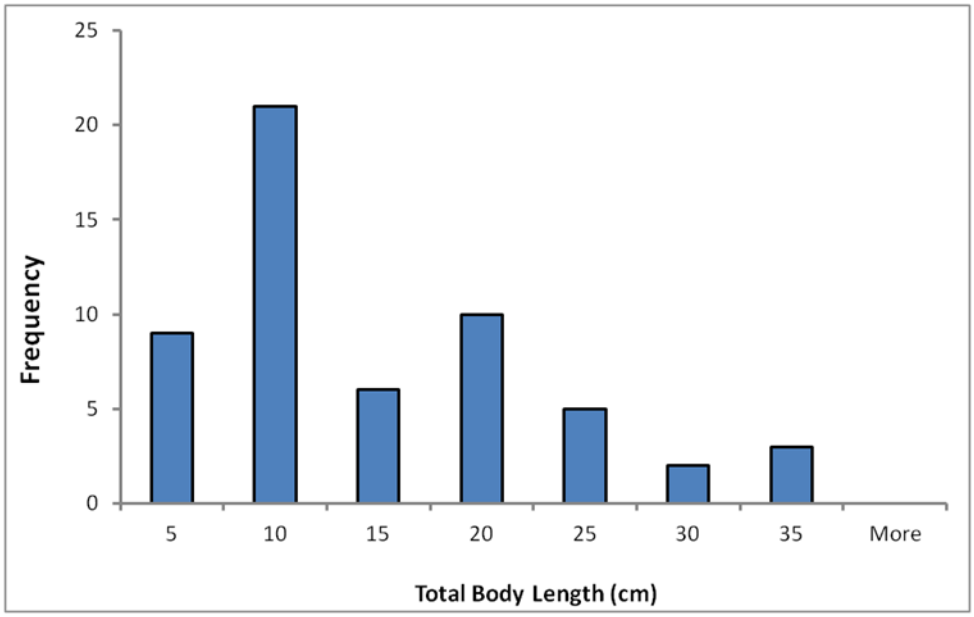

Figure 6.5 Variation in the total body length of *Teredothyra dominicensis* from Mediterranean sample sites.

The degradation of the Uluburun III shipwreck

A replica of the famous Uluburun shipwreck was built and capsized in October 2006 to commemorate the finding of the original wreck and to boost dive tourism in the region of Kaş, southern Turkey. Teredinid infestation was first noticed in August 2008 and by the summer of 2010, the wreck had disintegrated until only parts of the mast, frame and keel remained. Sampling between the summers of 2010 -2011 first revealed that the invasive Caribbean shipworm, *Teredothyra dominicensis*, was responsible for the rapid destruction of the wreck. Figure 6.6 shows a timeline from the capsizing of the wreck in 2007, to its complete disintegration by the summer of 2012 and demonstrates the destructive ability of the Teredinidae.

Summer 1982: A late Bronze Age shipwreck off Uluburun, 6 miles from Kaş, discovered by a local sponge diver.

1984 – 1994: Excavation of the wreck begins.

October 2006: a replica of the Uluburun ship is built to commemorate the original, promote diver tourism in the region and to train underwater archaeologists.

October 2006: The replica is deliberately capsized off the coast of Kaş.

May 2007: The wreck is in good condition and appears free from borer infestation.

August 2008: The first signs of infestation and damage are reported.

August 2009: The wreck's structural integrity had been weakened by borers and storms during the previous winter cause the wreck to fragment.

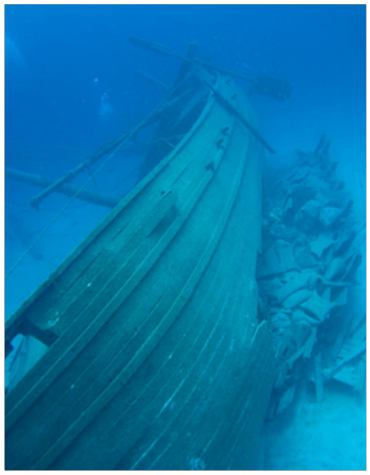

August 2010: Only the mast frame and keel remain, albeit heavily infested. The teredinids calcareous tunnels are clearly visible.

July 2011: The wreck's timber is severely degraded and held together by teredinids calcareous tunnels.

July 2011: Wooden bait panels secured to the mast in 2010 are retrieved the following summer.

July 2011: Wreck timber is retrieved for examination. Timber is heavily infested with teredinids and the wood boring amphipods, Chelura and Limnoria. The teredinids specimen, centred, measured in excess of 30 cm.

July 2011: A heavily infested piece of wreck timber.

Summer 2012: Wreck completely disintegrated.

Figure 6.6 A time-line of the Uluburun III shipwreck degradation by *Teredothyra dominicensis.*

Discussion

Prior to molecular based identification, teredinids were categorised based on pallet morphology. As pallets vary throughout ontogeny and are also influenced by ecological factors, identification based on these features is more assured if a profile of natural pallet variation is measured (Tan *et al.,* 1983; Turner, 1966; Cragg *et al.*, 2009). The profile of pallet variation between the invasive population and the native population of *T. dominicensis* indicate no morphological difference between the two sites. As cryptic species morphologically indistinguishable from 'true' species exist among the Teredinidae (Calloway & Turner, 1983), further means of identification are necessary. Molecular analysis using both COI-5P and 18s markers showed low interspecific genetic divergence between *T. dominicensis* specimens from the Caribbean, Mediterranean and Aegean. Furthermore, sequences were matched with those of *T. dominicensis* in GenBank, including a specimen from the Netherlands Antilles (Distel *et al.,* 2011). Thus, both morphological and molecular data confirm the invasive species identity as *T. dominicensis* and rule out the possibility of the Mediterranean population representing a cryptic species. Furthermore, both the sequence and morphological data provided herein improve the traceability of this poorly-studied invasive species.

Originally discovered off the coast of Dominica, *T. dominicensis* was thought to be exclusively confined to the Gulf of Mexico and Caribbean Sea (Bartsch, 1922; Turner, 1966). This species has never been documented in the Mediterranean, despite numerous and extensive surveys of the region (Roch, 1940; Turner, 1966; Sen *et al*., 2010). Due to the striking differences between the pallets of this species with the known teredinid fauna of the Mediterranean, misidentification is unlikely and, whilst there is a slim chance these surveys failed to find *T. dominicensis*, the pair-wise distance between specimens from the Caribbean and Mediterranean suggests a recent invasion. Specimens were obtained from the timber of a wreck which was deliberately capsized in 2006 to promote dive tourism in the region. Infestation was first recorded the following year, thus proving the first known reference point for larval colonisation of *T. dominicensis* in the Mediterranean.

T. dominicensis has been recorded outside of its natural distribution range once before, when small numbers (37 specimens, representing 0.2 % of the 17812 teredinids collected) were discovered during an extensive survey of Papua New Guinea (Rayner,

1983). The fact this species has never been found in surrounding regions, including major surveys of teredinid distribution around the Australian coast and Hawaiian waters (Edmondson, 1942; Ibrahim, 1981; McIntosh, 2012) and that specimens from Papua New Guinea were all found in deep water ports, suggests this species colonised from shipping ballast water. Given the pattern of ocean currents and the distance between the Mediterranean and Caribbean Seas, invasion of *T. dominicensis* via drift wood or by direct larval recruitment seems highly unlikely. Thus, we propose that the *T. dominicensis* was introduced to the Mediterranean via ballast water. This is believed to represent the world's largest invasion vector in Marine environments (Ruiz *et al.,* 1997), with thousands of species being transported around the globe in billions of gallons of seawater per day (Carlton, 2011). Furthermore, this mode of dispersal has been found to affect teredinid distribution (Gollasch, 2002).

The only previous report on the reproductive mode for *T. dominicensis* suggested the species represented a transition between broadcast spawning and brooding modes (Turner, 1966). However, this was based on a small number of poorly preserved specimens. Cultures reared over a year-long period did not spawn larvae and the large number examined specimens (Caribbean, Mediterranean and laboratory reared) failed to reveal brooding structures or internally developing larvae. A number of the laboratory cultures also released unfertilized eggs (averaging 50 μm in diameter). Free spawning suggests the eggs were ripe and their small size is comparable to other externally-fertilizing teredinids (Nair & Saraswathy, 1971). *T. dominicensis* spermatozoa also showed structural characteristics of externally-fertilizing bivalve spermatozoa, with four mitochondria gathered at the base of the sperm head (Popham, 1979), found in externally fertilizing teredinids (Popham, 1974). Thus, mode of fertilization for this species is likely to be external with larvae undergoing planktotrophic development, which typically lasts 20-25 days in other broadcast spawning teredinids (Nair & Saraswathy, 1971; Culliney, 1975).

Panels placed at the wreck site were infested exclusively by *T. dominicensis* specimens and the marked size distribution (from small, recently settled juveniles, to large, mature adults) suggests at least three settlement events over the ten month exposure period. Recruitment is unlikely to have taken place directly from the wreck site itself: having spent a number of weeks developing in the water column, larvae from local parents would disperse away from the area. It is also unlikely that larval supply was maintained from Caribbean ballast water, so larval recruitment probably originated from other

populations of *T. dominicensis* in the Mediterranean. With conditions in the region able to sustain breeding populations which produce viable larvae that can settle and metamorphose, *T. dominicensis* may now be considered as part of the established teredinid fauna in the Mediterranean.

Prior to its complete disintegration, the Uluburun III supported a substantial population of this invasive species over a period of five years, providing ample time for this species to disperse. Teredinids are prodigiously fecund: adult *Psiloteredo megatora* are estimated to produce over 10^7 eggs in a single spawning (Sigerfoos, 1908) and huge numbers of eggs are also produced by other broadcast-spawning teredinids (Turner, 1966). It has been suggested that other members of the Teredothyra genus are highly adapted to an oceanic existence (Edmondson, 1962). Thus, combined with the long planktotrophic larval period, it is likely that *T. dominicensis* has a huge dispersal potential. Over time, broadcast spawning teredinids are outcompeted by brooding species (McIntosh *et al.,* 2012); but *T. dominicensis* was the dominant species at the wreck site over a number of years and was the only species found infesting wooden panels placed at the wreck site. Furthermore, no brooding species were found in the wreck timber, even though the long-term brooder *L. pedicellatus* was found in driftwood close to the wreck site and other brooders, such as *Teredo navalis*, are known to exist in the region (Sen *et al.*, 2010). This monopolisation and dominance of the wood resource suggests substantial quantities of larvae in the region and the ability of this species to locally outcompete brooding species.

The appearance and establishment of a Caribbean shipworm in the Mediterranean is of concern. Tropical borers can grow to sizes far surpassing European borers (Castagna, 1961) and a number of specimens of *T. dominicensis* recovered from wooden panels showed growth of over 30 cm in a ten month period. Tropical borers are also known to be more destructive than their temperate counterparts (Edmondson, 1942; Southwell & Bultman, 1971), as demonstrated by the rapid destruction of the entire shipwreck, Uluburun III, in the space of just six years. The impact of global warming, particularly the rise in temperature of Mediterranean, also needs to be considered in relation to teredinid activity. An increase in the temperature and salinity of the region has already been observed (Gibelin & Déqué, 2003; Sánchez *et al.,* 2004) and is expected to continue over the coming decades (Giorgi & Lionello, 2008; Giannakopoulos *et al.,* 2009). The increase of these factors is known to extend teredinid distribution ranges (Borges *et al.*, 2010; Paalvast & van der Velde, 2011). Furthermore, warmer

temperatures are known to accelerate growth, increase boring activity (Eckelbarger & Reish, 1972), hasten maturity, reduce larval development time (Grave, 1928) and increase settlement rates (Ibrahim, 1981). Higher temperatures also prolong the breeding season, providing more opportunity for reproductive output thus increasing larval recruitment. Introduced tropical teredinids have also been shown to out-compete native species as they respond more favourably to environmental change (Hoagland & Turner, 1980). Thus, the warming of the Mediterranean will increase the threat posed by all teredinids in the region. Yet as the temperature and salinity become more similar to those in tropical regions, they also become more suitable for *T. dominicensis*, thus amplifying the threat this Caribbean species poses to submerged wood structures in the region.

Chapter Seven: General Discussion

Lyrodus pedicellatus specialisation towards xylotrophy

The anatomical adaptations and physiological mechanisms which allow *Lyrodus pedicellatus* to exploit two independent food sources, the wood through which it burrows and plankton filtered from the water column, were examined in Chapter two. The results indicate that *L. pedicellatus* has a limited capacity to process plankton, as evidenced by the reduced surface area of the gill during brooding, the relatively shallow food groove and the small labial palps. This is supported by the shell and pallet data from chapter 3, which compared the diameters of the calcareous structures of *L. pedicellatus* with *Nototeredo norvagica* – a planktotrophic teredinid (Purchon, 1941). The pallets of *L. pedicellatus* were slimmer throughout the species life-cycle than those of *N. norvagica*. Therefore the respiratory opening to the burrow, and thus the volume of water which may be drawn into the teredinid body cavity, was reduced. Furthermore, the ability of the species to capture plankton and generate a respiratory current would be limited due to the volume of larvae held on the parental gill; the shallow food-groove would only allow a small volume of particles to pass through to the mouth; and the labial palps are greatly reduced, thus limiting the ability of *L. pedicellatus* to process plankton.

Conversely, the digestive system of *L. pedicellatus* showed a number of adaptations consistent with xylotrophy. These include the elongated stomach and long intestine, both of which allow a more complete utilization of wood. The relatively large and specialised caecum with a twin-coiled typhlosole, which greatly increases the organ's surface area for nutrient absorption; and the digestive gland specialised for wood-digestion. The anatomical specialisation towards xylotrophy is also apparent in the calcareous structures which were analysed in Chapter four. The shell valves are broader relative to the pallets, thus the valves have a greater degree of contact with the anterior burrow which generates a greater volume of wood for ingestion during burrowing. Whilst *L. pedicellatus* is capable of filter-feeding and plankton undoubtedly provides a valuable source of nutrients (Morton, 1971), *L. pedicellatus* is predominantly a xylotroph and may complete an entire life-cycle feeding exclusively on wood (Gallager *et al.,* 1981).

It is not known whether the cellulolytic enzymes produced by the bacterial symbionts are utilized by the host, yet the large range of enzymes encoded in the bacterial genome suggest they play an important role in wood digestion (Yang *et al*., 2009). However, the mechanism underlying the transportation of these enzymes from the bacteriocytes on the gill to the digestive system remains unknown. Indeed it has been proposed that a duct connects the gills with the oesophagus in the species *Teredo furcifera* (Nair & Saraswathy, 1971), yet this duct has never been observed in other teredinid species (Moraes & Lopes, 2003). Chapter 2 sought to elucidate whether this duct was present in *L. pedicellatus,* using X-ray scanning micro computer tomography. This technique produced a 3-D rendered digital model of specimens, which could then be dissected in any plane. Furthermore, models could be traversed at 2 μm sections allowing the user to 'journey' through a specimen. Examination of the three-dimensional structure of the mouth, oesophagus and stomach of the *L. pedicellatus* failed to reveal a duct, opening or structure similar to the one described by Nair and Saraswathy (1971). Whilst this evidence is compelling, it does not conclusively rule out the presence of a duct-like structure in *L. pedicellatus*. Indeed, future studies should aim to utilize a range of microscopic techniques and examine a number of species, including *T. furcifera*, to determine whether this duct exists.

The endogenous production of cellulolytic enzymes by *Lyrodus pedicellatus*

It was initially thought that teredinid symbionts were the sole producers of cellulolytic enzymes, but recent research suggests that the hosts may contribute to the enzymatic deconstruction of wood (Betcher *et al*., 2012). Only a single report has investigated whether teredinids can endogenously produce cellulolytic enzymes (Honein *et al*., 2012) and this was of limited value as the transcriptome of whole specimens were sequenced. Thus no information was provided on the abundance of cellulolytic enzymes and the organs which produced them.

Chapter three details the transcriptomic survey of the major digestive organs in *L. pedicellatus* to determine the endogenous capability of the teredinid to produce cellulolytic enzymes. As transcription reflects active gene expression, this chapter provides an insight into organ function, thus directly correlates with the anatomical survey in Chapter two.

Analysis revealed that the digestive gland plays a fundamental role in wood digestion, producing a total of 26 different cellulolytic enzymes called glycoside hydrolases (GHs). It has previously been hypothesised that the caecum may represent a major site of enzyme transcription (Betcher *et al*., 2012). Yet the low abundance of cellulolytic enzymes transcripts suggests the caecum plays a minor role in cellulolytic enzyme production. In light of these findings, the current view on the role of caecum as the main site of enzyme transcription needs to be reconsidered. The findings suggest that the digestive gland produces cellulases which are likely secreted into the caecum, where wood digestion and nutrient absorption take place. Whilst the genome of *Teredinibacter turnerae* reveals genes encoding a range of cellulolytic enzymes, levels of gene expression (hence, protein production) from the symbionts remain unknown. Identification of all proteins present in the caecum would help determine the overall contribution to cellulolysis from the host and symbiont. Indeed, whilst termites possess a range of genes encoding cellulolytic enzymes, proteomic analysis revealed that the most abundant proteins in the hindgut were produced by their resident endosymbiont (Watanabe & Tokuda, 1998; Todaka *et al.*, 2007).

The apparent absence of a classic cellobiohydrolase from the transcriptomic data suggests that *L. pedicellatus* may utilize endoglucanases and processive endoglucanases to produce cellobiose units. Further examination of these enzymes is required in order to confirm their function. The activity of recombinant enzymes of interest could be assayed, thus proving their specificity *e.g.*, processive endoglucanases would be differentiated from endoglucanases by the production of cellobiose, and glucosidase would cleave cellobiose substrate. Identification of the activity of these two enzymes would confirm the shipworm has an endogenous capability to deconstruct lignocelluloses without the enzymes provided by the symbiont.

Further transcriptomic analysis of the crystalline style sac and intestine of *L. pedicellatus* should be undertaken and combined with data for the caecum, digestive gland and gill tissue, to provide a transcriptomic data set for the entire digestive system. This may potentially identify additional endogenously-produced GHs with specificity towards lignocellulose. Extraction of the crystalline style from the small cultured specimens proved challenging and the intestinal RNA yield was insufficient for further downstream processing. Establishing a culture of *L. pedicellatus* in larger blocks of wood, maintained at elevated temperatures, could increase growth rates, therefore increasing ease of dissection and tissue yield. High-performance liquid chromatography could be used to measure sugars present in the polymers

of wood fragments from the caecum, intestine and frass - the waste particles expelled by the shipworm. This would reveal the change in hemicellulose and cellulose content during digestion and identify the main regions of cellulose degradation in the digestive system.

Sequencing the genome of *L. pedicellatus* may reveal a number of genes encoding cellulolytic enzymes that were not present in the transcriptome. Furthermore, this will allow a direct comparison with the genome of the symbiont *Teredinibacter turnerae,* and with the marine wood-boring isopod, *Limnoria quadripunctata*, which is not associated with any bacterial symbionts. This would allow a direct comparison between two different digestive strategies (symbiosis and microbe exclusion) which tackle the same problem - overcoming the recalcitrance of lignocellulose and utilizing the glucose trapped in the plant cell wall as nutrition.

Aspects of the life history strategy of *Lyrodus pedicellatus*

Lyrodus pedicellatus is one of the most destructive teredinids and has achieved a cosmopolitan distribution in temperate and tropical waters (Nair & Saraswathy, 1971; Borges *et al*., 2012). The success of this species is primarily attributed to the long-term brooding strategy which allows larvae to settle on wood almost immediately after release, thus providing the greatest chance for offspring survival (Lebour, 1946; Turner & Johnson in Jones & Eltringham, 1971). Chapter four aimed to develop a greater understanding of the early life history of the long-term brooding teredinid *L. pedicellatus* and sets out the evidence that developing young may be matrotrophic, obtaining extra-embryonic nutrition from the adult.

Intense larval settlement rapid growth was observed in cultured specimens of *L. pedicellatus*. Metamorphosed larvae were observed growing at an average rate of 0.11 mm per day. The smallest fully developed individual containing larval broods was found at a body size of 4.46 mm in length. Thus using this minimum size of maturity and the known average growth rate, *L. pedicellatus* larvae may become fully developed brooding adults approximately 41 days after metamorphosis. This is far more rapid than the ten weeks previously noted by Turner and Johnson, in Jones and Eltringham (1971). This suggests individuals become sexually mature within weeks after metamorphosing as larvae. Brooding adults measuring 10 mm in length contained an average of 157 larvae at various developmental stages. This suggests that multiple fertilization events occur and staggered brooding allows a continual release of larvae during the breeding season.

Examination of the larval-parent interaction during brooding revealed that larvae are individually enclosed within a thin membranous brood-pouch and thus are unlikely to come into direct contact with the water which washes over the adult gill. Furthermore, the large number of larvae retained on the gills would appear to limit the adult's intake of water, therefore reducing availability of phytoplankton. This is supported by the X-ray scanning micro-computer tomography images and videos in Chapter two, which show transformation of the parental gills to accommodate a large number of larvae, individually housed in brood pouches. The larval velum appears to lack pre-oral cilia and has greatly reduced post-oral cilia, thus *L. pedicellatus* larvae appear poorly equipped for the opposed-band feeding mechanism described by Strathman & Grunbaum (2006). Therefore the larvae appear to lack the ability to feed on plankton during development. Yet long-term brooded larvae are provided with small eggs which appear insufficient to fuel the extensive growth of the prodissoconch II and dissoconch phase (Cragg *et al*., 2009). This suggests that larval growth is fuelled by extra-embryonic nutrition (Cragg *et al*., 2009) and the larvae of at least one long-term brooding species have been observed ingesting glycogen-forming cells of adult origin (Calloway, 1982). Results presented herein support this observation as cells were imaged budding off from the inner surface of the brood pouch, and were captured by the larvae. Examining the energetic content of the eggs and larval pediveligers will help determine the level extra-embryonic nutrition gained by the larvae. Transmission electron microscopy could be used to observe the glycogen transfer mechanism between the parent and brooded larvae. Examination of the larval stomach content will also reveal whether larvae are capable of suspension-feeding whilst retained on the paternal gill and whether the cells which appear to bud-off from the brood pouch lining are ingested by the larvae.

The ability of *L. pedicellatus* to derive nutrition exclusively from wood, allows the species to grow and reproduce continually year-round. This provides an advantage against species more reliant on planktotrophy for nutrition and those which produce larvae with an extended free-swimming developmental period. These species face seasonal checks in growth and potential limitations in larval dispersal when levels of phytoplankton are low. Thus, long-term brooders are probably the dominant species in oligotrophic waters, such is the case *Teredo bartschi* in the Gulf of Aqaba (Cragg *et al*., 2009).

Improving the taxonomic resolution and classification of the Teredinidae

Species identification within the Teredinidae is challenging and the taxonomy of this family existed in a state of "chaos" prior to Turner's (1966) classification. However a number of issues still persist, thus highlighting the necessity for a robust means of species identification. The molecular phylogeny of the Teredinidae outlined in Chapter five uses integrative taxonomic approach, combining ribosomal and nuclear markers, biogeographic information and anatomical characteristics to accurately identify teredinid species and increase the resolution of this taxonomically challenging group. This work improves upon the only existing molecular-based taxonomic survey using nuclear markers (Distel *et al.,* 2011) and includes eight species of teredinid which were previously unsequenced, achieving coverage of all the groups based on Turner's (1966) classification. Thus this work represents the most complete phylogenetic survey of the Teredinidae to date.

The mitochondrial cytochrome C oxidase I gene (COI-5P) has been adopted as the standard 'taxon barcode' for most animal groups (Herbert *et al*., 2003) and is by far the most represented in public reference libraries. At the time of writing (September 2013) the Barcode of Life Database (BOLD) included COI-5P sequences from over 1,300,000 specimens belonging to over 120,000 species across all phyla. However, the Teredinidae are represented by only four species on BOLD. As this system relies on the ability to match sequences with reference barcodes, taxonomic identification of the Teredinidae is limited. Thus, the acquisition of COI-5P sequences for a further eight species of teredinid represents a significant advance in molecular-based identification using mitochondrial markers.

The availability of both nuclear and mitochondrial sequences on a public database, such as GenBank and BOLD, will greatly assist future identification of teredinid species. This has a range of applications including tracking and monitoring the spread of invasive teredinids, distinguishing cryptic species and identifying specimens which are incomplete (Borges *et al*., 2012).

The acquisition of sequence data greatly assists species identification, yet anatomical, morphological and behavioural-based characterisation still remains a fundamental part of taxonomy. Members of the *Lyrodus* genus are the most difficult to identify due to the high degree of variation in pallet morphology (Nair & Saraswathy, 1971). Indeed, this has resulted in over 30 synonyms for *L. pedicellatus* alone (Turner, 1966; Turner, 1971). Furthermore, at

least two morphologically indistinguishable cryptic species of *L. pedicellatus* have been identified (Calloway & Turner, 1984; Borges *et al*,. 2012). Examination of the brooding strategy of one of these cryptic species revealed that larvae were released at the straight-hinged veliger stage, as opposed to the pediveliger stage of the 'true' *L. pedicellatus* species (Turner & Johnson in Jones & Eltringham, 1971; Calloway & Turner, 1984). Chapter four therefore assists the molecular-based identification of Chapter five, by providing information on a range of morphological characteristics. Mapping pallet variation through the life-cycle of *L. pedicellatus* provides a more secure means of pallet-based identification, and characterisation of brooding behaviour and larval development allows this species to be differentiated from cryptic species which may be morphologically indistinguishable.

Whilst molecular data exist for species representing all known teredinid groups described by Turner (Turner, 1966), the genera *Uperotus* and *Bactronophorus* remain unsequenced. Furthermore, at least two species of the sea grass borer *Zaschia* have been identified (Turner & Yakovlev, 1982; Yakovlev *et al*., 1998; Cragg, in Marshall & Beehler, 2007). However, these rare species are the least investigated among the Teredinidae and their taxonomic placement is unknown. Thus, in order to achieve a greater understanding of the evolutionary pathways and taxonomy of the Teredinidae it is necessary to obtain sequences from these individuals. Due to the difficulties in sequencing the COI-5P region in the Teredinidae, mitogenomic sequencing would allow targeted selection of a suitable mitochondrial region. This would assist in the design of primers more suitable. Furthermore, mitogenome phylogenetic comparisons may replace the current system of molecular taxon diagnosis as next generation sequencing becomes a more viable alternative due to the significant reduction in costs.

A Caribbean teredinid, *Teredothyra dominicensis*, invades the Mediterranean Sea

The rate of biological invasions has increased dramatically over the past few decades due to maritime and shipping activity (Cohen & Carlton, 1995; Seebens *et al.,* 2013). Indeed, a number of teredinid species are believed to have been transported beyond their natural range, resulting in a worldwide distribution (Hill & Kofoid, 1927; Turner, 1966; McIntosh *et al*., 2012). Whilst the problem associated with marine borers is a cosmopolitan issue, the spread of teredinids into new areas is still a major cause for concern. Historically, invasions have caused widespread destruction and this damage is often far more severe when exotic species

enter new areas (Kofoid & Miller, 1927). Yet given the economic importance of this issue, very few studies on teredinid invasion and establishment exist.

Chapter six reports a substantial population of the Caribbean shipworm, *Teredothyra dominicensis*, in the Mediterranean Sea. Identification was confirmed by comparing pallet morphologies and DNA sequences between indigenous Caribbean specimens and the invasive Mediterranean specimens. Examination of gamete structure and observations of breeding behaviour revealed this poorly studied species is an externally-fertilizing broadcast-spawner, with larvae which undergo a long developmental phase in the water column. This is of particular importance, as the most successful invading species are believed to be those with long-brooding and short free-swimming stages which can quickly colonise nearby substrata at high densities (Jablonski & Lutz, 1983). However, the timber from which this species was found did not contain any brooding teredinids, despite their prevalence in the region. Furthermore, panels placed at this site and recovered one year later were colonised exclusively by *T. dominicensis*. This suggests that breeding populations are present in the region, and these individuals can produce competent larvae in numbers large enough to outcompete brooding species.

Specimens were initially found in a wooden shipwreck, which was deliberately sunk in the autumn of 2006. Infestation was first noticed during the summer of 2007, which provides the first known recorded incident of *T. dominicensis* invading the Mediterranean Sea. By the summer of 2011 the entire shipwreck, bar parts of the mast, had been completely destroyed. However, this structure was so riddled with shipworm that it was held together by the calcareous tubes of the line the teredinid burrow. This study reports the first well-documented teredinid invasion, highlights the extensive damage which can be caused by non-indigenous invasive species and also represents an important case study on the disintegration of shipwrecks by marine borers.

Future research should aim to survey sites around the Mediterranean to determine the prevalence of *T. dominicensis*. Studies should also focus on aspects of larval development, particularly the duration of the larval free-swimming period. Modelling the invasive potential will identify the extent to which this species may spread throughout the region and the influence that global warming may have on distribution range. The Suez Canal provides a vector by which this species may invade the Red Sea. Wooden panels could be placed along the canal to determine borer biodiversity and whether *T. dominicensis* may invade beyond the

Mediterranean. *T. dominicensis* should be reared to determine the patterns of larval development which may elucidate how this broadcast spawning species was capable of outcompeting brooding species.

References

Adamkewicz, S. L., Harasewych M., G. *et al.* (1997). A molecular phylogeny of the bivalve molluscs. *Molecular Biology and Evolution* 14(6): 619-629.

Arantes, V. and Saddler, J. (2010). Access to cellulose limits the efficiency of enzymatic hydrolysis: the role of amorphogenesis. *Biotechnology for Biofuels* 3(1): 4.

Arnold, K., L. Bordoli, *et al*. (2006). The SWISS-MODEL workspace: a web-based environment for protein structure homology modelling. *Bioinformatics* 22(2): 195-201.

Artimo, P., M. Jonnalagedda, *et al*. (2012). ExPASy: SIB bioinformatics resource portal. *Nucleic Acids Research* 40(W1): W597-W603.

Atkins, D. (1937). On the ciliary mechanisms and interrelationships of lamellibranchs. Part III: types of lamellibranch gills and their food currents. *Quarterly Journal of Microscopical Science*, N. S., 79: 375–421.

Bartsch, P. (1922). A monograph of the American shipworms, *Govt. print. off*.

Bartsch, P. (1923). Stenomorph, a New Term in Taxonomy. *Science* 57(1472): 330.

Bazylinski D., A, Rosenberg F., A. (1983). Occurrence of a brush-border in the caecum (appendix) of several *Teredo* and *Bankia* species (Teredinidae, Bivalvia, Mollusca). *Veliger* 25: 251.

Betcher, M., A., Fung, J., M. *et al*. (2012). Microbial Distribution and Abundance in the Digestive System of Five Shipworm Species (Bivalvia: Teredinidae). *PLoS ONE* 7(9).

Biely, P. Vršanská, M. *et al*. (1997). Endo-β-1,4-xylanase families: differences in catalytic properties. *Journal of Biotechnology* 57(1–3): 151-166.

Bienhold, C., P. Ristova, P. *et al*. (2013). How Deep-Sea Wood Falls Sustain Chemosynthetic Life. *PLoS ONE* 8(1): e53590.

Bjoerdal, C., G. Gregory, D. (2011). WreckProtect: decay and protection of archaeological wooden shipwrecks. *Archaeopress*.

Bjordal, C., G. and T. Nilsson (2008). Reburial of shipwrecks in marine sediments: a long-term study on wood degradation. *Journal of Archaeological Science* 35(4): 862-872.

Blaxter, M., L. De Ley, P. *et al*. (1998). A molecular evolutionary framework for the phylum Nematoda. *Nature* 392(6671): 71-75.

Boraston, A., B., Bolam, D., N. *et al*. (2004). Carbohydrate-binding modules: fine-tuning polysaccharide recognition. *Biochemical Journal* 382: 769-781

Borges, L., M., S. Sivrikaya, H. *et al*. (2012). Investigating the taxonomy and systematics of marine wood borers (Bivalvia: Teredinidae) combining evidence from morphology, DNA barcodes and nuclear locus sequences. *Invertebrate Systematics* 26(5-6): 572-582.

Borges, L., M., S., Valente, A. *et al*. (2010). Changes in the wood boring community in the Tagus Estuary: a case study." *Marine Biodiversity Records* 3: Unpaginated.

Bourlat, S., J., Nielsen, C. *et al*. (2008). Testing the new animal phylogeny: a phylum level molecular analysis of the animal kingdom. *Mol. Phylogenet. Evol*. 49(1): 23-31.

Boyle, P. J. and Mitchell, R. (1978). Absence of Microorganisms in Crustacean Digestive Tracts. *Science* 200(4346): 1157-1159.

Brown, G. D. and Gordon, S. (2005). Immune recognition of fungal β-glucans. *Cellular Microbiology* 7(4): 471-479.

Bulatov, G., A. (1941). Response of the larvae of the Black Sea Teredo navalis *L.* to different water temperatures. *Dokl. Akad. Nauk. SSSR*, 32(4), 291-292.

Calloway, C. B. (1982). Parentally derived extra-embryonic nutrition in *Lyrodus pedicellatus* (Bivalvia, Teredinidae). *American Zoologist* 22(4): 860.

Calloway, C., B. and Turner R., D. (1983). Documentation and implications of rapid successive gametogenic cycles and broods in the shipworm *Lyrodus floridanus* (Bartsch) (Bivalvia, Teredinidae). *Journal of Shellfish Research* 3(1): 65-69.

Cantarel, B., L. Coutinho, P., M. *et al*. (2009). The Carbohydrate-Active EnZymes database (CAZy): an expert resource for Glycogenomics. *Nucleic Acids Research* 37(suppl 1): D233-D238.

Carlton, J., T. (1999). Molluscan invasions in marine and estuarine communities. *Malacologia* 41(2): 439-454.

Carlton. J., T. (2013). Ballast, in: Simberloff D. and Rejmanek, R. Encyclopaedia of Biological Invasions, University of California Press, Berkeley.

Castagna, M. and U. S. B. o. C. Fisheries (1961). Shipworms and Other Marine Borers, U.S. Department of the Interior, Fish and Wildlife Service, Bureau of Commercial Fisheries.

Clapp, W., F. (*1951)*. *Observations on living Teredinidae*. Fourth Progress Report, W. F. *Clapp* Laboratories, Inc., Duxbury, Mass., p. 1-9.

Coe, W., R. (1933). Destruction of Mooring Ropes by Teredo; Growth and Habits in an Unusual Environment. *Science* 77(2002): 447-449.

Coe, W., R. (1941). Sexual Phases in Wood-Boring Molluscs. *Biological Bulletin* 81(2): 168-176.

Cohen, A., N. and Carlton, J., T. (1995), Biological study: non-indigenous aquatic species in a United States estuary: a case study of the biological invasions of the San Francisco Bay and delta, University of California Final Report, National Technical Information Service, Springfield, VA 203pp.

Collins, T. Gerday, C. *et al*. (2005). Xylanases, xylanase families and extremophilic xylanases. FEMS *Microbiology Reviews* 29(1): 3-23.

Cragg, S. M., (2003). Marine wood-boring invertebrates of New Guinea and its surrounding waters. In, Marshall, A. J. and Beehler B., M., P. (2007). The ecology of Papua, Periplus Editions.

Cragg, S. M., Jumel, M., C. *et al*. (2009). The life history characteristics of the wood-boring bivalve *Teredo bartschi* are suited to the elevated salinity, oligotrophic circulation in the Gulf of Aqaba, Red Sea. *Journal of Experimental Marine Biology and Ecology* 375(1-2): 99-105.

Cragg, S. M., Pitman, A., J. *et al*. (1999). Developments in the understanding of the biology of marine wood boring crustaceans and in methods of controlling them. *International Biodeterioration & Biodegradation* 43(4): 197-205.

Cragg, S., M. and Icely, J., D. (1982). An interim report on studies of the tolerance of *Sphaeroma* (Crustacea: Isopoda) of CCA-treated timber. *International Research Group on Wood Preservation* Doc. 491.

Cragg, S., M. Daniel, G. (1992). *Chelura terebrans* (Crustacea: Amphipoda) is capable of degrading wood independently of its associate, *Limnoria*. *International Research Group on Wood Preservation* IRG/WP/92-4180: 1-9.

Culha, M. (2010). The Presence of *Teredo navalis* Linnaeus, 1758 (Mollusca, Bivalvia, Teredinidae) in the Southern Black Sea, Turkey. *Journal of Animal and Veterinary Advances* 9(10): 1515-1518.

Culliney, J., L. (1975). Comparative larval development of shipworms *Bankia gouldi* and *Teredo navalis*. *Marine Biology* 29(3): 245-251.

Dahiya, N. Tewari, R. *et al*. (2006). Biotechnological aspects of chitinolytic enzymes: a review. *Applied Microbiology and Biotechnology* 71(6): 773-782.

Daniel, G. Nilsson, T. *et al*. (1991). *Limnoria lignorum* ingest bacterial and fungal degraded wood. *Holz als Roh- und Werkstoff* 49(12): 488-490.

De Moraes, D., T. and. Lopes S., B., G., C. (2003). The functional morphology of *Neoteredo reynei* (Bartsch, 1920) (Bivalvia, Teredinidae). *Journal of Molluscan Studies* 69(4): 311-318.

Dean, R., C. (1978). Mechanisms of Wood Digestion in the Shipworm Bankia gouldi Bartsch: Enzyme Degradation of Celluloses, Hemicelluloses, and Wood Cell Walls. *Biological Bulletin* 155(2): 297-316.

Distel, D. L. Delong, E., F. *et al*. (1991). Phylogenetic characterization and *in situ* localization of the bacterial symbiont of shipworms (Teredinidae, Bivalvia) by using 16s-ribosomal-rna sequence-analysis and oligodeoxynucleotide probe hybridization. *Applied and Environmental Microbiology* 57(8): 2376-2382.

Distel, D. L., Beaudoin, D. J. *et al*. (2002). Coexistence of Multiple Proteobacterial Endosymbionts in the Gills of the Wood-Boring Bivalve *Lyrodus pedicellatus* (Bivalvia: Teredinidae). *Applied and Environmental Microbiology* 68(12): 6292-6299.

Distel, D., L. Amin, M. *et al*. (2011). Molecular phylogeny of Pholadoidea Lamarck, 1809 supports a single origin for xylotrophy (wood feeding) and xylotrophic bacterial endosymbiosis in Bivalvia. *Molecular Phylogenetics and Evolution* 61(2): 245-254.

Distel, D., L. and. Roberts S., J. (1997). Bacterial endosymbionts in the gills of the deep-sea wood-boring bivalves *Xylophaga atlantica* and *Xylophaga washingtona*." *Biological Bulletin* 192(2): 253-261.

Donlan, C., J. and Nelson P., A. (2003). Observations of invertebrate colonized flotsam in the eastern tropical Pacific, with a discussion of rafting. *Bulletin of Marine Science* 72(1): 231-240.

Eaton, R., A. and Hale D., M., D., C. (1993). Wood: Decay, Pests, and Protection, Chapman and Hall.

Eckelbarger, K., J. and Reish D., J. (1972). A first report of self-fertilization in the wood-boring family Teredinidae (Mollusca: Bivalvia). *Bull. South California Acad. Sci.* 71: 48-50.

Edmondson, C., H. (1942). Teredinidae of Hawaii. *Occasional Papers of Bernice P. Bishop Museum*, Honolulu, Hawaii 17: 97-150.

Edmondson, C., H. (1962). Teredinidae, ocean travellers. *Occasional Papers of Bernice P. Bishop Museum*, Honolulu, Hawaii 23(3).

Ekborg, N., A. Morrill, W. *et al*. (2007). CelAB, a multifunctional cellulase encoded by *Teredinibacter turnerae* T7902T, a culturable symbiont isolated from the wood-boring marine bivalve *Lyrodus pedicellatus*. *Applied and Environmental Microbiology* 73(23): 7785-7788.

Elshahawi, S., I. Trindade-Silva, A., E. *et al*. (2013). Boronated tartrolon antibiotic produced by symbiotic cellulose-degrading bacteria in shipworm gills. *Proceedings of the National Academy of Sciences of the United States of America* 110(4): E295-E304.

Eltringham, S., K. (Eds.), Les Perforants, les Champignons et les Salissures du Boisen Millieu Marin. OECD, Paris, pp. 74–91.

Field, K. Olsen, G. *et al*. (1988). Molecular phylogeny of the animal kingdom. *Science* 239(4841): 748-753.

Filho, C., S. Tagliaro, C., H. *et al*. (2008). Seasonal abundance of the shipworm *Neoteredo reynei* (Bivalvia, Teredinidae) in mangrove driftwood from a northern Brazilian beach. *Iheringia Serie Zoologia* 98(1): 17-23.

Fuller, S., C. Hu, Y., P. *et al*. (1989). Shell and pallet morphology in early developmental stages of *Teredo navalis* Linné (Bivalvia, Teredinidae). *Nautilus* 103(1): 24-35.

Gallager, S., M. Turner, R., D. *et al*. (1981). Physiological aspects of wood consumption, growth, and reproduction in the shipworm *Lyrodus pedicellatus* Quatrefages (Bivalvia:Teredinidae). *Journal of Experimental Marine Biology and Ecology* 52(1): 63-77.

Gibelin, A., L. and Déqué M. (2003). Anthropogenic climate change over the Mediterranean region simulated by a global variable resolution model. *Climate Dynamics* 20(4): 327-339.

Giorgi, F. and Lionello P. (2008). Climate change projections for the Mediterranean region. *Global and Planetary Change* 63(2-3): 90-104.

Gollasch, S. (2002). ″The importance of ship hull fouling as a vector of species introductions into the North Sea.″ *Biofouling* 18(2): 105-121.

Gollasch, S. and Daisie (2009). Species accounts of 100 of the most invasive alien species in Europe: *Teredo navalis* Linnaeus, common shipworm (Teredinidae, Mollusca).

Goodell, B., and Nicholas, D., D *et al.* (2003). Wood Deterioration and Preservation: Advances in Our Changing World, American Chemical Society.

Grave, B., H. (1928). Natural history of shipworm, *Teredo navalis*, at Woods Hole, Massachusetts. *Biological Bulletin* 55.

Greenfield, L. J. (1952). Observations on the Nitrogen and Glycogen Content of *Teredo* (*Lyrodus*) *Pedicellata* De Quatrefages at Miami, Florida. *Bulletin of Marine Science* 2(3): 486-496.

Greenfield, L., J. and Lane C., E. (1953). Cellulose digestion in *Teredo*. *Journal of Biological Chemistry* 204(2): 669-672.

Gregory, D. (2010). Shipworm Invading the Baltic? International Journal of Nautical Archaeology 39(2): 431-431.

Haga, T. and T. Kase (2013). Progenetic dwarf males in the deep-sea wood-boring genus Xylophaga (Bivalvia: Pholadoidea). *Journal of Molluscan Studies* 79: 90-94.

Hammen, C., S. (1968). Aminotransferase activities and amino acid excretion of bivalve molluscs and brachiopods. *Comparative Biochemistry and Physiology* 26(2): 697-70

Harvey, R. (1996). Deep water Xylophagaidae (Pelecypoda:Pholadacea) from the North Atlantic with descriptions of three new species. *Journal of Conchology* 35: 473-481.

Hebert, P., D. Cywinska, N. A, *et al*. (2003). Biological identifications through DNA barcodes. Proceedings of the Royal Society of London. Series B: *Biological Sciences* 270(1512): 313-321.

Hebert, P., D., N. and Gregory, T., R. (2005). The Promise of DNA Barcoding for Taxonomy. *Systematic Biology* 54(5): 852-859.

Hendy, I., W. Eme, J. *et al*. (2013). Dartfish use teredinid tunnels in fallen mangrove wood as a low-tide refuge. *Marine Ecology Progress Series* 486: 237-245.

Henrissat, B. and G. Davies (1997). Structural and sequence-based classification of glycoside hydrolases. *Current Opinion in Structural Biology* 7(5): 637-644.

Himmel, M. E., S. Y. Ding, *et al*. (2007). Biomass recalcitrance: Engineering plants and enzymes for biofuels production. *Science* 315(5813): 804-807.

Hiroki, K., R. Leonel, M., V. *et al*. (1994). Reproductive events of *Nausitora fusticula* (Jeffreys, 1860) (Mollusca, Bivalvia, Teredinidae). *Invertebrate Reproduction & Development* 26(3): 247-250.

Hoagland, K., E. and Turner R., D. (1980). Range Extensions of Teredinids (Shipworms) and Polychaetes in the Vicinity of a Temperate-Zone Nuclear Generating-Station. *Marine Biology* 58(1): 55-64.

Honein, K., G. Kaneko, *et al*. (2012). Studies on the cellulose-degrading system in a shipworm and its potential applications. Terragreen 2012: Clean Energy Solutions for Sustainable Environment. C. Salame, M. Aillerie and G. Khoury. 18: 1271-1274.

Hong, T., Y. and Meng M. (2003). Biochemical characterization and antifungal activity of an endo-1,3-β-glucanase of *Paenibacillus* sp. isolated from garden soil. *Applied Microbiology and Biotechnology* 61(5-6): 472-478.

Huang, Q., S., Xie, X., L. *et al*. (2012). The GH18 family of chitinases: their domain architectures, functions and evolutions. *Glycobiology* 22(1): 23-34.

Hyde, K., E. Jones, B., G. *et al*. (1998). Role of fungi in marine ecosystems. *Biodiversity & Conservation* 7(9): 1147-1161.

Ibrahim, J. (1981). Season of settlement of a number of shipworms (Mollusca : Bivalvia) in six Australian harbours. *Marine and Freshwater Research* 32(4): 591-604.

Isham, L. and T. JQ (1953). ″Some aspects of larval development and metamorphosis of *Teredo* (*Lyrodus*) *pedicellata* de Quatrefages.″ *Bull. Mar. Sci. Gulf Caribb*. 2: 574-589.

Jablonski, D. and R., A. Lutz (1980). Molluscan larval shell morphology: ecological and paleontological applications. Skeletal growth of aquatic organisms: biological records of environmental change. D. C. Rhoads and R. A. Lutz. New York, Plenum: 323-377.

Janeček, S. t. (1997). α-amylase family: Molecular biology and evolution. *Progress in Biophysics and Molecular Biology* 67(1): 67-97.

Janeway Jr, C. A. (1992). ″The immune system evolved to discriminate infectious nonself from noninfectious self.″ *Immunology Today* 13(1): 11-16.

Johnson, M., W. and Menzies R., J. (1956). The Migratory Habits of the Marine Gribble *Limnoria tripunctata* Menzies in San Diego Harbor, California. *Biological Bulletin* 110(1): 54-68.

Johnson, M., W. and R., C. Miller (1935). The Seasonal Settlement of Shipworms, Barnacles, and Other Wharf-pile Organisms at Friday Harbour, Washington, University of Washington Press.

Kawabata, S., I. Nagayama, R. *et al*. (1996). Tachycitin, a small granular component in horseshoe crab hemocytes, is an antimicrobial protein with chitin-binding activity. *Journal of Biochemistry* 120(6): 1253-1260.

Kelley, L., A. and Sternberg M., J., E. (2009). Protein structure prediction on the Web: a case study using the Phyre server. Nature Protocols 4(3): 363-371.

Kern, M.,. McGeehan, J., E. *et al*. (2013). Structural characterization of a unique marine animal family 7 cellobiohydrolase suggests a mechanism of cellulase salt tolerance. *Proceedings of the National Academy of Sciences of the United States of America* 110(25): 10189-10194.

King, A., J. Cragg, S., M. *et al*. (2010). Molecular insight into lignocellulose digestion by a marine isopod in the absence of gut microbes. *Proceedings of the National Academy of Sciences* 107(12): 5345-5350.

Klemm, D. Heublein, B, *et al*. (2005). Cellulose: fascinating biopolymer and sustainable raw material. Angew Chem Int Ed Engl 44(22): 3358-3393.

Knudsen. P. (1974). Pelemark-marine treborer. *Norsk Institut for Skogforskning* 1432 AS-NLH.

Kofoid, C., A. Miller, R., C. (1927). Marine borers and their relation to marine construction on the Pacific Coast: being the final report of the San Francisco Bay Marine Piling Committee, The Committee.

Kühne, H. and Becker G. (1964). Der Holz-Flohkrebs *Chelura terebrans* Philippi (Amphipoda, *Cheluridae*): Morphologie, Verbreitung, Lebensweise, Verhalten, Entwicklung und Umweltabhängigkeit, Duncker & Humblot.

Kühne, H., 1971. Identifications des crustace´s perforants des bois. In: Jones, E.B.G.,

Lane, C., E. Posner, G., S. *et al*. (1952). The Distribution of Glycogen in the Shipworm, *Teredo* (*Lyrodus*) *Pedicellata* Quatrefages. *Bulletin of Marine Science* 2(2): 385-392.

Lane, C., E. Tierney, J., Q. *et al*. (1954). The respiration of normal larvae of *Teredo bartschi* Clapp. 106: 323-327. *Biological Bulletin* 106: 323-327.

Larsson, A., M. Anderson, L. *et al*. (2006). Three-dimensional crystal structure and enzymic characterization of β-Mannanase Man5A from blue mussel *Mytilus edulis*. *Journal of Molecular Biology* 357(5): 1500-1510.

Lasker, R. and Lane C., E. (1953). The Origin and Distribution of Nitrogen in *Teredo Bartschi* Clapp. *Biological Bulletin* 105(2): 316-319.

Lazier, E., L. (1924). Morphology of the Digestive Tract of *Teredo Navalis*, University of California Press.

Lechene, C., P. Luyten, Y. *et al*. (2007). Quantitative imaging of nitrogen fixation by individual bacteria within animal cells. *Science* 317(5844): 1563-1566.

Levasseur, A. Drula, E. *et al*. (2013). Expansion of the enzymatic repertoire of the CAZy database to integrate auxiliary redox enzymes.″ *Biotechnology for Biofuels* 6(1): 41.

Lewis, N., G. and. Yamamoto, E. (1990). Lignin: Occurrence, biogenesis and biodegradation. *Annual Review of Plant Physiology and Plant Molecular Biology* 41(1): 455-496.

Li, H. and Greene L., H. (2010). Sequence and structural analysis of the chitinase insertion domain reveals two conserved motifs involved in chitin-binding. *PLoS ONE* 5(1): e8654.

Loader, N., J. Robertson, I. *et al.* (2003). Comparison of stable carbon isotope ratios in the whole wood, cellulose and lignin of oak tree-rings. *Palaeogeography, Palaeoclimatology, Palaeoecology* 196, 395-407.

Loosanoff, V., L., and Davis. H., C. (1963). Rearing of bivalve molluscs, p. 1-128. In F. S. Russell [ed.], Advances in marine biology, vol. 1. Academic Press, Inc., New York.

Lopes, S., G., B., C. and Narchi, W *et al*. (1998). Digestive system of *Nausitora fusticula* (Jeffreys, 1860) (Bivalvia, Teredinidae). *Veliger*, 41: 351–365.

Luyten, Y. *et al*. (2007). Quantitative imaging of nitrogen fixation by individual bacteria within animal cells. *Science* 317(5844): 1563-1566.

Luyten, Y., A. Thompson, J., R. *et al*. (2006). Extensive variation in intracellular symbiont community composition among members of a single population of the wood-boring bivalve *Lyrodus pedicellatus* (Bivalvia: Teredinidae). *Applied and Environmental Microbiology* 72(1): 412-417.

Macintosh, H. (2012). *Lyrodus turnerae*, a new teredinid from eastern Australia and the Coral Sea (Bivalvia: Teredinidae). *Molluscan Research* 32(1): 36-42.

MacIntosh, H., de Nys, R. *et al*. (2012). Shipworms as a model for competition and coexistence in specialized habitats. *Marine Ecology Progress Series* 461: 95-105.

Mann, R. and Gallager S., M. (1984). Physiology of the Wood Boring Mollusc *Martesia cuneiformis* Say. *Biological Bulletin* 166(1): 167-177.

Mann, R. and Gallager S., M. (1985). Physiological and biochemical energetics of larvae of *Teredo navalis* L. and *Bankia gouldi* (Bartsch) (Bivalvia: Teredinidae). *Journal of Experimental Marine Biology and Ecology* 85(3): 211-228.

Manyak, D., M. (1982). A Device for the Collection and Study of Wood-Boring Molluscs: Application to Boring Rates and Boring Movements of the Shipworm *Bankia gouldi*. *Estuaries* 5(3): 224-229.

Marsden, P., R., V. McElvogue, D. *et al*. (2009). The Mary Rose - Your Noblest Shippe: Anatomy of a Tudor Warship, Mary Rose Trust.

Martins-Silva M., A. and Narchi, W. (2008). Functional Anatomy of *Bankia fimbriatula* Moll & Roch, 1931 (Bivalvia: Teredinidae). *The Veliger* 50:4 pp309.

Miller, R., C. (1923). Variation in the pallets of *Teredo navalis* in San Francisco Bay. University of California Publications in Zoology 22: 401-414.

Miller, R., C. (1924). The Boring Mechanism of *Teredo*, University of California Press.

Miller, S., E. (2007). DNA barcoding and the renaissance of taxonomy. *Proceedings of the National Academy of Sciences* 104(12): 4775-4776.

Mohnen, D. (2008). Pectin structure and biosynthesis. *Curr Opin Plant Biol* 11(3): 266-277.

Monod, T., H. (1952). Note additionnelle sur le problem Senegalensis petiti. *Inst. Fran. Afr. Noire. Cat*. 8, 9-46, 59-62.

Moreira, L., R., S. and Filho E., X., F. (2008). An overview of mannan structure and mannan-degrading enzyme systems. *Applied Microbiology & Biotechnology* 79(2): 165-178.

Morton, B. (1970). The functional anatomy of the organs of feeding and digestion of *Teredo navalis* and *Lyrodus pedicellatus*. Proceedings of the Malacological Society of London 39(2-3): 151-167.

Morton, B. (1970). The functional anatomy of the organs of feeding and digestion of *Teredo navalis* and *Lyrodus pedicellatus*. Proceedings of the Malacological Society of London 39(2-3): 151-167.

Mount, D., W. (2007). Using the Basic Local Alignment Search Tool (BLAST). Cold Spring Harbour Protocols 2007(7): pdb.top17.

Nagabhushnanam, R. (1959). Observations on the biology of the wood boring mollusc *Bankia* (Liliobankia) *campanellata* (Mollusc). *Proc. 1st All India Congress of Zoology Jabalpur*, P. 30.

Nair, N. B. & Saraswathy, M. (1971). Biology of wood-boring teredinid molluscs. Advances in Marine Biology 9: 335-540.

Nair, N. B. (1956). The Development of the Wood-boring Pelecypod *Bankia indica* Nair. Offprint from J. Madras Univ. B., XXVI, No. 2, 1956, pp [303]-318

Nakashima, K. Watanabe, H. *et al*. (2002). Dual cellulose-digesting system of the wood-feeding termite, *Coptotermes formosanus* Shiraki. *Insect Biochemistry and Molecular Biology* 32(7): 777-784.

Nishimoto, A. Mito, S. *et al*. (2009). Organic carbon and nitrogen source of sunken wood communities on continental shelves around Japan inferred from stable isotope ratios. Deep Sea Research Part II: Topical Studies in Oceanography 56(19–20): 1683-1688.

Ochiai, M. and Ashida M. (2000). ″A Pattern-recognition Protein for β-1,3-Glucan: the binding domain and the cDNA cloning of β-1,3-Glucan recognition protein from the silkworm, *Bombyx mori. Journal of Biological Chemistry* 275(7): 4995-5002.

Oliver, A. C. 1962. An account of the biology of *Linittorid*. J. Inst. Wood Sci. 9: 32-91

Quayle, D. B. (1992). Marine wood borers in British Columbia, Dept. of Fisheries and Oceans.

O'Sullivan, A. (1997). Cellulose: the structure slowly unravels. *Cellulose* 4(3): 173-207.

Paalvast, P. and van der Velde G. (2011). New threats of an old enemy: The distribution of the shipworm *Teredo navalis* L. (Bivalvia: Teredinidae) related to climate change in the Port of Rotterdam area, the Netherlands. *Marine Pollution Bulletin* 62(8): 1822-1829.

Paalvast, P. and van der Velde G. (2013). What is the main food source of the shipworm (*Teredo navalis*)? A stable isotope approach. Journal of Sea Research 80(0): 58-60.

Paalvast, P. and van der Velde, G. (2011). Distribution, settlement, and growth of first-year individuals of the shipworm *Teredo navalis* L. (Bivalvia: Teredinidae) in the Port

of Rotterdam area, the Netherlands. *International Biodeterioration & Biodegradation* 65(3): 379-388.

Peberdy, J. F. (1990). Fungal cell walls — a review. biochemistry of cell walls and membranes in fungi. P. Kuhn, A. J. Trinci, M. Jung, M. Goosey and L. Copping, Springer Berlin Heidelberg: 5-30.

Pechenik, J. Perron, F. *et al*. (1979). The role of phytoplankton in the diets of adult and larval shipworms, *Lyrodus pedicellatus* (Bivalvia: Teredinidae). *Estuaries* 2(1): 58-60.

Pitson, S., M. Seviour, R., J. *et al*. (1993). Noncellulolytic fungal β-glucanases: Their physiology and regulation. *Enzyme and Microbial Technology* 15(3): 178-192

Plazzi, F., Ceregato, A. *et al*. (2011). A Molecular Phylogeny of Bivalve Molluscs: Ancient Radiations and Divergences as Revealed by Mitochondrial Genes. *PLoS ONE* 6(11): e27147.

Popham, J. D. (1974). Comparative morphometrics of the acrosomes of the sperms of *"*externally*"* and *"*internally*"* fertilizing sperms of the shipworms (Teredinidae, Bivalvia, Mollusca). *Cell and Tissue Research* 150(3): 291-297.

Popham, J. D. (1979). Comparative spermatozoon morphology and bivalve phylogeny.*"* *Malacological Review* 12(1-2): 1-20.

Popham, J., D. and Dickson M., R. (1973). *"*Bacterial associations in the *Teredo Bankia australis* (Lamellibranchia: Mollusca). *Marine Biology* 19(4): 338-340.

Potts, F. A. (1923). The structure and function of the liver of *Teredo*, the shipworm. *Biological Reviews* 1(1): 1-17.

Puls, J. (1997). Chemistry and biochemistry of hemicelluloses: Relationship between hemicellulose structure and enzymes required for hydrolysis. *Macromolecular Symposia* 120(1): 183-196.

Purchon, R. D. (1941). On the biology and relationships of the lamellibranch *Xylophaga dorsalis* (Turton). *Journal of the Marine Biological Association of the United Kingdom* 25(01): 1-39.

Quayle, D.B. (1959). The growth rate of *Bankia setacea* Tryon, in: Ray, D.L. (Ed.) (1959). Marine boring and fouling organisms: Symposium. Friday Harbor Symposia: pp. 175-183

Rancurel, P. (1951) A propos de la larve de Teredo pedi'celScltCa Quatrefages. Bulletin du Laboratoire de Dinard, Fasc. XXXIV p 18-25.

Raskoff, K. A., F. A. Sommer, *et al*. (2003). Collection and culture techniques for gelatinous zooplankton. Biol Bull 204(1): 68-80.

Rayner, S., M. (1983). Distribution of teredinids (Mollusca: Teredinidae) in Papua New Guinea. *Records of the Australian Museum* 35: 61-76.

Reguera, G. and Leschine S., B. (2001). Chitin degradation by cellulolytic anaerobes and facultative aerobes from soils and sediments. *FEMS Microbiology Letters* 204(2): 367-374.

Richards, T,. A. Jones, M., D., M. *et al*. (2012). Marine Fungi: Their Ecology and Molecular Diversity. *Annual Review of Marine Science* 4(1): 495-522.

Ridewood, W., G. (1903). On the structure of the gills of the Lamellibranchia. Philosophical Transactions of the Royal Society of London. Series B, *Containing Papers of a Biological Character* 195(207-213): 147-284.

Robertson, A., I. and. Daniel P., A (1989). *D*ecomposition and the annual flux of detritus from fallen timber in tropical mangrove forests. *Limnology and Oceanography* 34(3): 640-646.

Roch, F. (1940). Die Terediniden des Mittelmeeres, Deutsch-Italienisches Institut für Meeresbiologie zu Rovigno d'Istria.

Rotramel, G. (1975). Filter-feeding by the marine boring isopod, *Sphaeroma quoyanum* H. Milne Edwards, 1840 (Isopoda, Sphaeromatidae). *Crustaceana* 28(1): 7-10.

Ruiz, G. M. Carlton, J., T. *et al*. (1997). Global Invasions of Marine and Estuarine Habitats by Non-Indigenous Species: Mechanisms, Extent, and Consequences. *American Zoologist* 37(6): 621-632.

Sakamoto, K. Touhata, K. *et al*. (2007). Cellulose digestion by common Japanese freshwater clam *Corbicula japonica*. *Fisheries Science* 73(3): 675-683.

Sakon, J. and Karplus P., A. (1998). Structure and mechanism of endo/exocellulase E4 from *Thermomonospora fusca*. *Biophysical Journal* 74(2): A255-A255.

Sánchez, E. Gallardo, C. *et al*. (2004). Future climate extreme events in the Mediterranean simulated by a regional climate model: a first approach. *Global and Planetary Change* 44(1–4): 163-180

Santhakumaran, L. N. (1980). Two New Species of *Xylophaga* from Trondheimsfjorden, Western Norway (Mollusca, Pelecypoda). *Sarsia* 65(3-4): 268-272.

Santos, S., M., L. Tagliaro, C., H. *et al*. (2005). Taxonomic implications of molecular studies on northern Brazilian Teredinidae (Mollusca, Bivalvia) specimens. *Genetics and Molecular Biology* 28(1): 175-179.

Scheller, H., V. and Ulvskov P. (2010). Hemicelluloses. *Annu Rev Plant Biol* 61: 263-289.

Scheltema, R. S. (1971). Dispersal of phytoplanktotrophic shipworm larvae (Bivalvia, Teredinidae) over long distances by ocean currents. *Marine Biology* 11(1): 5-11

Sellius, G. (1733). Got. Sellii Historia naturalis teredinis seu xylophagi marini, tubulo-conchoidis speciatim.

Sen, S. Sivrikaya, H. *et al*. (2010). Fouling and boring organisms that deteriorate various European and tropical woods at Turkish seas. *African Journal of Biotechnology* 9(17): 2566-2573.

Shallom, D. and Shoham Y. (2003). Microbial hemicellulases. *Current Opinion in Microbiology* 6(3): 219-228.

Si, A. Alexander, C., G. *et al*. (2000). Habitat partitioning by two wood-boring invertebrates in a mangrove system in tropical Australia. *Journal of the Marine Biological Association of the United Kingdom* 80(6): 1131-1132.

Sigerfoos, C., P. (1908). Natural history, organization, and late development of the Teredinidae, or ship-worms. United States, *Department of Commerce and Labor, Bureau of Fisheries, Bulletin* 27(639): 191-231.

Singh, A., P. (2012). A review of microbial decay types found in wooden objects of cultural heritage recovered from buried and waterlogged environments. *Journal of Cultural Heritage* 13(3, Supplement): S16-S20.

Smant, G. Stokkermans, J., P. *et al*. (1998). Endogenous cellulases in animals: isolation of beta-1, 4-endoglucanase genes from two species of plant-parasitic cyst nematodes. *Proceedings of the National Academy of Sciences of the United States of America* 95(9): 4906-4911.

Somerville, C. (2006). Cellulose Synthesis in Higher Plants. *Annual Review of Cell and Developmental Biology* 22(1): 53-78.

Southwell, C. R. and Bultman J., D. (1971). Marine borer resistance of untreated woods over long periods of immersion in tropical waters. *Biotropica* 3(1): 81-107.

Stanton, S. A. (2012). *Structure and function of the external ciliation of larval bivalves with different life history strategies*. Ph.D. University of Portsmouth, United Kingdom.

Steiner, G. and S. Hammer (2000). ″Molecular phylogeny of the Bivalvia inferred from 18S rDNA sequences with particular reference to the Pteriomorphia.″ *Geological Society, London, Special Publications* 177(1): 11-29.

Strathmann, R., R. Hughes, T., P. *et al*. (2002). Evolution of local recruitment and its consequences for marine populations. *Bulletin of Marine Science* 70(Supplement 1): 377-396.

Svensson, B. (1994). Protein engineering in the α-amylase family: catalytic mechanism, substrate specificity, and stability. *Plant Molecular Biology* 25(2): 141-157.

Tamura, K., D. Peterson, *et al*. (2011). MEGA5: Molecular Evolutionary Genetics Analysis Using Maximum Likelihood, Evolutionary Distance, and Maximum Parsimony Methods. *Molecular Biology and Evolution* 28 (10): 2731 -2739.

Tan, A., S. Hu, Y., P. *et al*. (1993). Shell and pallet morphology of early developmental stages of *Bankia gouldi* (Bartsch, 1908) (Bivalvia, Teredinidae). *Nautilus* 107(2): 63-75.

The Woodshole Oceanographic Institution Annual Report (1952).

Thiel, M. (1999). ″Reproductive biology of a wood-boring isopod, *Sphaeroma terebrans*, with extended parental care.″ *Marine Biology* 135(2): 321-333.

Thiel, M. and Gutow L. (2005). The ecology of rafting in the marine environment. II. The rafting organisms and community. Oceanography and Marine Biology - an Annual Review, Vol. 43. R. N. Gibson, R. J. A. Atkinson and J. D. M. Gordon. 43: 279-418.

Tjoelker, L., W. Gosting, L. *et al*. (2000). Structural and functional definition of the human chitinase chitin-binding domain. *Journal of Biological Chemistry* 275(1): 514-520.

Turner, R. (1976). Some factors involved in the settlement and metamorphosis of marine bivalve larvae. [in] Sharpley & Kaplan (eds.), Proc. 3rd. International Biodegradation Symposium, pp.409-416.

Turner, R. and Calloway, C., B. (1987). Species pairs in the Teredinidae. *International research group on wood preservation*, Document No: IRG/WP/4142: 1-2

Turner, R. D. (1966). A Survey and Illustrated Catalogue of the Teredinidae: (Mollusca: Bivalvia), Museum of Comparative Zoology, Harvard University.

Turner, R. D. (1971). Identification of marine wood boring molluscs. Marine borers and fouling organisms of wood. E. B. G. Jones and S. K. Eltringham. Paris, OECD: 17-64.

Turner, R. D. (2002). ″On the subfamily Xylophagainae (family Pholadidae, Bivalvia, Mollusca). Bulletin of the Museum of Comparative Zoology 157(4): 223-307.

Turner, R. D. and Yakovlev Y. (1983). Dwarf males in the Teredinidae (Bivalvia, Pholadacea). *Science* 219(4588): 1077-1078.

Tyler, P. A., C. M. Young, *et al*. (2007). Settlement, growth and reproduction in the deep-sea wood-boring bivalve mollusc *Xylophaga depalmai*. *Marine Ecology-Progress Series* 343: 151-159.

Voight, J. R. (2007). Experimental deep-sea deployments reveal diverse Northeast Pacific wood-boring bivalves of Xylophagainae (Myoida : Pholadidae). *Journal of Molluscan Studies* 73: 377-391.

Voight, J. R. (2009). Diversity and reproduction of near-shore Vs offshore wood-boring bivalves (Pholadidae: Xylophagainae) of the deep eastern Pacific ocean, with three new species. *Journal of Molluscan Studies* 75: 167-174.

Voight, J. R. and Segonzac M. (2012). At the bottom of the deep blue sea: a new wood-boring bivalve (Mollusca, Pholadidae, Xylophaga) from the Cape Verde Abyssal Plain (subtropical Atlantic). *Zoosystema* 34(1): 171-180.

Umezurike, G., M. (1975). The subunit structure of beta-glucosidase from *Botryodiplodia theobromae*. Biochemical Journal 179(3):503-7.

Wang, M., Liu, K. *et al*. (2013). The structural and biochemical basis for cellulose biodegradation. *Journal of Chemical Technology & Biotechnology* 88(4): 491-500.

Warnecke, F. Luginbuhl, P. *et al*. (2007). Metagenomic and functional analysis of hindgut microbiota of a wood-feeding higher termite. *Nature* 450(7169): 560-565.

Watanabe, H., Noda, H. *et al*. (1998). A cellulase gene of termite origin. *Nature* 394(6691): 330-331.

Waterbury, J. B., C. B. Calloway, *et al*. (1983). A cellulolytic nitrogen-fixing bacterium cultured from the gland of Deshayes in shipworms (Bivalvia, Teredinidae). *Science* 221(4618): 1401-1403.

Watson, B. J. Zhang, H.*et al*. (2009). Processive endoglucanases mediate degradation of cellulose by *Saccharophagus degradans*. *Journal of Bacteriology* 191(18): 5697-5705.

Wilson, D. B. (2008). Three microbial strategies for plant cell wall degradation. *Annals of the New York Academy of Sciences* 1125(1): 289-297.

Xu, B., Hägglund, P. *et al*. (2002). Endo-β-1,4-Mannanases from blue mussel, *Mytilus edulis*: purification, characterization, and mode of action. *Journal of Biotechnology* 92(3): 267-277.

Yakovlev, Y. M., Drozdov, A. L. *et al*. (1998). Peculiarities of reproduction and gamete structure of the shipworm *Zachsia zenkewitschi* (Bivalvia: Teredinidae). Korean Journal of Malacology 14(1): 1-8.

Yang, J. C., Madupu, R. *et al*. (2009). The complete genome of *Teredinibacter turnerae* T7901: an intracellular endosymbiont of marine wood-boring bivalves (shipworms).″ *PLoS ONE* 4(7)

Zehr J. P., Carpenter, E. J., Villareal, T. A. (2000). New perspectives on nitrogen-fixing microorganisms in tropical and subtropical oceans. Trends Microbiol. 8(2):68-73.